**Faculty of Engineering**
Sanitary Engineering Department

# Study of Water and Wastewater in New Burj Al Arab City

A Thesis submitted in partial fulfillment of the requirements for the degree of Master of Science
In
Sanitary Engineering

**Presented by**

Mohamed Gharib Abd El Ghani Mujahid

B.Sc. in Power and Electrical Machinery Engineering,
Faculty of Engineering, Menoufia University, 2007

*November 2020*

**Faculty of Engineering**
Sanitary Engineering Department

Approval Sheet

# Study of Water and Wastewater in New Burj Al Arab City

**A Thesis Submitted by**

Mohamed Gharib Abd El Ghani Mujahid

B.Sc. in Power and Electrical Machinery Engineering,
Faculty of Engineering, Menoufia University, 2007

For the Degree of Master of Science in
Sanitary Engineering

| *Examiners'Committee* | *Approved* |
|---|---|
| **Prof. Dr. Fifi Mohamed Elsayed**<br>Full Time Professor of Sanitary Engineering<br>Alexandria University | ……………… |
| **Prof. Dr. Mohamed Tarek Sorour**<br>Professor of Sanitary Engineering<br>Alexandria University | ……………… |
| **Prof. Dr. Medhat Abd El Moaty Mostafa**<br>Professor of Sanitary Engineering<br>Alexandria University | ……………… |

Date of discussion: 16/11/2020

**Faculty of Engineering**
Sanitary Engineering Department

Supervisory Committee

# Study of Water and Wastewater in New Burj Al Arab City

**A thesis Submitted by**

Mohamed Gharib Abd El Ghani Mujahid

B.Sc. in Power and Electrical Machinery Engineering,
Faculty of Engineering, Menoufia University, 2007

| *Supervisors committee* | *Signature* |
|---|---|
| **Prof. Dr. Fifi Mohamed Elsayed**<br>Full Time Professor of Sanitary Engineering<br>Alexandria University | .................. |
| **Dr. Mai Abd El Fattah Fayed**<br>Lecturer of Sanitary Engineering<br>Alexandria University | .................. |
| **Dr. Samia Abd El Rahman Aly**<br>Lecturer of Sanitary Engineering<br>Alexandria University | .................. |

# ACKNOWLEDGEMENTS

First of all, praise is to Allah for helping me in making this thesis possible.

I Would like to express my sincere gratitude to

**Prof. Dr. Fifi Mohamed Elsayed,**

**Prof. Dr. Hamdy Seif,**

**Dr. Mai Abd El Fattah Fayed,** And

**Dr. Samia AbdEl Rahman Aly**

For their continuous support, guidance, and efforts highly contributed to the success of this study that I never would have reached on my own.

I wish to thank all my family members, especially my father, mother, wife, sisters, daughter, my son for their encouragement**.**

Finally, I ask Allah to bless all giving them long life and continuous pleasure**.**

# DECLARATION

I declare that no part of the work referred to this thesis has been submitted in support of an application for another degree or qualification from this or any other university or institution**.**

Student Name: Mohamed Gharib Abd El Ghani Mujahid.

Signature:

# TABLE OF CONTENTS

# NOMENCLATURE

| **English Symbols** | |
|---|---|
| a, b | The coefficients of the given functions. |
| c1, c2 | The acceleration constants |
| $C_{E,t}$ | The energy-related cost for the year (t) |
| $C_t$ | The annual cost operation of the RO plant |
| $C_{(PV)t}$ | The same annual cost operation and maintenance |
| $D$ | Pipe diameter |
| Ediff,hor | The diffuse solar irradiance |
| Edir,hor | The direct solar irradiance |
| EGlob,hor | The global irradiance |
| E,extra | The extraterrestrial irradiance |
| $E_{Total}$ | Total required energy of the RO plant |
| $E_{(desalination)}$ | High pressure pumps energy requirements |
| $E_{(el)t}$ | The amount of conventional electrical energy from the unified electricity grid |
| $E_{(Lifting\ pumps)}$ | High lifting pumps energy requirements |
| $E_{(PV)t}$ | The photovoltaic system produces the same amount of energy produced in the year |
| $E_{(\text{transfer}\ pumps)}$ | Transfer pumps energy requirements |
| $f$ | Coefficient of friction |
| $ff$ | Membrane active area |
| $f(x)$ | The fitness function |
| $F_d$ | The design flow rate of high lift pumps |
| $F_{lifting\ pumps}$ | Lift pump flow rate |
| $F_{pump}$ | Pump flow rate |
| $F_{Total}$ | The total amount of product water to be produced by membranes. |
| $F(x)$ | The objective function |
| $gbest_i$ | The overall best value |
| H | The outlet pressure |
| $H_F$ | The friction losses |
| $H_l$ | The lost head |
| $H_P$ | The total head |
| $H_M$ | The minor losses |
| $H_{static}$ | The static head |
| $i$ | The discount rate of the RO plant |
| $iter$ | The present iteration number |
| $i_{(PV)}$ | The discount rate of the PV system |
| I | The current |
| $I_0$ | The initial capital investment of the RO plant |
| Impp | The rated current at the maximum power-point |
| Isc | The short circuit current |
| $I_{(PV)0}$ | The initial capital investment of PV system |

| | |
|---|---|
| $k$ | A scaling constant |
| $K_M$ | The minor losses coefficient |
| $L$ | The length of force main-line |
| n | The number of years. |
| $n(pv)$ | The PV system lifetime |
| $N_E$ | The total number of elements |
| $N_{EpV}$ | The total number of membrane elements per Pressure Vessels |
| $N_{lifting\ pumps}$ | The total number of lifting pumps |
| $N_{pump}$ | The total number of transfer pumps |
| $N_V$ | The total number of pressure vessels |
| $NW_{2032}$ | The net additional water capacity required until 2032 |
| $N_{WorKing\ \ pumps}$ | The total number of working pumps |
| m | The scaled index |
| $pbest_i$ | The value of the fitness for particle |
| Pmpp | The rated power at the maximum power-point |
| $P_{Total}$ | The total required power of the RO plant |
| $P_t$ | The population |
| $P_{t\ ,predicted}$ | The type of analytical function used. |
| $P_{t\ ,real\ value}$ | The existing recorded data |
| $p_{Water}$ | The amount of water produced in a year by the RO plant |
| $P_{(desalination)}$ | The total power consumption of high-pressure pumps are used to achieve this high feed pressure for the RO process |
| $P_{(el)t}$ | The cost of the unit of conventional electrical energy from the unified electricity grid in the year (t) |
| $P_{(integration)t}$ | The cost of the electric power unit for the integration of conventional from the unified electricity grid and the power energy from the PV system in the year (t) |
| $P_{(PV)t}$ | The cost of the unit of electrical energy from the photovoltaic system in the year (t) |
| $Power_{(Total\ lifting\ \ pumps)}$ | The total power consumption of high lifting pumps |
| $Power_{(Total\ transfer\ pumps)}$ | The total power consumption of transfer pumps |
| $Q_P$ | The required permeate flow |
| r1, r2 | Random numbers |
| R | The forecasting error |
| S | The sum of the squared prediction errors. |
| $S_E$ | The average flux |
| $Specific\ energy_{(desalination)}$ | The specific energy high-pressure pumps are used to achieve this high feed pressure for the RO process |
| $Specific\ energy\ _{(Lifting\ pumps)}$ | The specific energy of lifting pumps |
| $Specific\ energy_{(\text{transfer}\ pump)}$ | The specific energy of transfer pumps |
| $Total\ specific\ energy$ | The total specific energy of the RO plant |
| $TW_{2032}$ | The total estimated water amount by the year 2032 |
| V | The voltage |
| $Vi$ | The velocity of the particle ( i ) |
| Vmpp | The rated voltage at the maximum power-point |

| | |
|---|---|
| Voc | The open-circuit voltage |
| $w$ | The particle's inertia weight |
| $w_{max}$ | The maximum values of the inertia weight |
| $w_{min}$ | The minimum values of the inertia weight |
| $W_{40}$ | The amount of water received from the Kilo 40 station |
| $W_{reuse}$ | The amount of treated wastewater reused |
| $x_i$ | The $i_{th}$ year in which the population $P_t$ is considered. |
| $x_o$ | The base year |
| $X$i | The $i_{th}$ particle |
| **Greek Symbols** | |
| $\eta_{motor}$ | The motor efficiency |
| $\eta_{pumps}$ | The pump efficiency |
| $\eta_{VFD}$ | The variable-frequency drive efficiency |
| **Subscripts** | |
| a-Si:H | Hydrogenated amorphous silicon |
| B | Boron |
| Ba | Barium |
| Ca | Calcium |
| CdTe | Cadmium telluride |
| Cl | Chloride |
| $CO_2$ | Carbon dioxide |
| $CO_3$ | Carbon trioxide |
| CuInGaSe2=CIGS | Copper indium gallium diselenide. |
| f-Si | Thin-film polycrystalline silicon |
| F | Fluorine |
| GaAs | A compound semiconductor form by Gallium (Ga) and Arsenic (As) |
| HCO3 | Carbonic acid |
| K | potassium |
| Mg | Magnesium |
| Na | Sodium |
| NH4 | Ammonium |
| $NO_3$ | Nitrate |
| PH | A scale used to specify how acidic or basic a water-based solution |
| $PO_4$ | Phosphate |
| $SiO_2$ | Silica |
| $SO_4$ | Sulfate |
| Sr | Strontium |

# LIST OF ABBREVIATIONS

| | |
|---|---|
| *AC* | Alternating Current |
| A.C | The Annual Capital Cost |
| A.O.C | The Annual Operation and Maintenance Cost |
| BCM | Billion Cubic Meters |
| BOS | Balance of System |
| C.C | The Capital Cost |
| CPV | Concentrating PV Photovoltaic |
| CRF | The Capital Recovery Factor |
| *DC* | Direct Current |
| DOD | The Depth of Discharge |
| DSSC | Dye-Sensitized Solar Cells |
| ED | Electro-Dialysis |
| EGP | Egyptian Pound |
| ERD | Energy Recovery Devices |
| ETC | Evacuated Tubes Collector |
| Fit | The Fitness Function |
| FPC | The Flat-Plate Collectors |
| GA | The Genetic Algorithm |
| GDP | Gross Domestic Product |
| GHG | The Global Greenhouse Gas |
| ha | Hectare |
| HPP | The High-Pressure Pump |
| LCOE | The Levelised Cost of Electricity. |
| LCOW | The Levelised Cost of Water |
| LD | Liquid Discharge. |
| L/C/D | Liters per Capita per Day |
| LID | Light-Induced Degradation |
| MED | Multi-Effect Distillation |
| MPP | The Maximum Power-Point |
| MSF | Multi-Stage Flash |
| MTES | The Minimum Thermodynamic Energy of Separation |
| NEA | Nuclear Energy Agency |
| OECD | Organization for Economic Co-Operation and Development |
| PF | The Peak Factor |
| POP | Population in Thousands |
| PR | Performance Ratio |
| PSO | The Particle Swarm Optimization Technique |
| PV | Photovoltaic |
| PV-RO | The Solar Photovoltaic Panels Coupled to Reverse Osmosis Desalinate Water System |
| R&D | Research and Development |
| RO | Reverse Osmosis |
| RR | The Recovery Ratio |
| SE | Solar Energy |
| SOC | The battery State of Charge |

| | |
|---|---|
| STC | Standard Test Conditions |
| SWRO | Seawater Reverse Osmosis |
| VC | Vapor Compression |
| T.A.C | Total Annual Cost |
| TDS | Total Dissolved Solids |
| UPVC | Unplasticized Polyvinyl Chloride |
| USD | United States Dollar |
| VFD | A Variable-Frequency Drive |
| ZLD | Zero Liquid Discharge |
| ZVI | Zero Valente Iron. |

# LIST OF FIGURES

# LIST OF TABLES

# ABSTRACT

In the presence of overpopulation in Egypt in the last decades, it was necessary to establish and expand new cities to accommodate this overcrowding. Hence, these new cities need water, where the Nile water budget is $55.5x10^9$ $m^3$/ year in Egypt and this budget is fixed. So the only option needed to manage our resources efficiently is by searching and developing other resources, like using seawater desalination and reuse the tertiary treated wastewater to reduce the depletion of water resource-limited for future generations**.**

The new city of Burj Al-Arab is a sample of the new (residential and industrial) cities that have been studied in this thesis. This thesis develops a framework for strategic planning to support decision-making in water and wastewater infrastructure planning. That is to strengthen and expand the existing water and sanitation facilities of the Burj Al-Arab city. This is to accommodate the expected population increase until 2032, with taking into consideration the comparison between the three suggested configurations of the solar photovoltaic panels coupled to reverse osmosis desalinate water system (PV-RO) and a study of the feasibility of using seawater desalination by using (PV-RO) technology as a second alternative source of Nile water. That is to supply the city with drinking water to cover future needs. This is in line with the directives of the government in Egypt**.**

The water demands and wastewater discharges were estimated for all uses. This is done by using the forecasted population census and the general plan for urban and industrial development in Burj Al-Arab city. The laws and consumption rates concerning the estimation of water demand and wastewater discharges stipulated in the Egyptian code were applied to the design and implementation of drinking water and sanitation projects. The current situation has been assessed of drinking water and wastewater facilities in the Burj Al Arab City, and weaknesses have been identified to develop solutions within the proposed strategic planning. In this thesis, several different techniques and software programs have been exposed to help in selecting optimal solutions**.**

# CHAPTER 1

# INTRODUCTION

# INTRODUCTION

## 1.1 Introduction

Individuals need water for drinking, cooking, and bathing; communities need water for agriculture and industry. In many parts of the world, water is a major source of energy and means of transportation. Beyond these obvious uses, there is also a complex relationship between water and sanitation and their role in alleviating poverty, safeguarding human health, advancing educational opportunities, and reducing gender inequity [1].

For these reasons, Egypt's millennium development goals set two specific global water targets: by 2032, to halve the proportion of people without safe drinking water, and to halve the proportion of people lacking adequate sanitation [2].

**Figure (1.1)** shows how the water-related issue was in 1995 and the forecast of how worse could it be in 2025. The world will face severe water shortages. The countries that have water withdrawal as a percentage of total available water from 10% to 20% would become even more water-stressed reaching numbers from 20% to 40%. The situation would be even rougher with the countries that already were water-stressed. A solution to the problem could be water desalination from the sea and oceans. More and more countries will rely on this method and supply desalinated water to the population [3].

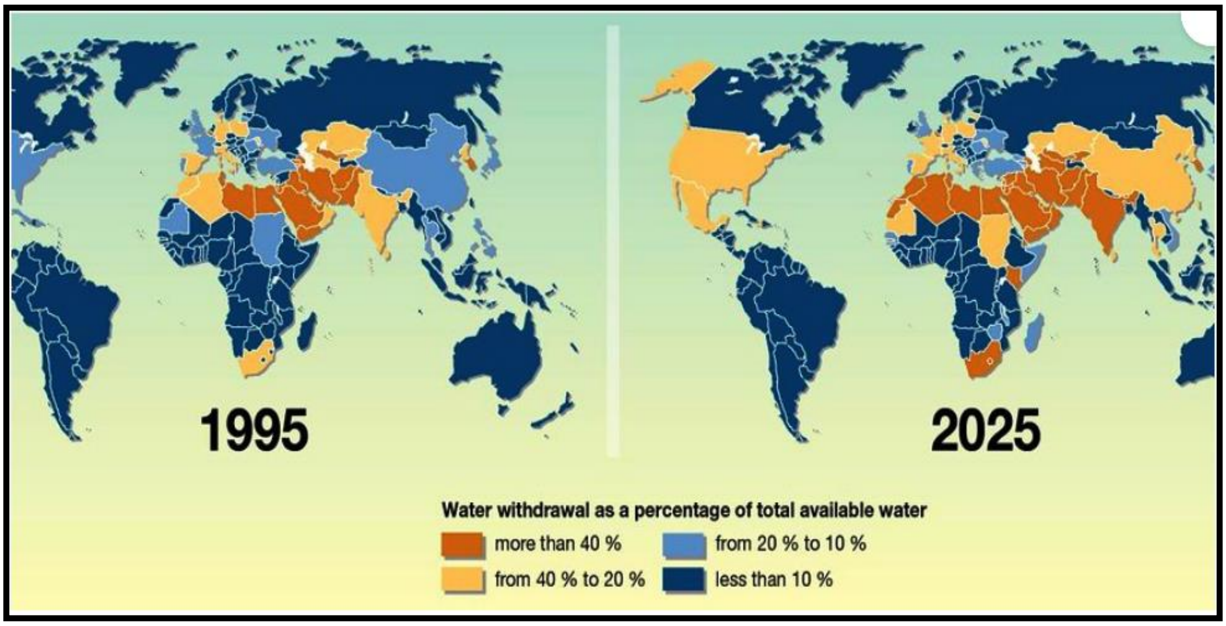


**Figure (1.1): Forecast of water scarcity in 2025 UNEP 2009 [3].**

In the presence of overpopulation in Egypt in the last decades, it was necessary to establish and expand new cities to accommodate this overcrowding. Hence, these new cities need water, where the Nile water budget is $55.5x10^9$ $m^3$/ year in Egypt and this budget is fixed. So the only option needed to manage our resources efficiently is by searching and developing other resources than the Nile water like using the seawater desalination and reuse the tertiary treated wastewater [2].

## 1.2 Research Problem

The new city of Burj Al-Arab is an example of the new (residential and industrial) city that has been studied in this thesis. The main objective of the thesis is to proposed strategic planning for drinking water and wastewater projects. This is to strengthen and expand the existing water and wastewater facilities to cover the future needs of the Burj Al-Arab city, to accommodate the expected population increase until 2032. Taking into consideration the weakness of the current water and wastewater systems like the lack of available water rations for Burj Al-Arab city. More economical use of water, reducing distribution losses and increased use of reused water can help alleviate this problem. But if there is still a shortfall then desalination of seawater may be a good option to cover that shortfall. This is in line with the state's tendency to find alternatives to conventional water sources and also reduce the dependency on water allocations from the Nile water [4, 5].

## 1.3 Aim and Objectives

The specific goals of this research study are the following:

**1-** Study and evaluate the position of wastewater and drinking water supply works to calculate the requirements of the strategic plan.

**2-** Propose a framework for strategic planning to support decision-making in water and wastewater infrastructure planning. That is to strengthen and expand the existing water and sanitation facilities to cover the future needs of the Burj Al-Arab city. Determining a minimum cost for long-term strategic planning for water and wastewater projects to supply the users within a set of technical, economic, and political constraints.

**3-** Within the framework of this thesis, a simplified approach was proposed, which allows a quick but relatively precise assessment of the investment as well as of the operational cost of solar desalination plants configurations. The best configuration will be selected as a second alternative source of Nile water. The three representative utility-scale of the solar photovoltaic panels coupled to reverse osmosis desalinate water System (PV-RO system configurations) that have been analyzed as follows:

**A- The first configuration, (PV-RO system with PV solar panels only).**

**B- The second configuration, (PV-RO system with PV solar panels and Batteries).**

**C- The third configuration, (PV-RO system with PV solar panels and electricity grid).**

## 1.4 Research Methodology

This study mainly relied on the following methodology:

**1-** Long-term forecasting of the population increase is performed for Burj Al-Arab city until 2032 using two methods (linear, exponential) that are specified in the Egyptian code for the implementation of drinking water and wastewater projects. The forecast was calculated by using three techniques: extrapolation of trend curves, genetic algorithm (GA), and particle swarm optimization technique (PSO). All of these techniques have been implemented with MATLAB software and the best results have been selected.

**2-** Estimating water demand and wastewater discharge for all uses. According to the Egyptian code and by using the forecasted population census and the general plan for urban and industrial development in the Burj Al-Arab city.

**3-** Evaluate the existing water and sanitation facilities. Also, to do the strategic planning for the drinking water and wastewater projects.

**4-** Selecting the optimal strategic planning for drinking water and sanitation projects to strengthen existing facilities and expand the existing water and sanitation facilities for coverage of future needs. This is to accommodate the expected population increase until 2032 of the Burj Al-Arab city. Taking into consideration the precise assessment and study of the possibility of using the PV-RO system. In addition, the results will show the sensitivity of the Levelised Cost of Water (LCOW) as a function of selected key parameters. The designs have been carried out according to the manufacturer‘s recommended specifications using a commercially available simulation tool (IMSDesign software program and PVsyst software program)**.**

# CHAPTER 2

# LITERATURE REVIEW

# LITERATURE REVIEW

## 2.1 Introduction

There is a very important question about the possibility of feeding new cities with clean drinking water in the future. The new Burj Al-Arab is a sample of existing residential and industrial new cities that studies in this thesis. It is one new city of the first generation in Egypt, was established by presidential decree No.506 in 1979, and adopted in the planning on the Dutch experience. Which is planned to accommodate 750,000 people with an area of about 191.83 square kilometers (47,403 acres), located just about 60 km in the direction of West Alexandria, Egypt [4]. The current population is 140,000 residents in according to the last population census of 2017. The general plan of the new Burj Al Arab city is shown in **Figure (2.1)**. The Mediterranean coast is about seven kilometers. It's a site feature that is the city located on high ground above the sea level to 25 meters, making the climate is dry and is not humid [4]**.** The necessary data for the drinking water and wastewater systems in the new city of Burj Al-Arab that will be used in this thesis is presented in **Appendix (A)** [4 - 6]**.**


**Figure (2.1): The general plan of the new Burj Al-Arab city [7].**

Source: The google earth website, 2019.

## 2.2 The Current Status of the Water in Egypt

Egypt is an arid country, which covers an area of about 1,001,450 km$^2$ of which only 4% is occupied by its population. The population was increased during the last 50 years from 19 million in 1947 to about 100 million in 2018 of whom about 99% are concentrated on the Nile Valley and Delta. The agriculture requirements exceed 80% of the total water demand. In view of the expected increase in water demand from other sectors, such as municipal and industrial water supply, the development of Egypt‘s economy strongly depends on its ability to conserve and manage its water resources [8]. Meanwhile, water demand is continually increasing due to population growth, industrial development, and the increase in living standards. The per capita share of water has dropped dramatically to less than 1000 $m^3$/ capita, which is classified as the water poverty limit. It is projected that the value decreases to 500 $m^3$/ capita in the year 2025 [8]. Most cultivated lands are located close to the Nile banks, its main branches, and canals. Currently, the inhabited area is about 5.3 million hectares and the cultivated agricultural land is about 3.3 million hectares. The crop area declined from 0.17 hectares/ capita in 1960, 0.08 hectares/ capita in 1996 to about 0.04 hectares/ capita in 2012. The sharp decline of both cultivated land and crop area per capita resulted in a decrease in crop production. This affects directly on food security at individual, family, community, and country levels [8]**.**

## Water Resources in Egypt

Water resources in Egypt are**:**

1- Nile River**;** 2- Rainfall**;** 3- Groundwater in the deserts and Sinai and**;**

4- Non-conventional water resources**.**

Each resource has its limitation on use, whether these limitations are related to quantity, quality, space, time, or cost. The following is a description of each resource [8]**.**

### A. Nile River Water

The Nile River inside Egypt is completely controlled by the Aswan dam in addition to a series of seven barrages between Aswan and the Mediterranean Sea and Nile water budget is 55.5 x $10^9$ $m^3$/ year to Egypt. Egypt relies on the available water storage of Lake Nasser to sustain its annual share of water. Nile water comprises about 91.5% of the total freshwater supply and 97% of renewable water supplies in Egypt [9]**.**

- ❖ Water supplies and demands in Egypt are given in **Table (2.1).**

### B. Rainwater

Rainfall is limited to the coastal strip running parallel to the Mediterranean Sea and occurs only in winter. The amount is small ranging between 80 to 280 mm/ year and provides an overall volume of about 1.3 billion $m^3$/ year. Rain is also erratic with respect to space and time and is mainly utilized for agricultural purposes. The rainfall amount cannot be considered a reliable source of water due to high spatial and temporal variability [10]**.**

### C. Groundwater

Although there is less groundwater than Nile water, the existence of aquifers in the desert, where no Nile water can be conveyed, makes this resource extremely precious. Desert aquifers are most deep and non-renewable, meaning that they are mined and the cost of exploitation is high [8 and 11]. The second source of groundwater is the Nile aquifer, which lies below cultivated land in the valley and Delta. The reservoir is fed by surplus irrigation water and seepage from the Nile and its branches. Water in the reservoir is shallow and renewable and the quality is not as good as the deep groundwater in the desert. The total available storage of the Nile aquifer is estimated at 500 BCM but the maximum renewable amount (the aquifer safe yield) is around 7.5 BCM. The existing rate of groundwater abstraction in the Valley and Delta regions is about 5.1 BCM/ year, which is still below the potential safe yield of the aquifer. The third, smaller groundwater reservoir is the coastal aquifer, which is fed by rain falling on the coastal strip, forming lenses of freshwater, which sit above the saline groundwater and run parallel to the shoreline [8 and 11].

**Table (2.1): The water supplies and demands in Egypt in BCM per year [8].**

| | 1990 | 2000 | 2025 |
|---|---|---|---|
| Water supplies | | | |
| Nile water | 55.5 | 55.5 | 55.5 |
| Groundwater: | | | |
| - in the Delta and New Valley | 2.6 | 5.1 | 6.3 |
| - in the desert | 0.5 | 1.0 | 2.0 |
| Reuse of agricultural drainage water | 4.7 | 7.0 | 8.0 |
| Treated sewage water | 0.2 | 0.7 | 3.8 |
| Total | 63.5 | 69.4 | 75.6 |
| Water demands | | | |
| Agriculture | 49.7 | 59.9 | 61.5 |
| Households | 3.1 | 3.1 | 5.1 |
| Industry | 4.6 | 6.1 | 8.6 |
| Navigation | 1.8 | 0.3 | 0.4 |
| Total | 59.2 | 69.4 | 75.6 |

Source: Abdel-Shafy. H., 2013.

### D. Non-Conventional Water Resources

Given the continuous need to increase water resources and bridge the gap between supply and demand; Egypt has a long history of water reuse. While conventional (renewable) resources are extremely scarce, non-conventional water sources provide highly valued supplies. This water is generally used for agriculture, landscaping, and industrial uses through specialized processes, these sources include:

- **The Reuse of Treated Sewage Water**

Currently, Egypt produces an estimated 7.6 BCM of sewage water per year (see **Figure (2.3)**). Of that 2017, about 3.8 BCM per year is treated, but only 0.7 BCM per year is utilized for agriculture (0.26 BCM is undergoing secondary treatment and 0.44 BCM undergoing primary treatment), mainly direct reuse in desert areas or indirect reuse through mixing with agricultural drainage water [8, 12, and 13].

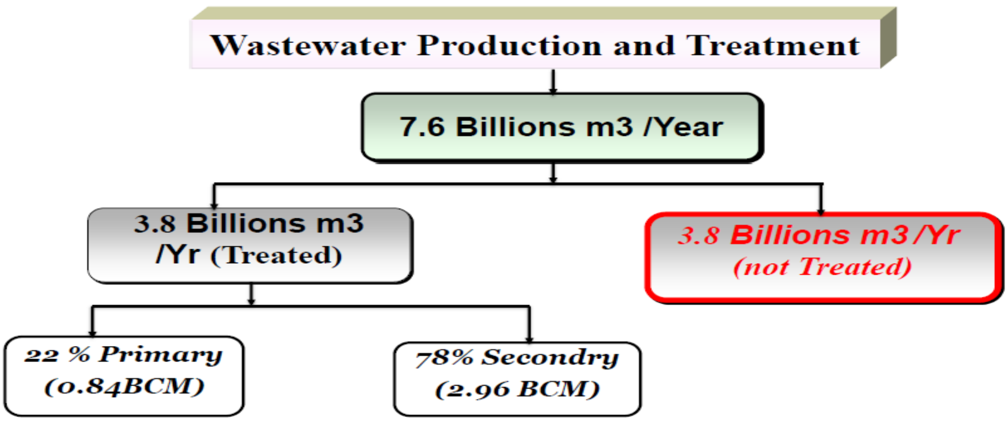


**Figure (2.2): The current wastewater production and treatment (2017) [13].**
Source: Holding Company for Water and Wastewater Website, 2017.

- **The Reuse of Treated Agricultural Drainage Water**

The amount of water that returns to drain from irrigated lands is relatively high about (25% - 30%). The total amount of reused water is estimated to be 7 BCM in 2013. The reuse practi-ces increase the overall efficiency of the system as compared to the efficiency of modern irrigation systems. Reuse of non-conventional water sources such as agricultural drainage water and treated sewage water cannot be added to Egypt's freshwater resources. In fact, using these sources is a recycling process of the previously used Nile fresh water in such a way that improves the overall efficiency of the water distribution system. However, appropriate strategies are needed for managing soil, water, and crops when these resources are used for irrigation [8].

- **Desalination of Sea Water**

The desalination of seawater in Egypt has been given low priority. The reason is due to the cost of treating seawater which is high compared with other sources; even the unconventional sources such as drainage reuse. The future use of such resources for other purposes (agriculture and industry) will largely depend on the rate of improvement in the technologies used for desalination and the cost of power. The amount of desalinated water in Egypt has been in the order of 0.03 BCM/ year in 2017 [8].

## 2.3 The Current Situation of Water and Wastewater System for Alexandria City

### 2.3.1 Alexandria City

Alexandria Governorate area is 2,679 km$^2$ with a total population of 5,163,750 people, according to the primary data Estimated on 18/ 4/ 2017 for the central agency for public mobilization and statistics – Egypt [14].

### 2.3.2 Water Service

Alexandria is served with 11 water treatment plants with a design capacity of 3,567,000 m$^3$/ day; the total actual capacity is 2,720,000 m$^3$/ day. This means that the stations are working with almost around 76.28% of their design capacity. Also, Alexandria is served with 41 lift stations. The Average water consumption is 527 liters/ person/ day [5].

### 2.3.3 Sewer Service

Alexandria is served with 20 wastewater treatment plants with a design capacity of 1,668,080 $m^3$/ day; the total actual capacity is 1,255,767 $m^3$/ day. This means that the stations are working with almost around 75% of their design capacity. Also, Alexandria is served by 165 lift stations. The force main lengths are about 196.25 km with diameters between (200 - 2250) mm. The network length is about 4400 km. The Average daily disposal of sewage is 243 liters/ person/ day [6].

## 2.4 The Current Situation of Water and Wastewater System for New Burj Al-Arab City:

- **The current situation of the water sources for the new Burj Al-Arab city**

The new city of Burj Al-Arab depends on a drinking water station in Kilo 40, (Alexandria Cairo desert road) in providing drinking water. The station has an existing design capacity of 566,000 $m^3$/ day. New Burj Al Arab's share of the total capacity of the Kilo 40 station is About 166,000 $m^3$/ day and the rest capacity is 400,000 $m^3$/ day dedicated to feeding the Northern Coast and Matrouh [4 and 5]. The drinking water station at Kilo 40 was the construction of three stages as shown in **Figure (2.3)**. The rest of the necessary current data for the drinking water and wastewater systems in the new city of Burj Al-Arab that will be used in this thesis is presented in **Appendix (A).**

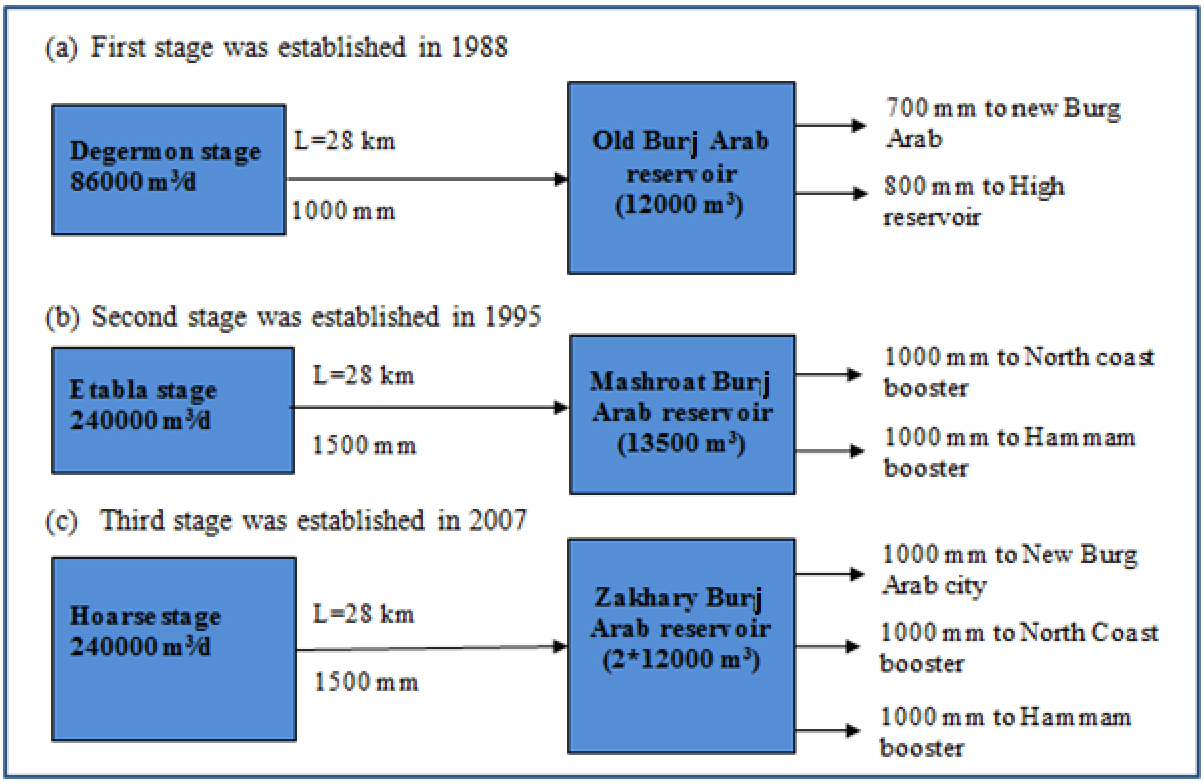


**Figure (2.3): The construction of three stages of a drinking water station at Kilo 40 [5].**

## 2.5 Overview of Desalination

Increased demand for water is a global problem. In many parts of the world, local demand is outstripping conventional resources. More economical use of water, reducing distribution losses and increased use of recycled water can help alleviate this problem but if there is still a shortfall then the desalination of seawater or brackish water may be an option (World Bank, 2004) [15]. Seawater Reverse Osmosis (SWRO) desalination has emerged as one of the technologies of choice to alleviate the problems of freshwater shortages. Since the 1990s, reverse osmosis (RO) has been adopted in most arid and semi-arid regions around the world. Frequent droughts, climate changes, and seasonal shifts worldwide, in addition to population growth and depleted traditional water resources, are among a myriad of factors that have forced many coastal communities to seek reliable alternative sources of potable water. As shown in **Table (2.2)**, the abundance of seawater (about 97% of the volume of water on earth) makes it an attractive supply source, at least for communities living in the vicinity of coastlines [16]**.**

**Table (2.2): Data on approximate volumes of global water resources [16].**

| Water Source | Water Volume ($km^3$) | Fresh Water (%) | Total Water (%) |
|---|---|---|---|
| Oceans, seas, bays | $1.338 \times 10^9$ | – | 96.539 |
| Ice caps, glaciers, permanent snow | $2.406 \times 10^7$ | 68.700 | 1.7364 |
| Groundwater, fresh | $1.053 \times 10^7$ | 30.060 | 0.7598 |
| Groundwater, saline | $1.285 \times 10^7$ | – | 0.9272 |
| Soil moisture | $1.650 \times 10^4$ | 0.047 | 0.0012 |
| Ground ice and permafrost | $3.000 \times 10^5$ | 0.857 | 0.0216 |
| Lakes, fresh | $9.100 \times 10^4$ | 0.260 | 0.0066 |
| Lakes, saline | $8.540 \times 10^4$ | – | 0.0062 |
| Atmospheric water | $1.290 \times 10^4$ | 0.037 | 0.0009 |
| Swamp water | $1.147 \times 10^4$ | 0.030 | 0.0008 |
| River flows | $2.120 \times 10^3$ | 0.006 | 0.0002 |
| Biological water | $1.120 \times 10^3$ | 0.003 | 0.0001 |
| Total freshwater | $3.503 \times 10^7$ | 100 | – |
| Total water reserves | $1.386 \times 10^9$ | – | 100 |

Source: Shiklomanov, I., 1993**.**

Aside from its rich content of nutrients, bacteria, and viruses, seawater contains high concentration levels of total dissolved solids (TDS). The total dissolved solids (TDS) of Mediterranean Seawater in the vicinity of Sidikerir Region, west of Alexandria, Egypt, as shown in **Table (2.3)** [17]**.**

While this is a typical concentration level in most oceans, TDS levels vary among different oceans and seas. Although seawater TDS concentration shown here totals 38,490 mg/ L (or parts per million), these levels fluctuate considerably [17]. This largely depends on the seasonal variations during the hydrologic cycle and geographical regions. Seawater TDS concentrations range between 7,000 and 45,000 mg/ L (and sometimes higher), as shown in **Table (2.4)** [15]. Water is classified in terms of different ranges of TDS concentration, as shown in **Table (2.5).**

**Table (2.3): The range and the seasonal values of seawater TDS concentration level at the SidiKerir region during 2012 - 2013 [17].**

| Season | Concentration (mg/ L) |
|---|---|
| Spring | (38260 to 38690)<br>The Average = 38475 |
| Summer | (37910 to 39710)<br>The Average = 38810 |
| Autumn | (37510 to 38850)<br>TheAverage = 38180 |
| Winter | (38440 to 38570)<br>The Average = 38505 |
| Annual | (37510 to 39710)<br>The Average =38490 |

Source: Abdel-Halim. A. M., 2016.

**Table (2.4): Seawater sources and their respective TDS concentrations [15].**

| Source | Concentration (mg/ L) |
|---|---|
| Baltic Sea | 7,000 |
| Oceans | 35,000 |
| Closed Seas | 38,000 |
| Red Sea | 41,000 |
| Arabian Gulf | 45,000 |
| Aral Sea | 29,000 |

Source: The World Bank, 2004.

**Table (2.5): Water, classified in terms of TDS [15].**

| Concentration (mg/ L) | Classification |
|---|---|
| TDS ≤ 1,000 | Potable water |
| 1,000 ≤ TDS ≤ 5,000 | LSB water |
| 5,000 ≤ TDS ≤ 15,000 | HSB water |
| 7,000 ≤ TDS ≤ 50,000 | Seawater |

LSB**:** Low Salinity Brackish**;** HSB**:** high Salinity Brackish[ 15]**.**

Source: The World Bank, 2004.

Additionally, potable water may be categorized with respect to its organoleptic properties (predominantly taste quality), in a manner shown in **Table (2.6)** [18]**.**

**Table (2.6): Potable water organoleptic properties [18].**

| Concentration (mg/ L) | Classification |
|---|---|
| TDS ≤ 300 | Excellent |
| 300 < TDS ≤ 600 | Good |
| 600 < TDS ≤ 900 | Fair |
| 900 < TDS≤ 1,200 | Poor |
| TDS >1,200 | Unacceptable |

Source: World Health Organization, 2003.

In order to transform seawater into safe drinking water, TDS levels have to be reduced. This is achieved by using desalting technologies that have traditionally included thermal processes such as multi-effect distillation (MED), multi-stage flash (MSF) distillation, and vapor compression (VC)[16]. Newer technologies include membrane and ion-exchange processes such as seawater reverse osmosis (SWRO) desalination as well as electro-dialysis (ED). Some of these processes are also combined together in some instances, creating a hybrid setup to achieve optimal desalination and reduce energy consumption [19].

- **Brief description of some desalination technologies and processes**

There are two groups of desalination currently in use: physical processes, such as reverse osmosis (RO), and chemical processes, such as the newer zero-valent iron (ZVI) technology, discovered in 2010 and just starting to be commercialized. Throughout this chapter, desalination has been mainly reviewed as a purely physical process: the physical separation of salt and water. In this sense, water desalination is fundamentally a thermodynamic process with a minimum required work that is intrinsic thereto. This is known as the minimum thermodynamic energy of separation (MTES); the lowest possible energy that is required to separate the solute from water. Attempts to minimize energy consumption toward MTES are only beneficial if they are also economically viable. A wise choice of making an advantageous desalination plant also depends on the TDS of the input and output water (see **Figure (2.4)**) [19]. Desalination systems may be loosely classified as a membrane or thermal technologies and as large-scale or small-scale systems. For a large scale, we may think of freshwater production capacities above 100,000 $m^3$/ day. Small-scale systems may extend well below 10,000 $m^3$/ day [20].

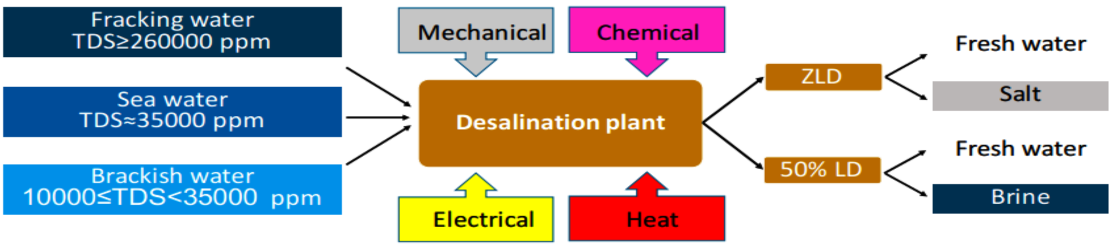


**Figure (2.4): Inputs and outputs of a typical desalination process. TDS, total dissolved salts; LD, liquid discharge; ZLD, zero liquid discharge (2019) [19].**

Source: Ahmadvand. S., 2019.

➡ A brief description of the three most important techniques for desalination will be done as follows:

## 1- Reverse osmosis (RO)

RO is a desalination process with the use of semi-permeable membranes which allow the passage of water molecules but not the dissolved salts. In an RO process, seawater is firstly pre-treated to remove suspended solids. Sufficient pressure is then applied with the use of high-pressure pumps to force water passing through the semi-permeable membranes, leaving the dissolved salts behind. Desalinated water then undergoes post-treatment, such as PH adjustment and disinfection, to make it suitable for drinking. The above process is depicted in **Figure (2.5)** [21].

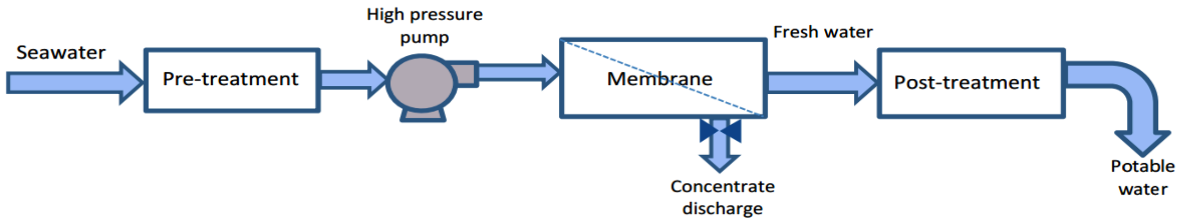


**Figure (2.5): The basic process of reverse osmosis [21].**

Source: Research Office Legislative Council Secretariat, 2015.

## 2- Multi-stage flash evaporation (MSF)

MSF is a type of thermal desalination which has already been in use since around the 1960s. The first desalination plant in Hong Kong, which was built in the 1970s, adopted the MSF technology. MSF facilities consist of some chambers connected with each successive chamber operating at a progressively lower pressure. Source water/pre-treated water (i.e. feed water) first passes from back to front through a tubing system to the brine heaters, where water is heated under high pressure. The heated water then enters the first chamber at reduced pressure, causing it to boil rapidly with a portion evaporating into vapor (see **Figure (2.6)**). In each successive chamber that operates at reduced pressure, the same process repeats. The vapor generated by evaporation is converted into freshwater by condensation [21].

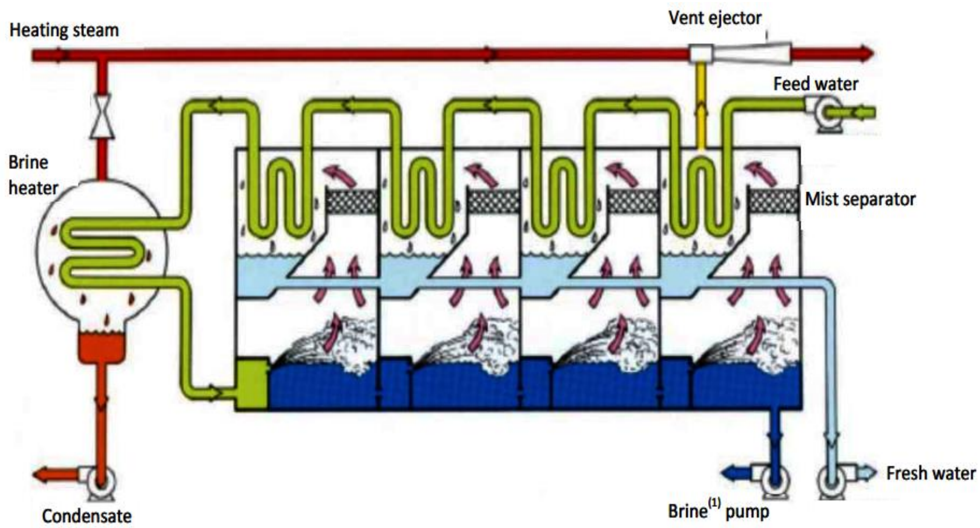


**Figure (2.6): The basic process of multi-stage flash evaporation [21].**

Note: Brine is the high salty solution after partial evaporation [21].

## 3- Multi-effect distillation (MED)

Similar to MSF, MED is an evaporation process going through a series of chambers (also known as "effects"), with each successive chamber operating at a progressively lower pressure. Yet MED differs from MSF in that the vapor formed in one chamber condenses in the next chamber with the heat released acting as a heating source. In addition, feed water is sprayed over the tube bundle on top of each chamber in a typical MED process. As shown in **Figure (2.7)**, external steam is introduced in the first chamber and feed water evaporates as it absorbs heat from the steam. The resulting vapor enters through the tube to the second chamber at reduced pressure. The heat released by condensation causes the feed water in the second chamber to evaporate partly. The process repeats in the third chamber and so on. In each chamber, the vapor condensing into freshwater inside the tube is then pumped out [21].

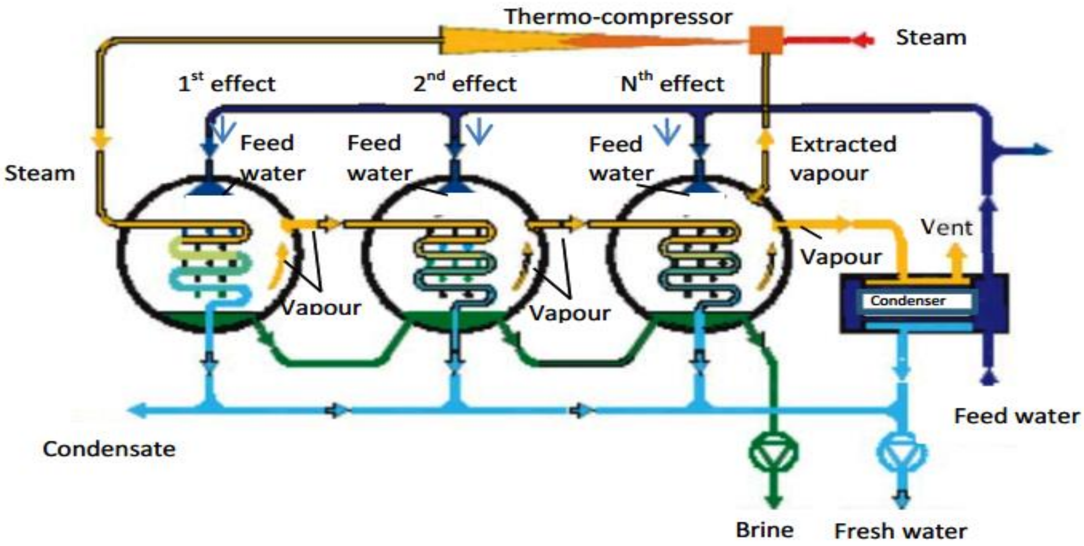


**Figure (2.7): The basic process of multi-effect distillation [21].**

Source: Research Office Legislative Council Secretariat, 2015.

A wide variety of additional desalination technologies exists, at varying stages of maturity. Electro-Dialysis (ED) has been in use for brackish water for decades. Membrane distillation, thermo-lytic forward osmosis, and humidification-dehumidification are in the early stages of industrial development, with advantages in important niche applications. None of these have been deployed for large-scale seawater desalination, and in most cases, the target applications are quite different; however, hybrid systems that combine two or more desalination technologies have the potential to increase water recovery and consequently reduce brine management costs or lower energy requirements per unit water production. Research in this area is quite active [19]. In the past decade, the dominance of RO over other desalination techniques has been due to its high scalability and relatively low energy requirement, neglecting the extra energy required for any additional treatment and the quality of this energy (**Figure (2.8)**).

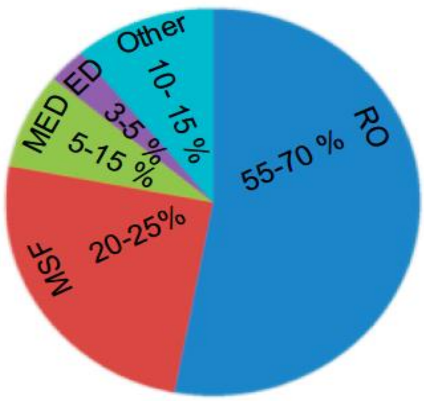


**Figure (2.8): Contribution of different techniques in the current water desalination market in 2019.**

Source: Ahmadvand. S., 2019.

## 2.6 Overview of Renewable Energy

Energy and freshwater production are heavily interconnected, termed the "water-energy nexus". The majority of the water on earth is in the oceans with high salinity and otherwise captured in the icecaps and glaciers, while most of the human energy usage (~90%) originates from fossil fuels. Water desalination is the manifestation of the water-energy nexus with all the strategic considerations regarding the availability of both of them (**Figure (2.9)**) [19].

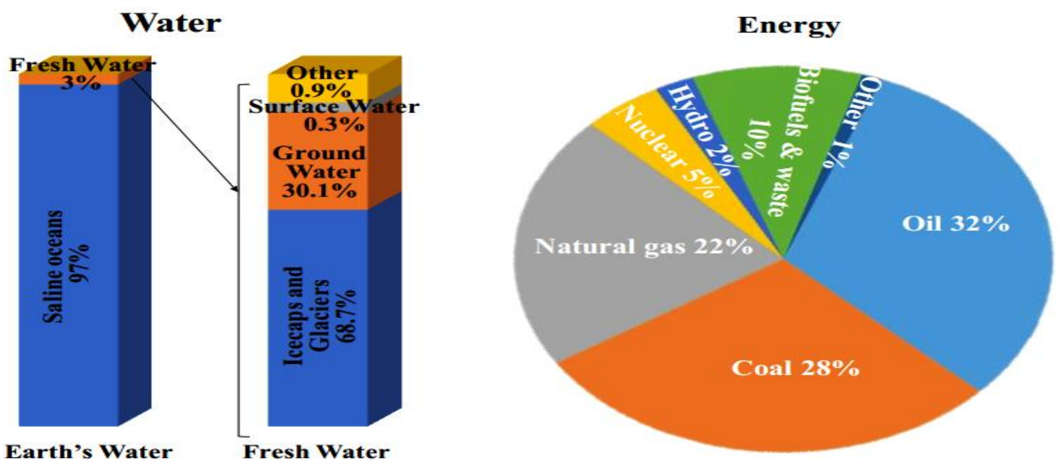


**Figure (2.9): Current availability of water and energy resources (2019) [19].**

Source: Ahmadvand. S., 2019.

Global atmospheric $CO_2$ levels have nearly doubled in the last 169 years and are predicted to double again in the next 100 years. An accompanying **The World Meteorological Organization** report on greenhouse gas concentrations shows that 2015-2019 has seen a continued increase in carbon dioxide ($CO_2$) levels and other key greenhouse gases in the atmosphere to new records, with $CO_2$ growth rates nearly 20% higher than the previous five years. $CO_2$ remains in the atmosphere for centuries and the ocean for even longer. Preliminary data from a subset of greenhouse gas observational sites for 2019 indicate that $CO_2$ global concentrations are on track to reach or even exceed 410 ppm by the end of 2019. This is causing a global temperature increase of more than 2 degrees Celsius above pre-industrial levels (see **Figure (2.10)**) and a significant sea-level rise caused by the melting of the polar ice caps [22].

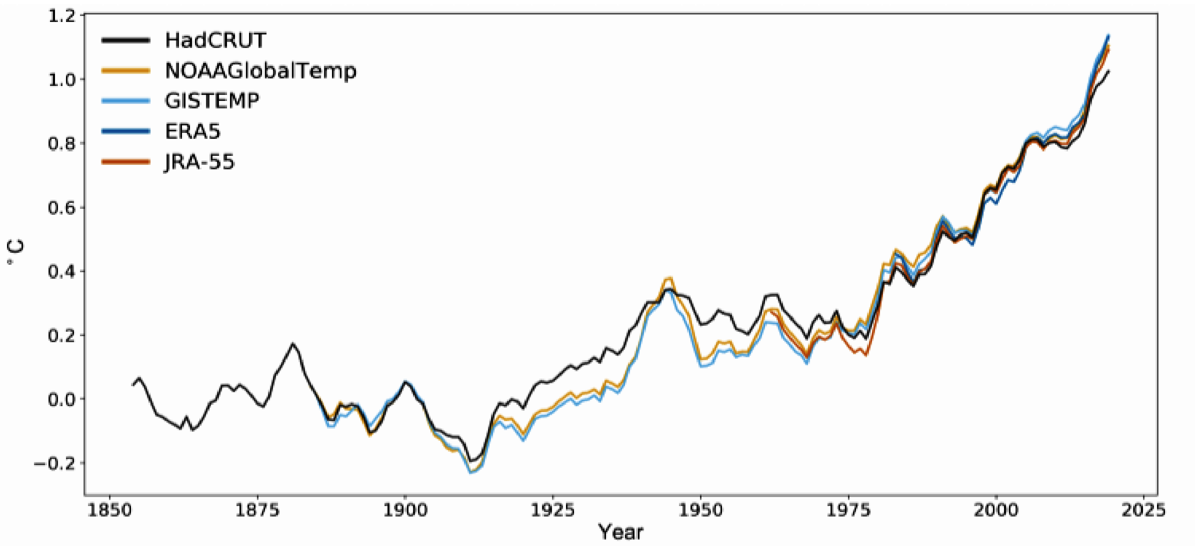


**Figure (2.10): Global mean temperature difference from 1850- 1900 (℃) (relative to pre-industrial) for five data sets: HadCRUR.4.6.0.0, NOAAGlobalTemp v5, GISTEMP v4, ERA5, and JRA-55 (2019) [22].**

Source: The World Meteorological Organization, 2019.

It is generally accepted that around 75% of the additional $CO_2$ has arisen from the combustion of fossil fuels (for the provision of electricity, heat, and transport) and the other 25% from human alteration of the land uses. Climate Change is recognized as the most serious and threatening global environmental problem. While natural variation in climate over time is normal, humans are contributing to climate change through the emission of substantial amounts of greenhouse gases. The resulting rise in the Earth's temperature contributes to man-made climate change. Renewable energy is energy that comes from natural resources such as wind, sunlight, ocean (waves and tide), and geothermal heat, which is naturally replenished. Each source has its characteristics that influence how and where they are used [24].

In this thesis, the main reasons for using renewable energy (Solar energy) to generate electrical energy are:

- It reduces reliance on fossil fuels, with taken economic conditions into consideration.
- It is considered to be a clean source of energy that can be harvested without damaging the environment; and
- Its sources are infinite and it can be continuously harnessed.
- Solar energy is the most readily applicable source of renewable energy to be integrated with desalination technology. It can produce the heat and electricity required by all desalination processes. Worldwide, various renewable energy sources are used for desalination, as illustrated in **Figure (2.11)** [25].

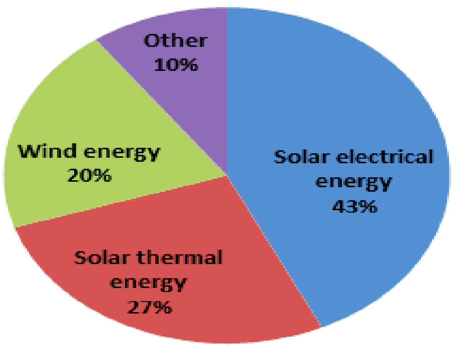


**Figure (2.11): Renewable energy sources for desalination worldwide (in %) in 2017 [25].**

Source: Olsson. G., 2018.

➧ A brief description of the most important renewable energy resources will be done as follows:

## 2.6.1 Biomass Energy

Biomass is a renewable energy resource derived from the carbonaceous waste of various human and natural activities. Biomass can be divided into four subcategories:

1. Wood, logging, and agricultural residue;
2. Solid industrial waste;
3. Animal dung;
4. Landfill biogas.

The potential of landfill gas is dependent on environmental considerations and waste management practices. The potential available for exploitation increases as a controlled landfill replaces other dumps and uncontrolled tipping. Biomass production requires land. The net energy production per hectare of various crops depends on climatic and soil conditions [26].

### 2.6.2 Wind Energy

Wind power is the conversion of wind energy into more useful forms, usually electricity using wind turbines. Most modern wind power is generated in the form of electricity by converting the rotation of turbine blades into electrical current by using an electrical generator [25].

### 2.6.3 Geothermal Energy

Geothermal power is generated wherever water comes in contact with hot rocks below the earth's surface. Geothermal energy plants generate electricity and heat by harnessing the heat energy contained within the earth. The earth transfers its energy to deep-lying circulating water, which the plants access with wells and pumps. Geothermal energy is attractive because it creates almost no environmental pollution. However, the number of sites where geothermal energy can be economically extracted is limited [27].

### 2.6.4 Hydropower

The history of using hydropower reaches back many centuries. Initially, watermills were used to convert hydropower into mechanical energy. Electricity generation from hydropower started at the end of the 19th century and has achieved technical sophistication. A weir creates a height (or 'potential') difference (also called a 'head') between the water before and after the weir. This potential difference can be utilized by a power plant. The water flows through a turbine, which transforms the potential energy into mechanical energy. An electric generator converts this into electricity [28].

### 2.6.5 Solar Energy

Solar radiation is available at any location on earth (see **Figure (2.12))**. The total world average power at the earth's surface in the form of solar radiation exceeds the total current energy consumption by 15,000 times, but its low density and geographical and time variations pose major challenges to its efficient utilization [26].

The solar source is generally assessed on the following criteria:

- Power density or irradiance.
- Angular distribution.
- Spectral distribution.

The maximum power density of sunlight on earth is approximately 1Kw/ $m^2$ irrespective of location. Solar radiation per unit of the area during a period is defined as energy density or insolation [26]. For many practical applications of solar energy, the absolute value of yearly insolation is less important than the differences in average monthly insolation values.

These differences vary greatly: from 25% close to the equator to a factor of 10 in the most northern and southern areas [26]. Since the average power density of solar radiation is 100-300 W/ $m^2$.

➡ Preliminary solar resource assessment will include the following:

- Clear sky seasonal solar irradiance data.
- Site insolation data for evaluating the economics of solar energy projects.
- Review of land or surfaces available for solar systems.
- Energy infrastructure, population density, geographical conditions review.
- Technical potential for solar project development.

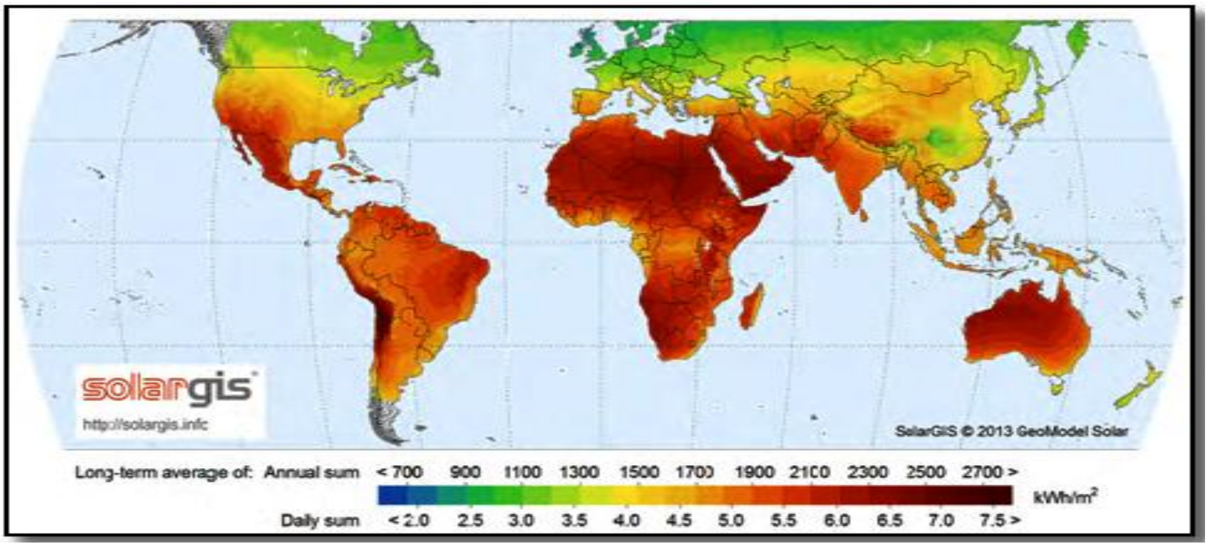


**Figure (2.12): Global insolation map (2014) [29].**

Source: Jäger. K., 2014.

- ## Solar Technologies

Solar Energy (SE) cost has fluctuated during the last decades. In the 1970s oil crises began which caused a resurgence of interest in other forms of energy such as solar. In the 1990s and especially in Japan and Germany, solar energy has been restored due to many factors, i.e. global warming and environmental awareness, availability of energy resources, and industrial countries' policy. The energy supply has been forecasted to the year 2100 as presented in **Figure (2.13)** [30].

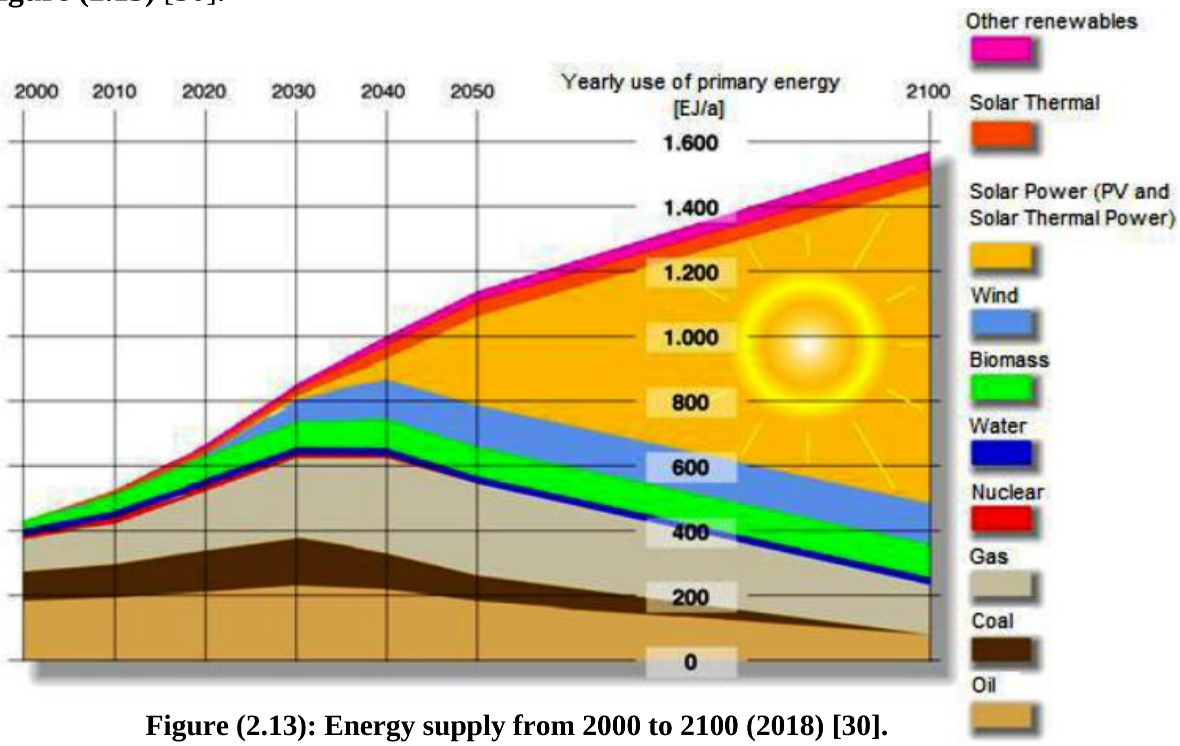


**Figure (2.13): Energy supply from 2000 to 2100 (2018) [30].**

Source: Alsumiri. M., 2018.

Until 2030, the global energy demand is expected to grow at a rate of 2.5%. Also, it has been estimated that this growth in electricity demand requires cumulative investments of 22 trillion United States dollars (USD) which means that approximately 1.1 trillion USD of investment is required per annum. The projected capacity of power generation is 4,800 GW by the end of 2030. Since one-third of the global greenhouse gas (GHG) emissions are produced by the power sector, it becomes necessary to direct these investments to renewable energy technologies [30]**.**

- The solar energy technologies can be categorized as follows**:**

**A. Solar thermal energy conversion is to convert solar radiation to:**

- **Water heating technologies**

Water heating represents huge energy consumption, especially in the winter season. Moreover, some applications such as swimming pools water heating consume high energy which needs further technology improvement [30]. The well-known main water heating technologies are**:**

**i. The Flat-Plate Collectors (FPC) technology**

The major component of a typical flat-plate collector system is a glazed dark-colored or particularly coated solar heat-absorber. A network of copper tubes is connected with the plate. The network of tubes is placed in a glazed glass-covered insulator box. The glazed glass is used to protect the collection panels from dust, moisture, and other contaminants. Also, by using glazed glass a greenhouse effect is provided which can minimize energy dissipation. When light radiation falls on it, water or glycol solution that is in the copper tubes is heated up by the absorption of thermal energy in the glass and tube. Then solar radiation can be converted into usable heat energy [30]**.**

**ii. Evacuated tubes collector (ETC) technology**

This technology is considered as the modification of the flat-plate technology. This type can be used in domestic applications. The main working part is the Evacuated tubes. The thermal energy of sunlight is absorbed then converted to heat that can be used in eating applications. Solar thermal collectors use quite a few types of evacuated tubes, i.e. "twin-glass tube", which is used by Apercus collectors. This type of tube is popular because of its many advantages like reliability, performance, and cost-effectiveness. **Figure (2.14)** shows the operation of evacuated tubes that contain dual glass tubes manufactured from extremely strong borosilicate glass. The outer tube is transparent and the inner tube is coated with an aluminum nitride coating. The sunlight is allowed to pass through the outer layer with negligible reflection and the light is collected by the inner tube. Hence, the reflection losses are minimized by improving the absorption of solar radiation which is achieved by using such arrangement of selective surfaces [30]**.**

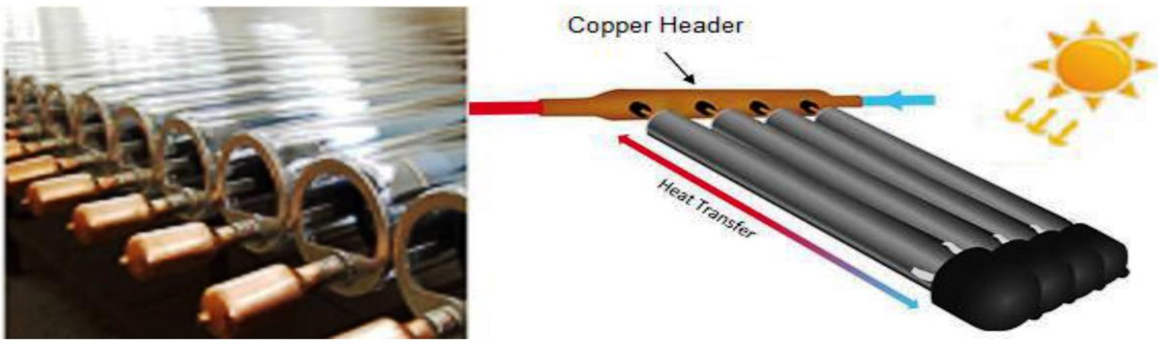


**Figure (2.14): Evacuated tubes [30].**

Source: Alsumiri. M., 2018.

Pumping out the air which is normally present between the glass layers and heating the top surface of the tube takes place during the process of manufacturing. This process allows the two tubes to fuse together in order to create a single evacuated tube without gases. The vacuum is formed by this evacuation process, which helps in improving the performance of the evacuated tubes. The vacuum prevents the leakage of heat energy between the tubes' layers, which means that there will be no exhausting energy. Solar radiation is absorbed and converted to heat by the evacuated tube. Moreover, the vacuum influences thermal insulation. As a result, the outer tube remains at a temperature just above the ambient temperature while the inner area of the tube reaches 150$^{o}$C. Based on the above, the performance of the evacuated tube water heaters is satisfactory even in cold weather, while the performance of the flat plate collectors is inadequate in these circumstances because of heat losses [30]**.**

- **Solar thermal electricity generation**

There are three different approaches for solar thermal electricity generation. All require sunlight to be collected and concentrated to provide a high-energy source. The first uses a parabolic trough-shaped mirror to focus the energy contained in sunlight onto an energy collector at the focus of the parabola (see **Figure (2.15)**). These parabolic trough solar units can bed employed in massive arrays to provide a large generating capacity (see **Figure (2.16)**) [27]. The second approach called a solar tower, employs a solar energy collector mounted atop a large tower. A field of a mirror is used to direct sunlight onto the collector where the concentrated heat is used in a power generation system (see **Figure (2.17)**). Both this and the parabolic trough system can be used to build utility-sized power plants. The third system, usually called the solar dish, comprises a parabolic dish with a solar heat engine mounted at its focus (see **Figure (2.18)**). Dishes are usually only 10–50 KW in capacity but can achieve high energy conversion efficiency. Fields of dishes are needed to produce a high-capacity power plant [27]. There is also a novel technique being explored in Australia called a solar chimney. This involves building a massive greenhouse, in the center of which is an extremely tall chimney. The chimney sucks hot air from the greenhouse, creating a massive updraft. Fans or turbines placed inside the chimney can capture energy from this updraft to generate electricity. It is estimated that 40 km$^2$ of greenhouse and a chimney 1000 m high will be needed to generate 200 KW [27]**.**

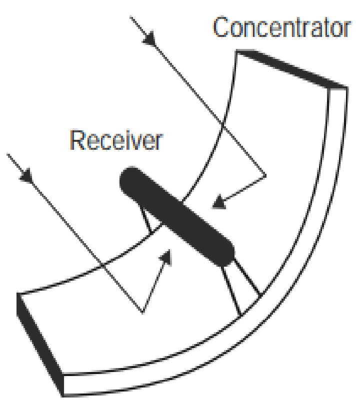


**Figure (2.15): A solar trough system [27].**

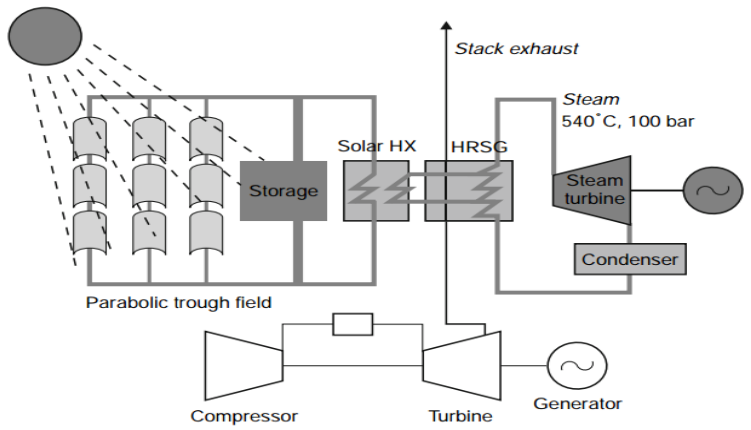


**Figure (2.16): An integrated-solar-thermal/ combined cycle power plant utilizing solar troughs [27].**

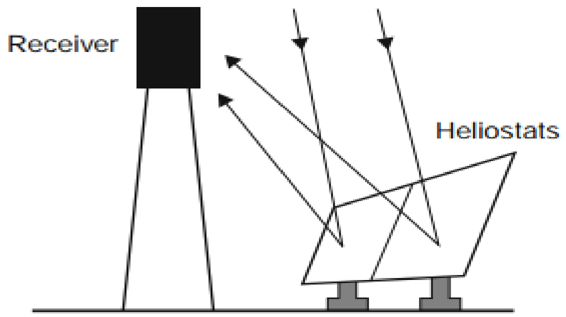


Figure (2.17): A solar tower system [27].

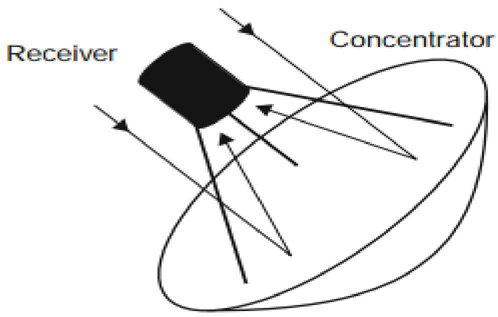


Figure 2.18 A solar dish [27].

## B. Photovoltaic applications

Photovoltaic (PV) devices or solar cells which means the direct conversion of solar irradiance to electricity (see **Figure (2.19)**) [29]. The efficiency of different technologies varies between (6% - 47.1%) for amorphous silicon-based solar cells with multiple-junction production cells (see **Figure (2.20)**) [31]. Currently, there is a wide range of PV cell technologies on the market. Depending mainly on the basic material used and their level of commercial maturity, PV cell technologies are usually classified into three generations as illustrated in **Figure (2.21)**; namely, first-generation, second-generation, and third-generation technologies [32]**.**

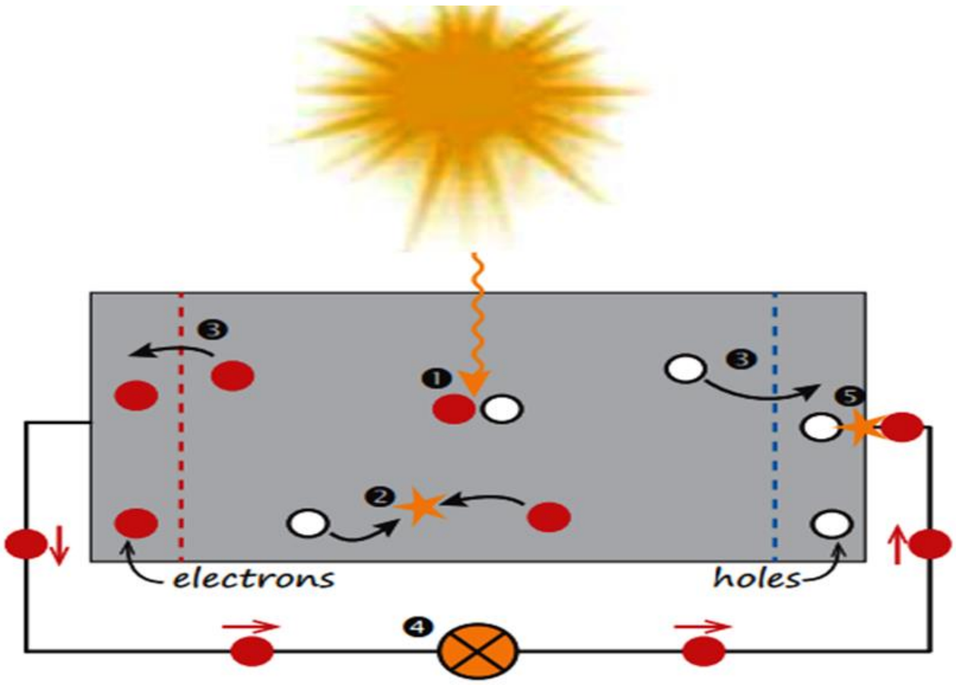


**Figure (2.19): A very simple solar cell model. ❶ The absorption of a photon leads to the generation of an electron-hole pair. ❷ Usually, the electrons and holes will combine. ❸ With semipermeable membranes, the electrons and the holes can be separated. ❹ The separated electrons can be used to drive an electric circuit. ❺ After the electrons passed through the circuit، they will recombine with holes [29].**

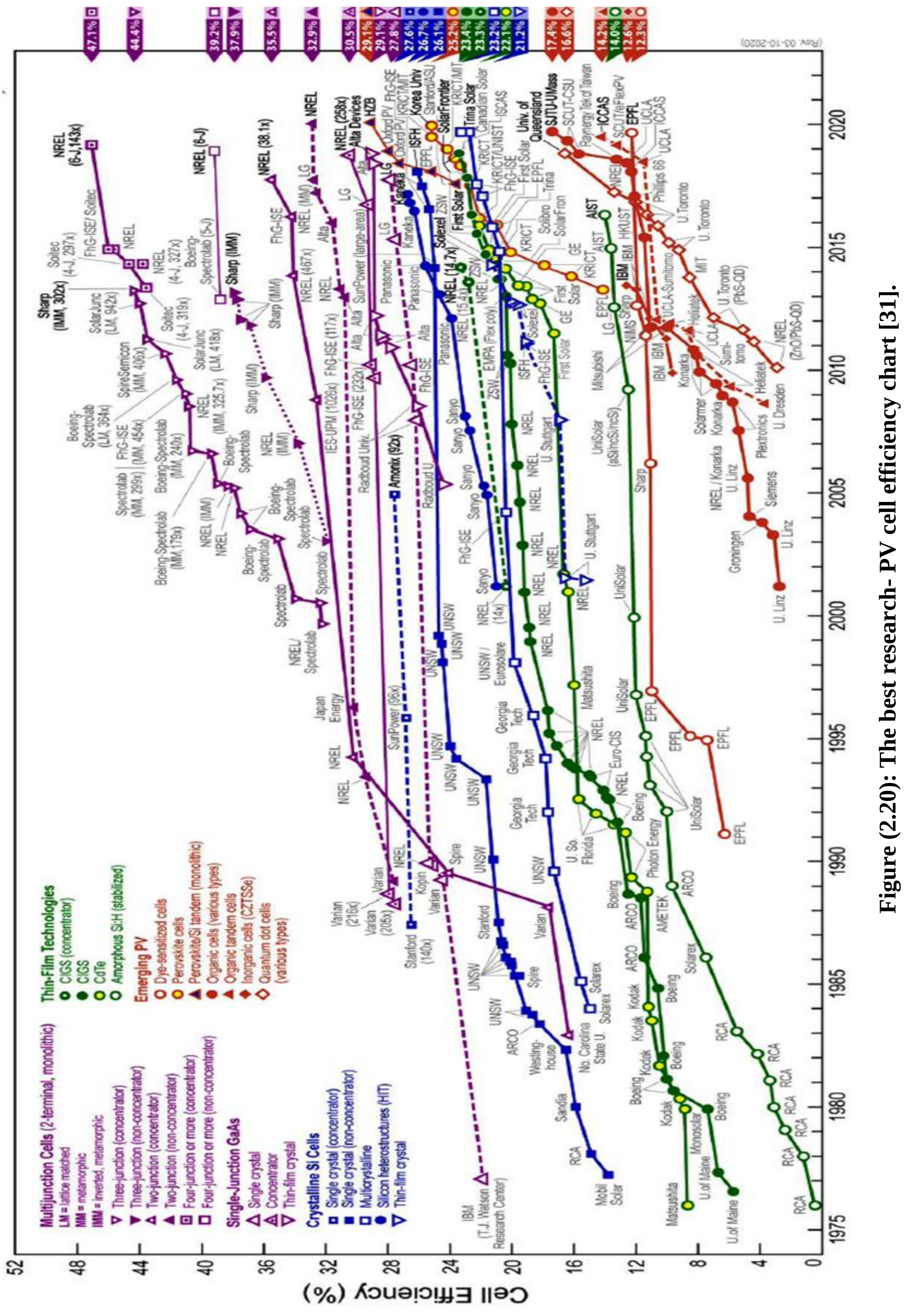


**Figure (2.20): The best research- PV cell efficiency chart [31].**

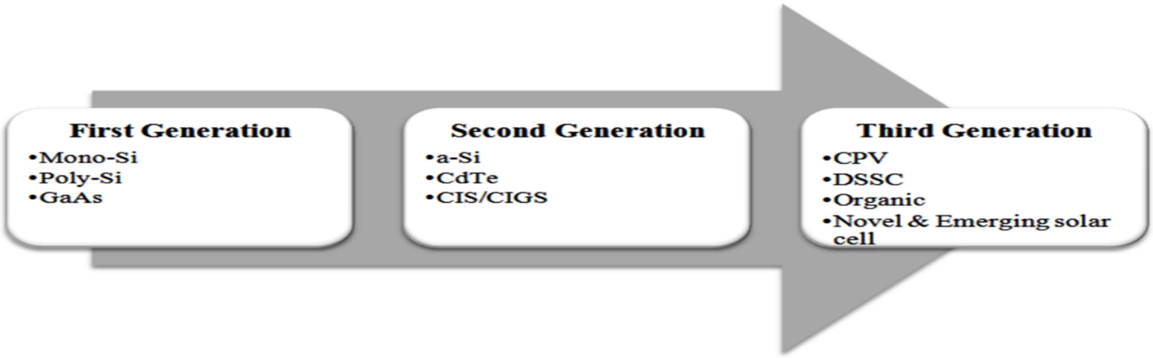


**Figure (2.21): PV cell technologies [32].**

The first practical use of solar cells was the generation of electricity on the orbiting satellite (Vanguard 1) in 1958. These first solar cells were made from single-crystal silicon wafers and had an efficiency of 6%. The space application was for some time the only application of solar cells. The mono-crystalline silicon wafer-based solar cells that had been used in space became also the first solar cells to be used for terrestrial generation of electricity. In order to increase the efficiency of mono-crystalline solar cells and to lower their price, crystalline silicon solar cell technology has improved dramatically in the past twenty years and today it is the dominant solar cell technology. Crystalline silicon solar cell technology represents today not only mono-crystalline silicon wafer-based solar cells but also poly-crystalline silicon solar cells.TheGaAs is a compound semiconductor form by Gallium (Ga) and Arsenic (As) that has a similar crystal structure as silicon. Compared to silicon-based solar cells, GaAs have higher efficiency and less thickness. all of these technologies are considered the first generation solar cells for terrestrial applications. As this technology has matured, costs have become increasingly dominated by material costs, namely those of the silicon wafer, the glass cover sheet, and encapsulants [32]**.**

In order to decrease the material costs of crystalline silicon solar cells, research has been directed to develop low-cost thin-film solar cells, which represent **second-generation solar cells** for terrestrial application[32]. Several semiconductor materials are potential candidates for thin-film solar cells, namely copper indium gallium diselenide (CuInGaSe2 = CIGS), cadmium telluride (CdTe), hydrogenated amorphous silicon (a-Si:H) thin-film polycrystalline silicon (f-Si). The titanium oxide nanocrystals covered with organic molecules represent so-called dye-sensitized nano-structured solar cells [32]. **The third-generation solar cells** are at the precommercial stage and vary from the technologies under the demonstration (e.g. multi-junction concentrating PV) to novel concepts that still require basic Research and development (R&D) activities. There are four types of third-generation PV technologies: Concentrating PV (CPV), Dye-sensitized solar cells (DSSC), Organic solar cells, and Novel and emerging solar cell concepts [32]**.**

## 2.7 Overview of the PV system components

In summary, a PV solar system consists of three parts**:**
i) PV modules or solar arrays**;**
ii) balance of system**;**
iii) electrical load [29]**.**

- The different components of a PV system are schematically presented in **Figure (2.22)** will be discussed as follows**:**

**i) PV modules or solar arrays:**

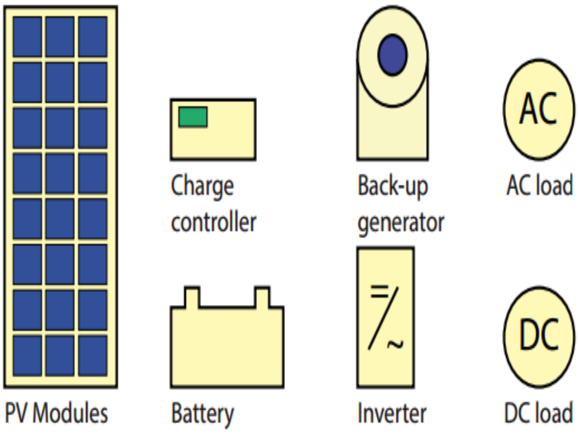


**Figure (2.22): A schematic of the different components of a PV system [29].**

As we have seen earlier in this section, a solar cell can convert the energy contained in the solar radiation into electrical energy. Due to the limited size of the solar cell, it only delivers a limited amount of power under fixed current-voltage conditions that are not practical for most applications. In order to use solar electricity for practical devices, which require a particular voltage and/ or current for their operation, a number of solar cells have to be connected together. **Figure (2.23(a)**) shows a crystalline solar cell. For the moment we will consider only modules that are made from this type of solar cell. A PV module is a larger device in which many solar cells are connected, as illustrated in **Figure (2.23(b))**. The names PV module and solar module are often used interchangeably. A solar panel, as illustrated in **Figure (2.23(c))**, consists of several PV modules that are electrically connected and mounted on a supporting structure. Finally, a PV array consists of several solar panels. An example of such an array is shown in **Figure (2.23(d))**. This array consists of two strings of two solar panels each, where string means that these panels are connected in series [29]**.**

- **Series and parallel connections in PV modules**

If we make a solar module out of an ensemble of solar cells, we can connect the solar cells in different ways: first, we can connect them in a series connection as shown in **Figure (2.24 (a and b))**. And the total current in a string of solar cells is equal to the current generated by one single solar cell. **Figure (2.24(d))** shows the I-V curve of solar cells connected in series. We can connect solar cells in parallel as illustrated in **Figure (2.24(c))** if cells are connected in parallel; the voltage is the same overall solar cells, while the currents of the solar cells add up [29]**.**

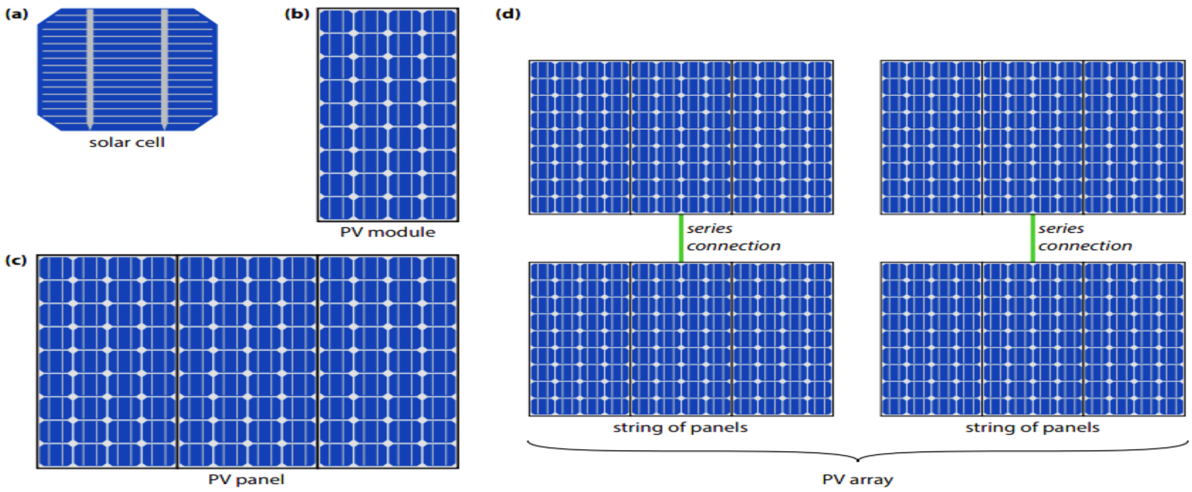


**Figure (2.23): The PV array structure [29].**

### The PV I-V Curve under Standard Test Conditions (STC)

**Figure 2.24(d)** shows a generic current-voltage (I-V) curve for a PV module, identifying several key parameters including the open-circuit voltage $V_{OC}$ and the short circuit current $I_{SC}$. Also shown is the product of voltage and current, that is, the power delivered by the module. The maximum power point (MPP) is that spot near the knee of the I-V curve at which the product of current and voltage reaches its maximum. Since PV I-V curves shift all around as the amount of insolation changes and as the temperature of the cells varies, STC has been established to enable fair comparisons of one module to another [33].

Those test conditions include a solar irradiance of 1 KW/ $m^2$ (1sun) with spectral distribution, corresponding to an air mass ratio of 1.5 (AM 1.5). The standard cell temperature for testing purposes is 25◦C (it is important to note that 25◦ is cell temperature, not ambient temperature). Manufacturers always provide performance data under these operating conditions [33].

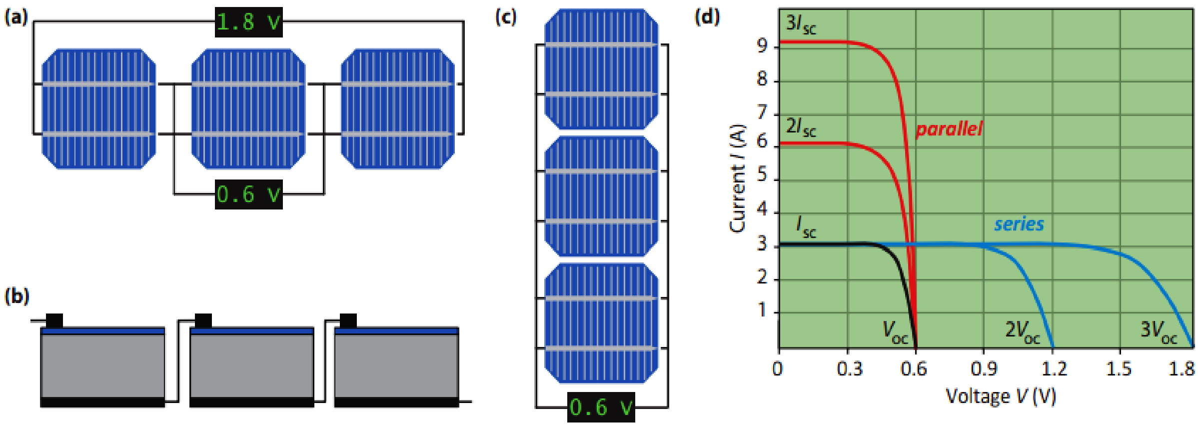


**Figure (2.24): Series and parallel connection of three solar cells [29].**

Source: Jäger. K., 2014.

### ii) Balance of System (BOS):

Although solar panels are the heart of a PV system, many other components are required for a working system, which we already discussed very briefly above. Together, these components are called the balance of system. Which components are required depends on whether the system is connected to the electricity grid or whether it is designed as a stand-alone system [29].

➡ The most important components belonging to the BOS are:

- **A mounting structure** is used to fix the modules and to direct them towards the sun **(Figure 2.25)**. It is divided into two types:

1- Fixed-array design, usually, PV modules are mounted using a fixed tilt installation structure, which keeps the tilt and azimuth angles unaltered [34].

2- Tracking systems-array design, tracking systems are the racks that allow the collector to track the movement of the sun across the sky are quite cost-effective [33].

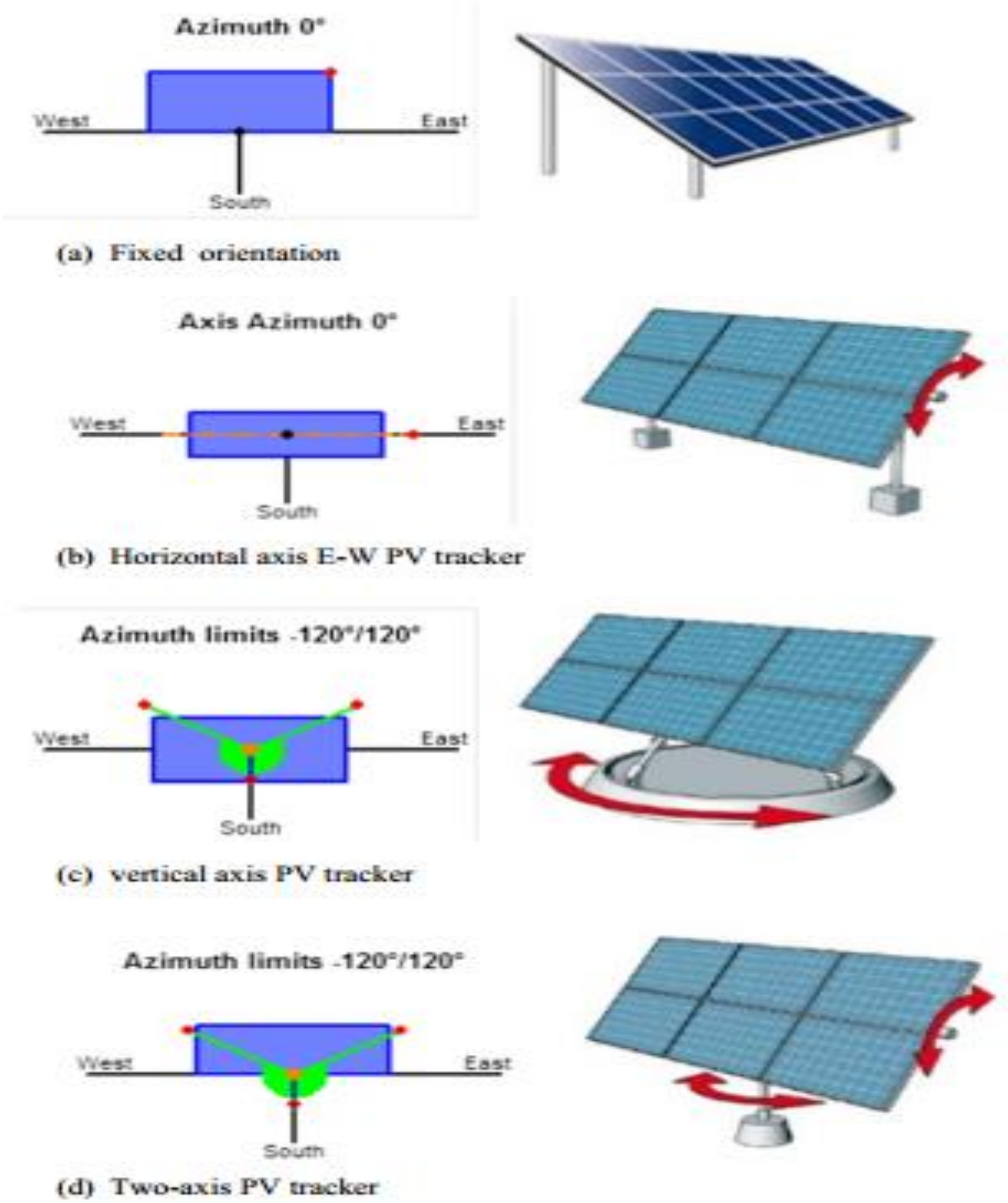


**Figure (2.25): Illustration of the PV tracker: (a) Fixed mounted orientation, (b) single-axis, horizontal axis E-W PV tracker, (c) single-axis vertical axis PV tracker, and (d) two-axis PV tracker (PVSyst 6.8.6 © software) [34].**

- **There are two types of sun trackers:**

  a. One-axis tracker, which tracks the sun at only one angle during the day [33].
  b. Two-axis tracker, which tracks the sun from east to west during the day, and from north to south during the seasons of the year. In this thesis the main reasons for using the two-axis tracker, which can increase the energy yield up to 40 percent over the year compared to the fixed-array design [34 and 35].

- **Energy storage** is a vital part of stand-alone systems because it assures that the system can deliver electricity during the night and in periods of bad weather. Usually, batteries are used as energy-storage units [29]**.**
- **DC-DC converters** are used to convert the module output, which will have a variable voltage depending on the time of the day and the weather conditions, to a fixed voltage output that e. g. can be used to charge a battery or that is used as input for an inverter in a grid-connected system [29]**.**
- **Inverters or DC-AC** converters are used in grid-connected systems to convert the DC electricity originating from the PV modules into AC electricity that can be fed into the electricity grid [29]**.**
- **Cables** are used to connect the different components of the PV system and to the electrical load [29]**.**

**iii) Electrical load**

Even though not a part of the PV system itself, the electric load, i.e. all the electric appliances that are connected to it have to be taken into account during the planning phase. Further, it has to be considered whether the loads are AC or DC loads [29]**.**

### Types of PV Systems

PV systems can be very simple, consisting of just a PV module and load, as in the direct powering of a water pump motor. As illustrated in **Figure (2.26 (a))**, this only needs to operate when the sun shines. However, when for example a whole house should be powered, the system must be operational day and night. It also may have to feed both AC and DC loads, have reserve power, and may even include a backup generator. Depending on the system configuration, we can distinguish three main types of PV systems: stand-alone, hybrid, and grid-connected. As illustrated in **Figure (2.26 (b, c, and d))**. The Large PV grid-connected fields act as power stations from that all the generated PV electricity is directly transported to the electricity grid. And this system is used in my thesis point. The basic PV system principles and elements remain the same. Systems are adapted to meet particular requirements by varying the type and quantity of the basic elements. Modular system design allows easy expansion when power demands change [29]**.**

## 2.8 Overview of Long-Term Population Forecasting

The design of the water supply and sanitation scheme is based on the projected population of a particular city, estimated for the design period. Any underestimated value will make the system inadequate for the purpose intended; similarly overestimated value will make it costly [36]**.**

The design population is estimated with all factors governing the future growth and development of the project area in the industrial, commercial, educational, social, and administrative spheres. The design of the water supply and sanitation scheme is based on the projected population of a particular city or town and also estimates the design period of the components of all structures of water supply and sanitation depends on the projection of the population. Changes in the population of the city over the years occur, and the system should be designed to take into account the population at the end of the design period [37 and 38]**.**

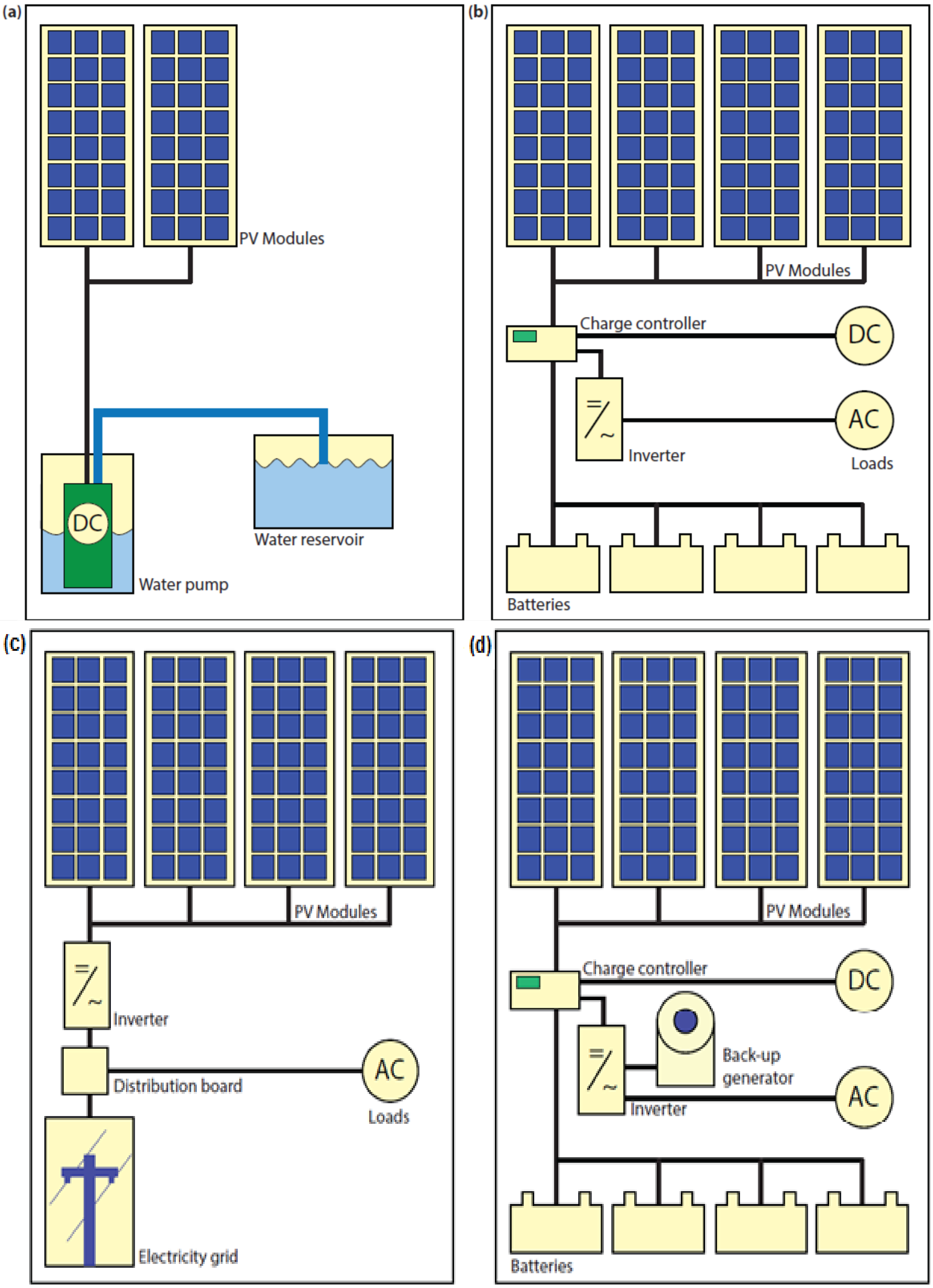


**Figure (2.26): Schematic representations of the different PV systems** [29]**.**

Source: Jäger. K., 2014.

Long-term population forecasting can be obtained by using conventional techniques such as the extrapolation of trend curves technique, the Box-Jenkins technique, the end-user technique … etc. Also, this forecasting can be obtained by using modern techniques such as genetic algorithm, artificial neural network, particle swarm optimization technique … etc. In order to obtain possible more accurate results, both conventional and modern techniques can be applied [36 - 39]. The techniques that will be used for long-term population forecasting in this report are reviewed as follows**:**

### 2.8.1 Long-term Population Forecasting by Using Conventional Technique

The conventional population forecasting technique uses a mathematical formula to fit successive values of the variables from which projections are made by extrapolation. This technique utilizes models based on the transformation of data, which are used for curve fitting. In practice, different techniques are used in combination to produce new and better long-term population forecasting results by applying many simple approximations, which are: linear, geometrical, and exponential equations … etc. In these approximations, the future population is predicted using the available past historical data [36, 37, and 39]**.**

Some of the standard analytical functions are used in trend curve fitting**:**

1. Extrapolation of trend curves using **Arithmetical progression method** or (**The linear approximation** )

$$P_t = a + bX_i \tag{2.1}$$

2. Extrapolation of trend curves using **Ethiopian statistical authority** or (**The exponential approximation**)

$$P_t = e^{a+bX_i} \tag{2.2}$$

where, $P_t$ = The forecasted population.

$$X_i = x_i - x_o \tag{2.3}$$

where, $x_i$ = The $i_{th}$ year in which the population $P_t$ is considered; $x_o$= The base year; *(a) and (b)* = The coefficients of the given functions**.**

Two simple approximations, which are linear and exponential analytical functions, are applied. The most common curve-fitting technique for finding the coefficients of linear and exponential analytical functions respectively in a given forecast is by the method of least squares. In regression-based models, the prediction error is minimized to zero by using the least-squares approach as given in the following equation**:**

$$S = \sum_{i=1}^{n} ( P_{t\,,real\,value} - P_{t\,,predicted} )^2 \tag{2.4}$$

where, *n* = The number of years; $P_{t\,,real\,value}$ = The existing recorded data; $P_{t\,,predicted}$ = The type of the analytical function used; *S* = the sum of the squared prediction errors**.**

In this method, the variable *S* is equalized to zero after being differentiated to each coefficient. In this way, the normal equations are attained. In the least-squares method, linear and exponential regression models are explained in detail below and used as $P_{t\,,predicted}$ in **Equation (2.4)** [36, 37, and 39]**.**

- **Population forecasting by using a linear regression model**

The linear population forecasting may be expressed by **Equation (2.1)**, in order to predict the population correctly; the sum of the squares of the errors should be minimal [36, 37, and 39]**.**

For *S* being minimal, the conditions are**:**

$$\frac{\partial S}{\partial a} = 0 \tag{2.5}$$

$$\frac{\partial S}{\partial b} = 0 \tag{2.6}$$

Applying **Equations (2.5 and 2.6)** on **Equation (2.4)**, the coefficients (a) and (b) are determined by the following equations**:**

$$a = \frac{1}{n}\sum_{i=1}^{n} P_{t\,(i)} \tag{2.7}$$

$$b = \sum_{i=1}^{n} P_{t\,(i)} X_i \Big/ \sum_{i=1}^{n} X_i^2 \tag{2.8}$$

- **Population forecasting by using the exponential regression model**

The exponential population forecasting may be expressed by the **Equation (2.2)**, in this equation, the estimation of coefficients (a) and (b) can be simplified by taking the natural log of the equation, as follows**:**

$$Ln\ P_{t\,(i)} = a + b\,X_i \tag{2.9}$$

$$Y_i = a + b\,X_i \tag{2.10}$$

where, $(Y_i = Ln\ P_{t\,(i)})$ (2.11)

Similarly, as a linear regression model, applying **Equations (2.5 and 2.6)** on **Equation (2.4)**, the coefficients (a) and (b) are determined by the following equations**:**

$$a = \frac{1}{n}\sum_{i=1}^{n} Y_i \tag{2.12}$$

$$b = \sum_{i=1}^{n} Yi\,Xi \Big/ \sum_{i=1}^{n} X_i^2 \tag{2.13}$$

where, *n* = The number of historical data years [36, 37, and 39]**.**

## 2.8.2 Long-term Population Forecasting by Using Modern Techniques

Modern techniques aim to find the optimum solutions to the optimization problems where the optimum solution may be either the least or the most. The prediction of the population is considered one of the optimization problems. Then, modern optimization techniques are applied. Two of these techniques will be applied, namely genetic algorithm and particle swarm optimization technique. The values of the coefficients (a) and (b), which are obtained by using the conventional technique, are used in these techniques to obtain the optimal values of them to get more accurate results of the population forecasting of the Burj Al-Arab city**.**

### 2.8.2.1 Genetic Algorithm (GA)

A GA is a numerical optimization method that employs a search process imitated from the mechanism of biological selection and biological genetics. They combine survival of the fittest among those feasible solutions in the form of string structures (or genes), and a randomized formation exchange to form a search algorithm. GA uses the binary representation, each solution or chromosome is sub-divided into genes, each gene consists of a binary string. The length of each gene string is not important to be the same [40 - 43]**.**

It depends on the lower and upper limits of the parameters. In every generation, a new set of string solutions is created from the fittest of the old string solutions set. While randomized they efficiently use historical information to speculate on new search points with expected improved performance. The control variables have to be represented as strings. During the search procedure, initially many solutions are randomized. Each solution string-fitness is computed. The higher fitness solution string has more probability to have more copies. This copying procedure is called selection. The crossover uses for innovating the solution strings while the mutation can help the solution strings to have a wider area of feasible solutions. **The Mutation** is also introduced as a technique to avoid being trapped in local optima and force diversity in the population in the final generations. These three genetic operations, namely, **Selection**, **Crossover**, and **Mutation** process the initial population of guesses, then the new generation solution strings exist, the processes of GA technique for a certain problem to obtain the optimal solution are shown in **Figure (2.27)**. These new generation solution strings start the genetic operations again and again till the feasible solution is satisfied [40 - 43]**.**

**Fitness function**

GA represents the survival of the fittest principle of nature to make a search process. Therefore, GA is usually suitable for solving maximization problems. Minimization problems are usually converted into maximization problems using some suitable transformation [41]. The fitness function *f(x)* for maximization problems can be used the same way as the objective function *F(x)* as follows**:**

$$f(x) = F(x) \tag{2.14}$$

The fitness function for the minimization problem can be obtained from the objective function using the following equation**:**

$$f(x) = \frac{1}{1 + F(x)} \tag{2.15}$$

In this thesis, GA is employed to find the optimal values of the coefficients and exponents (a) and (b) in **Equations (2.1 and 2.2)** that minimizes the absolute sum of the forecasting error (*R*) which is obtained from the following equation**:**

$$R = P_{t\,,real\,value} - P_{t\,,predicted} \tag{2.16}$$

From **Equation (2.15)**, the fitness function (Fit) is**:**

$$Fit = 1/\left(1 + k \sum_{i=1}^{n} |R|\right) \quad (2.17)$$

Where, $k$ is a scaling constant [41]**.**

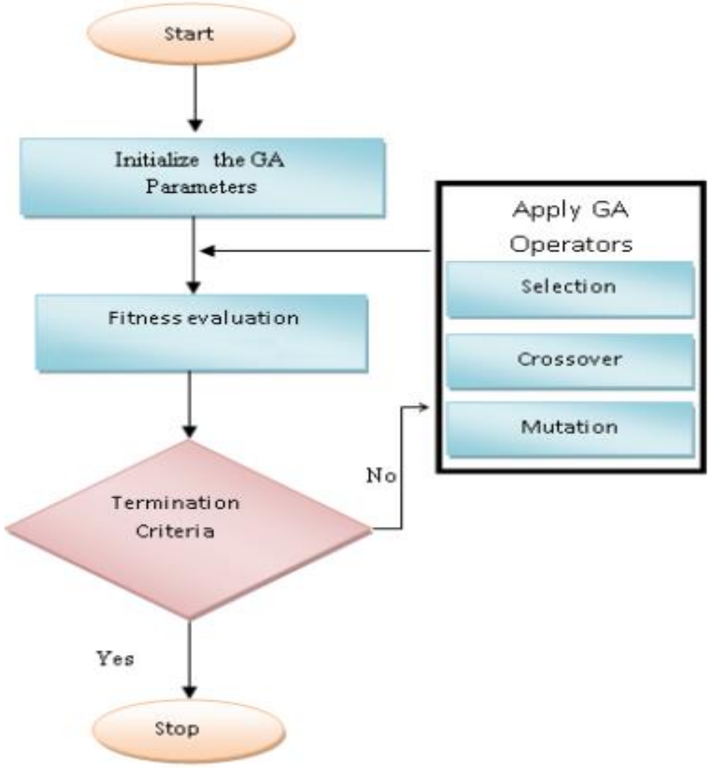


**Figure (2.27): Flow chart of GA [43].**

Source: Shabir. S., 2016**.**

### 2.8.2.2 Particle Swarm Optimization Technique (PSO)

A PSO algorithm is a kind of swarm intelligence (SI) technology, which was initially proposed by Eberhart and Kennedy in 1995. Inspired by birds flocking, the core concept of PSO is to find out the optimal or sub-optimal of an objective function through the cooperation and information sharing among particles. Since PSO is efficient, simple, and robust, it has been widely used in multi-objective optimization [43 - 50]**.**

The classic PSO starts with a population of random solutions 'particles' in a D-dimension space. The $i_{th}$ particle is represented by *Xi =(xi1, xi2, …,xiD).* Each particle keeps track of its coordinates in hyperspace, which are associated with the fittest solution it has achieved so far. The value of the fitness for the particle ($pbest_i$) is also stored as *Pi = (Pi1, Pi2, …, PiD).* The global version of the PSO keeps track of the overall best value ($gbest_i$) is also stored as *Pg = (Pg1, Pg2, …, PgD),* and its location, obtained thus far by any particle in the population. The PSO consists of, at each step, changing the velocity of each particle towards its $pbest_i$ and $gbest_i$ according to **Equation (2.18).** The velocity of particle i is represented as

*Vi = (vi1, vi2,…, viD)* [43 - 50]. Acceleration is weighted by a random term, with separate random numbers being generated for acceleration towards $pbest_i$ and $gbest_i$. **Figure (2.28)** shows the basic concept behind the PSO technique, the position of the $i_{th}$ particle is then updated according to the following equations**:**

$$v_{i,t+1}^{d} = wv_{i,t}^{d} + c_1\, r_1\left(P_{i,t}^{d} - x_{i,t}^{d}\right) + c_2\, r_2\left(P_{l,t}^{d} - x_{i,t}^{d}\right) \tag{2.18}$$

$$x_{i,t+1}^{d} = x_{i,t}^{d} + v_{i,t+1}^{d} \tag{2.19}$$

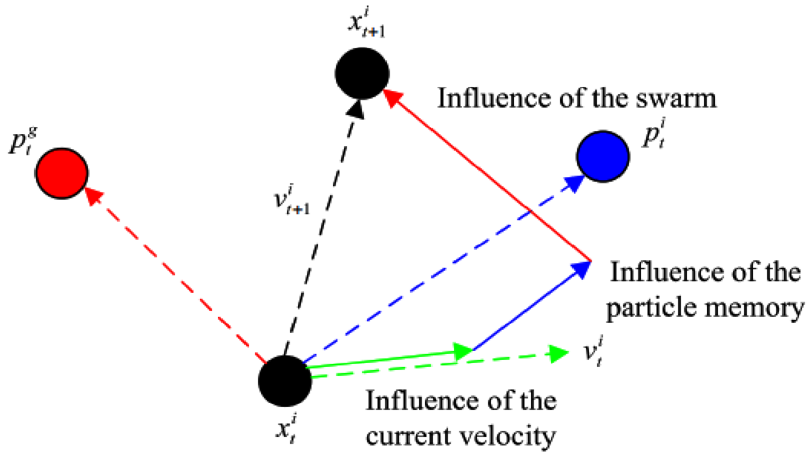


**Figure (2.28): Basic concepts of PSO technique [49].**

where $P_l$ was the optimal position in the local neighborhood; *w* is the particle's inertia weight, *c1* and *c2* are positive constants, called acceleration constants; *r1* and *r2* represent random numbers, following the uniform distribution over (0, 1)**.**

The inertia weight (*w*) is set during the learning according to the following equation**:**

$$w = w_{max} - \left[(w_{max} + w_{min})/\, iter_{max}\right] \times iter \tag{2.20}$$

In the above equation, $iter_{max}$ is the maximum number of iterations, $iter$ are the present iteration numbers, $w_{max}$, and $w_{min}$ are the maximum and minimum values of the inertia weight, respectively [43 - 50]**.**

For population forecasting problem the classic PSO is efficient to find out the optima of an objective function, In this thesis, the range of the search space for each variable can be determined according to the values of the coefficients (a) and (b) which are obtained from the conventional technique. The mentioned algorithms are run several times and then optimal results are selected, the processes of the PSO technique for a certain problem to obtain the optimal solution are shown in **Figure (2.29).**

**Fitness function**

The fitness function *f(x)* for this optimization problem can be used the same way as the objective function F(x) as shown in **Equation (2.14)**. In this thesis, the PSO technique is employed to find the optimal values of the coefficients (a) and (b) in **Equations (2.1 and 2.2)** that minimizes the absolute sum of the forecast error (R) which can be obtained from **Equation (2.17).**

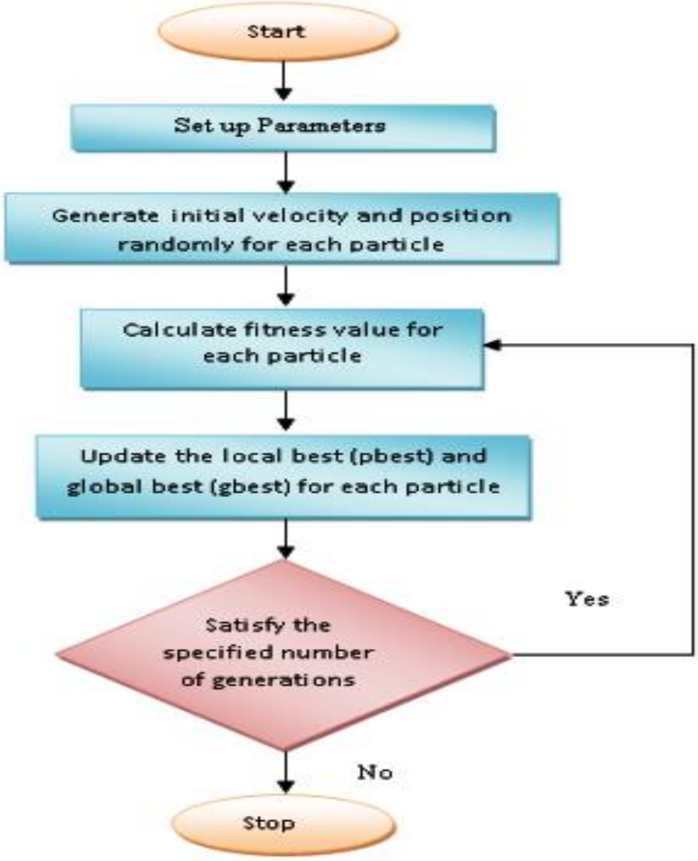


**Figure (2.29): Flow chart of PSO [43].**

# CHAPTER 3

# MATERIALS AND METHODS

# MATERIALS AND METHODS

## 3.1 Introduction

This chapter is devoted to specifying the steps and the methodology taken in carrying out the research endeavor. The current situation has been assessed of drinking water and wastewater facilities in the Burj Al Arab city, and weaknesses have been identified to develop solutions within the proposed strategic planning. In this chapter, several different techniques and software programs have been exposed to help in selecting optimal solutions**.**

As concluded from **Chapter (1)**, three PV-RO system configurations are suggested to cover expands of the Burj Al Arab city. A PV system and solar energy, in general, is a sustainable and an ideal energy source for a place with high solar resources like Egypt [29]. The PV energy system is the most readily applicable source of renewable energy to be integrated with RO desalination technology. Moreover, reverse osmosis is currently the cheapest and most appropriate desalination process in seawater. It will reduce the dependence on the Nile water as a source of freshwater [25]. For these reasons, in this chapter, the feasibility of PV-RO plants operating at the maximum attainable recovery rate (RR) is investigated in terms of their energy performance and life cycle unit water costs. The designs will be carried out according to the manufacturer‘s recommended specifications using a commercially available simulation tool (IMSDesign and PVsyst V6.86 software programs). The most important parameters, which determine the feasibility of PV-RO systems, are the Levelized Cost of Water (LCOW) of the entire plant. The basic data input for planning refers to**:**

- Water demand**;**
- RO plant size**;**
- PV potential of the selected region**.**

Results are provided for the**:**

- Annual energy flows**;**
- The price per cubic meter of water produced (LCOW), and**;**
- The investment cost for the entire unit**.**

The comparison and study of three representative utility scales, solar reverse osmosis desalination (PV-RO system) configurations taking into consideration. After the comparison, the best alternative will be selected as a second alternative source of Nile water. This is to supply the Burj Al Arab city with drinking water to cover future needs until the year of the target (2032). The sequence of the supposed strategic planning for drinking water projects is presented in **Figure (3.1).**

The methodology adopted for the research is illustrated as follows: There are five distinct components of the study, viz: Collecting the necessary data of drinking water and sanitation facilities; Long-term forecasting of the population increase is made of the Burj Al-Arab city until 2032; Estimation of the water demand and wastewater discharges of the new Burj Al-Arab city until 2032; The existing water and wastewater facilities will be evaluated, as well as the utilization of tertiary treated wastewater and reuse in the irrigation of green areas, according to environmental laws that govern it; The optimal strategic planning for drinking water projects will be made to strengthen existing facilities by using PV-RO plants. A detailed description of the individual components in the following sub-sections**.**

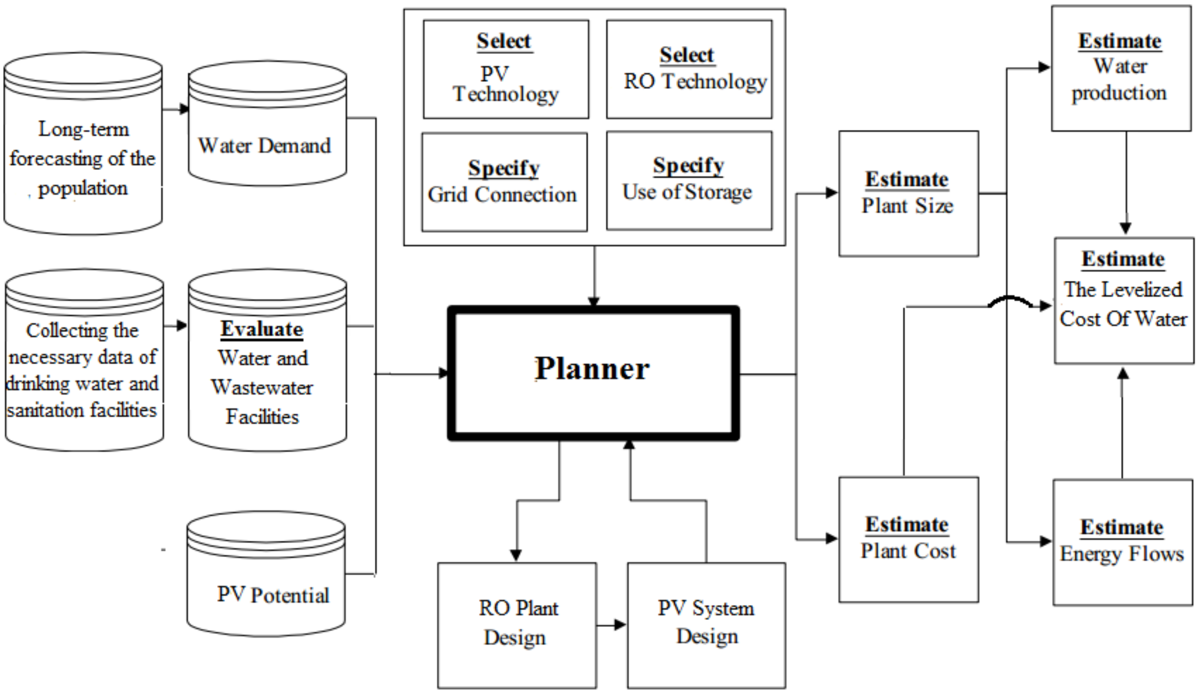


**Figure (3.1): The sequence of the supposed strategic planning for water and wastewater projects.**

## 3.2 Collect the Necessary Data and Reviewing Some Previous Studies of Drinking Water and Sanitation Facilities

**The following records and reports were reviewed to collect data:**

Annual records and reports from Sewerage company of Alexandria; The new Burj Al-Arab authority (Facilities management); and Water company of Alexandria. These reports regarding the current state of water and sewage system components in the Burj Al-Arab city were reviewed. As described in **Chapter (2)** and **Appendix (A)** [4, 5, and 6]**.**

## 3.3 Long-term Forecast of the Population Increase of Burj Al-Arab City until 2032

The current population is 140,000 residents in according to the last population census of 2017. Estimates of the historical data of the population of the new Burj Al-Arab city from 2011 to 2016 (according to the data of the facilities management of new Burj Al-Arab development authority data, that is by multiplying the actual occupancy rate of housing units by the average design number of residents per housing unit in each year) as shown in the following table**:**

**Table (3.1): The historical population data for the new Burj Al-Arab city [4 and 14].**

| Year | Population (thousands) | Year | Population (thousands) |
|---|---|---|---|
| 2011 | 68 | 2015 | 116 |
| 2012 | 80 | 2016 | 128 |
| 2013 | 92 | 2017 | 140 |
| 2014 | 104 | | |

After collecting these population figures, the population at the end of the design period is predicted using various methods as suitable for that city considering the growth pattern followed by the city [37]. Long-term population forecasting can be obtained by using two methods (linear, exponential) that are specified in the Egyptian code for the implementation of drinking water and wastewater projects. Long-term population forecasting can be calculated by using three techniques: extrapolation of trend curves, genetic algorithm (GA), and particle swarm optimization technique (PSO) [38]. In order to obtain possible more accurate results, both conventional and modern techniques can be applied in the MATLAB software program to get the long-term forecasting of the population growth of the Burj Al-Arab city until 2032. The best results will be selected. So, the planning is more realistic to estimate the water demand for residential areas in addition to estimating the water demand for all other uses in the city**.**

## 3.4 Estimating the Water Demand and Wastewater Discharges

In this section, the water demands and wastewater discharges will be estimated for all uses. This is done by using the forecasted population census and the general plan for urban and industrial development in Burj Al-Arab city. The laws and consumption rates concerning the estimation of water demand and wastewater discharges stipulated in the Egyptian code will be applying for the design and implementation of drinking water and sanitation projects. Detailed descriptions of the individual components (water demands and wastewater discharges which will be estimated) are described in the following sub-sections**.**

### 3.4.1 Estimating the Water Demand

In this sub-section, the forecasted population census and the general plan for urban and industrial development in Burj Al-Arab city (that mentioned in **Appendix (A) - Tables (A.3 - A.9**) will be used. In addition to applying the laws and consumption rates concerning the estimation of water demand stipulated in the Egyptian code for the design and implementation of drinking water and sanitation projects (as shown in **Table (3.2)**). This is to estimate the water demand for all uses that mentioned as follows**:**

1- The water demand of residential areas**;**
2- The water demand of industrial areas**;**
3- The water demand of construction works**;**
4- The water demand of swimming pools and lakes**;**
5- The water demand of the tourism sector and entertainment**;**
6- The water demand of the regions of universities and research centers**;**
7- The water demand of hospitals and medical centers**.**

### 3.4.2 Estimating the Wastewater Discharges

The wastewater facilities will be evaluated, as well as the utilization of tertiary treated wastewater and reuse in the irrigation of green areas in accordance with the environmental laws that govern it. This evaluates based on calculating the quantities of domestic wastewater discharges and industrial wastewater. Then, will compare them with the design capacities of the proposed lifting and treatment plants to ensure their capacity to accommodate future discharges. This will be done in the next chapter**.**

In this sub-section the forecasted population census and the general plan for urban and industrial development in Burj Al-Arab city (that mentioned in **Appendix (A) - Tables (A.3 - A.9**) will be used. In addition to applying the laws and consumption rates concerning the estimation of water demand stipulated in the Egyptian code for the design and implementation of drinking water and sanitation projects (as shown in **Table (3.2)**). This is to estimate the wastewater discharges for all uses that mentioned as follows**:**

The wastewater discharges in the new city of Burj Al Arab will be estimated in parts. So that the amount of wastewater that reaches each treatment plant is estimated separately. This is for facilitating the evaluation process for each station separately. The estimation process will be divided as follows**:**

- First, estimate the amounts of domestic wastewater that will be treated in the western tertiary treatment plant**.**
- Second, estimate the amounts of industrial wastewater that will be divided into two parts**:**

a) Estimation of the amount of industrial wastewater that will be treated in the proposed western industrial wastewater treatment plant**.**

b) Estimating the amount of industrial wastewater that will be treated in the eastern industrial wastewater treatment plant**.**

**Table (3.2): The design standards are used for drinking water and drainage projects [51 and 52].**

| No | Parameter | Designed criteria |
|---|---|---|
| 1 | The consumption rate for residential areas | 280 liters/ person/ day |
| 2 | The consumption rate for Sporting Clubs District | 50 liters/ person/ day |
| 3 | The consumption rate for the tourist resort hotel | 50 liters/ person/ day |
| 4 | The consumption rate for the Galleries and conference | 5 $m^3$/ hectare/ day |
| 5 | The consumption rate for parks | 50 liters/ person/ day |
| 6 | The consumption rate for hospitals and medical centers | 500 liters/ bed/ day |
| 7 | The consumption rate for universities and research centers | 50 liters/ person/ day |
| 8 | The consumption rate for swimming pools and lakes | 1500 $m^3$/ hectare/ day |
| 9 | The consumption rate for construction works | 62 $m^3$/ day per hectare development annually. |
| 10 | The consumption rate for the industrial zones | 1 L/ sec/ hectare |
| 11 | The consumption rate for storage areas | 5 $m^3$/ hectare/ day |
| 12 | The consumption rate for the logistics area, customs department, dry port, and free zone | 5 $m^3$/ hectare/ day |

**Table (3.2): The design standards are used for drinking water and drainage projects [51 and 52].**

| No | Parameter | Designed criteria |
|---|---|---|
| 13 | The economically designed velocity of pipes | Ranges between (1 - 2) m/ s |
| 14 | Maximum monthly consumption | 1.3 × Average daily housing consumption + the needs for the tourism sector and entertainment + the water needs for hospitals and medical centers + the water needs of the regions of universities and research centers + the water needs of construction works + the water needs of swimming pools and lakes + the needs for water for industrial use. This rate is used to determine the design capacity of the stations. |
| 15 | Maximum daily consumption | 1.5 × Average daily housing consumption + the needs for the tourism sector and entertainment + the water needs for hospitals and medical centers + the water needs of the regions of universities and research centers + the water needs of construction works + the water needs of swimming pools and lakes + the needs for water for industrial use. This rate is used to determine the design capacity of storage works, main water lines, and sub-lines. |
| 16 | Groundwater storage tanks capacity | Maximum daily consumption (maximum monthly consumption) + 80 % of fire requirements |
| 17 | Force main | Maximum daily discharge + fire discharge |
| 18 | Average wastewater flow | Estimated at 80 % of average daily water consumption |
| 19 | Maximum design sanitation discharges (for calculating the capacity of lift stations) | Peak factor (PF) × average wastewater flow + other flows including the flows of the prison and industries activities + rain flows |
| 20 | PF (The peak factor) | $PF = 1 + 14/(4 + \sqrt{POP})$ When POP > 8000 capita<br>$PF = 5/POP^{0.167}$ When POP ≤ 8000 capita<br>POP = population in thousands. |

**Notes:**

**[1]** Water leachate: Due to the location of the city in a desert area the groundwater is deep, and the value of the leachate that has reached the sewerage network has been neglected [4].

**[2]** Rainwater: It will be assumed that the amount of rainwater reaching the network is equivalent to about 15% of the average consumption amount.

## 3.5 The Reverse Osmosis Systems Coupled to the Solar Photo-voltaic Panels to Desalinate Water Systems (PV-RO Systems)

In the presence of overpopulation in Egypt in the last decades, it was necessary to establish and expand new cities to accommodate this overcrowding. Hence, these new cities need water, where the Nile water budget is $55.5x10^9$ $m^3$/ year in Egypt and this budget is fixed. So the only option needed to manage our resources efficiently is by searching and developing other resources than the Nile water. So, the solar photovoltaic panels coupled to reverse osmosis desalinate water Systems (PV-RO Systems) may be a good suggested option in this thesis [2].

Within the framework of this thesis, a simplified approach has been elaborated, which allows a quick but relatively precise assessment of the investment as well as of the operational cost of the three PV-RO systems configurations included in this thesis. Also, the results will show the sensitivity of the Levelised Cost of Water (LCOW) as a function of selected key parameters. After this analysis and comparison, the best alternative will be selected. This is to cover the increase in the demand for potable water due to the forecasted increase of the population and the various activities in the new city of Burj Al-Arab until the year of the target (2032). Details of the individual system components are provided below.

- **The three suggested PV-RO plant configurations are as follows:**

**A-** PV-RO system with PV solar only**:** in this case, the solar photovoltaic (PV) power station is the only electricity source for the reverse osmosis (RO) desalination plant. Accordingly, the operation of the RO desalination plant is intermittent (see **Figure (3.2)**).

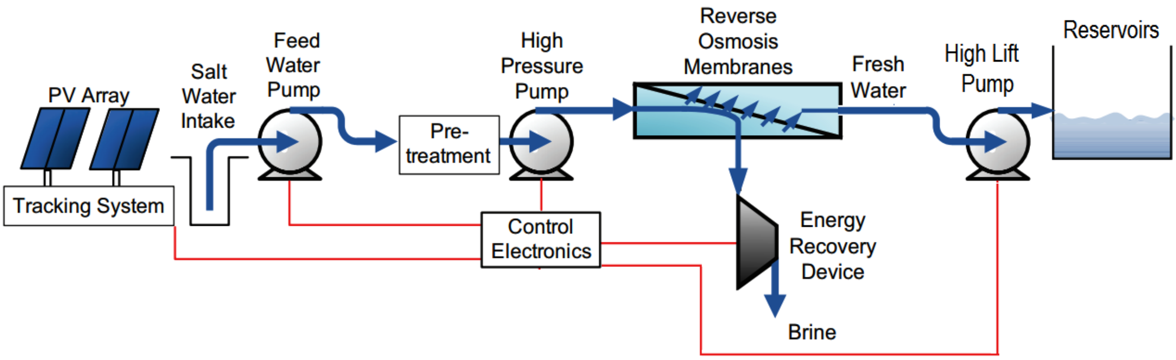


**Figure (3.2): Schematic representations of PV-RO system with PV solar panels only.**

**B-** PV-RO system with PV solar and batteries**:** the RO operation time is extended by batteries with three full load hour capacity. Accordingly, the operation of the RO desalination plant is intermittent (see **Figure (3.3)**).

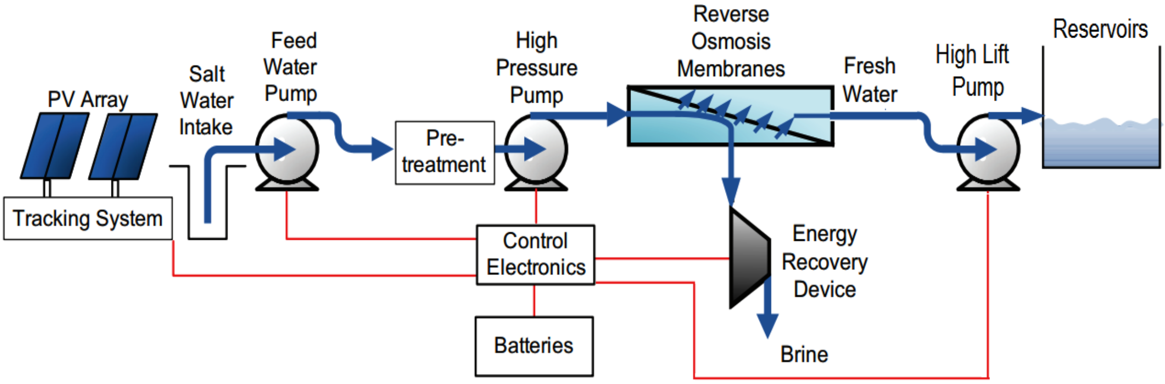


**Figure (3.3): Schematic representations of PV-RO system with PV solar panels and batteries.**

**C-** PV-RO system with PV solar and electricity grid**:** The PV is designed in order to cover the electricity requirements of the RO plant. The continuous operation of the RO desalination plant is guaranteed by the backup electricity is provided by the grid (see **Figure (3.4)).**

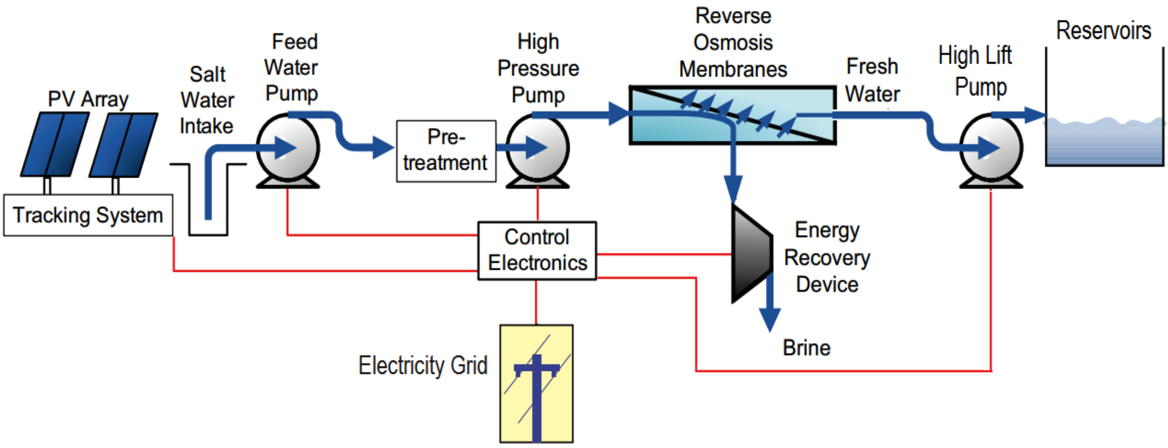


**Figure (3.4): Schematic representations of PV-RO system with PV solar panels and electricity grid.**

In these PV-RO systems, the control electronics direct power from the PV panels, the batteries, and the electricity grid to the pumps to pressurize the incoming water. The water is driven through the reverse osmosis membrane array by the high pressure, producing high salt concentration brine on the pressured side and freshwater on the low-pressure side at the end of the array. The high-pressure brine passes through an energy recovery device, such as a pressure exchanger or turbine, to recover the useful energy in the brine before it exits the system [58]**.**

## 3.5.1 The (PV- RO) System Design Calculations

In the following paragraphs, the fundamental principles of the design process will be given. The following steps are guidelines to design a reverse osmosis plant coupled to PV panels [55]**.**

**Step 1: Determine the product volume requirement**

First of all, a good evaluation should be carried out to determine the customer's water requirements**.**

$$F_{Total} = maximum\ monthly\ discharge\ +\ 7\ \% \tag{3.1}$$

where, $F_{Total}$ = Total amount of product water to be produced by membranes ($m^3$/ d) [52]**.**

**Step 2: Determine the characteristics of the feed water and maximum water recovery possible during desalination**

The design calculations presented down here are based on seawater analysis of Egypt offshore. The most important required chemical components for plant design are shown in **Table (3.3)**. Elements will be calculated according to the needs of feed water capacity, feed water salinity, feed water fouling tendency, required productivity, and salt rejection, as well as energy requirements and IMSDesign software, which will be used to help design and give the information required for the RO designed systems. This software is available on (The Website of Hydranautics Company) [53]**.**

**Table (3.3): Seawater analysis (Sidikerir Region, west of Alexandria, Egypt offshore sample during the summer season with water temperature 25(°C)) [17 and 54].**

| | | | |
|---|---|---|---|
| PH | 8 | $CO_3$ | 18.9 mg/ l |
| Cations | mg/ l | Anions | mg/ l |
| Ca | 463 | $HCO_3$ | 163 |
| Mg | 1367 | $SO_4$ | 2915 |
| Na | 11600 | Cl | 21045 |
| K | 419 | F | 0 |
| $NH_4$ | 540 | $NO_3$ | 750 |
| Ba | 0 | $PO_4$ | 0 |
| Sr | 0 | $SiO_2$ | 2 |
| TDS | 39284 | B | 0 |

The quality of the feed water gives an estimation of the maximum recovery ratio (RR) a RO plant can achieve. Membrane fouling is the limiting factor for the recovery ratio due to scaling. At the critical recovery ratio, crystal formation in the brine stream would appear due to the saturation point of the salt. RO plants should never be operated above this critical recovery ratio. **Table (3.4)** gives some guidance to the recovery ratio (water recovery) of seawater [56]**.**

**Product water target salinity**

- While water with salinities up to 1,000 mg/ l is suitable for drinking [15]**.**
- In this thesis, the product water salinity is targeted to be in the range of 500 mg/ l to increase water acceptability by the population. Moreover, water with 500 mg/ l salinity is suitable for irrigating almost all crops without yield losses [18]**.**

**Table (3.4): Typical RO plant concentrates quality [56].**

| Parameter | Seawater |
|---|---|
| Feed TDS, mg/ L | 30,000 - 40,000 |
| Water recovery, % of feed | 40 - 60 |
| Concentrate quantity, % of feed | 40 - 60 |
| Concentrate TDS, mg/ L | 60,000 - 80,000 |

- **Note:** Seawater recovery ratio**:** 40% < RR>60 % (Taken ~ 40%)**.**

➧ **Step 3: Consider pre-treatment requirements**

Seawater pretreatment is a key component of every membrane desalination plant. The main purpose of the pretreatment system is to remove particulate, colloidal, organic, mineral, and microbiological contaminants contained in the source seawater and to prevent their accumulation on the downstream seawater reverse osmosis (SWRO) membranes (i.e., to protect the membranes from fouling). The content and nature of foul-ants contained in the source seawater depend on the type and location of the desalination plant intake [57]. A pre-treatment system requires additional water for maintenance purposes such as backwash, etc. Therefore the feed pumps must supply an additional volume of water for the pre-treatment system and not only for the RO membranes. **Equation (3.2)** will give the total water supply per day (to be provided by the feed pumps) [52 and 56]**.**

$$F_{Total\ (Feed)} = \frac{maximum\ monthly\ discharge + 7\ \%}{RR} \tag{3.2}$$

where, $F_{Total\ (Feed)}$ = Total water amount to be supplied ($m^3$/ d); $RR$ = Maximum recovery ratio allowed, obtained from **Step 2.**

**Step 4: Consider post-treatment and brine discharge**

Both the product and brine water need to be treated before it can be used or discharged back into the sea**.**

- **Product water treatment:**

The product water needs to be stabilized and disinfected before it can be used. For disinfection purposes, chlorine is normally added together with ultraviolet light. It is mainly done for the prevention of biological growth in pipelines and reservoirs. Furthermore, a desalination plant can easily remove the carbonate, calcium, and magnesium from the water which makes it corrosive. Therefore the product water needs to be stabilized before it can be used as drinking water [56]**.**

- **Brine discharge:**

In this step, the designer must understand that discharge of high saline brine water to the environment can have a significant negative impact on the fauna and flora. Again, experts need to address this important issue and assess the discharge method. There are mainly two options for the discharging method, namely to use an evaporation pond or to discharge the brine back into the feed water source (e.g. the sea). Evaporation ponds can only be used in small RO applications but will have an extra cost. In this is a case where the brine water is returned to the feed water source (e.g. the sea), currents, marine life, the inflow of large rivers, etc. must be considered during the design. On the microscopic level measurements such as the colloidal, organic and biological amounts are important and must be monitored by specialists [56]**.**

**Step 5: Calculate the feed pressure requirement and the number of membranes required**

**a) High-pressure feed pump**

The selection of the high-pressure pump (HPP) with energy recovery devices (ERD) depends on the minimum and maximum flow rates, discharge pressure required, suction pressure available, and the maximum temperature, where these parameters can be obtained from the IMSDesign detailed report**.**

**b) The reverse osmosis membrane system**

The key components of the RO separation system include filter effluent transfer pumps, high-pressure pumps, reverse osmosis trains, energy recovery equipment, and the membrane cleaning system. The following steps were used to design the membrane assembly of the SWRO desalination plant [58]**.**

- **Selection of membrane element type**

Elements will be selected according to feed water salinity, feed water fouling tendency, required productivity, and salt rejection, as well as energy requirements, where the membrane will be selected for the designed plant, is SWC6 and IMSDesign software. **Table (3.5)** lists all the specifications of SWC6 MAX membranes**.**

- **Selection of average membrane flux**

The flux design selection depends on experimental data, an experience where the typical membrane design fluxes based on the feed supply. The (Maximum) recommended design flux for this plant is **13.5 l/ m²-h** [58].

**Table (3.5): Membrane specifications (SWC6 MAX) [53].**

| **Performance** | |
|---|---|
| Permeate flow | 50 $m^3$/ d |
| Salt rejection | 99.8% (99.7 % min) |
| Applied pressure | 55 bar |
| **Type** | |
| Configuration | Spiral Wound |
| Membrane polymer | Composite Polyamide |
| Membrane active Area | 40.8 $m^2$ |
| **Application data** | |
| Maximum applied pressure | 83 bar |
| Maximum chlorine concentration | < 0.1 ppm |
| Maximum operating temperature | 45 $^oC$ |
| (pH) Range, continuous (Cleaning) | 2-11 |
| Maximum feed water turbidity | 1.0 NTU |
| Maximum feed water SDI (15 mints) | 5 |
| Maximum feed flow | 17.0 $m^3$/ h |
| Minimum ratio of concentrate to permeate flow for any element | 5:1 |
| Maximum pressure drop for each element | 15 psi |

- **Number of elements needed**

The number of elements ($N_E$) can be calculated using **Equation (3.3)** by dividing the design permeates flow rate ($Q_P$) by the design flux ($S_E$) and by the membrane active area ($ff$) of the chosen element ($ft^2$ or $m^2$) [58].

$$N_E = \frac{Q_P}{ff.\ S_E} \tag{3.3}$$

- **Number of pressure vessels needed**

For this plant, 6-element vessels will be used, so, the number of pressure vessels will be**:**

$$N_V = \frac{N_E}{N_{EpV}} \tag{3.4}$$

where**,** $N_V$ = Total number of pressure vessels**;** $N_{EpV}$ = Total number of membrane elements per Pressure Vessel**.**

- **Number of stages selection**

The stage number of the RO plant describes the number of pressure vessels in series, where the inlet feed water will go through till it leaves the desalination plant as brine. Typically, the number of serial element positions is linked with the system recovery and the number of stages, for the designed SWRO plant the recovery is 40% and one stage plant will be selected to avoid the expected scaling problems and the uncaring in operation and monitoring of the plant. The RO stages consist of ten parallel RO trains with $N_V$ pressure vessels. Each pressure vessel contains six spiral wound RO membranes [58]**.**

### Step 6: Estimate the energy requirements of the RO plant

#### a) High-pressure pumps energy requirements ($\mathbf{E}_{(\mathbf{desalination})}$)

High-pressure pumps are used to achieve this high feed pressure. However, this results in high energy demands ($\mathbf{E}_{(\mathbf{desalination})}$) for the RO process [56].

The $E_{desalination}$ can be obtained from IMSDesign detailed report (pump report).

#### b) Additional systems energy requirements

Apart from the desalination energy, the RO plant needs basic electricity for auxiliary systems, lighting, etc. By using a slight over-estimated pressure for the pre-treatment and post-treatment depending on the design. The following sub-sectors will give an estimated energy requirement for these systems.

- **Transfer pumps (Feed water pumps) energy requirements ($\mathbf{E}_{(\mathbf{Transfer\ pumps})}$) and lifting pumps energy requirements ($\mathbf{E}_{(\mathbf{Lifting\ pumps})}$)**

Transfer pumps are used to pump the clarified seawater to the pressure required by the pre-treatment stage. Lifting pumps will be used to lift water from the RO station to the ground tanks in the new Burj Al-Arab city. The $\mathbf{E}_{(\mathbf{Transfer\ pumps})}$ and $\mathbf{E}_{(\mathbf{Lifting\ pumps})}$ can be calculated as follows [52]:

$$N_{pumps} = \left( {}^{F_d}\!/_{F_{pumps}} + 50\ \%\ \text{stand by} \right),\ \text{Assume } F_{pump} = 3600\ m^3/h \tag{3.5}$$

where, $N_{pumps}$ = Total number of pumps; $F_d$=Design flow rate; $F_{pumps}$ = The pump flow rate.

Power consumed by each pump:

$$p_{motor} = \frac{\gamma \times F_{pump} \times H_P}{75 \times 1.36 \times \eta_{pump} \times \eta_{motor} \times \eta_{VFD}} \tag{3.6}$$

The pumps energy requirements are:

$$Power_{Total\ pump} = p_{motor} \times N_{WorKing\ pumps} \tag{3.7}$$

$$E = Power_{Total\ pump} \times \text{Hours of operation} \tag{3.8}$$

$$\text{Specific energy} = \frac{E}{\text{Total Water production}} \tag{3.9}$$

where, $Power_{Total\ pump}$ = Total power consumption of pumps (KW); $H_P$ = The pump total head (m); $\eta_{pump}$ = The pump efficiency; $\eta_{motor}$ = The motor efficiency; $\eta_{VFD}$ = The variable-frequency drive efficiency; $N_{WorKing\ pumps}$= Total number of working pumps; E = Total energy requirements of pumps (KWh); Specific energy = The specific energy of pumps (KWh/ $m^3$).

**Note:** The length of force mainline between the RO plant and Burj Al-Arab reservoirs = 16 Km (see **Figure (3.5)**; The elevation of RO plant location = 18 m; The elevation of Burj Al-Arab reservoirs = 25 m [7]. The calculation of the head for transfer and lifting pumps can be found in **Appendix (B)**. **Table (3.6)** lists all the transfer pumps and lifting pumps design parameters.

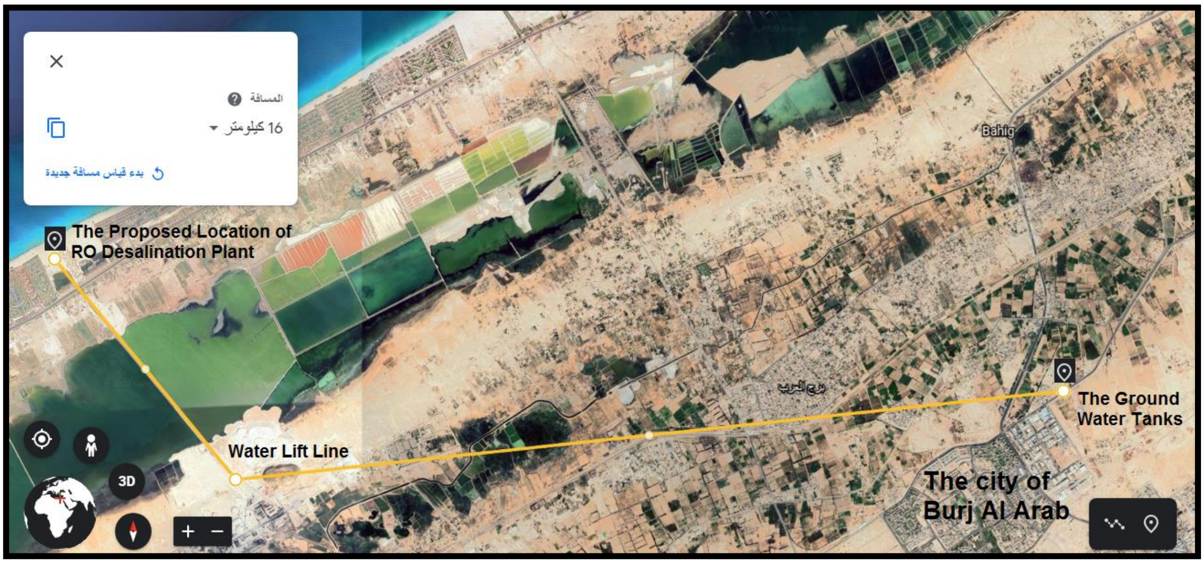


**Figure (3.5): Location of suggested RO plant (Three PV-RO systems configurations) [7].**

**The total power required for the RO plant can be calculated as follows:**

$$P_{Total} = (P_{(desalination)} + Power_{(Total\ transfer\ pumps)} + Power_{(Total\ lifting\ pumps)}) \tag{3.10}$$

**Table (3.6): Transfer and lifting pumps design parameters.**

| Water source | Transfer pumps | Lifting pumps |
|---|---|---|
| $F_d$ | $F_{Total\ (Feed)}$ | maximum monthly discharge |
| $F_{pump}$ | 3600 $m^3$/ h | 3600 $m^3$/ h |
| $H_P$ | 4.5 bar | 2.84 bar |
| $\eta_{pumps}$ | 0.87 | 0.87 |
| $\eta_{motor}$ | 0.95 | 0.95 |
| $\eta_{VFD}$ | 0.97 | 0.97 |

$$E_{Total} = (E_{(desalination)} + E_{pre\ (\text{transfer}\ pumps)} + E_{(Lifting\ pumps)}) \tag{3.11}$$

$$Total\ specific\ energy = (\ Specific\ energy_{(desalination)} + Specific\ energy_{\ (\text{transfer}\ pumps)} + Specific\ energy_{\ (Lifting\ pumps)}) \tag{3.12}$$

where, $P_{Total}$ = Total required power of the RO plant (KWh); $P_{(desalination)}$ = Total power consumption of high-pressure pumps are used to achieve this high feed pressure for the RO process (KW); $Power_{(Total\ transfer\ pumps)}$ = Total power consumption of transfer pumps (KW); $Power_{(Total\ lifting\ pumps)}$ = Total power consumption of lifting pumps (KW); $E_{Total}$ = Total required energy of the RO plant (KWh/ $m^3$); $E_{(desalination)}$ = Total energy consumption of high-pressure pumps are used to achieve this high feed pressure for the RO process (KWh); $E_{pre\ (\text{transfer}\ pumps)}$ = Total energy consumption of transfer pumps (KWh); $E_{(Lifting\ pumps)}$ = Total energy consumption of lifting pumps (KWh); $Total\ specific\ energy$ = The total specific energy of the RO plant (KWh/ $m^3$); $Specific\ energy_{(\text{transfer}\ pumps)}$= The specific energy of transfer pumps (KWh/ $m^3$); $Specific\ energy_{\ (Lifting\ pumps)}$ = The specific energy of lifting pumps (KWh/ $m^3$) ); $Specific\ energy_{(desalination)}$ = The specific energy high-pressure pumps are used to achieve this high feed pressure for the RO process (KWh/ $m^3$).

### Step 7: The photovoltaic systems (PVs) design calculations

In this section, PVsyst simulation tool is used to design and model the PV energy supply. PVsyst performs yearly simulations using hourly weather data which are more accurate than manual calculations using average monthly or yearly irradiation data. PVsyst also performs detailed analysis on the performance of the battery bank, particularly in terms of the battery state of charge (SOC), which helps in obtaining more accurate battery sizing [60].

It is important to keep in mind that the irradiation value strongly depends on the station of the year, reaching its maximum values in summer and minimum values in winter this is for the PV system part. On the other side the maximum demand for clean water in the summer and minimum demand in winter, and maximum values in feed water salinity for RO system in summer and minimum values in winter. To accomplish a correct design, one must select the summer values.

#### [1] The meteorology data for design and analyze solar system

- **A Geographical site defined:**

The coordinates will be defined by the **Google Earth Map** to get the parameters of the defined site, as shown in **Table (3.7)** [7]. Using these parameters and entering them into a PVsyst simulation program to get monthly meteorology data on the PV system site. The entire results of the simulation can be found in **Appendix (C)**. The PVsyst program contains many monthly meteorology data, including it from the appropriate websites in meteorology data like NASA-SSE and PVGIS-ESRA database [60].

**Table (3.7): Details of geographical coordinates and locations that are used [7].**

| Site name | | Country | Region |
|---|---|---|---|
| SidiKerir | | Egypt | Africa |
| Time zone | Latitude | Longitude | Altitude |
| UT + 2 | 30° 92' N | 29° 44' E | 18 m above sea level |

- **Solar irradiation**

Solar irradiation is expected to play a major role in PV system sizing [29]. For this reason, the different solar-driven desalination plant configurations considered in this study are investigated. Solar radiation is scattered and reflected when passing through the atmosphere. Rays of extraterrestrial irradiance (E,extra) are virtually parallel. Terrestrial sunlight, on the other hand, consists of direct and diffuse components (see **Figure (3.6)**) [60].

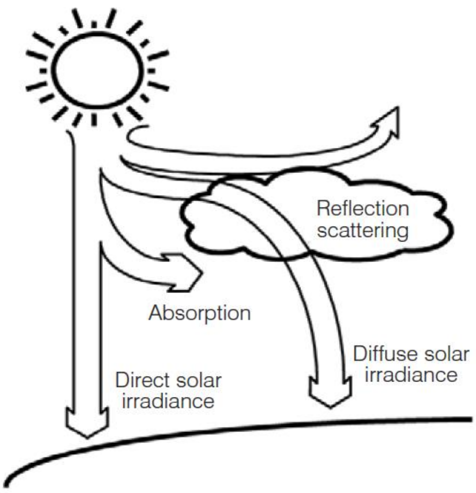


**Figure (3.6): Sunlight passing through the atmosphere [28].**

Direct solar radiation casts shadows, because it is directional, coming directly from the sun; diffuse irradiation, on the other hand, has no defined direction. The total irradiance on a horizontal surface on Earth is also called global irradiance (EGlob,hor) [28]. It is the sum of the direct solar irradiance (Edir,hor) and the diffuse solar irradiance (Ediff,hor) on the horizontal surface:

$$\text{EGlob,hor} = \text{Edir,hor} + \text{Ediff,hor} \tag{3.13}$$

$$\text{Clearness Index} = [\text{EGlob, hor}/ \text{E, extra}] \tag{3.14}$$

❖ **Figure (3.7)** shows only the irradiation section of the simulation at the Sidi-Kerir PV system site**.**

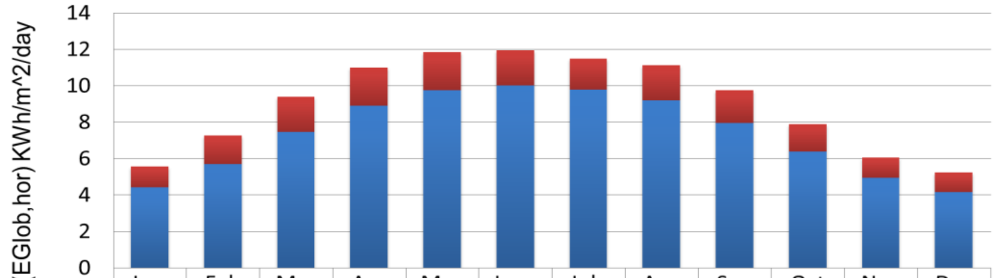


| | Jan | Feb | Mar | Apr | May | June | July | Aug | Sep | Oct | Nov | Dec |
|---|---|---|---|---|---|---|---|---|---|---|---|---|
| (Ediff,hor) KWh/m2/day. | 1.15 | 1.56 | 1.94 | 2.09 | 2.11 | 1.92 | 1.7 | 1.94 | 1.79 | 1.52 | 1.11 | 1.09 |
| (Edir,hor ) KWh/m2/day. | 4.41 | 5.71 | 7.45 | 8.9 | 9.74 | 10.03 | 9.78 | 9.19 | 7.96 | 6.37 | 4.95 | 4.16 |

**Figure (3.7): The irradiation section results of the simulation using PVsyst software [60].**

## [2] Photovoltaic system design

- **Array sizing**

The PV array is designed based on the module specifications of the TP6H72M-440-L module (**Table (3.8)**). The U-value used to calculate the thermal losses, hence the array temperature is assumed to be constant at 20 W/ $m^2$.K based on PVsyst recommendation for free-standing arrays which is based on the assumption of a constant wind velocity due to the lack of reliable data on the coefficient of wind velocity at (PVsyst) [60]**.**

- **Module orientation and operating hours**

The module orientation (Two-axis tracker) and the exact operating time of the RO plant are chosen such that the incident solar irradiation in each month matches the load energy requirements as much as possible to minimize the required battery bank capacity and array size. In this case, the system operates more efficiently particularly in terms of minimizing the wasted PV array energy when the batteries are fully charged and the number of hours when the PV system cannot meet the load energy requirements [29]**.**

The suitable operating hours for each season at SidiKerir region are shown in **Table (3.9)** which as expected, increases in seasons with high solar irradiation and therefore matches the expected increase in water consumption caused by the high ambient temperature. It should be noted that the operating hours are varied such that their daily average is always 8 hours [60]**.**

In this study the feasibility of a PV-driven RO plant is investigated under daytime-only operation, 24 hours operation (with battery system), and PV solar integrated with electricity grid-driven RO plant. In the first case, the PV-RO plant operates only during the daytime and for 8 hours on average with small availability rates (33.3%). In the second case, the PV-RO plant operates the whole day, i.e. 24 hours, which increases the availability rates (90%) of the plant but at the expense of requiring a larger battery bank and array size. In the third case, the PV-RO plant operates all day, that is, 24 hours, which increases the availability rates (90%) of the plant but at the expense of the need for panels, transformers, and cables to connect and transmit electrical energy from the unified public grid to the desalination plant [60]**.**

**Table (3.8): System parameters that are used in designing the PV energy supply [60].**

| PV module specifications | | Reference |
|---|---|---|
| Vmpp (STC) | 42.6 V | Module specifications based on Technology**:** Monocrystal **Manufacturer:** Talesun Solar **Model**: TP6H72M-440-L **[60]**. |
| Impp (STC) | 10.33 A | |
| Pmpp (STC) | 440.2 | |
| Voc (STC) | 50.8 V | |
| Isc (STC) | 10.90 A | |
| Module efficiency (STC) | 21.9% | |
| Voc temperature coefficient (STC) | -170 mV/ C° | |
| Isc temperature coefficient (STC) | 5.5 mA/ °C | |
| Max. power temperature coefficient (STC) | -0.38 %/ C° | |
| Battery specifications | | **Manufacturer, model:** LG Chem, EM048290P5B1 290Ah **[60].** |
| Battery voltage | 51.4 V | |
| Battery capacity | 3.81 KWh | |
| Coulombic efficiency | 96 % | |
| Inverter specifications | | **Manufacturer, model:** Zeversolar, Zeverlution Pro 40K-MV **[60].** |
| Nominal AC power | 40 KWac | |
| Nominal voltage | 600 V | |
| European average efficiency | 98.2 % | |
| Array De-rating factors | | Array De-rating factors taken as standard PVsyst default values **[60].** |
| Mismatch losses | 1.1 % | |
| Module quality loss | -0.8 % | |
| Ohmic wiring losses | 1.5 % at STC | |
| Annual soil losses | 3.0 % | |
| Light Induced Degradation (LID) | 2.0 % | |
| Thermal loss factor | U (const) 20.0 W/ m².K | |

**Table (3.9): Optimal operating hours of the RO plant when designed to operate only during the daytime [60].**

| Season operating | Time | Total hours |
|---|---|---|
| Winter | 7:30 to 14:00 | 6.5 |
| Spring and Summer | 7:30 to 16:30 | 9 |
| Autumn | 7:30 to 15:00 | 7.5 |

- **Battery sizing**

The battery type recommended for use in a solar PV system is a deep cycle battery. A deep cycle battery is specifically designed to be discharged to low energy levels and rapid recharged or cycle charged and discharged day after day for years. The battery should be large enough to store sufficient energy to operate the appliances at night and on cloudy days. The amount of rough energy storage required is equal to the multiplication of the total power demand and the number of autonomy days. The term days of autonomy means the number of days a battery bank can provide the appliances you have connected to the system without a recharged by the solar panels. The battery bank capacity for both the day only and 24 hours operation cases is designed such that the maximum depth of discharge (DOD) does not exceed 75%. While for standalone designs, 3.5 to 5 days of autonomy are usually recommended for PV-driven loads. For the day and night operation, the battery bank is selected to provide one day of autonomy assuming that it will be more economical to store water needed for urgent uses, i.e. domestic purposes, on cloudy days rather than oversizing the battery bank. With such smaller battery sizes, the number of hours at which the battery bank will not be able to supply the load due to low State of Charge (SOC), particularly during cloudy days, is expected to increase which will be examined during the analysis [61 and 62]. The technical data for the components of the PV system is provided in **Appendix (C).**

**[3] Estimate the Levelized cost of electricity of the PV system**

- **Cost reviews**

Several studies have reviewed published PV system costs. This thesis did a similar work, where cost data from some publications were used to develop the tables providing cost ranges for different PV systems [63 - 73]**.**

- **Measuring the Cost of Renewables**

According to OECD and NEA (2018), the cost of electricity can be categorized into three different levels**:**

**A- PV plant (PV system)-level costs;**
**B- Grid-level system costs;**
**C- External or social costs outside the electricity system.**

The plant-level cost is commonly referred to as the technology cost, described as the Levelised Cost of Electricity (LCOE), which represents the lifetime costs divided by the electricity production. Grid-level system costs concern the costs at the level of the electricity system, linked through the transmission and distribution grids. The third category includes items that impact the well-being of individuals and communities outside the electricity sector [63]. Known as external or social costs, such costs include the impacts of local and regional air pollution, climate change…, etc**.**

**A- PV system costs**

The PV system involves several kinds of costs and revenues over a long time during the planning, construction, operation, and decommissioning phases, which results in complicated cash flows. There are well-established methodologies applied in any kind of industry to compare different projects involving cash flows over several years. The most commonly applied indicators used in the evaluation of investments are the "amortization factor" or the "annualized life cycle cost method" was used. The situation is similar in energy projects, where the price at which the generated electricity can be sold has to be known. In that case, the concept of the LCOE has been introduced, which is an assessment of the price at which the electricity would have to be sold for the project to break even and is calculated by dividing the discounted costs over the lifetime of the project by the discounted energy produced over the same period. **Equation (3.15)** is obtained for the Levelised Cost of Electricity ($\mathrm{LCOE}_{t,n}$) of PV-generated power [64]**.**

$$\mathrm{LCOE}_{t,n} = \frac{sum\ of\ costs\ over\ lifetime}{sum\ of\ electrical\ energy\ produced\ over\ lifetime} = \frac{I_{(PV)0} + \sum_{t=1}^{n(pv)} \frac{C_{(PV)t}}{\left(1+i_{(PV)}\right)^{t}}}{\sum_{t=1}^{n(pv)} \frac{E_{(PV)t}}{\left(1+i_{(PV)}\right)^{t}}} \qquad (3.15)$$

where, the initial capital investment is ($I_{(PV)0}$ ), it is assumed that every year (from year 1 to year $n(pv)$) the photovoltaic system produces exactly the same amount of energy produced in a year ($E_{(PV)t}$) and has exactly the same annual cost operation and maintenance ($C_{(PV)t}$), $i_{(PV)}$ represents the discount rate [64].

- **Financial variables and plant lifetime**

**i. Discount rate ($i_{(PV)}$)**

As discussed in the above sections, cost assessment methods require the use of a discount rate to account for the value of money over time and the risk or uncertainty of future cash flows. In fact, a discount rate picked a value, usually between 5% and 10% (see **Table (3.10)**) [65 and 66].

**Table (3.10): The discount rate of the PV system available in the literature and the actual values selected for the cost estimation.**

| Discount rate | Reference | Value used |
|---|---|---|
| 5-8% | [65] | 5% |
| 10% | [66] | |

**ii. PV system lifetime ($n(pv)$)**

The methodology for evaluating the LCOE of PV system projects requires the definition of the PV system lifetime ($n(pv)$), i.e the number of years for which the future cash flows will be taken into account. Normally this is defined by the decision-makers, who have to fix the period of time over which they want to calculate the return on their investment, respecting the technical constraints of the PV system and its components. The residual value of the PV system at the end of this period has to be taken into account. In general, it is common to choose a period between 20 and 40 years. In most cases, 25 years are chosen, as shown in **Table (3.11)** [60 and 65 - 69].

- **Assumptions and estimations of input data**

If a correct and detailed equation is used to calculate the costs, the quality and detail of the input data, and the accuracy of the assumptions about future performance, costs and revenues will be the main elements that define how relevant or reliable the results are. These assumptions and estimations are discussed in this sub-section [64].

**i. Capital Costs ($I_{(PV)0}$ )**

The PV system consists of the PV modules, the mounting supports, the battery bank, the solar inverter, and the interactive inverter that in addition to the balance of system (BOS) which includes the wiring, instrumentation, and other electrical equipment [29]. In fact, the average price of the PV module picked a value (see **Tables (3.12)**), usually between (550 and 850) USD/ KW [66, 68, and 71]. For the solar inverters, their price is usually between (130 - 900) USD/ KW (see **Tables (3.12)**) [65, 66, 68, and 71]. Regarding the battery bank, numerous cost values are used in the literature ranging from (540 - 4592) USD/ KW as shown in **Tables (3.12)** [67 - 68, and 72]. While a value of 1500 USD/ KW is used in this study as a cheaper alternative is likely to be available locally without compromising the battery lifetime. Regarding the battery lifetime, while a typical lifetime of 10 years is expected, a conservative value of 5 years is used to account for the effect of high temperature in Egypt which is expected to reduce the battery lifetime by 50% [60].

Finally, for BOS and Mounting structure costs, the higher cost will be chosen because the tracking system used is a two-axis tracker (see **Tables (3.12)**) [66, 68, and 71]**.**

**Note:** Solar PV panels can last 25 years or more. The storage batteries and inverters are likely to need replacing in the lifetime of the needed PV system. **Table (3.13)** shows the batteries and inverters' costs based on the project lifetime**.**

**Table (3.11): PV system components lifetime available in the literature and the actual values selected for the cost estimation.**

| PV module lifetime (Project lifetime) | Reference | Value used |
|---|---|---|
| 25 Years | [66] | 25 Years |
| 40 Years (15 years of residual life in addition to the 25year service life) | [65] | |
| 25 Years | [67] | |
| 20 – 25 Years | [68] | |
| **Inverter lifetime** | **Reference** | **Value used** |
| 15 years | [65] | 15 years |
| 5 – 10 years | [68] | |
| **Battery lifetime** | **Reference** | **Value used** |
| 15 years | [67] | 5 years |
| 5 years | [60] | |
| 10 years | [69] | |

- **Note:** The values of both the land cost and the degradation factor have been neglected**.**

### ii. Operating Costs ($C_{(PV)t}$)

For the operation and maintenance costs, including labor costs, different figures are used in the literature (**see Table (3.14)**). In this study, the annual operation cost is assumed to be 1.5 % of the capital cost which gives annual cost values close to the average of those used in the literature [65 - 68, and 71]**.**

### B- Grid-level system costs

This includes the cost of linked through the transmission and distribution grid infrastructure. This group can be termed system costs or additional costs [70]. Regarding the grid-level system costs some papers introduce the Levelized transmission cost in the overall cost calculation, ranging from (2.91 - 4.1) USD/ MWh (see **Table (3.15)**) [68 and 70]**.**

### C- External or social costs

Depending on the circumstances, cost reductions might occur because of the reduced fuel costs for conventional generators, reduced CO2 and other pollutant emissions costs, a reduced need for additional generation capacity, a reduced need for transmission infrastructure, and/ or reduced transmission system losses. This group can be termed benefits or avoided costs [63]. Regarding external or social system costs, some papers introduce the Levelized carbon (Tax) cost in the overall cost calculation, ranging from ($9.7\times10^{-3}$ - $28.1\times10^{-3}$) USD/ KWh (see **Table (3.16))** [73 and 74]**.**

**Table (3.12): PV system capital costs available in the literature and the actual values selected for the cost estimation.**

| Solar PV costs | Reference | Value used |
|---|---|---|
| ( 550 - 680)USD/ KW | [66] | 600 USD/ KW |
| 556 USD/ KW | [71] | |
| (660 - 850) USD/ KW | [68] | |
| **Inverter or converter costs** | **Reference** | **Value used** |
| ( 130 - 160)USD/ KW | [66] | 160USD/ KW |
| (420 - 900) USD/ KW | [65] | |
| 132 USD/ KW | [71] | |
| (230 -750) USD/ KW | [68] | |
| **Battery costs** | **Reference** | **Value used** |
| Storage type (2hrs) 540 USD/ kW | [67] | 1500 USD/ kW |
| Storage type (1hrs) (1228 - 1294) USD/ kW | [72] | |
| Storage type (2hrs)(1535 - 1824) USD/ kW | [72] | |
| Storage type (4hrs) (2612)USD/ kW | [72] | |
| Storage type (6hrs) (1500) USD/ kW | [72] | |
| Storage type (8hrs) (4592) USD/ kW | [72] | |
| Storage type (48hrs) (2794) USD/ kW | [72] | |
| (1200 - 1500) USD/ kW | [68] | |
| **Mounting structure costs** | **Reference** | **Value used** |
| ( 550 - 680)USD/ KW | [66] | 600 USD/ KW |
| 556 USD/ KW | [71] | |
| (660 - 850) USD/ KW | [68] | |
| **Balance of system (BOS) costs** | **Reference** | **Value used** |
| ( 470 - 540)USD/ KW | [66] | 540 USD/ KW |
| 433 USD/ KW | [71] | |

**Table (3.13): The batteries and inverters cost base on the project lifetime.**

| Item | Item lifetime (Years) | Project lifetime (Years) | The actual value used of cost (USD/ KW) | The cost base on the project lifetime (USD/ KW) |
|---|---|---|---|---|
| Inverter | 15 | 25 | 160 | 25/ 15 × 160 = 266.6 |
| Battery | 10 | 25 | 1500 | 25/ 10 × 1500 = 3750 |

**Table (3.14): PV system operating costs available in the literature and the actual values selected for the cost estimation.**

| O&M costs | Reference | Value used |
|---|---|---|
| (1% - 2%) of the capital cost. | [66] | 1.5 % of the capital cost |
| (7.42 - 32.80) USD/ KW-year | [65] | |
| (25+7.25 = 32.25) USD/ KW-year | [67] | |
| 25 USD/ KW-year | [71] | |
| 40 - 126 USD/ KW-year | [68] | |

**Table (3.15): Levelized transmission cost available in the literature and the actual values selected for the cost estimation.**

| The levelized transmission cost | Reference | Value used |
|---|---|---|
| 2.91 - 3.83 USD/ MWh | [70] | 3.3 USD/ MWh<br>$3.3 \times 10^{-3}$ USD/ KWh |
| 4.1 USD/ MWh | [68] | |

**Table (3.16): Emission factor for electricity and carbon Tax available in the literature and the actual values selected for the cost estimation.**

| Emission factor for electricity and carbon tax | Reference | Value used |
|---|---|---|
| (0.5 - 0.8 kg CO2-e/ KWh)<br>(19.39 USD/ ton carbon)<br>($9.7\times10^{-3}$ - $15.5\times10^{-3}$ USD/ KWh) | [73] | (0.5 kg CO2-e/ KWh)<br>(19.39 USD/ ton carbon)<br>($9.7\times10^{-3}$ USD/ KWh) |
| (1.22 kg CO2-e/ KWh)<br>(23 USD/ ton carbon)<br>($28.1\times10^{-3}$ USD/ KWh) | [74] | |

**Step 8: Estimate the Levelized Cost of Water (LCOW) of the RO plant**

- **Cost reviews**

Several studies have reviewed published RO desalination system costs. This thesis did a similar work, where cost data from some publications were used to develop the tables providing cost ranges for RO desalination technology powered by conventional sources and renewable energy. All these papers classify costs based on technology and energy source and sometimes plant size [74 - 80].

- **Investment evaluation indicators**

Desalination plants involve several kinds of costs and revenues over a long period of time during the planning, construction, operation, and decommissioning phases, which results in complicated cash flows. There are well-established methodologies applied in any kind of industry to compare different projects involving cash flows over several years. The most commonly applied indicators used in the evaluation of investments are the “amortization factor” or the “annualized life cycle cost method” was used. The situation is similar in energy projects, where the price at which the generated electricity can be sold has to be known. In that case, the concept of Levelized Cost of Electricity (LCOE) has been introduced, which is an assessment of the price at which the electricity would have to be sold for the project to break even and is calculated by dividing the discounted costs over the lifetime of the project by the discounted energy produced over the same period. By adapting that concept for desalination and other water production technologies, **Equation (3.16)** is obtained for the Levelized Cost of Water (LCOW) [75].

$$\text{LCOW} = \frac{sum\ of\ costs\ over\ lifetime}{sum\ of\ the\ amount\ of\ water\ produced\ over\ lifetime} = \frac{I_0 + \sum_{t=1}^{n} \frac{C_t}{(1+i)^t}}{\sum_{t=1}^{n} \frac{P_{Water}}{(1+i)^t}} \qquad (3.16)$$

where, the initial capital investment is ($I_0$ ), it is assumed that every year (from year 1 to year $n$) the desalination plant produces exactly the same amount of water produced in a year

($p_{Water}$) and has exactly the same annual cost operation ($C_t$), $i$ represents the discount rate [75].

- **Production water ($p_{Water}$)**

The annual water production ($p_{Water}$) is usually calculated simply as the product of the plant capacity with the plant availability. The plant availability is estimated after taking into account the planned maintenance and unplanned downtime. However, the plant availability is taken into account at a reasonable rate between 85% and 95% for availability in conventional systems, or between 25% and 33% for systems that use PV solar energy and do not have any backup or energy storage [74 and 75]. **Table (3.17)** provides an overview of some availability rates that will be used.

**Table (3.17): The availability rates of the RO plant available in the literature and the actual values selected for the cost estimation.**

| Availability | Reference | Value used |
|---|---|---|
| 85% - 95% | [75] | 90% |
| 90% | [74] | |
| 25% - 33% (PV powered) | [75] | 29% |

- **Financial variables and plant lifetime**

**i. Discount rate (i)**

As discussed in the above sections, cost assessment methods require the use of a discount rate to account for the value of money over time and the risk or uncertainty of future cash flows. In fact, a discount rate picked a value, usually between 5% and 10% (see **Table (3.18))** [74 and 75].

**Table (3.18): The discount rates of the RO plant available in the literature and the actual values selected for the cost estimation.**

| Discount rate (i) | Reference | Value used |
|---|---|---|
| 6.5% - 10% | [75] | 5% |
| 5 % | [74] | |

**ii. Plant lifetime (n)**

The methodology for evaluating the feasibility of desalination projects requires the definition of the plant lifetime (n), i.e the number of years for which the future cash flows will be taken into account. Normally this is defined by the decision-makers, who have to fix the period of time over which they want to calculate the return on their investment, respecting the technical constraints of the plant and its components. The residual value of the plant at the end of this period has to be taken into account. In general, it is common to choose a period between 10 and 30 years. In most cases, 25 years are chosen, as shown in **Table (3.19)** [74 - 76].

**Table (3.19): The lifetime of the RO plant available in the literature and the actual values selected for the cost estimation.**

| Plant lifetime (years) | Reference | Value used |
|---|---|---|
| 10 - 30 | [75] | 25 |
| 20 | [74] | |
| 25 | [76] | |

- **Assumptions and estimations of input data**

If a correct and detailed equation is used to calculate the costs, the quality and detail of the input data, and the accuracy of the assumptions about future performance, costs and revenues will be the main elements that define how relevant or reliable the results are. These assumptions and estimations are discussed in this section [75]**.**

**i. Capital Costs ($I_0$ )**

Capital Costs take into consideration the desalination technology, including standard pre-treatment and post-treatment equipment and materials costs (usually in USD/ $m^3$/ day) in their calculation. In order to do that, the plant design has to be known, which depends on choices made by the customer (for example the type of energy recovery equipment used), energy generation hardware costs have to be taken into account, and plant scale [75]. The Capital cost of a plant is estimated using a Capacity Factored Estimate. The cost of a new plant is derived from the cost of a similar plant of known capacity, with a similar production route, but not necessarily the same end product (the product should be relatively similar, however). It relies on the nonlinear relationship between capacity and cost as shown in follows **Equation:**

$$\left[\frac{\text{capital cost plant1}}{\text{capital cost plant2}}\right] = \left[\frac{\text{plant capacity1}}{\text{plant capacity2}}\right]^{m} \tag{3.17}$$

where, m = the scale index [exponent]. The m used in the capacity factor equation is the slope of the log curve that has been drawn to reflect the change in the cost of a plant as it is made larger or smaller. The methodology of using the capacity factor is sometimes referred to as the “six tenth factor” method because of the reliance on an exponent of 0.6 if no other information is available [74]. **Table (3.20)** provides an overview of some capital costs that will be used to derive the capital cost of the suggested plant [77]**.**

**Table (3.20): Overview of SWRO plant capital costs in the Mediterranean area that used in desalination cost analysis [77].**

| Plant name and location | Operation year | Size ($10^3 \times m^3$/ day) | Capital cost ( million USD) | |
|---|---|---|---|---|
| | | | Total (million USD) | USD/ $m^3$/ day |
| Sorek, Israel | 2013 | 624 | 480 | 0.77 |
| Magtaa, Algeria | 2009 | 500 | 512 | 1.02 |
| Larnaca, Cyprus | 2001 | 64 | 80.0 | 1.25 |
| Larnaca, Cyprus | 2009 | 62 | 80 | 1.29 |
| Hamma, Algeria | 2008 | 200 | 272.2 | 1.36 |
| Ashdod, Israel | 2011 | 320 | 444 | 1.39 |

**ii. In this is a thesis there are additional capital costs that must take into consideration, like:**

**The capital cost of water transmission line:** The estimated cost of constructing a water transmission line with a diameter of 1500 mm and a length of approximately 16 km long is about $160\times 10^6$ EGP ≈ $10\times 10^6$ USD at 23/ 4/ 2020, Calculated basis on 10000 EGP/ m/ line ≈ 625 USD/ m/ line according to the Egypt building index.

**The capital cost of ground storage tanks:** The estimated cost of constructing ground storage water tanks with a capacity of 15000 $m^3$/ tank is calculated basis on 2000 EGP/ $m^3$/ tank ≈ 125 USD / $m^3$/ tank at 23/ 4/ 2020 according to the Egypt building index.

- **Note:** The values of both the land cost and the degradation factor have been neglected.

**iii. Operating Costs (Ct)**

**1- Chemicals and other consumables:**

The requirements for chemicals depend on the type of desalination plant and the feed water quality. These chemicals' cost values range from 0.019 to 0.064 USD/ $m^3$. **Table (3.21)** provides an overview of some discount rate will be used [75 and 77 - 79].

**Table (3.21): The chemical costs of the RO plant available in the literature and the actual values selected for the cost estimation.**

| Chemicals costs | Reference | Value used |
|---|---|---|
| 0.019 - 0.05 USD/ $m^3$ | [75] | 0.02 USD/ $m^3$ |
| 0.045 - 0.064 USD/ $m^3$ | [78] | |
| 0.0482 USD/ $m^3$ | [79] | |
| 0.02 USD/ $m^3$ | [77] | |

**2- Labor:**

The labor costs can vary widely depending on the country, the exact location, the technology, the specific design, and the scale of the plant. **Table (3.22)** takes the specific costs used in some of the reviewed papers to give a taste of the values used [74, 75, 77, and 79].

**Table (3.22): The specific costs for the labor of the RO plant available in the literature and the actual values selected for the cost estimation.**

| Specific costs for labor | Reference | Value used |
|---|---|---|
| 0.02 - 0.1 USD/ $m^3$ | [75] | 0.02 USD/ $m^3$ |
| 0.02 USD/ $m^3$ | [74] and [77] | |
| 0.027 USD/ $m^3$ | [79] | |

**3- Maintenance:**

One of the major maintenance costs for RO is membrane replacement, with a replacement rate that varies between 5 and 20% (see **Table (3.23)**) [74 - 76, and 79]. In the case where PV was considered as the source of energy, 40% was used to account for the negative effect that varying pressure might have on the membranes. Regarding other maintenance costs, like a replacement of parts, pumps, etc, they are often ignored, or they are accounted for by adding annually to the costs a certain percentage of the capital costs, ranging between 1 and 4%. Some examples are provided in **Table (3.24)** [74 - 75, and 78 - 79].

**Table (3.23): The membrane replacement rate and cost of the RO plant available in the literature and the actual values selected for the cost estimation.**

| - Membrane replacement rate.<br>- Replacement cost. | Reference | Value used |
|---|---|---|
| (5 - 20% / yr)<br>N/A | [75] | Membrane replacement rate = (15 %/ yr) (Grid powered)<br><br>membrane cost = 0.28 USD/ $m^2$<br>846.40 USD/ element |
| (20% / yr)<br>membrane cost of 9 USD / $m^2$ | [74] | |
| (15 % / yr)<br>membrane cost of 0.28 USD/ $m^2$<br>846.40 USD/ element | [76] | |
| (14.3 % / yr)<br>N/A | [79] | |
| (40 % / yr) (PV powered)<br>846.40 USD/ element | [75] | (40 %/ yr) (PV powered)<br>846.40 USD/ element |

**Table (3.24): Other maintenance costs of the RO plant available in the literature and the actual values selected for the cost estimation.**

| Other maintenance costs | Reference | Value used |
|---|---|---|
| 1.5% - 4% of capital costs | [75] | 1.5% of capital costs |
| 2% of capital costs | [74] | |
| 1% - 3% of capital costs | [78] | |
| 1% of capital costs | [79] | |

**4- Brine disposal:**

Regarding RO brine disposal cost is about 0.04 USD/ $m^3$ [74 and 75].

**5- Energy**

However, there are some cases, where energy contributes mainly through capital costs when the desalination plant includes an integrated system or a common electricity supply system such as (conventional electricity from the unified electricity grid + photovoltaic system) [75].

For calculating the energy-related cost for year t ($C_{E,t}$) the following equation can be used:

$$C_{E,t} = E_{(el)t} \times P_{(el)t} + E_{(PV)t} \times P_{(PV)t} \tag{3.18}$$

where $E_{(el)t}$ and $E_{(PV)t}$ are the amount of conventional electricity energy from the unified electricity grid and electrical energy from photovoltaic system respectively used by the RO plant in year $t$ and $P_{(el)t}$ and $P_{(PV)t}$ the cost of the unit of conventional electrical energy from the unified electricity grid and electrical energy from photovoltaic system respectively in a year$(t)$ [75]. The way to account for the cost of energy ($P_{(el)t}$ and $P_{(PV)t}$) depends on whether it is generated on-site or provided externally (for example the electrical energy cost from the grid = 1.25 Egyptian Pound/ kWh ≈ 0.079 USD/ kWh at 23/ 4/ 2020) [80]**.**

For PV system generation, if the energy and desalination plants are operated by the same entity, the initial costs related to energy generation (for equipment, engineering, etc.), must be taken into account as part of the capital costs, leaving only the associated running costs (like fuel, maintenance, and personnel costs) to be used in **Equation (3.16)**. An alternative approach (PV systems), will be calculated separately (LCOE) and use that as the cost of the unit of electricity [75]. The cost of the electric power unit for the integration of conventional from the unified electricity grid and the power energy from the PV system ($P_{(integration)t}$), in the year *(t)* will calculate as follow**:**

$$P_{(integration)t} = \frac{E_{(el)t} \times P_{(el)t} + E_{(PV)t} \times P_{(PV)t}}{E_{(el)t} + E_{(PV)t}} \tag{3.19}$$

# CHAPTER 4

# RESULTS AND DISCUSSION

# RESULTS AND DISCUSSION

## 4.1 Introduction

The main objective of this chapter is to present the results of strategic planning for the drinking water projects of the new city of Burj Al-Arab. This is for strengthening and expands the existing water facilities in the Burj Al-Arab city to accommodate the expected population increase until 2032. The comparison between the feasibility of using the PV-RO plant will be also investigated for the three suggested configurations is taken into consideration. The best configuration will be selected as a second alternative source of Nile water. This is to cover the increase in the demand for potable water due to the forecasted increase of the population and the various activities in the new city of Burj Al-Arab until the year of the target (2032). Also in this chapter, a strategic plan for sanitation works will be studied. This plan, including the future needs of the new Burj Al-Arab city, according to current trends and projects with a view to developing the current situation**.**

The water demands and wastewater discharges will be estimated for all uses. This is done by using the forecasted population census and the general plan for urban and industrial development in Burj Al-Arab city. The laws and consumption rates concerning the estimation of water demand and wastewater discharges stipulated in the Egyptian code will be applying for the design and implementation of drinking water and sanitation projects. The wastewater discharges in the new city of Burj Al Arab estimate on parts. So that the amount of wastewater that reaches each treatment plant is estimated separately. This is to facilitate the evaluation process for each station separately. This evaluates based on calculating the quantities of domestic wastewater discharges and industrial wastewater. Then, will compare them with the design capacities of the lifting and treatment plants to ensure their capacity for future discharges. The methodologies mentioned in **Chapter (3**) were used and the result was obtained. This result of the strategic plan is divided into parts to evaluate the wastewater works and to calculate the requirements of the drinking water feeding works as follows**:**

## 4.2 Population Forecasting

This sub-section is carried out to verify the application of conventional (the extrapolation of trend curves method) and modern techniques (GA and PSO) for population forecasting of The Burj Al-Arab city up to the year 2032. All of these techniques were applied in the MATLAB Software program. Using the historical data of the population of the Burj Al-Arab city from the year 2011 to the year 2017(see **Table (3.1)**, **Chapter (3)**)**.**

### 4.2.1 Population Forecasting by Using the Conventional Technique

Two approximations of the extrapolation of trend curves are applied to this data to forecast the population of the Burj Al-Arab city**.**

❖ **Application and results for linear regression**

Population forecasting of the Burj Al-Arab city can be obtained by using **Equation (2.1)** in **Chapter (2)** when the linear regression model is used**.** The coefficients (a) and (b) in **Equation (2.1)** can be determined by using **Equations (2.7** and **2.8)** in **Chapter (2)** and using the historical data shown in **Table 3.1**. The population coefficients (a) and (b) are equal to (104) and (12) respectively**.**

❖ **Application and results for exponential regression**

Also, population forecasting of the Burj Al-Arab city can be obtained by using **Equation (2.2)** when the exponential regression model is used. The population coefficients (a) and (b) in **Equation (2.2)** can be determined by using **Equations (2.12** and **2.13)** in **Chapter (2)** and using the historical data shown in **Table (3.1)**. The population coefficients (a) and (b) are equal to (4.6) and (0.1) respectively**.**

### 4.2.2 Population Forecasting by Using Modern Techniques

GA and PSO techniques are applied to estimate the parameters of linear and exponential regression models using the historical data shown in **Table (3.1)** to forecast the population of the Burj Al-Arab city. According to the values of the population coefficients (a) and (b), which are obtained using a conventional technique, the range of the search space for both GA and PSO technique for (a) and (b) using a linear regression model is taken for the population forecasting as (100:110) and (11.5:12.5) respectively, and with using the exponential regression model is taken as (4:5) and (0.08:0.12) respectively for the population**.**

### 4.2.3 Application and Results

**Figure (4.1)** and **Table (4.1)** show the population forecasting of the Burj Al Arab city from the year 2017 to the year 2032 by two different methods (linear, exponential) by using three techniques (extrapolation of trend curves, GA and PSO)**.**

### 4.2.4 Choice of the Best Results of the Population Forecasting

Long-term population forecasting has been presented in this section to know the population development of the Burj Al-Arab city up to the year 2032**.**

❖ **Extrapolation of the trend curves technique has been applied as a conventional technique. The remarkable results of this application are:**

**1.** In linear regression, the coefficients (a) and (b) for the population are equal to (104) and (12) respectively, and the population forecasting of Burj Al-Arab city in 2032 is equal to 320,000 people**.**
**2.** In exponential regression, the coefficients (a) and (b) for the population are equal to (4.6) and (0.1) respectively, and the population of Burj Al-Arab city in 2032 is equal to 601,845 people**.**

❖ **The coefficients and exponents using the extrapolation of trend curves technique are used in the GA and PSO technique which has been applied as modern techniques to obtain possible more accurate results. The results of both GA and PSO technique applications are:**

**a)** The range of the search space for both GA and PSO technique for (a) and (b) by using the linear regression model is taken for the population forecasting as (100:110) and (11.5:12.5) respectively, and the population forecasting of the Burj Al-Arab city in 2032 by using both GA and PSO techniques is equal to (320,009 people) and (321,921 people) respectively**.**

**b)** The range of the search space for both GA and PSO technique for (a) and (b) by using the exponential regression model is taken as (4:5) and (0.08:0.12) respectively of the population. And the population forecasting of the Burj Al-Arab city in 2032 by using both GA and PSO techniques is equal to (686,303 people) and (727,375 people) respectively**.**

**Table (4.1): The population forecasting results, that obtained by using the different techniques until 2032.**

| Year | Forecasted Population, (Thousands) | | | | | |
|---|---|---|---|---|---|---|
| | Extrapolation Technique | | GA | | PSO | |
| | Linear Approx. | Exponential Approx. | Linear Approx. | Exponential Approx. | Linear Approx. | Exponential Approx. |
| 2011 | 68 | 73.7 | 67.998 | 68.123 | 67.679 | 72.791 |
| 2012 | 80 | 81.45 | 79.999 | 76.045 | 79.786 | 81.224 |
| 2013 | 92 | 90.017 | 91.999 | 84.887 | 91.892 | 90.633 |
| 2014 | 104 | 99.484 | 104 | 94.757 | 103.999 | 101.133 |
| 2015 | 116 | 109.947 | 116 | 105.776 | 116.106 | 112.848 |
| 2016 | 128 | 121.51 | 128 | 118.075 | 128.213 | 125.921 |
| 2017 | 140 | 134.29 | 140.001 | 131.804 | 140.319 | 140.508 |
| 2018 | 152 | 148.413 | 152.002 | 147.13 | 152.426 | 156.786 |
| 2019 | 164 | 164.022 | 164.002 | 164.239 | 164.533 | 174.948 |
| 2020 | 176 | 181.272 | 176.003 | 183.336 | 176.64 | 195.215 |
| 2021 | 188 | 200.337 | 188.003 | 204.654 | 188.747 | 217.83 |
| 2022 | 200 | 221.406 | 200.004 | 228.45 | 200.853 | 243.064 |
| 2023 | 212 | 244.692 | 212.004 | 255.014 | 212.96 | 271.222 |
| 2024 | 224 | 270.426 | 224.005 | 284.667 | 225.067 | 302.641 |
| 2025 | 236 | 298.867 | 236.005 | 317.767 | 237.174 | 337.701 |
| 2026 | 248 | 330.3 | 248.006 | 354.717 | 249.28 | 376.821 |
| 2027 | 260 | 365.037 | 260.006 | 395.963 | 261.387 | 420.475 |
| 2028 | 272 | 403.429 | 272.007 | 442.004 | 273.494 | 469.184 |
| 2029 | 284 | 445.858 | 284.007 | 493.4 | 285.6 | 523.537 |
| 2030 | 296 | 492.749 | 296.0077 | 550.771 | 297.707 | 584.185 |
| 2031 | 308 | 544.572 | 308.008 | 614.814 | 309.814 | 651.86 |
| 2032 | 320 | 601.845 | 320.009 | 686.303 | 321.921 | 727.375 |

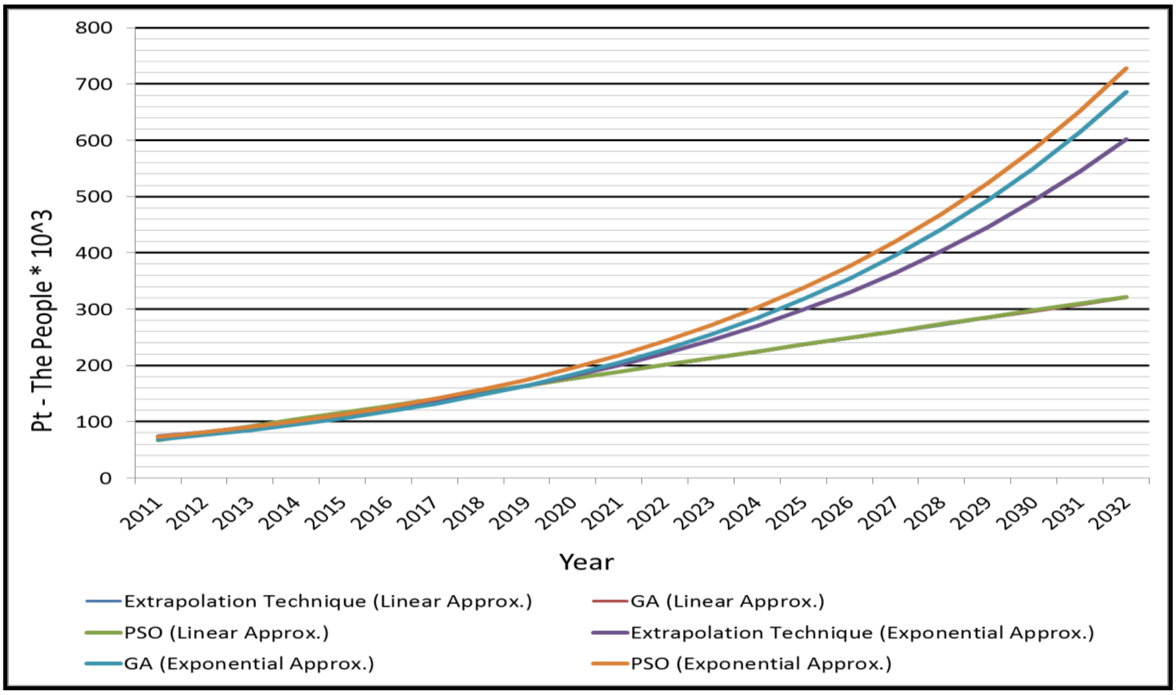


**Figure (4.1): The forecasted population of Burj Al-Arab city until 2032 by using conventional and modern techniques.**

**The outcome of this section:**

From the obtained results and **Figure (4.1)**, we can deduce the following conclusions**:**

**1-** In linear regression models, the population forecasted is increasing at a constantly increasing rate. While, in exponential regression models, the population forecasted is increased with variable and fast increasing rate**.**

**2-** The results obtained from the exponential regression models are more accurate than the results obtained from the linear regression models because the population forecasted increasing rate in the exponential regression models is suitable for the nature of the population development in the Burj Al-Arab city where will be one of the important industrial cities in Egypt in the near future. Therefore, the increase in the population will be faster due to the increase in job opportunities, which is an attractive factor for the population**.**

**3-** From the previous results also, it can be found that the population forecasting results by using the PSO for the exponential regression model have the best results (727,375 people) compared to the other models. This is because the population forecasting results using this model adapt to the actual peak population of the Burj Al-Arab city from the year 2012 to the year 2017 as shown in **Table (4.2)**. PSO can be implemented simply, and the convergence speed is quick without too many parameters, and it has the good global searching ability because the information of particle is single-directional, each particle would remember the past position, and the convergence is very quick, but at the same time, it is easy to fall into local optima**.**

**Table (4.2): Actual and forecasted population from the year 2012 to the year 2017 [4].**

| Year | 2012 | 2017 |
|---|---|---|
| Actual Population, (Thousands) | 80 | 140 |
| Forecasted Population, (Thousands) | 81.22 | 140.5 |

## 4.3 Estimating the Water Demand and Wastewater Discharges

This strategic plan serves as a framework and basis for decision making and detailed planning in a Fifteen-years planning horizon divided into three stages (five-year plans), such as the first planning stage (from 2017 to 2022), the second planning stage (from 2022 to 2027), and the third planning stage from (2027 to 2032)**.**

### 4.3.1 Estimating the Water Demand

The materials and methods mentioned in **Sub-section (3.4.1)** of **Chapter (3)** were used and the results were obtained**.**

❖ **Figure (4.2)** shows the results of the average water daily consumption for Burj Al-Arab city up to the year 2032. **Table (4.3)** shows the results of the design flows of potable water demand throughout the various stages of development**.**

**The outcome of this section:**

**The maximum monthly consumption of water required for all uses during the development period:** were calculated for 2032 as mentioned in the Egyptian code of design principles and conditions of implementation for drinking water and drainage, which was (498,187 $m^3$/ day)**.**

**Table (4.3): The design flows of potable water throughout the various stages of development.**

| Year | 2017 | 2022 | 2027 | 2032 |
|---|---|---|---|---|
| The average daily housing consumption ($m^3$/ day) | 39200 | 68058 | 117733 | 203665 |
| The needs for Water for Industrial Use ($m^3$/ day) | 80483 | 155705 | 181680 | 183034 |
| The water needs of construction works ($m^3$/ day) | 23215.5 | 33780 | 33410 | 18500 |
| The water needs of swimming pools and lakes ($m^3$/ day) | 1260 | 4470 | 11400 | 11400 |
| The needs of the tourism sector ($m^3$/ day) | 695 | 5150 | 8688 | 9583 |
| The water needs of the regions of universities and research centers ($m^3$/ day) | 2295 | 4661 | 7314 | 7800 |
| The water needs of hospitals ($m^3$/ day) | 105 | 1405 | 3055 | 3105 |
| The total average daily consumption ($m^3$/ day) | 147254 | 273229 | 363280 | 437087 |
| The maximum monthly consumption ($m^3$/ day) | 159014 | 293646 | 398600 | 498187 |
| The maximum daily consumption ($m^3$/ day) | 166854 | 307258 | 422147 | 538920 |
| The maximum hour consumption ($m^3$/ day) | 176654 | 324273 | 451580 | 589836 |
| The fire requirements $m^3$/ day ($m^3$/ day) | 1944 | 1944 | 1944 | 1944 |

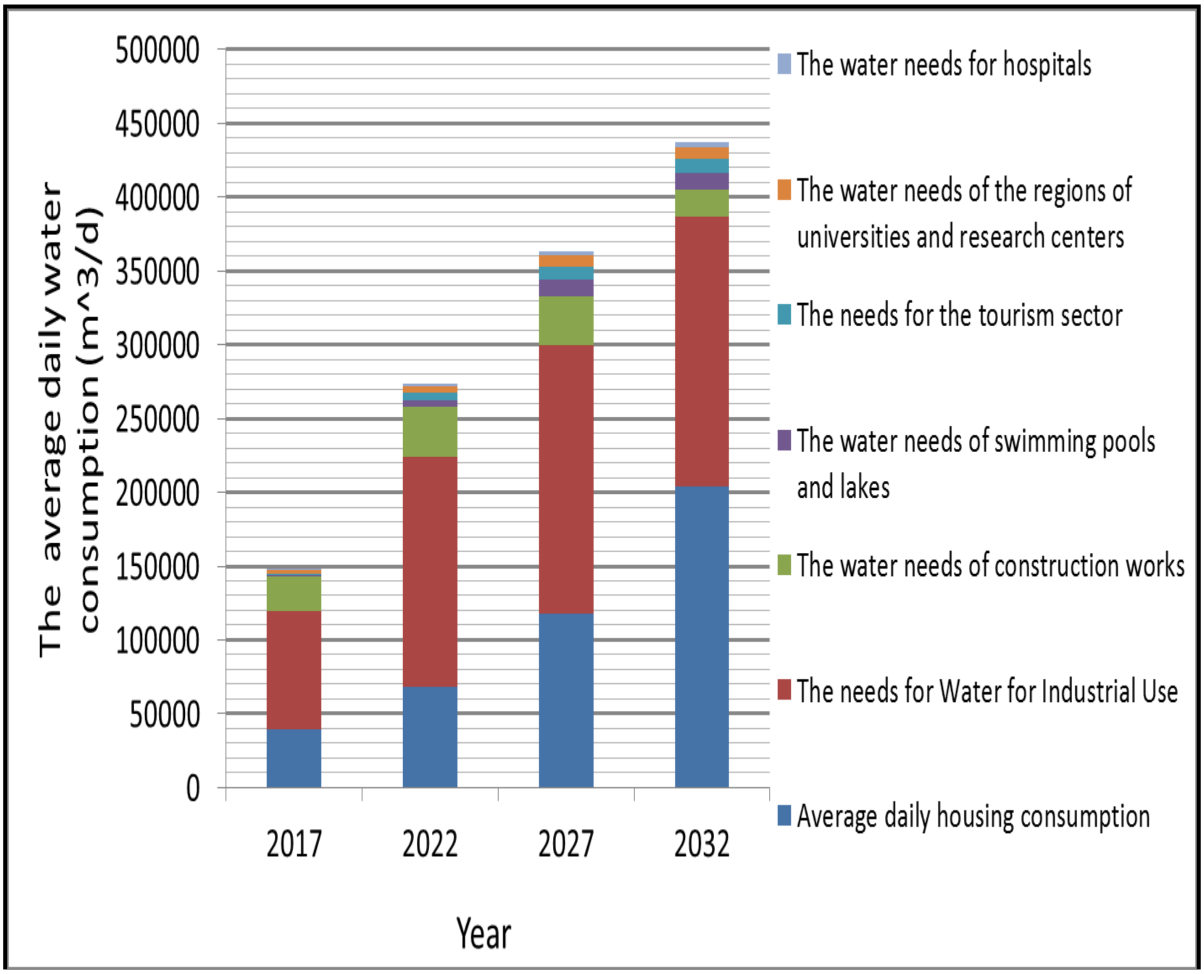


**Figure (4.2): The total average daily consumption for the Burj Al-Arab city until 2032.**

**Table (4.4): The water consumption, domestic flows, and design flow of sewage during development stages.**

| Year | 2017 | 2022 | 2027 | 2032 |
|---|---|---|---|---|
| Average daily domestic consumption ($m^3$/ day) | 39200 | 68058 | 117733 | 203665 |
| The needs of the tourism sector ($m^3$/ day) | 695 | 5150 | 8688 | 9583 |
| The water needs for hospitals ($m^3$/ day) | 105 | 1405 | 3055 | 3105 |
| The water needs of the regions of universities and research centers ($m^3$/ day) | 2295 | 4661 | 7314 | 7800 |
| The Average human daily consumption of water ($m^3$/ day) | 42295 | 79274 | 136790 | 224153 |
| The Average human discharges of wastewater ($m^3$/ day) | 33836 | 63419.2 | 109432 | 179322 |
| The discharge that coming from the prison Al Gharbaniyat ($m^3$/day) | 5000 | 5000 | 5000 | 5000 |
| The Rainwater flows ($m^3$/ day) | 6344.25 | 11891.1 | 20518.5 | 33623 |
| Population (In thousand people) | 140 | 243 | 420 | 727 |
| Peak factor (PF) | 1.884 | 1.715 | 1.572 | 1.452 |
| The maximum daily discharge in summer ($m^3$/ day) | 55754 | 100129 | 169148 | 273984 |
| The maximum design discharge ($m^3$/ day) | 84683.8 | 140955 | 220034 | 330470 |
| The maximum design discharge (L/ Sec) | 980.136 | 1631.42 | 2546.69 | 3824.89 |

## 4.3.2 Estimating the Wastewater Discharges

The materials and methods mentioned in **Sub-section (3.4.2)** in **Chapter (3**) were used and the results were obtained**.**

- **Table (4.4**) shows the results of the amount of water and domestic discharges resulting from the different uses. That's expected to be served by the western tertiary treatment plant being implemented and the design flow of wastewater during different stages of development**.**
- **Table (4.5)** shows the results of the discharges resulting from the previously mentioned industrial zones. That planned to service by the proposed western industrial drainage plant as part of the work of separating the industrial wastewater flows from the domestic wastewater flows**.**
- **Table (4.6)** shows the results of the industrial areas serviced by the eastern station for industrial discharge, as well as the water needs of each area, and its discharge and the combined discharges distributed in different stages of development**.**
- The following **Figure (4.3)** and **Table (4.7)** shows the maximum design flows of wastewater throughout the various stages of development for the Burj Al-Arab city up to the year 2032**.**

**The outcome of this section:**

The domestic maximum design flow resulting from the different uses expected to be served by the western tertiary treatment plant is about **330,470 $m^3$/ day** at 2032. The industrial maximum design flow resulting from the different industrial zones expected to be served by the proposed western industrial treatment plant is about **62,027 $m^3$/ day** at 2032. The industrial maximum design flow resulting from the different industrial zones expected to be served by the eastern industrial treatment plant is about **84,400 $m^3$/ day** at 2032**.**

**Table (4.5): The industrial areas to be serviced by the proposed western industrial wastewater treatment plant are distributed at various stages of development.**

| Year | 2017 | 2022 | 2027 | 2032 |
|---|---|---|---|---|
| The third industrial zone (acres) | 504 | 504 | 504 | 504 |
| The extension of the third industrial zone (acres) | 0 | 300 | 397 | 397 |
| The fourth industrial zone (acres) | 751 | 751 | 751 | 751 |
| The extension of the fourth industrial zone (acres) | 0 | 476 | 476 | 476 |
| The total area (acres) | 1255 | 2128 | 2128 | 2128 |
| The total area (hectare) | 527.1 | 893.8 | 893.8 | 893.8 |
| The water needs ($m^3$/ day) | 45541 | 77221 | 77221 | 77221 |
| The third industrial (workshops and stores) (acres) | 149 | 149 | 149 | 149 |
| The area (hectare) | 62.6 | 62.6 | 62.6 | 62.6 |
| The water needs ($m^3$/ day) | 313 | 313 | 313 | 313 |
| The total water needs ($m^3$/day) | 45854 | 77534 | 77534 | 77534 |
| The total wastewater flows ($m^3$/ day) | 36683 | 62027 | 62027 | 62027 |
| The maximum design flow ($m^3$/ day) | 36683 | 62027 | 62027 | 62027 |
| The maximum design flow (L/ Sec) | 424.6 | 717.9 | 717.9 | 717.9 |

**Table (4.6): The industrial areas serviced by the eastern station for industrial discharge are distributed at different stages of development.**

| Year | 2017 | 2022 | 2027 | 2032 |
|---|---|---|---|---|
| The first industrial zone (acres) | 205 | 205 | 205 | 205 |
| The second industrial zone (acres) | 742 | 742 | 742 | 742 |
| The fifth industrial zone (acres) | 0 | 469 | 674 | 674 |
| The total area (acres) | 947 | 1621 | 3749 | 1621 |
| The total area (hectare) | 397.74 | 680.82 | 1574.58 | 680.82 |
| The water needs ($m^3$/ day) | 34365 | 58823 | 58823 | 58823 |
| The textile and textile industries complex (acres) | 0 | 282 | 422 | 422 |
| The textile and textile industries complex (hectare) | 0 | 118.44 | 177.24 | 177.24 |
| The water needs ($m^3$/ day)<br>The rate of water consumption, 200 $m^3$/ hectare/ day | 0 | 23688 | 35448 | 35448 |
| The engineering and chemical industries zone (acres) | 0 | 176 | 352 | 440 |
| The engineering and chemical industries zone (hectare) | 0 | 73.92 | 147.84 | 184.8 |
| The water needs ($m^3$/ day)<br>The rate of water consumption, 20 $m^3$/ hectare/ day | 0 | 1478 | 2957 | 3696 |
| The small industries complex (acres) | 0 | 115 | 115 | 115 |
| The small industries complex (hectare) | 0 | 48.3 | 48.3 | 48.3 |
| The water needs ($m^3$/ day)<br>The rate of water consumption, 15 $m^3$/ hectare/ day | 0 | 725 | 725 | 725 |
| The second industrial (workshops and stores) (acres) | 127 | 127 | 127 | 127 |
| The valley of technology (acres) | 0 | 582 | 873 | 1038 |
| The smart village (acres) | 0 | 125 | 250 | 378 |
| The logistics area (acres) | 0 | 315 | 496 | 496 |
| The customs department and dry port (acres) | 0 | 276 | 276 | 276 |
| The free zone (acres) | 0 | 678 | 678 | 678 |
| The total area (acres) | 127 | 2103 | 3242 | 3242 |
| The total area (hectare) | 53.3 | 883.3 | 1361.6 | 1361.6 |
| The water needs ($m^3$/ day)<br>The rate of water consumption, 5 $m^3$/ hectare/ day | 267 | 4416 | 6808 | 6808 |
| The total water needs ($m^3$/ day) | 34632 | 89130 | 104761 | 105500 |
| The total wastewater flows ($m^3$/ day) | 27706 | 71304 | 83809 | 84400 |
| The maximum design flow ($m^3$/ day) | 27706 | 71304 | 83809 | 84400 |
| The maximum design flow (L/ Sec) | 320.7 | 825.3 | 970 | 976.9 |

**Table (4.7): The maximum design flows of wastewater throughout the various stages of development.**

| Year | 2017 | 2022 | 2027 | 2032 |
|---|---|---|---|---|
| The domestic maximum design flow resulting from the different uses expected to be served by the western tertiary treatment plant ($m^3$/ day). | 84684 | 140955 | 220034 | 330470 |
| The industrial maximum design flow resulting from the different industrial zones is expected to be served by the proposed western industrial treatment plant ($m^3$/ day). | 36683 | 62027 | 62027 | 62027 |
| The industrial maximum design flow resulting from the different industrial zones is expected to be served by the eastern industrial treatment plant ($m^3$/ day). | 27706 | 71304 | 83809 | 84400 |

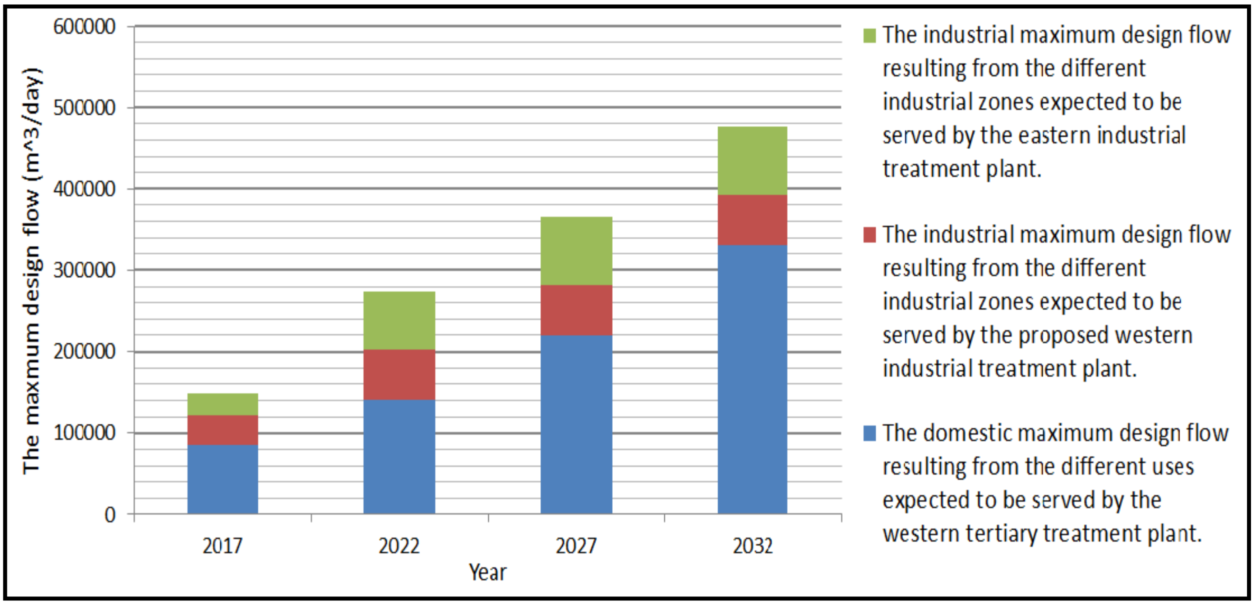


**Figure (4.3): The maximum design flows of wastewater throughout the various stages of development.**

## 4.4 Evaluation of the Position of the Wastewater Works to Calculate the Requirements of the Strategic Plan

In this section, the position of the wastewater works is evaluated in terms of separating human wastewater from industrial wastewater. Solutions have been studied and recommendations are obtained, namely, there is no need to increase the design capacity of the wastewater works. This is because the wastewater works can accommodate estimated flows until the target year. A detailed study was done as follows**:**

### 4.4.1 The Evaluation of the Position of the Domestic Wastewater Treatment Plant

In this sub-sector, the current necessary data about the western tertiary treatment station in the new city of Burj Al-Arab mentioned in the **sector (A-3)** in **Appendix (A)** has been reviewed. Solutions have been studied and recommendations are obtained, namely, there is no need to increase the design capacity of the western tertiary treatment station. This is because the western tertiary treatment station can accommodate estimated flows**.**

- **A detailed study is as follows:**

The western tertiary treatment station is implemented to deal with domestic flows. The design capacity is 115,000 $m^3$/ day for the first stage of the western tertiary treatment station, which was implemented. The design capacity of the western tertiary treatment station will increase to be 345,000 $m^3$/ day at the completion of the three stages before 2032, with a capacity of 115,000 $m^3$/ day for each stage [4].

**The outcome of this section:**

In reviewing the western tertiary treatment station's planned flows and expected flows of the new Burj Al-Arab city and the different stages of development that are estimated as shown in **Table (4.4)**. The maximum design flow is 330,470 $m^3$/ day in 2032. It is clear that the western tertiary treatment station is sufficiently designed (345,000 $m^3$/ day) to accommodate the city's flows to the target year.

### 4.4.2 The Evaluation of the Position of the Main Lift Stations for Domestic Discharges

In this sub-sector, the current necessary data about the works of the main lifting stations that are scheduled to lift domestic discharges directly to the western tertiary treatment station in the new city of Burj Al-Arab that is mentioned in the **sector (A-3)** in **Appendix (A)** has been reviewed. Solutions have been studied and recommendations are obtained, namely, there is no need to increase the design capacity of the main lifting stations that are scheduled to lift domestic discharges directly to the western tertiary treatment station. This is because the main lifting stations that are scheduled to lift domestic discharges directly to the western tertiary treatment station can accommodate estimated flows.

- **A detailed study is as follows:**

The main lifting stations that are scheduled to lift domestic discharges directly to the western tertiary treatment station have a total design capacity of about 443,000 $m^3$/ day as shown in **Table (4.8)** [4].

**The outcome of this section:**

In reviewing the main lifting stations that are scheduled to lift domestic discharges directly to the western tertiary treatment station planned flows and expected flows of the new Burj Al-Arab city and the different stages of development that are estimated as shown in **Table (4.4).** The maximum design flow is 330,470 $m^3$/ day in 2032. It is clear that the main lifting stations that are scheduled to lift domestic discharges directly to the western tertiary treatment station are sufficiently designed (443,000 $m^3$/ day) to accommodate the city's flows to the target year [4].

### 4.4.3 The Evaluation of the Position of the Proposed Western Industrial Wastewater Treatment Plant

In this sub-sector, the current necessary data about the proposed western industrial wastewater treatment plant in the new city of Burj Al-Arab mentioned in the **sector (A-3) in Appendix (A)** has been reviewed. Solutions have been studied and recommendations are obtained, namely, there is no need to increase the design capacity of the proposed western industrial wastewater treatment plant. This is because the proposed western industrial wastewater treatment plant can accommodate estimated flows.

**Table (4.8): The lift stations for lifting human flows to the western treatment station [4].**

| Main lift stations | Design capacity ($m^3$/ day) | Areas serviced by the station | Point of discharge |
|---|---|---|---|
| Lifting station (D) phase II | 73,000 | South of the second and third neighborhoods and the university area | The western tertiary treatment station |
| The fourth and fifth neighborhoods lift station | 104,000 | The flows of the fourth and fifth neighborhoods in addition to the flows of the proposed lift station next to the lift station (A) for the service of the first district and north of the second and third neighborhoods and the eastern central axis | |
| The north of the sixth neighborhood lift station | 95,040 | The flow of the sixth neighborhood and part of the flow of the Middle central axis | |
| The north of the eighth neighborhood lift station | 86,400 | The flow of the eighth neighborhood and part of the flow of the middle central axis | |
| The seventh neighborhood lift station | 34,560 | The flow of the Seventh neighborhood and Agharbanaat Prison | |
| The eleventh neighborhood lift station | 50,000 | The flow of the eleventh, twelfth, and thirteenth residential neighborhoods, specialty resort, gardens, and amusement park | |
| The total flows | 443,000 | ($m^3$/ day) | |

- **A detailed study is as follows:**

The capacity of the proposed western industrial wastewater treatment plant is about 65,000 $m^3$/ day [4].

- **The outcome of this section:**

In reviewing the proposed western industrial wastewater treatment plants planned flows and expected flows of the new Burj Al-Arab city and the different stages of development that are estimated as shown in **Table (4.5)**. The maximum design flow is 62,000 $m^3$/ day in 2032. It is clear that the western tertiary treatment station is sufficiently designed (65,000 $m^3$/ day) to accommodate the city's flows to the target year [4].

### 4.4.4 The Evaluation of the Position of the Eastern Industrial Wastewater Treatment Plant, That Under Development

In this sub-sector, the summary of current necessary data about the eastern industrial wastewater treatment plant (The Eastern Oxidation Plant) in the new city of Burj Al-Arab is mentioned in the **sector (A-3)** in **Appendix (A)** has been reviewed. Solutions have been studied and recommendations are obtained, namely, there is no need to increase the design capacity of the eastern industrial wastewater treatment plant. This is because the eastern industrial wastewater treatment plant can accommodate estimated flows.

- **A detailed study is as follows:**

The existing eastern industrial wastewater treatment plant is being rehabilitated and expanded to increase the capacity of the eastern industrial wastewater treatment plant from 36,000 $m^3$/ day to 100,000 $m^3$/ day [4]**.**

**The outcome of this section:**

As mentioned in **Table (4.6)**. The industrial wastewater discharges of the rest industrial zones that are serviced by the eastern industrial wastewater treatment plant are estimated for these areas by 84,400 $m^3$/ day at 2032. This means no need to increase the design capacity. Because the capacity after the expansion (100,000 $m^3$/ day) is sufficient to treat the industrial wastewater of the area, that is serviced from this plant [4]**.**

### 4.4.5 The Evaluation of the Position of the Main Lift (d) Station for Industrial Discharges

In this sub-sector, the summary of current necessary data about the lifting station (d) in the new city of Burj Al-Arab that is mentioned in the **sector (A-3)** in **Appendix (A)** has been reviewed. Solutions have been studied and recommendations are obtained, namely, there is no need to increase the design capacity of the lifting station (d). This is because the lifting station (d) can accommodate estimated flows**.**

- **A detailed study is as follows:**

As for the lifting station (d), which is supposed to serve the third industrial zone, its extension, the workshop zone, the fourth industrial zone, and its extension. Its point of discharge is the proposed western industrial wastewater treatment plant and design capacity 77,760 $m^3$/ day and the 1000 mm lifting line [4]**.**

**The outcome of this section:**

Where the future discharges are estimated for these areas that are served by the lifting station (d) by 62,027 $m^3$/ day at 2032, as mentioned in **Table (4.5)**. This means no need to increase the design capacity. Because the current capacity (77,760 $m^3$/ day) of the lifting station (d) is sufficient to lift the industrial wastewater of the area are serviced from this plant [4]**.**

- **Note**: The discharges of the rest industrial zones are received to the eastern industrial wastewater treatment plant by slope lines [4]**.**

## 4.5 The Evaluation of the Position of the Drinking Water Feeding Works to Calculate the Requirements of The Strategic Plan

In this sub-sector, the current necessary data about the works of water supply in the new city of Burj Al-Arab that is mentioned in **Chapter (2)** and **sector (A-2)** in **Appendix (A)** has been reviewed**.** The new city of Burj Al-Arab depends on a drinking water station in Kilo 40, (Alexandria-Cairo desert road) in providing drinking water. The station has an existing design capacity of about **566,000 $m^3$/ day**. New Burj Al-Arab's share of the total capacity of the Kilo 40 station is About **166,000 $m^3$/ day** and the rest capacity is **400,000 $m^3$/ day** dedicated to feeding the northern coast and Matrouh [4]**.**

There is a proposal to use treated water from the western domestic tertiary treatment station to irrigate green areas, which is currently being implemented. The amount of water required for the irrigation process of green spaces in the city was estimated at **78,000 $m^3$/ day** [4]. From the estimation of the quantities of water required for all uses during the development period in the new Burj Al-Arab city that is illustrated in **Table (4.3)**. It turns out that the city needs to raise the capacity of the water supply from **166,000 $m^3$/ day** to **498,000 $m^3$/ day** to cover the maximum monthly consumption in 2032. This means that the water needs will be triple their capacity. There are three suggested available configurations of PV-RO plant as an alternative for water supply will be studied to choose the best economical one to cover the future capacity deficit of the water supply that feeds the city with water. The net additional water capacity required until 2032 can obtain by the following **Equation:**

$$NW_{2032} = TW_{2032} - W_{40} - W_{reuse} \tag{4.1}$$

$NW_{2032}$ = 498000 – 166000 – 78000 = (254,000 $m^3$/ day)

where, $NW_{2032}$ = the net additional water capacity required until 2032; $TW_{2032}$ = the total estimated water amount by the year 2032; $W_{40}$ = the amount of water received from the Kilo 40 station; $W_{reuse}$ = the amount of reused treated wastewater**.**

- **The outcome of this section:**

The net additional water capacity required for the new city of Burj Al-Arab until 2032 is 254,000 $m^3$/ day**.**

## 4.6 Design of the (PV-RO) System

The design of the (PV-RO) System was based on the design steps given in **Chapter (3)**. All the assumptions and estimated parameters are explained and the results are given for each step**.**

- **Step 1: The product volume requirement**

**Equation (3.1)** is applied and the total amount of product water for three suggested configurations of the PV-RO plant is calculated**:**

$F_{Total} = \text{maximum monthly discharge} + 7\,\%$ = (271,780 $m^3$/ day)

- **Step 2: The characteristics of the feed water and maximum water recovery possible during desalination**

  - The characteristics of the feed water were illustrated in **Chapter (3) - Table (3.3).**
  - The maximum water recovery possible during desalination is taken at 40%**.**
  - Product water target salinity was illustrated in **Chapter (3),** (The product water salinity is targeted to be in the range of 500 mg/ l)**.**

### Step 3: Pre-treatment requirements

**Equation (3.2)** is applied and the total water supply per day (to be provided by the feed pumps) for three suggested configurations of the PV-RO plant is calculated**:**

$$F_{Total\ (Feed)} = \frac{maximum\ monthly\ discharge + 7\ \%}{RR} = (679{,}450\ m^3/\ day)$$

**The outcome of step 3:**

- **Figure (4.4)** shows the design flow rates of the desalination plant**.**
  - Maximum supply to pre-treatment system: (679,450 $m^3$/ day)**.**
  - Maximum product water from RO plant: (254,000 $m^3$/ day)**.**

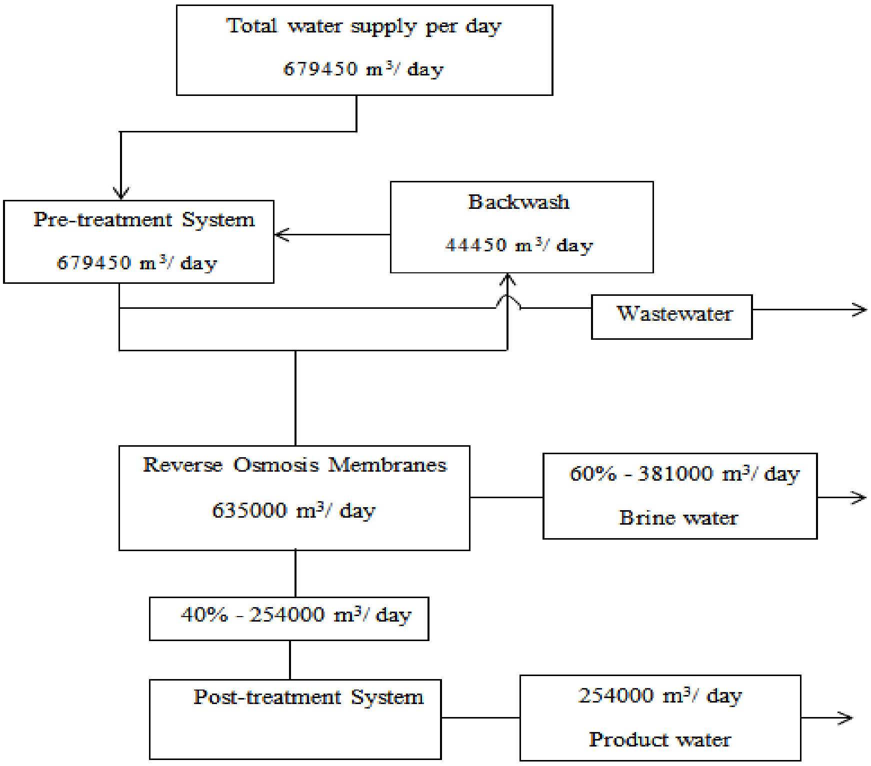


**Figure (4.4): Flow diagram of the desalination plant.**

### Step 4: Consider post-treatment and brine discharge

**[1] Consider post-treatment**

In this sub-sector, the current necessary data about the works of ground storage in the new city of Burj Al-Arab that is mentioned in **Appendix (A)** has been reviewed. Solutions have been studied and recommendations are obtained, namely, increasing the number of ground reservoirs. This is because the existing ground tanks in the city have insufficient capacity to meet the requirements of the future needs for the continuity of efficiently feeding of water. This creates a great risk if the water plant stops production or breaks the water lines. The Produced water from the RO plant needs to be stabilized and disinfected before it can be used and for these reasons the importance of the ground tanks**.**

- **A detailed study is as follows:**

**The Total Ground Storage Capacity Requirement**

There are two ground reservoirs with a capacity of 24,000 $m^3$ that are implemented in the city. Thus, the total ground tanks capacity for the city is currently 48,000 $m^3$ [4]. The ground tanks will be designed as following (see **Table (3.2)**):

**The total ground storage requirements** = maximum daily consumption - maximum monthly consumption + 80% of the fire requirements**.**

From **Table (4.3)**, a value of maximum daily consumption, maximum monthly consumption, and fire requirements can be obtained. And these values can be compensated in the previous equations, to get the results are shown in **Table (4.9).**

**Table (4.9): High and ground storage needs during different periods of development.**

| Year | 2017 | 2022 | 2027 | 2032 |
|---|---|---|---|---|
| The capacity of the existing and under construction ground tanks ($m^3$) | 48000 | 48000 | 48000 | 48000 |
| The total ground storage capacity requirements ($m^3$) | 41300 | 75000 | 101000 | 123000 |
| The shortage of ground storage capacity ($m^3$) | 0 | 27000 | 53000 | 75000 |

As shown in **Table (4.9)**, the total required capacity of the ground tanks in the city is currently 32,500 $m^3$ and will rise to about 123,000 $m^3$ in the target year. Thus, there is a need to establish new ground reservoirs with a capacity of 75,000 $m^3$ to suffice the city until the year target 2032**.**

**[2] Brine Discharge**

The brine water will be released into the sea. This outfall technique should be investigated by a specialist to determine if any damage to the environment may accrue**.**

**The outcome of step 4:**

The establishment of five ground storage reservoirs for drinking water is proposed with a capacity of 15,000 $m^3$/ tank with a total capacity of about 75,000 $m^3$, this capacity is sufficient for the city until 2032. Thus, the city's ground storage capacity is raised from 48,000 $m^3$ to 123,000 $m^3$. It is proposed to establish the ground storage tanks according to hydraulic studies of the water network as well as the topography of the city**.**

**Step 5: Calculate the feed pressure requirement and the number of membranes required**

Integrated Membrane Solutions Design (IMSDesign) software was used to design, optimize and analyze the performance of the designed plant and testing the configuration according to seawater analysis shown in **(Table (3.3)** in **Chapter (3))**. **Table (4.10)** shows the design parameters of the designed RO desalination plant, including the amount of pressure required for the desalination process. The additional technical data for the components of the RO system and the results of the simulation are provided in **Appendix (D).**

**Table (4.10): Reverse osmosis plant design parameters.**

| Design parameters | Pass 1 | Total system |
|---|---|---|
| Company name | Hydranautics | |
| Design software used | IMS design | |
| Pressure vessels configuration | 1 stage | |
| No. of trains | | 10 |
| Permeate recovery % | 40 | 40 |
| Average flux, lmh | 13.5 | |
| No. of pressure vessels | 318 | 3180 |
| No. of membranes | 1908 | 19080 |
| No. of membranes per pressure vessels | 6 | |
| Nominal diameter, inch | 8 | |
| Membrane model | SWC6 MAX | |
| Max. operating pressure, bar | 83 | |
| Working pressure, bar | 51 | |
| ph | 8 | |
| Temperature, $^oC$ | 25 | |
| Feed flow, $m^3/d$ | 63500 | 635000 |
| Permeate flow, $m^3/d$ | 25400 | 254000 |
| Concentrate flow, $m^3/d$ | 38100 | 381000 |
| Fouling factor, % | 96 | 96 |
| Concentrate salinity, mg/ l | 65163.20 | 65163.20 |
| Permeate salinity, mg/ l | 433.86 | 433.86 |
| Feed salinity, mg/ l | 39282.93 | 39282.93 |

**The outcome of step 5:**

In order to increase the product volume, resulting from a low recovery ratio, a single array Multi-Element (See **Figure (4.5)**) is often used in the feed water has a higher salt concentration. The pressure vessel and membrane configuration are exactly the same as the **Single Element System**, but with a number of elements in parallel. A larger pump is required to supply the right amount flow rate to the membranes. In the Burj Al-Arab case, this configuration was used. Four large pumps **(4 × 6118.3 KW = 24,473 KW)** were connected in parallel to supply **10 RO trains** with feed water. Note that each train contains **318 pressure vessels**. Each pressure vessel contains **six spirals** wound RO membranes. That is more than **19080 membrane elements.**

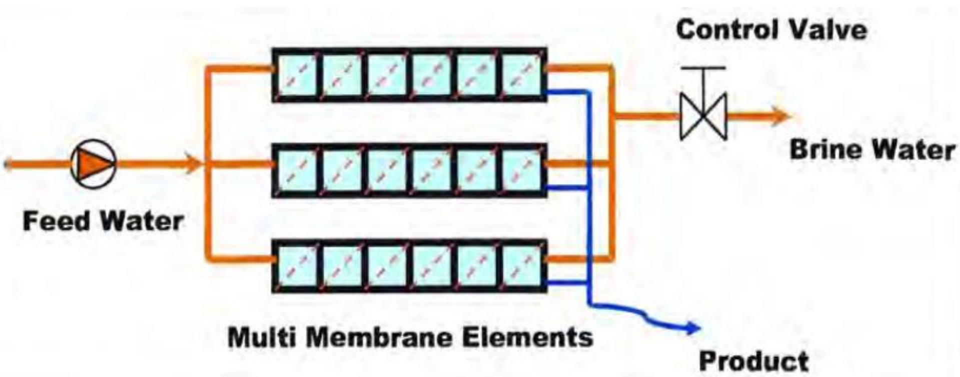


**Figure (4.5): Multi RO membrane element process.**

### Step 6: Estimate the energy requirements of the RO plant

#### [1] High-pressure pumps energy requirements ($E_{(desalination)}$)

High pressure pumps (HPP) are used to achieve this high feed pressure. However, this results in high energy demands ($E_{(desalination)}$) for the RO process [56]. Therefore, a high-pressure pump with energy recovery devices (ERD) will be chosen to reduce the energy used in the desalination process. The selection of the high-pressure pump with energy recovery devices (ERD) depends on the minimum and maximum flow rates, discharge pressure required, suction pressure available, and the maximum temperature, where these parameters are obtained from the IMSDesign detailed report. The $E_{(desalination)}$ and other design parameters of the high-pressure feed pumps can be obtained from an IMSDesign detailed report (see **Table (4.11)).**

**Table (4.11): High pressure pumps design parameters [53].**

| Power Calculation (with ERD) | Pass 1 | Total system |
|---|---|---|
| Working pressure, bar | 51 | |
| Pump/Boost pressure, bar | 26.7 | |
| Product flow $m^3$/ d | 25400 | 254000 |
| Pump flow $m^3$/ d | 63500 | |
| Total number of transfer pumps | (4 main + 2 stand by) | |
| Pump efficiency % | 87 | |
| Motor efficiency % | 95 | |
| Variable Frequency Drive(VFD) efficiency % | 97 | |
| Brake horse power BHP | 3280.6 | |
| Total pumping power KW | 2447.3 | 24473 |
| Total energy consumption of pumps KWh | 58735.2 | 587352 |
| Pumping specific energy KWh/ $m^3$ | 2.31 | 2.31 |

#### [2] Transfer pumps (Feed water pumps) energy requirements ($E_{(Transfer\ pumps)}$) and lifting pumps energy requirements ($E_{(Lifting\ pumps)}$)

**Equations (3.5 - 3.12)** are applied and the energy requirements of the transfer pumps and lifting pumps ($E_{(Transfer\ pumps)}$ and $E_{(Lifting\ pumps)}$) are calculated for the three suggested PV-RO plant configurations. **Tables (4.12** and **4.13)** show the design parameters of the transfer Pumps and Lifting pumps**.**

#### The outcome of step 6:

The total power required for the RO plant can be calculated as follows**:**

#### The first ( Power MW):

$$P_{Total} = (P_{(desalination)} + Power_{(Total\ transfer\ pumps)} + Power_{(Total\ lifting\ pumps)})$$

$$P_{Total} = (24473 + 4402.4 + 1041.9) = 29917.3 \text{ KW} \approx 30 \text{ MW}$$

**The second (Energy MWh):**

$$E_{Total} = (E_{(desalination)} + E_{pre\,(\text{transfer}\ pumps)} + E_{(Lifting\ pumps)})$$

$$E_{Total} = (587352 + 105657.6 + 25005.6) = 718015 \text{ KWh} \approx 720\text{MWh}$$

**The third (specific energy KWh/ m$^3$):**

$$Total\ specific\ energy = \left(\frac{E_{(desalination)}}{Total\ Water\ production} + \frac{E_{pre\,(\text{transfer}\ pumps)}}{Total\ Water\ production} + \frac{E_{(Lifting\ pumps)}}{Total\ Water\ production}\right)$$

$$Total\ specific\ energy = (2.31 + 0.42 + 0.1) = 2.83 \text{ KWh/ m}^3$$

**Table (4.12): Transfer pumps design parameters.**

| Power Calculation (with ERD) | Total system |
|---|---|
| Pump pressure (bar) | 4.5 |
| Feed water flow m$^3$/ d | 679450 |
| Pump flow m$^3$/ d | 86400 |
| Total number of transfer pumps | (8 main + 4 stand by) |
| Pump efficiency % | 87 |
| Motor efficiency % | 95 |
| Variable Speed Drive (VFD) efficiency % | 97 |
| Power consumed by each pump KW | 550.3 |
| Total pumping power KW | 4402.4 |
| Total energy consumption of transfer pumps KWh | 105657.6 |
| Pumping specific energy KWh/ m$^3$ | 0.42 |

**Table (4.13): Lifting pumps design parameters.**

| Power Calculation (with ERD) | Total system |
|---|---|
| Pump pressure (bar) | 2.84 |
| Water flow m$^3$/ d | 254000 |
| Pump flow m$^3$/ d | 86400 |
| Total number of transfer pumps | (3 main + 2 stand by) |
| Pump efficiency % | 87 |
| Motor efficiency % | 95 |
| Variable Speed Drive (VFD) efficiency % | 97 |
| Power consumed by each pump KW | 347.3 |
| Total pumping power KW | 1041.9 |
| Total energy consumption of transfer pumps KWh | 25005.6 |
| Pumping specific energy KWh/ m$^3$ | 0.1 |

### Step 7: The photovoltaic systems (PVs) design calculations

In this report, solar energy was considered a renewable energy source for the RO plant. SO, the feasibility study of the PV-RO plant was investigated for the three suggested configurations mentioned in **the sector (3.5)** in **Chapter (3).**

PVsyst V6.86 software program was used to design, optimize, sizing PV arrays and battery banks and analyze the performance of the designed PV system. The input data of details of the defined site was obtained from **(Table (3.7)** in **Chapter (3))**. The input data of system parameters were used in designing the PV was obtained from **(Table (3.8)** in **Chapter (3))**. The input data of the financial variables and plant lifetime, capital costs values, operating costs values, grid-level system costs values, and external or social costs values were obtained from **(Tables (3.10 - 3.16)** in **Chapter (3)).**

After the design of the PV system using the PVsyst V6.86 software program and obtaining the outputs that are used as input data of **Equations (3.15)** to estimate the LCOE of PV generated power for each configuration**.**

- **Table (4.14)** shows the unit energy cost (USD/ KWh) for all PV system configurations. The additional technical data for the components of the PV system and the results of the simulation are provided in **Appendix (C).**

**Figure (4.14): The unit energy cost (USD/ kWh) for all PV system configurations.**

| Identifier | PV solar only | PV solar and batteries | PV solar and electricity grid |
|---|---|---|---|
| PV configuration | Two-axis tracking | Two-axis tracking | Two-axis tracking |
| Average RO load (KW) | 30000 | 30000 | 30000 |
| Global horizontal irradiation (daily inputs) (total KWh/ $m^2$/ year) | 3055 | 3055 | 3055 |
| PV module dc efficiency (%) | 21.9 | 21.9 | 21.9 |
| PV system efficiency (%) | 17.68 | 16.85 | 17.68 |
| Solar Fraction ($E / E_{TOTAL}$) (%) | 29.27 (From the PV) | 61.41 (29.27 From the PV) + (32.14 From the batteries) | 100 (29.27 From the PV) + ( 70.73 From the grid) |
| PV capital cost (USD/ KW) | 1706.6 | 7504.5 | 1706.6 |
| PV O&M cost (USD/ KW/ year) | 25.6 | 112.7 | 25.6 |
| PV lifetime (years) | 25 | 25 | 25 |
| Discount rate (%) | 5 | 5 | 5 |
| Grid selling price (USD/ KWh) | | | 0.079 |
| Levelized transmission cost and distribution grid infrastructure (USD/ KWh) | | | $3.3 \times 10^{-3}$ |
| Emission factor for Electricity and Carbon Tax (USD/ KWh) | | | $9.7\times10^{-3}$ |
| LCOE solar electricity (USD/ KWh) | 0.1 | 0.21 | 0.1 |
| LCOE mix electricity into RO (USD/ KWh) | 0.1 | 0.21 | 0.086 |

### The outcome of step 7:

This section presents the economic study (LCOE) of the generated unit energy cost (USD/ KWh) from the three PV system configurations (see **Figure (4.6)** and **Figure (4.7)**).

- The PV-RO system with PV solar and electricity grid has the lower unit energy cost (0.086 USD/ KWh) and the higher solar fraction ratio (100%).
- The PV-RO system with PV solar only has the unit energy cost equal to (0.1 USD/ KWh) and a lower solar fraction ratio (29.27%).
- The PV-RO system with PV solar and batteries has the higher unit energy cost (0.21 USD/ KWh) and the solar fraction ratio equal to (61.41 %).

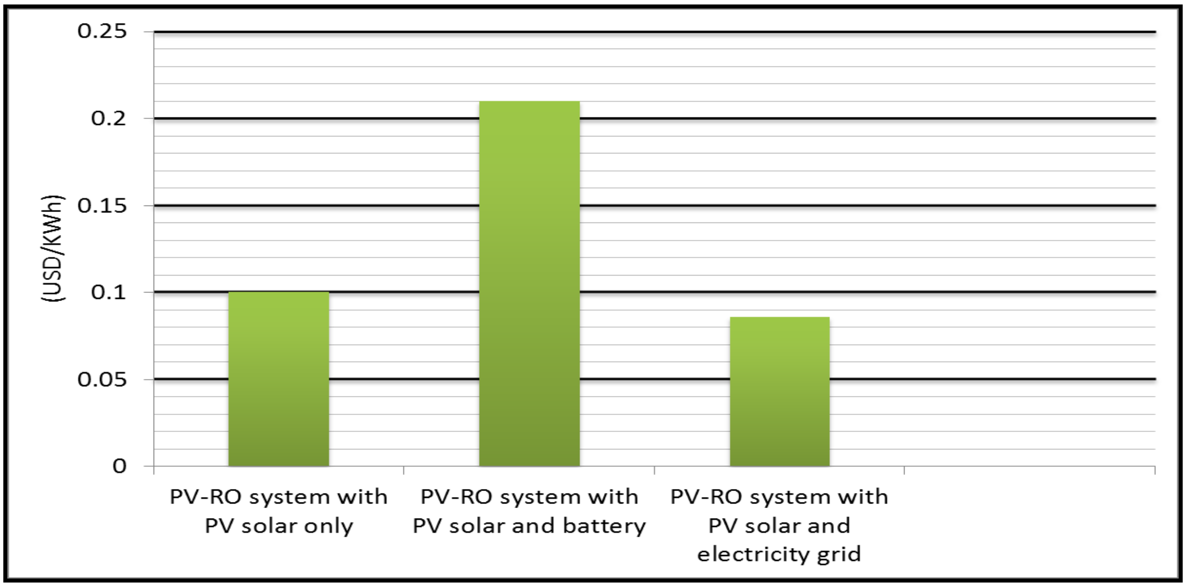


**Figure (4.6): The unit energy cost (USD/ KWh) for all PV system configurations.**

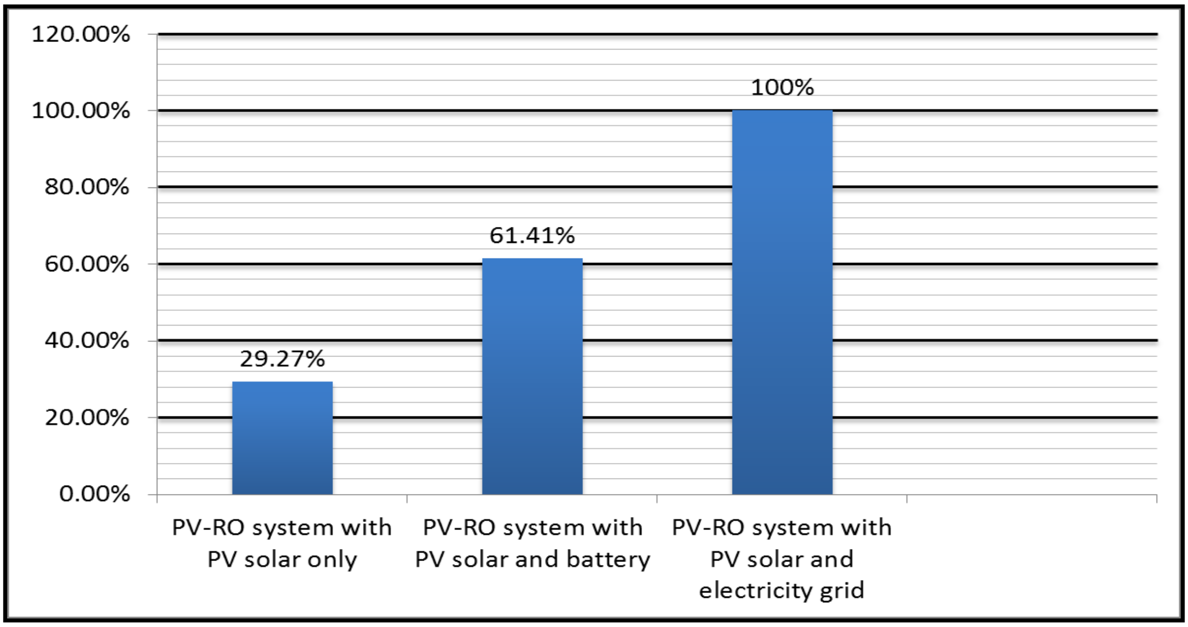


**Figure (4.7): The solar fraction ($E/ E_{TOTAL}$) ratio for different PV configurations.**

### Step 8: Estimate the Levelized Cost of Water (LCOW) of the RO plant

Initially, the capital costs must be taken into consideration in making the economic calculations of the desalination plant by reverse osmosis. The cost of a new plant is derived from the cost of a similar plant of known capacity, but not necessarily the same end product (the product should be relatively similar, however).

The RO plants' capital costs mentioned in **Table (3.20)** in **Chapter (3)** are used as input data of **Equations (3.17)** to estimate the equivalent capital cost of RO plant at 254,000 $m^3$/ day capacity. **Table (4.15)** shows the actual capital costs for the SWRO plants in the Mediterranean area available in the literature and their equivalent capital cost of RO plants at 254,000 $m^3$/ day capacity. The equivalent average equivalent capital cost was selected (280 million USD) that is used as the cost estimation input.

The financial variables and plant lifetime, Capital costs values, and operating costs values mentioned in **Tables (3.18 - 3.24)** in **Chapter (3)** are used as input data of **Equations (3.16)** to estimate the LCOW. The availability rates mentioned in **Table (3.17)** in **Chapter (3)** and solar fraction mentioned in **Table (4.14)** are used to estimate the actual amount of water produced in the year that is used as input data of **Equations (3.16)** to estimate the LCOW too.

**Table (4.15): The capital costs for the SWRO plants in the Mediterranean area available in the literature and the actual value selected for the cost estimation.**

| Plant name and location | Size ($m^3$/ day) | The proposed RO plant Size ($m^3$/ day) | Capital cost (million USD) | The equivalent capital cost of RO plants at 254,000 $m^3$/ day capacity (million USD) | Value used |
|---|---|---|---|---|---|
| Sorek, Israel | 624000 | 254000 | 480 | 279.9 | The Average of the equivalent capital cost of RO plants with 254,000 $m^3$/ day capacity is selected for the cost estimation = 280 million USD |
| Magtaa, Algeria | 500000 | | 512 | 341 | |
| Larnaca, Cyprus | 64000 | | 80.0 | 182.9 | |
| Larnaca, Cyprus | 62000 | | 80 | 186.4 | |
| Hamma, Algeria | 200000 | | 272.2 | 314.2 | |
| Ashdod, Israel | 320000 | | 444 | 386.5 | |

- As mentioned, all the three suggested PV-RO plant configurations are assumed to have the same design capacity of 254,000 $m^3$/ day. A salinity of 39,282 ppm has been assumed.
- The first part of the comparison includes an overview of the main technical data, as presented in **Table (4.16).**

#### The outcome of step 8:

- The comparison of the LCOW shows that (under the given assumptions) the PV-RO system with PV solar and electricity grid (grid backup) configuration is the best-performing one because it gave the lowest cost of cubic meter production **(0.892 USD/ $m^3$)**, which is due to the low cost of unit energy for the integration of electricity of the grid and the PV system of **(0.086 USD/ KWh)** and high RO plant availability rate of 90%). **Figure (4.8**) shows the breakdown of the annualized cost of the (PV-RO system with PV solar and electricity grid) configuration. The breakdown includes capital costs of the RO plant, Energy costs, net maintenance costs, and net other operating costs. In this scenario, energy accounts for 27.24% of the water production cost.

**Table (4.16): Comparison of investment, operation cost, and LCOW.**

| Identifier | Units | PV-RO system with PV solar only | PV-RO system with PV solar and battery | PV-RO system with PV solar and electricity grid |
|---|---|---|---|---|
| The design capacity of the RO plant | m³/ d | 254000 | 254000 | 254000 |
| Working pressure | bar | 51 | 51 | 51 |
| Permeate recovery | % | 40 | 40 | 40 |
| The design capacity of the PV system | MW | 30 | 30 | 30 |
| Discount Rate | % | 5 | 5 | 5 |
| RO plant lifetime | Year | 25 | 25 | 25 |
| PV System Efficiency | % | 17.68 | 16.85 | 17.68 |
| RO plant Availability rate ≈ Solar Fraction | % | 29 | 61 | 90 |
| The actual amount of water produced in the year | m³/ d | 73660 | 154940 | 228600 |
| Amount of water produced in the year | m³/ yr | 26885900 | 56553100 | 83439000 |
| Capital Expense | | | | |
| RO capital cost | USD | $280\times 10^6$ | $280\times 10^6$ | $280\times 10^6$ |
| The capital cost of water transmission line | USD | $10 \times 10^6$ | $10 \times 10^6$ | $10 \times 10^6$ |
| The capital cost of ground storage tanks | USD | $9.375\times 10^6$ | $19.375\times 10^6$ | $9.375\times 10^6$ |
| The total capital cost | USD | $299.375\times 10^6$ | $299.375\times 10^6$ | $299.375\times 10^6$ |
| Energy Expense | | | | |
| Total specific energy | KWh/ m³ | 2.83 | 2.83 | 2.83 |
| The unit energy cost for all PV system configurations | USD/ KWh | 0.1 | 0.21 | 0.086 |
| Energy expense | USD/ m³ | 0.283 | 0.594 | 0.243 |
| Net energy cost | USD/yr | $7.61\times10^6$ | $33.59\times10^6$ | $20.28\times10^6$ |
| Membrane replacement cost and Other maintenance costs | | | | |
| Total elements | Number | 19080 | 19080 | 19080 |
| Membrane replacement rate | %/ yr | 40 | 40 | 15 |
| The membranes that replaced it | Number | 7632 | 7632 | 2862 |
| Replacement cost | USD/ element | 846.40 | 846.40 | 846.40 |
| Replacement cost for elements | USD/ yr | $6.46\times10^6$ | $6.46\times10^6$ | $2.42\times10^6$ |
| Other maintenance costs | USD/ yr | $4.49\times10^6$ | $4.49\times 10^6$ | $4.49\times10^6$ |
| Net maintenance costs (M costs) | USD/yr | $10.95\times10^6$ | $10.95\times10^6$ | $6.91\times10^6$ |
| Other operating costs | | | | |
| The chemical costs | USD/ m³ | 0.02 | 0.02 | 0.02 |
| The specific costs for labor | USD/ m³ | 0.02 | 0.02 | 0.02 |
| Brine disposal cost | USD/ m³ | 0.04 | 0.04 | 0.04 |
| The total of other operating costs | USD/ m³ | 0.08 | 0.08 | 0.08 |
| Net other operating costs (O costs) | USD/ yr | $2.15\times10^6$ | $4.52\times10^6$ | $6.68\times10^6$ |
| The annual cost of operation and maintenance | | | | |
| The annual cost of (O and M) | USD/ yr | $13.1\times10^6$ | $15.47\times10^6$ | $13.59\times10^6$ |
| The total annual cost of operation, maintenance, and energy | | | | |
| The annual cost of (Energy , O, and M) | USD/ yr | $20.71\times10^6$ | $49.06\times 10^6$ | $33.87\times10^6$ |
| Water Production Cost (LCOW) | | | | |
| LCOW | USD/ m³ | 2.278 | 1.585 | 0.892 |

- PV-RO system with PV solar and batteries configuration delivers high LCOW **(1.585 USD/ m³)**, which is due to the intermittent operation of the desalination plant (the (PV+ battery) system covers 61% of the capacity of the RO plant). Also, the still relatively high investment, operation, and maintenance costs for the battery. This characteristic can also be appreciated in **Figure (4.9)**, which shows the share of capital cost, operation cost, and electricity on the LCOW**.**

- PV-RO system with PV solar only configuration delivers much higher LCOW **(2.279 USD/ m³)**, which is due to the photovoltaic system operates only during daylight hours, which is solely used for the supply of the desalination plant (as no electricity is fed from the electricity network in these cases). Electricity generated by the photoelectric system covers 29% of the capacity of the RO plant (RO plant Availability rate ≈ Solar Fraction) and this results in less water produced, which causes the price of cubic meters produced from the water to rise**.**

- **Table (4.17)** shows the investment plan of the proposed (PV-RO system with PV solar and the electricity grid with 254,000 m$^3$/ day capacity) project and displays the descriptive data for proposed projects of water, to clarify the purpose of the project**.**

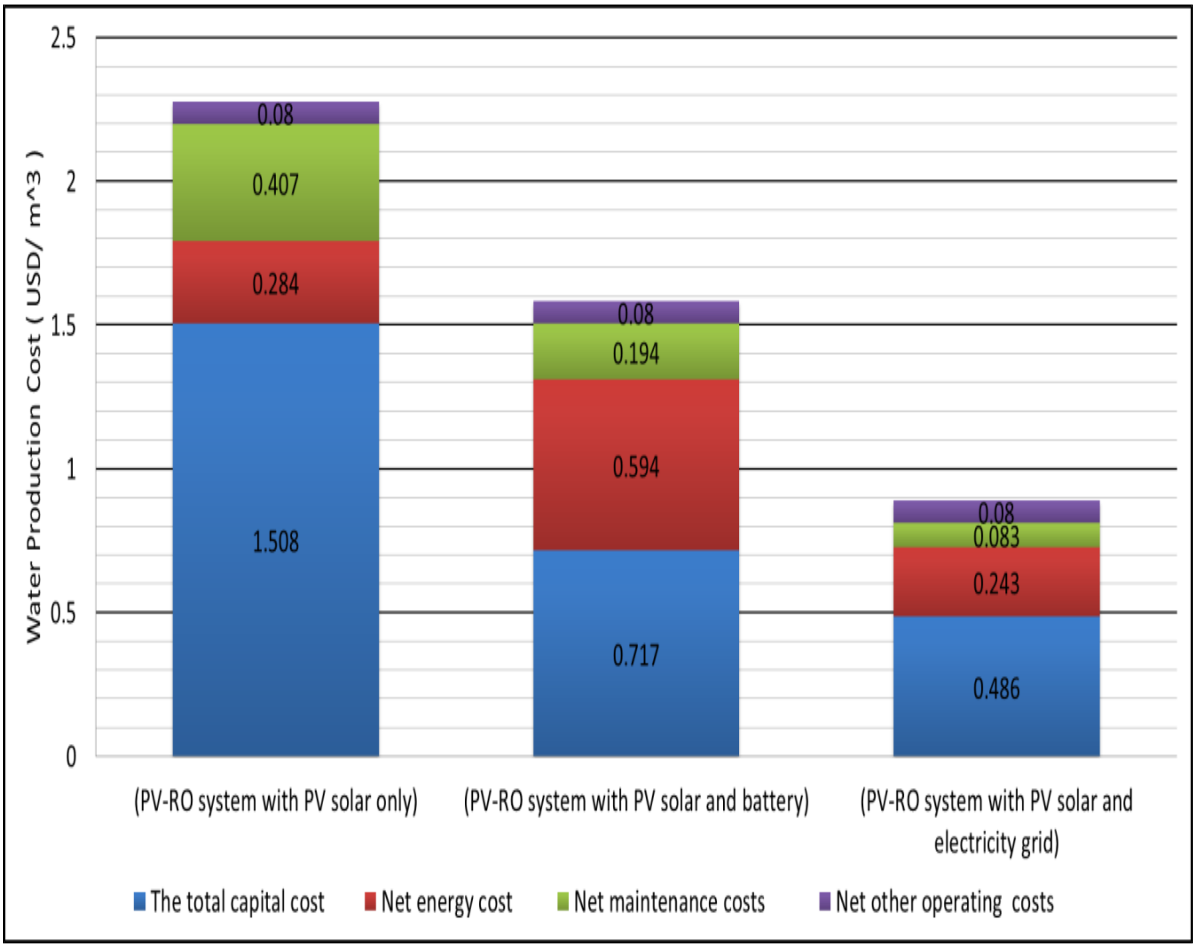


**Figure (4.8): LCOW comparison by configuration and by cost item.**

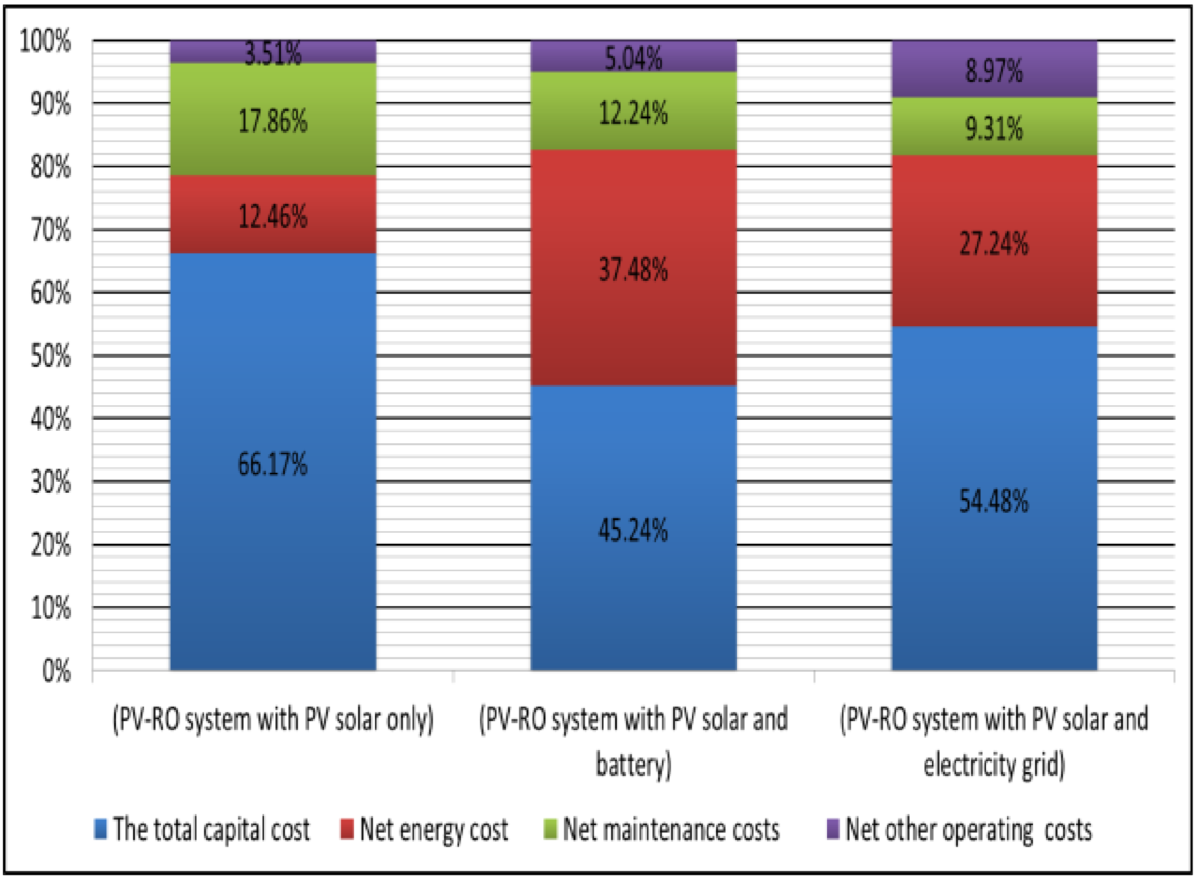


**Figure (4.9): Water production cost breakdown for the three PV- RO configurations (in %).**

**Table (4.17): The investment plan for the proposed project (PV-RO system) with PV solar and the electricity grid with a capacity of 254,000 $m^3$/ day.**

| No | Project | Cost (USD) |
|---|---|---|
| 1 | Establishment of RO plant with 254,000 $m^3$/ day capacity.<br>*The costs for investment are calculated basis on (1,100 USD/ $m^3$). | $280\times10^6$ |
| 2 | Establishment of PV system with 30 MW capacity.<br>*The costs for investment are calculated basis on (1,706,600 USD/ MW). | $51.198\times10^6$ |
| 3 | Establishment of new water transport lines with diameters of 1500 mm from the water RO plant to ground tanks location.<br>*The costs for investment are calculated basis on (625 USD/ m/ line). | $10\times10^6$ |
| 4 | Establishment of five ground tanks with a capacity of 15,000 $m^3$/ tank.<br>*The costs for investment are calculated basis on (125 USD/ $m^3$/ tank). | $9.375\times10^6$ |
| The total project cost (USD) | | $350.573\times10^6$ |

# CHAPTER 5

# CONCLUSIONS AND RECOMMENDATIONS

# CONCLUSIONS AND RECOMMENDATIONS

## 5.1 Conclusions

**In General, according to the results obtained from this study the main conclusions could be represented as follow:**

1- **Population studies:** The Long-term forecasted population size of the Burj Al-Arab city were calculated for 2032 using two methods (linear and exponential approximation) mentioned in the Egyptian code of design principles and conditions of implementation for drinking water and drainage. This forecasted population size was calculated by three techniques to include conventional techniques such as extrapolation of trend curves, and modern techniques such as GA and PSO. The population forecasting results by using the PSO for the exponential regression model have the best results (727,375 people) compared to the other models. This is because the population forecasting results using this model are adapted to the actual peak population of the new Burj Al-Arab city from the year 2012 to the year 2017. The population forecasted increasing rate in the exponential regression models is suitable for the nature of the population development in the Burj Al-Arab city where will be one of the important industrial cities in Egypt in the near future. Therefore, the increase in the population will be faster due to the increase in job opportunities, which is an attractive factor for the population. Also, the PSO can be implemented simply, and the convergence speed is quick without too many parameters, and it has the good global searching ability because the information of particle is single-directional, each particle would remember the past position, and the convergence is very quick, but at the same time, it is easy to fall into local optima.

2- **The maximum monthly consumption of water required for all uses during the development period:** The water demand rates of the Egyptian code of design principles and conditions of implementation for drinking water and drainage were used to determine the water demand of the new city of Burj Al-Arab. The estimated water demand was 498,187 $m^3$/ day (by the year 2032).

3- **The quantities of wastewater discharge for all uses during the development period:** The wastewater discharges are estimated for all uses by using the forecasted population census, the general plan for urban and industrial development in the Burj Al-Arab city, and applying in the laws concerning the estimation of wastewater discharges stipulated in the Egyptian code for the design and implementation of drinking water and sanitation projects. The wastewater discharges in the new city of Burj Al-Arab were estimated on parts. So that the amount of wastewater that reaches each treatment plant is estimated separately. This is to facilitate the evaluation process for each station separately. The estimation process is divided as follows:

   - **The quantities of domestic wastewater discharges:** The discharge rates of the Egyptian code were used to determine the wastewater discharges of the new city of Burj Al-Arab and the domestic flows expected to reach the sewerage network. The estimated wastewater discharges were 330,470 $m^3$/ day (by the year 2032).
   - **The quantities of industrial wastewater discharges:** There are many industrial activities in the new city of Burj Al-Arab, in accordance with the proposal to separate the human drainage from industrial drainage; the industrial drainage was estimated to treat with the following stations:

- **The quantities of the industrial discharges which are to be treated at the western station for industrial discharge:** The estimated industrial waste-water discharges were 62,027 $m^3$/ day (by the year 2032).
- **The quantities of the industrial discharges which are to be treated at the eastern station for industrial discharge:** The estimated industrial waste-water discharges were 84,400 $m^3$/ day (by the year 2032).

4- **Evaluation of the position of the wastewater works to calculate the requirements of the strategic plan:** The position of the wastewater works is evaluated in terms of separating the human wastewater from the industrial wastewater. Solutions have been studied and recommendations are obtained, namely, there is no need to increase the design capacity of the wastewater works. This is because the wastewater works can accommodate estimated flows until 2032.

5- **Evaluation of the position of the drinking water feeding works to calculate the requirements of the strategic plan:** The position of the drinking water feeding works is evaluated. Solutions have been studied and recommendations are obtained, namely, there is a need to increase the capacity of the drinking water feeding works by 254,000 $m^3$/ day for the new city of Burj Al-Arab until 2032.

6- **The requirements in the drinking water feeding work:** There are three the PV-RO plant suggested configurations, available as alternatives for water supply are studied to choose the best one to supply the city during the development period. These configurations are:

- **The first configuration:** PV-RO system with PV solar panels only.
- **The second configuration:** PV-RO system with PV solar panels and Batteries.
- **The third configuration:** PV-RO system with PV solar panels and electricity grid.

**The results of LCOW comparison of the configurations**

- The first configuration (The cost per cubic meter of water produced is **2.278 USD/ $m^3$**).
- The second configuration (The cost per cubic meter of water produced is **1.585 USD/ $m^3$**).
- The third configuration (The cost per cubic meter of water produced is **0.892 USD/ $m^3$**).

According to the results, the third configuration is the best economic configuration, because it has the lowest cost of a cubic meter of water. The PV-RO system with PV solar and the electricity grid (with 254,000 $m^3$/ day capacity at an estimated cost of $350.573\times10^6$ USD) project should be implemented. This is to overcome the weaknesses of the water system, and also to prevent any shortfall in services. There are other benefits to the project, such as reducing dependence on Nile water to benefit from it in other landlocked areas and also reducing harmful gases resulting from electricity generation by traditional methods used in the desalination of seawater.

## 5.2 Recommendations

The recommendations of this study are the following:

1- There is no need to increase the design capacity of the wastewater works.
2- The (PV-RO system) with PV solar and the electricity grid with a 254,000 $m^3$/day capacity project should be implemented.

# CHAPTER 6

# REFRENCES

# REFRENCES


[1] Wikipedia site (2017). available from: https://ar.wikipedia.org/wiki/%D9%85%D8%A7%D8%A1

[2] Gad. W. A. (2017). Water Scarcity in Egypt: Causes and Consequences. *Iioabj Journal*, Vol. 8, pp. 40-47, April 2017.

[3] United Nations Environmental Programme UNEP- GRiD (2009). Increased Global Water Stress. Accessed 15.08.11. available from: https://www.grida.no/resources/5625

[4] Facilities Management of New Burj Al-Arab Development Authority (2017). Annual facilities evaluation report, 2017.

[5] Alexandria Water Company AWCO - General administration of drinking water in the new Burj Al-Arab area (2017). Annual water facilities evaluation report, 2017.

[6] Alexandria Sewerage Company ASDCO (2017) - General Administration of Sewage Sector Burj Al-Arab. Annual wastewater facilities evaluation report, 2017.

[7] The google earth web site (2019). available from: https://www.google.com.eg/intl/ar/earth/

[8] Abdel-Shafy. H. & Mohamed-Mansour. M. S. (2013). Overview on water reuse in Egypt: Present and Future. *Research gate*, issue 14, pp. 17-25, January 2013.

[9] AbuZeid. K. & Elrawady. M. (2014). 2030 Strategic Vision for Treated Waste-water Reuse in Egypt. *Water resource management program – CEDARE*.

[10] Mostafa. H., El-Gamal. F., & Shalby. A. (2005). Reuse of low quality water in Egypt. *CIHEAM / EU DG research, options Méditerranéennes*, pp. 93- 103.

[11] Ashour. M. A., El Attar. S. T., Rafaat. Y. M., & Mohamed. M. N. (2009). Water Resources Management in Egypt. *Journal of engineering sciences, Assiut University*, Vol. 37, No. 2, pp. 269-279, March 2009.

[12] Expert Consultation Wastewater Management in the Arab World (2011): Water Reuse in the Arab World from Principle to Practice. *A Summary of Proceedings Expert Consultation Wastewater Management in the Arab World*, Dubai-UAE May 2011. https://www.researchgate.net/publication/264232759

[13] Holding Company for Water and Wastewater Website (2017). Annual report, 2017. available from: https://www.hcww.com.eg

[14] Central Agency for Public Mobilization and Statistics – Egypt (2017). available from: https://www.capmas.gov.eg/Pages/StatisticsOracle.aspx?Oracle_id=1966&year=2017&page_id=5109&YearID=23354

[15] The World Bank (2004). Seawater and Brackish Water Desalination in the Middle East, North Africa and Central Asia: A Review of Key Issues and Experience in Six Countries. Publ. No.: 33515, pp. 31-32, December 2004. available from: http://siteresources.worldbank.org/INTWSS/Resources/Desal_mainreportFinal2.pdf

[16] Shiklomanov, I. (1993). World Fresh Water Resources. In P.H. Gleick (Ed.) Water in Crisis: A Guide to the World's Fresh Water Resources. *Oxford University Press*, New York, pp.13-24.

[17] Abdel-Halim. A. M. & Aly-Eldeen. M. A. (2016). Characteristics of Mediterranean Sea water in vicinity of Sidikerir Region, west of Alexandria, Egypt. *Egyptian Journal of Aquatic Research*, 42, 133–140, 21 June 2016.

[18] World Health Organization (2003). Total Dissolved Solids in Drinking-Water: Background Document for Development of WHO Guidelines for Drinking-Water Quality. Publ. No.: WSH/03.04/16, Retrieved May 8, 2011. available from: http://www.who.int/water_sanitation_health/dwq/chemicals/tds.pdf

[19] Ahmadvand. S. , Abbasi. B., Azarfar. B., Elhashimi. M., Zhang. X. & Abbasi. B. (2019). Looking beyond energy efficiency: an applied review of water desalination technologies and an introduction to capillary-driven desalination. *MDPI*, *Water*, 11, 696; doi:10.3390/w11040696. April 2019. available from: www.mdpi.com/journal/water

[20] Lienhard. J. H., Thiel. G. P., Warsinger. D. M., & Banchik. L. D. (2016). Report of a workshop conducted at the Massachusetts Institute of Technology in association with the Global Clean Water Desalination Alliance. October 2016.

[21] Research Office Legislative Council Secretariat (2015). Seawater desalination technologies. September 2015. available from: https://www.legco.gov.hk/research-publications/english/1415fs07-seawater-desalination-technologies-20150930-e.pdf

[22] The World Meteorological Organization (2019). Global Climate in 2015-2019: Climate change accelerates. September 2019. available from: https://public.wmo.int/en/media/press-release/global-climate-2015-2019-climate-change-accelerates

[23] Hamilton. K. (1998). The Oil Industry And Climate Change. *Climate Campaign, Greenpeace international*, August 1998.

[24] Mayo County Council (2011). Renewable Energy Strategy For County Mayo2011-2020", Ordnance Survey Ireland, 2011.

[25] Olsson. G. (2018). Clean Water Using Solar and Wind. Outside the Power Grid. First published © *IWA Publishing*, pp.74&112,This eBook was made Open Access in January 2019. available from: https://iwaponline.com/ebooks/book-pdf/520710/wio9781780409443.pdf

[26] World Energy Council (2004). Renewable Energy Projects Handbook. *World Energy Council*, pp.3-4 & 12-13, *April* 2004.

[27] Sorensen. B. (2009). Renewable Energy Focus Handbook. First published © *Elsevier Inc*, All rights reserved, pp.425, 322-325. available from: http://www.elsevierdirect.com/9780123747051

[28] Quaschning. V. (2005). Understanding Renewable Energy Systems. *First published © Carl Hanser Verlag GmbH & Co KG*, All rights reserved, pp.28-29 & 52-53.

[29] Jäger. K., Isabella. O., Smets. A. H. M., van Swaaij. R. A., & Zeman. M. (2014). Solar Energy , Fundamentals, Technology, and Systems. *Delft University of Technology*, pp.25& 307, Sep 2014.

[30] Alsumiri. M. & El Khashab. H. (2018). Solar Energy Technology Choice Development. *published by EDP Sciences*. available from: http://creativecommons.org/licenses/by/4.0/

[31] National Renewable Energy Laboratory (NREL) (2020). The Best Research-Cell Efficiency Chart. available from: https://www.nrel.gov/pv/assets/pdfs/best-research-cell-efficiencies.20200218.pdf

[32] Abdo. T. & EL-Shimy. M.(2014). Quantitative Characterization and Selection of Photovoltaic Technologies. *16th International Middle- East Power Systems Conference – MEPCON*. December 2014.

[33] Masters. G. M. (2004). Renewable and Efficient Electric Power Systems , *Stanford University, John Wiley & Sons, Inc, New Jersey*, pp.473- 475 & 419.

[34] Alkaff. S. A., Shamdasania. N. H., Ii. G. Y., & Venkiteswaran. V. K. (2019). A Study on Implementation of PV Tracking for Sites Proximate and Away from the Equator. *Researchgate, Springer Nature Singapore Pte Ltd*, March 2019. available from: https://www.researchgate.net/publication/331532305

[35] Patel. M. R. (1999). Wind and Solar Power Systems. *U.S. Merchant Marine Academy, Kings Point*, New York, CRC Press LLC, pp.152- 153.

[36] Gawatre. D. W., Kandgule. M. H., & Kharat. S.D. (2016). Comparative Study of Population Forecasting Methods. *IOSR Journal of Mechanical and Civil Engineering*. IOSR-JMCE., Volume 13, Issue 4 Ver. V, pp 16-19, Jul - Aug 2016.

[37] Mekonnen. Y. A. (2018). Population Forecasting for Design of Water Supply System in Injibara Town, Amhara Region, Ethiopia. *Civil and Environmental Research*. Vol.10, No.10, pp 54-65, 2018.

[38] Chi G. & Ventura S. J. (2011 b). Population Change and Its Driving Factors in Rural, Suburban, and Urban Areas of Wisconsin, USA, 1970–2000. *International Journal of Population Research*, 1–14, 2011.

[39] Gulseven. O. (2016). Forecasting Population and Demographic Composition of Kuwait Until 2030. *International Journal of Economics and Financial Issues*. Vol 6 • Issue 4 • pp 1429-1435, 2016.

[40] wikipedia web site (2020). Genetic algorithm. available from: https://en.wikipedia.org/wiki/Genetic_algorithm

[41] Bodenhofer. U. (1999). Genetic Algorithms: Theory and Applications. *held at the Johannes Kepler University, Linz, during the winter term*, pp. 11-16, January 1999. https://www.researchgate.net/publication/200048792

[42] Thede. S. (2004). An introduction to genetic algorithms. Copyright © 2004 by the Consortium for Computing Sciences in Colleges, *ResearchGate*, October 2004 . available from: https://www.researchgate.net/publication/228609251

[43] Shabir. S. & Singla. R. (2016). A Comparative Study of Genetic Algorithm and the Particle Swarm Optimization. *International Journal of Electrical Engineering*. ISSN 0974-2158 Volume 9, Number 2, pp. 215-223, 2016.

[44] wikipedia web site (2020). Particle swarm optimization. available from: https://en.wikipedia.org/wiki/Particle_swarm_optimization

[45] Singh. S. (2014). A Review on Particle Swarm Optimization Algorithm. *International Journal of Scientific & Engineering Research*, ISSN 2229-5518, Volume 5, Issue 4, pp 551-553, April 2014.

[46] Jamous. R. A., El.Seidy. E., & Bayoum. B. I. (2016). A Novel Efficient Forecasting of Stock Market Using Particle Swarm Optimization with Center of Mass Based Technique. *(IJACSA) International Journal of Advanced Computer Science and Applications*, Vol. 7, No. 4, pp 342-347, 2016.

[47] Parsopoulos. K. E. (2015). Particle Swarm Methods. *Department of Computer Science & Engineering, University of Ioannina, Ioannina, Greece. © Springer International Publishing AG*, pp 7-10, 2015. available from: http://www.cs.uoi.gr/~kostasp/papers/B05.pdf

[48] Engelbrecht. A.P. (2007). Computational Intelligence: An Introduction. Second Edition, Chapter 16, Particle Swarm Optimization, © *2007 John Wiley & Sons, Ltd*, available from: https://web2.qatar.cmu.edu/~gdicaro/15382/additional/CompIntelligence-Engelbrecht-ch16.pdf

[49] Wang. D. (2017). Particle swarm optimization algorithm: an overview. *ResearchGate*, January 2017. available from: https://www.researchgate.net/publication/312519986

[50] Kaveh. A. (2017) Advances in Metaheuristic Algorithms for Optimal Design of Structures. Chapter 2, Particle Swarm Optimization, © *Springer International Publishing AG*, pp 11-17, 2017.

[51] Housing and Building National Research Center (HBRC) (2010). The Egyptian Code for the foundations of the Design and Implementation Conditions for Pipelines used in Drinking Water and Sewage Networks, 2010.

[52] Housing and Building National Research Center (HBRC) (2015). The Egyptian code of Design Principles and Conditions of Implementation for Drinking water and Drainage Purification Plants.101/3 .Egypt: HBRC, 2015.

[53] Hydranautics - A Nitto Group Company (2020). IMSDesign software. available from: https://membranes.com/solutions/software/

[54] Zaki. H. R. (2009). Environmental Parameters of Alexandria Inshore North Western Coastal Area, Egypt. *World Applied Sciences Journal 7 (6). © IDOSI Publication*, pp 715-725, 2009.

[55] Swartz1. C., Plessis. J. D., Burger. A., & Offringa. G. (2006). A desalination guide for South African municipal engineers. *Water Institute of South Africa (WISA) Biennial Conference, Durban, South Africa*, pp 641-647, 21-25 May 2006. available from: https://www.ajol.info/index.php/wsa/article/download/47845/34215

[56] American Water Works Association (2007). Reverse Osmosis and Nanofiltration. Manual of Water Supply Practices—M46, Second Edition, ©*1999, 2007 American Water Works Association*.

[57] Voutchkov. N. (2010). Considerations for Selection of Seawater Filtration Pretreatment System. *ResearchGate*, October 2010. available from: https://www.researchgate.net/publication/222421014

[58] Ezzeghni. U. (2018). Designing and optimizing 10,000 $m^3$/ day conventional SWRO desalination plant. *ResearchGate*, September 2018. available from: https://www.researchgate.net/publication/328228568

[59] Ezzeghni. U. (2018). The Optimal Membrane Type for the Next Membrane Replacement of Tajoura SWRO Desalination Plant. *ResearchGate*, October 2018. available from: https://www.researchgate.net/publication/328080209

[60] PVsyst - Photovoltaic system study Program (2020). General organization of the help, PVsyst SA,( Route du Bois-de-Bay 107),1242 Satigny ,Switzerland. available from: www.pvsyst.com

[61] P.Manimekalai (2013). An Overview of Batteries for Photovoltaic (PV) Systems. *ResearchGate & International Journal of Computer Applications (0975 – 8887),* Volume 82 – No 12, November 2013. available from: https://www.researchgate.net/publication/266499481

[62] Bin Sopian. K., Elbreki. A., Ruslan. M. H., & Al-Shamani. A. N. (2016). A stand-alone Photovoltaic System Design and Sizing: a Greenhouse Application in Sabha City: Case study in Libya. *ResearchGate*, August 2016. available from: https://www.researchgate.net/publication/317166386

[63] OECD and NEA (2018). The Full Costs of Electricity Provision. Paris: OECD. available from: https://www.oecd-nea.org/ndd/pubs/2018/7441-full-costs-2018-es.pdf

[64] Zhou. Y. & Gu A. (2019). Learning Curve Analysis of Wind Power and Photovoltaics Technology in US: Cost Reduction and the Importance of Research, Development and Demonstration. *MDPI. Sustainability*, 11, 2310; doi:10.3390/su11082310. April 2019. available from: https://res.mdpi.com/d_attachment/sustainability/sustainability-11-02310/article_deploy/sustainability-11-02310-v2.pdf

[65] National Institute of Standards and Technology (NIST) (2016). Energy and Economic Implications of Solar Photovoltaic Performance Degradation. *NIST Special Publication 1203*. January 2016. available from: https://nvlpubs.nist.gov/nistpubs/SpecialPublications/NIST.SP.1203.pdf

[66] Al Matin. M. A. (2019). LCOE Analysis for Grid-Connected PV Systems of Utility Scale Across Selected ASEAN Countries. *The Economic Research Institute for ASEAN and East Asia (ERIA)*, Discussion Paper Series No. 305, 2019. available from: https://www.eria.org/uploads/media/discussion-papers/LCOE-Analysis-For-Grid-Connected-PV-Systems-Of-Utility-Scale-Across-Selected-ASEAN-Countries.pdf

[67] Ocon. J. D & Bertheau. P. (2019). Energy Transition from Diesel-based to Solar Photovoltaics-Battery-Diesel Hybrid System-based Island Grids in the Philippines – Techno-Economic Potential and Policy Implication on Missionary Electrification. *Journal of Sustainable Development of Energy, Water and Environment Systems*. Volume 7, Issue 1, pp 139-154, 2019. available from: https://doi.org/10.13044/j.sdewes.d6.0230

[68] Van Den Akker. J. H. A. (2017). Overview of costs of sustainable energy technologies. Energy production: on-grid, mini-grid and off-grid power generation and supply and heat applications, *Advisory Services on Climate, Energy and Development Issues (ASCENDIS)*, 2017. available from: https://jhavdakk.home.xs4all.nl/ASCENDIS%20Cost%20of%20energy%20v2a.pdf

[69] Worighi. I., Geury. T., El-Baghdadi. M., Van Mierlo J., Hegazy. O., and Maach. A. (2019). Optimal Design of Hybrid PV-Battery System in Residential Buildings: End-User Economics, and PV Penetration. *Applied sciences, MDPI Journal © 2019 by the authors*. available from: https://res.mdpi.com/d_attachment/applsci/applsci-09-01022/article_deploy/applsci-09-01022.pdf

[70] Energy Information Agency United States (EIA) (2020). Levelized Cost and Levelized Avoided Cost of New Generation Resources in the Annual Energy Outlook 2020. available from: https://www.eia.gov/outlooks/aeo/pdf/electricity_generation.pdf

[71] Abu-Rumman. A. K., Muslih. I., & Barghash. M. A.(2017). Life Cycle Costing of PV Generation System. *Journal of Applied Research on Industrial Engineering*. Volume 4, Issue 4, pp 252–258, 2017. available from: http://www.journal-aprie.com/article_54724_4e5a256ff89a93cd0a5b12c5116c96f3.pdf

[72] Graham, P., Hayward, J., Foster, J., & Havas, L. (2019). GenCost 2019-20: preliminary results for stakeholder review CSIRO, Australia. © *Commonwealth Scientific and Industrial Research Organisation*, 2019.

[73] Abazza. H. (2012). Economic Considerations for Supplying Water Through Desalination in South Mediterranean Countries. Sustainable Water Integrated Management - Support Mechanism (SWIM- SM). *Project funded by the European Union*, pp 12- 13, August 2012. available from: http://www.swim-sm.eu/files/Economic_Considerations_on_Desalination_Final.pdf

[74] Kesieme. U. K., Milne. N. A., Aral. H., Cheng. C. Y., & Duke. M. (2013). Economic analysis of desalination technologies in the context of carbon pricing, and opportunities for membrane distillation. Desalination, 323, ISSN 0011-9164, pp 1-26, 2013. available from: http://vuir.vu.edu.au/21957/1/paper_kesieme%20post%20print.pdf http://vuir.vu.edu.au/21957/

[75] Papapetrou. M., Cipollina. A., La Commare. U., Micale. G., Zaragoza. G., & Kosmadakis. G. (2017). Assessment of methodologies and data used to calculate desalination costs. *IRIS UniPA University of Palermo Institutional Repository*, Desalination publications 419, DOI: 10.1016/j.desal.2017.05.038 pp 8–19, 2017. available from: https://iris.unipa.it/retrieve/handle/10447/245083/444208/Desalination%20costs%20paper-%20Papapetrou2017%20pre-print.pdf https://iris.unipa.it/handle/10447/245083#.XqBFR_37TIU

[76] Ezzeghni. U. (2018). The Optimal Membrane Type for the Next Membrane Replacement of Tajoura SWRO Desalination Plant. *ResearchGate*, October 2018. available from: https://www.researchgate.net/publication/328080209

[77] The World Bank (2019). The Role of Desalination in an Increasingly Water-Scarce World. *International Bank for Reconstruction and Developmen*, pp 19 & 23-24 & 31, March 2019. available from: https://idadesal.org/wp-content/uploads/2019/04/World-Bank-Report-2019.pdf

[78] Bhojwani. S., Topolski. K., Mukherjee. R., Sengupta. D., & El-Halwagi. M. M. (2018). Technology review and data analysis for cost assessment of water treatment systems. *Science of the Total Environment*, 651, pp 2749–2761, October 2018. available from: https://doi.org/10.1016/j.scitotenv.2018.09.363

[79] Priel. M. (2003). Comparative Cost of UF vs. Conventional Pretreatment for SWRO Systems. *ResearchGate*. January 2003. available from: https://www.researchgate.net/publication/266499481

[80] The Electricity Utility and Consumer Protection Regulatory Agency (2020). The electricity energy cost from the grid for supply (380 V) Water and sanitation stations. available from: http://egyptera.org/ar/Tarrif2019.aspx

# APPENDIX A

# THE CURRENT SITUATION OF WATER AND WASTE-WATER SYSTEM FOR NEW BURJ AL-ARAB CITY

# THE CURRENT SITUATION OF WATER AND WASTE-WATER SYSTEM FOR NEW BURJ AL-ARAB CITY

## A-1: Introduction

In this appendix, the data are presented in a summary of the current situation of the drinking water and wastewater system in the new city of Burj Al-Arab. In addition to the necessary data about all the added land areas needed for all the uses distributed in the development stages in the new Burj Al-Arab city. This will be mentioned as follows**:**

## A-2: The Current Situation of the Water System for the New Burj Al-Arab City

- **Figure (A.1)** shows the current status of the drinking water system. The water system for new Burj Al-Arab city has many assets as follows**:**

### A. Bahij Lift Station

Due to the distance is far between the city and the drinking water station, a Bahij lift station was established in the new city of Burj Al-Arab. And the Bahij lift station receives the entire production of a drinking water station in kilo 40 except for some small quantities estimated at 10,000 $m^3$/ day to feed Burj Al Arab airport and some surrounding communities [4, 5]**.**

### B. Sub Lift Station

The lift sub-station is located in the second industrial zone. This station has a set of pumping pumps, a ground reservoir for drinking water with a capacity of 12,000 $m^3$, and a cylindrical reinforced concrete high tank at an altitude of 50 meters with a capacity of 2000 $m^3$. But it is not used currently because the station depends on direct pumping to raise pressure on the water network. The capacity of the lift station is about (24,000 $m^3$/ day). And the lifting station was used to re-strengthen the pressure water network in the second industrial and the third and fourth. The ground reservoir is fed from a Bahij lift station by an 800 mm conveyor line made of pre-stressed concrete and flexible cast, plus a flexible cast line of 700 mm diameter [4]**.**

### C. Water Supply Networks

The water produced from the drinking water station in kilo 40 transfers to the Bahaj lift station through three water lines with a length of about 28 km long. It consists of a water transport line is made of (1000mm diameter) flexible cast pipe and two lines made of (1500mm diameter) pre-stressed concrete pipes [4, 5]**.**

A number of pumping lines exit from the Bahij station divided as follows**:**

1. Three water pumping lines made of (1000mm diameter) pre-stressed concrete pipes to deliver water to the North Coast lifting stations**.**
2. One water pumping line is made of (1000mm diameter) GRP pipes to feed the new Burj Al-Arab city**.**

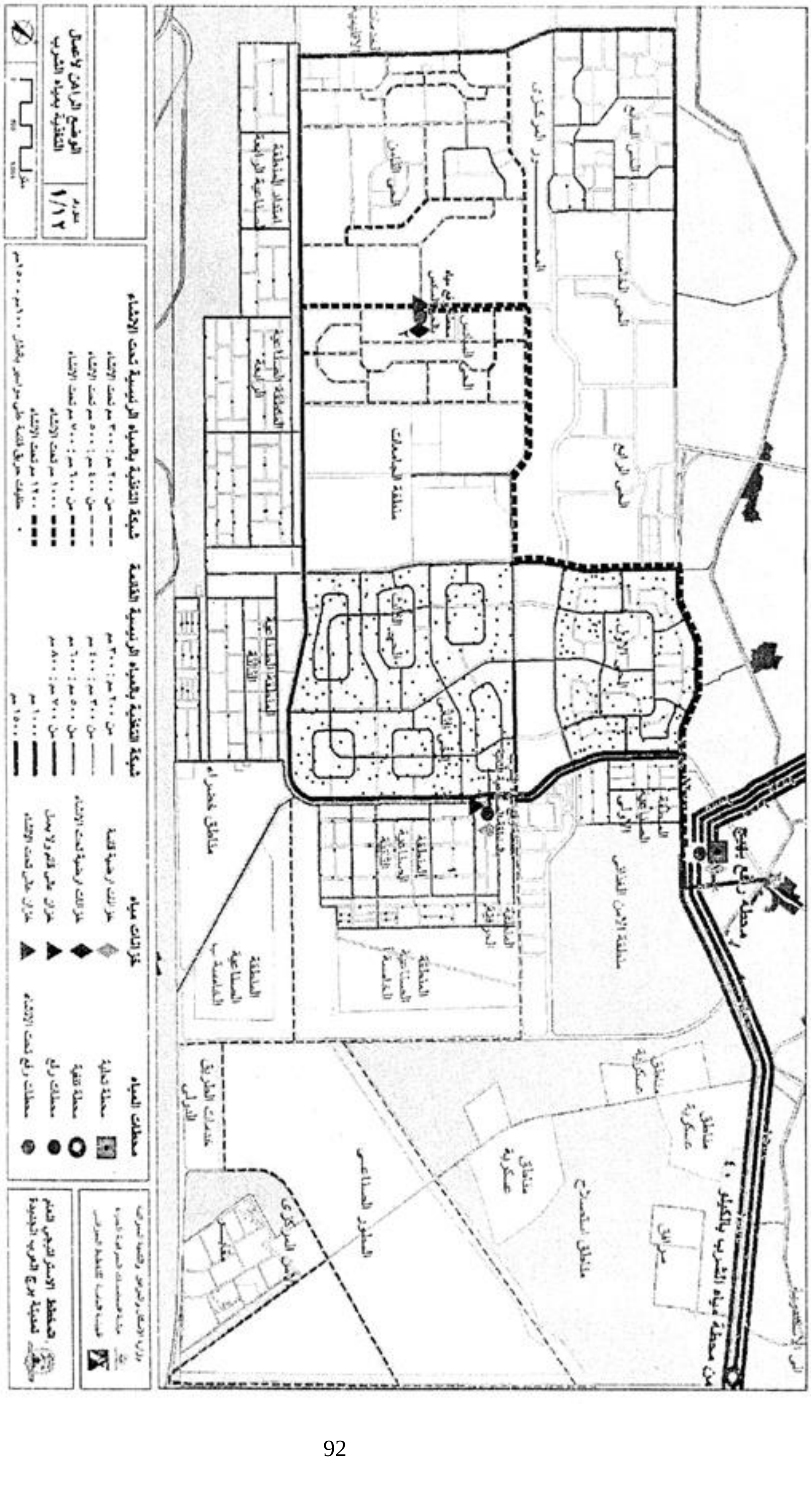

**Figure (A.1): The current status of drinking water supply** [4].

3. There are also additional transmission lines made of (800mm diameter) pre-stressed/ flexible cast iron pipes as well as (700mm diameter) flexible cast pipes to feed the city and linking to existing reservoirs in the second industrial zone**.**
4. A (1200/ 1000 mm diameter) GRP water transmission line is currently being implemented from the Bahaj lift station to the ground storage tanks under construction in the sixth residential district**.**

The total length of water transport pipes in the new city of Burj Al-Arab is estimated at 128km long, including the water transmission lines from the water station in kilo 40 to the Bahij station [4, 5]**.**

The main and secondary water network in the new city of Burj Al-Arab consists of pipes with diameters ranging from 100 mm to 1000 mm with a total length of 474 km long. The main lines around the new city of Burj Al-Arab are implemented with diameters ranging from 500 mm to 1000 mm and made of GRP, pre-stressed concrete, and flexible cast iron [4, 5]**.**

Defect of the secondary water distribution network, about 40% to 50% of the pipes are asbestos, with a total length of 208 km, with graduated diameters up to 500 mm diameter. The majority of asbestos pipes are located in the first residential district and industrial zone (1), (2), and (3) [4, 5]**.**

The internal water networks for the fifth, sixth and eighth districts are currently being designed, reviewed and implemented [4, 5]**.**

## D. Ground and High Storage

**• Ground reservoirs**

The Bahij lift station has four ground reservoirs, three of them with a capacity of 12,000 $m^3$ for the tank and one tank with a capacity of 13,500 $m^3$, and a total storage capacity of about 49,500 $m^3$. The ground storage capacity in the new city of Burj Al-Arab is estimated at 12,000 $m^3$, which is the first stage reservoir of the station, while the rest of the ground storage is to feed the Northern Coast to the city of Marsa Matruh [4, 5]. Also, there is another ground reservoir located in the city at the location of the existing high reservoir in the second industrial zone with a capacity of 12,000 $m^3$ and consists of four parts, each one has a capacity of 3000 $m^3$ [4, 5]**.**

Currently, two ground tanks with a total capacity of 24000 $m^3$ and one high tank with a capacity of 2000 $m^3$ are being implemented, as part of the project on the water GRP (1200/ 1000) mm line with a length of 9.68 km from the Bahij lifting station to tanks. That is being implemented and with a total cost of $143\times10^6$ EGP [4, 5]**.**

- **High reservoirs**

There is a high tank located in the second industrial zone at the location of the lift sub-station, it is a capacity of 2000 $m^3$ and the tank is in good condition and is not working now due to the direct pumping from the ground tank by the station. There is a decrease in the pressure of the water network in some residential areas such as neighborhoods (No.7 and No.9) in the first district and also neighborhood (No.4) in the third district Due to a difference in the levels up to 30 meters between some residential areas and the location of lift stations [4, 5].

In order to develop the current situation, two ground tanks with a capacity of 12,000 $m^3$ per tank are currently being constructed, a high reservoir with a capacity of 2000 $m^3$ at an altitude of 30 meters, according to the height limits in the area. The project also includes the implementation of conveyor lines from the Bahij lift station to the reservoirs with diameters of 1200 mm/ 1000 mm made of GRP and also the link on the line (700 mm) in the city of Mubarak for scientific research [4, 5].

## E. Fire Hydrants

The industrial zones and their extension, the (first, second, and third) neighborhoods have about 620 fire hydrants of the ground type, which are mounted on lines of 100-150mm. The number of fire hydrants in the third industrial zone is 22 fire hydrants, the second industrial zone is 27 fire hydrants, Storage of the second industrial zone is 25 fire hydrants, and the fourth industrial zone and its extension is 55 fire hydrants. The rest of the fire hydrants are distributed to the first, second, and third districts [4, 5].

## F. The Current Status of Green Landscaping

The new city of Burj Al Arab does not have a private network to irrigate the green areas for the lack of water quantities. The green areas of the city are irrigated through two systems:

- Exits with meters on the drinking water network and is used to irrigate the green areas in the large green areas in the existing neighborhoods.
- The green areas of the islands and the small green areas are irrigated through three agricultural tractors with tanks by three daily cycles per tractor.
- The Burj Al-Arab city authority calculates the drinking water company for the amount of water consumed according to the reading of the meters installed on the irrigation outlets [4, 5].
- **Note:** There is a proposal to use treated water from the western domestic tertiary treatment station to irrigate green areas, which is currently being implemented [4]. The amount of water required for the irrigation process of green spaces in the city was estimated at 78,000 $m^3$/ day.

### G. The Current Water Consumption Rates

The amount of water consumed in the new city of Burj Al Arab is estimated at 147,254 $m^3$/ day, according to the data from the Bahij lifting station and distributed as follows:

- Consumption rate for residential usage is about 280 L/ person/ day, with a total consumption of about 39,200 $m^3$/ day, representing about 26.6% of the total amount of water consumed in the city.
- The amount of water consumed in industrial areas is about 80,483 $m^3$/ day, and this is representing about 54.62% of the total amount of water consumed in the city.
- The amount of water used in the construction works in the city is about 23,216 $m^3$/ day, and this is representing about 15.78% of the total amount of water consumed in the city.
- The amount of water used in other uses is about 4355 $m^3$/ day and represents about 3% of the total amount of water consumed in the city. **Figure (A.2)** shows the water consumption by customer type in the new city of Burj Al Arab [4].

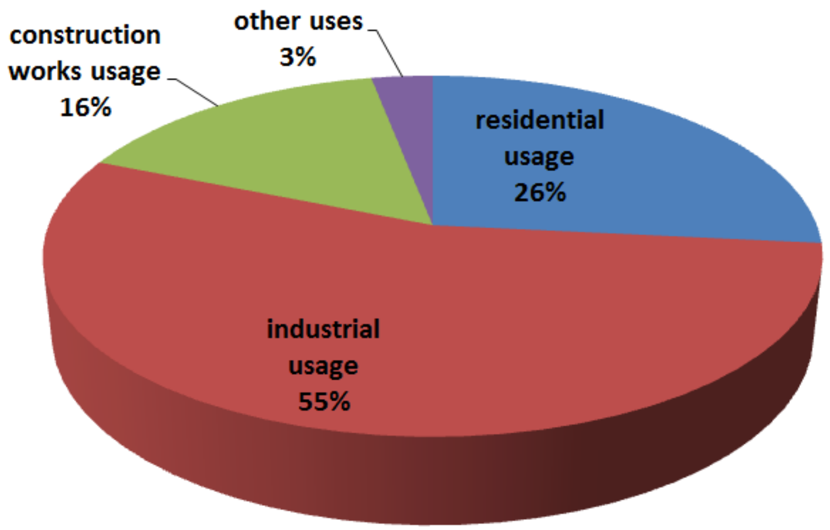


**Figure (A.2): The water consumption by customer type in the new city of Burj Al-Arab [4].**

## A-3: The Current Situation of the Wastewater System for the New Burj Al-Arab City

Wastewater discharges resulting from the new city of Burj Al-Arab are collected through a sloping network made of pottery pipes or PVC plastic or concrete. The length of the drainage network in the city is about 301 km long; including the sewage collection lines that serving the lifting stations, and drainage diameters ranging from 160 mm to 1000 mm [4, 6]**.**

The wastewater discharges from the first residential district and the engineer's residences are collected to the Lifting Station (B) that located in the north-west of the first residential district and for the lifting station (B) to the main lift station (A) that is located in the north of the first industrial zone that lifts wastewater discharges to the oxidation pond treatment plant that located in the east of the city [4, 6]**.**

The rest of the streets of the first district are collected through sewage collection lines directly into the main lift station (A). And Sewage water is collected from the central axis and some areas in the second and third districts in sewage collection lines connected to the main lift station (A), the other areas in the second and third districts, to the south-west of the third industrial zone, which lifting by the lift station (D) into a temporary pond at the site of the new treatment plant currently under construction. For the first industrial zone, wastewater is collected by the slope network connected to the station (A). The effluents generated from the second industrial zone are discharged to the (1000 mm diameter) main collection line directly to the oxidation pond treatment plant located east of the city [4, 6]**.**

Wastewater discharges from the third industrial zone are also collected at the station (C) and to lift this wastewater to the treatment plant with an oxidation pond located in the east of the city. The fourth industrial zone is serviced by the lift station (D). The networks in the extended area of the 4th industrial zone have been implemented, and the collected water shall be disposed of at the lift station (E) which shall lift the drainage water to the lift station (D) [4, 6]. The wastewater discharges produced from the Gharbaniyat prison are discharged to the Lift Station (6), which is located northwest of the seventh district and from there to Lift Station (5) located at the north of the first industrial zone, and from the lift station (5) to the oxidation pond treatment plant that is located at the east of the city [4, 6]**.**

Note the stations (5) and (6) are operated by the Ministry of the Interior and the lift station (6) has finally been connected to the 7th district residential lift station. **Table (A.1)** shows the sewage pumping stations of the new city of Burj Al Arab and the operational position of each station. Stations (5) and (6) are located in the city, but they do not serve them as they specialize in raising sewage from the Gharbaniyat prison to the eastern treatment plant. **Figure (A.3)** shows the current status of wastewater pumping stations and treatment plants [4, 6]**.**

**Table (A.1): The Sewage pumping stations for the new city of Burj Al Arab [4, 6].**

| NO | Lift Station | Point of Discharge | Capacity (m3/day) | Delivery Line | Executive position |
|---|---|---|---|---|---|
| 1 | station (A) | The Eastern treatment plant | 64800 | 1000 mm | Operating |
| 2 | station (B) | station (A) | 3120 | 500 mm | Operating |
| 3 | station (C) | The Eastern treatment plant | 43920 | 800 mm Delivery Line -slope line 800 /1000 mm | Operating |
| 4 | station (D) | The temporary pond at the site of the Western treatment station | 77760 | 1000 mm | Operating |
| 5 | station (E) | station (D) | 31104 | 500 mm Delivery Line -slope line 800 / 900 /1000 mm | Operating |
| 6 | 7th district residential lift station | The Western treatment station | 34560 | 600 mm | Operating |
| 7 | 4th district residential lift station | The Western treatment station | 104000 | 1200 mm | Under Operating |
| 8 | Developer lift station | The Eastern treatment plant | …………… | 900 mm | Under design and subtraction |
| 9 | Station (6) | Station (5) | Unavailable | 500 mm | Operating |
| 10 | Station (5) | The Eastern treatment plant | Unavailable | 500 mm | Operating |

## • Sewage Treatment Plants in the City of Burj Al-Arab

The following is a summary of the Sewage treatment plants in the city of Burj Al-Arab**:**

### 1- The eastern treatment plant

The existing eastern treatment plant consists of 18 ponds for wastewater treatment with natural ventilation. It is a current design capacity of 36,000 $m^3$/ day, and it is currently being developed and expanded. The station receives the flows of all the existing industrial zones. As well as the flows of the residential districts (The first, north of the second and third districts). And the discharges that come from the eastern central axis, as well as the flows, are received from the Gharbaniyat prison [4, 6]**.**

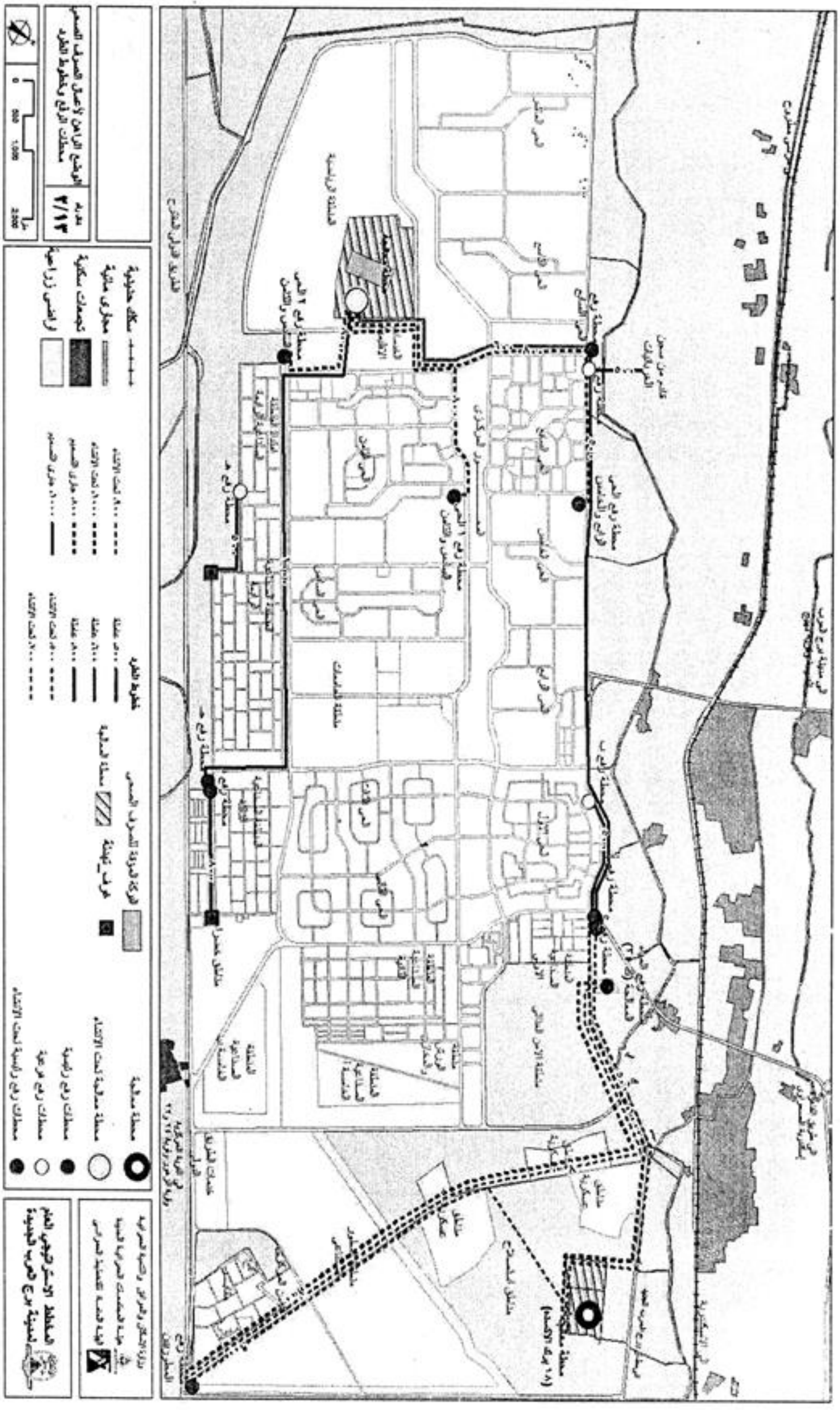

**Figure (A.3): The current status of wastewater pumping stations and treatment plants [4].**

The treated water of the plant is disposed of through an 800 mm diameter slop line to the treated water lifting plant (lifting station K 34) to be pumped through the lifting plant to the Agricultural channel (1/ 11) by a 700 mm diameter delivery line made of the pre-stressed concrete (It has not been run until this date). The treated wastewater is used in the irrigation of 600 acres of tree forests. In the case of non-conformity of the water discharged from the station to the specifications and conditions required after the treatment. The water is recycled in the treatment plant by the recycling pumps in the station [4, 6]**.**

**2- The temporary pond:**

A sanitation pond was established in the western part of the city at the site of the current treatment plant. The pond is used temporarily until the completion of the implementation of the three-stage wastewater treatment plant. The temporary pool serves south of the second district, south of the third district, the seventh district, and the fourth industrial zone [4, 6]**.**

## • The Current Projects in the Wastewater Sector

The following is a summary of the wastewater projects being executed in the new city of Burj Al Arab**:**

**1- The project of separating industrial wastewater from domestic wastewater**

The project of separating industrial wastewater from domestic wastewater is studied by the EGC consulting office. The study suggested that the household discharges resulting from all the existing neighborhoods in the city and planned neighborhoods should be received by the western treatment plant. That is currently being implemented [4, 6]**.**

The study also proposed the establishment of a lifting station. This is a proposed station located next to the existing lift station (A) with a capacity of 50,000 $m^3$/ day. To be used to receive the domestic flows resulting from the first neighborhoods and north of the second and third neighborhoods and the eastern central axis. The study also proposed the fourth neighborhood lift station. Its design capacity has been increased to 104,000 $m^3$/ day to cover the upcoming flows [4, 6]**.**

The study also proposed the construction of the second stage of the lifting station (d) with a capacity of 73,000 $m^3$/ day. This station will lift the collected domestic wastewater from (the south of the second and third neighborhoods and the university area) to the western treatment station through the proposed line of 900 mm diameter [4, 6]**.**

The study also noted that the lift station in the ninth district of the future design capacity 66,000 $m^3$/ day to collect and lift the flows of the ninth and tenth district and the sports area to the western treatment station [4, 6]**.**

It should be noted that in the proposed plan some of the names of the neighborhoods have been changed as follows**:**

- **a)** The fourth neighborhood name changed to the sports clubs are**;**
- **b)** The eighth neighborhood was divided into the eighth and ninth neighborhoods in the proposed plan**;**
- **c)** The ninth neighborhood name changed to the eleventh neighborhood**;**
- **d)** The tenth neighborhood name changed to the twelfth neighborhood**;**

**e)** The sports area name changed to the thirteenth neighborhood and the food security zone in the proposed plan**.**

The study also suggested dealing with the industrial wastewater produced by all the industrial zones in the eastern treatment plant that's being developed, except for the discharge of industrial wastewater from the third industrial zone and its expansion. As well as the fourth industrial zone and its extension should be received by the proposed western industrial wastewater treatment plant. This western industrial wastewater treatment plant is next to the western wastewater treatment plant. This study estimated the capacity of the proposed western industrial drainage plant is about 65,000 $m^3$/ day [4, 6]**.**

**Table (A.2)** shown the composition of the industrial wastewater produced by the third industrial zone and its expansion, as well as the fourth industrial zone and its extension [6]. These industrial wastewater discharges are supposed to be treated by the western industrial waste-water treatment plant. This composition is according to the sample taken from the sump of the main lifting station (D) that lifting all the wastewater from the industrial areas. This lift station is currently being pumped into a temporary lake, which is supposed to establish the western industrial wastewater treatment plant instead of it. **Figure (A.4)** shows the percentage of water consumed by the various industries in these industrial zones, of which about 80% reaches the sewage network [4]**.**

## 2- Rehabilitation and expansion project of the eastern oxidation plant

Due to the increased flow resulting from the different uses of the new city of Burj Al-Arab, rehabilitation and expansion are underway of the existing treatment plant in the eastern part of the city to increase the capacity of the planned plant from 36,000 $m^3$/ day to 100,000 $m^3$/ day. The development and expansion works were started in March 2008 by the Egyptian contracting company (Mokhtar Ibrahim) [4, 6]**.**

**Table (A.2): The composition of industrial wastewater (in g/ $m^3$) [6].**

| Parameter/ Metal | g/ $m^3$ | Parameter/ Metal | g/ $m^3$ |
|---|---|---|---|
| Temperature [°C] | 20 | Copper | 0.09 |
| COD | 2065 | Cadmium | ------- |
| BOD | 840 | Chromium | 0.011 |
| Oil and Greases | 21 | Nickel | 0.006 |
| Total nitrogen | 1.18 | Lead | 0.04 |
| Total phosphorus | 1.15 | pH | 7.2 |
| Suspended solids | 426 | Sulfide | 1.6 |
| Soluble solids | 716 | *E. coli* | $16*10^8$ |

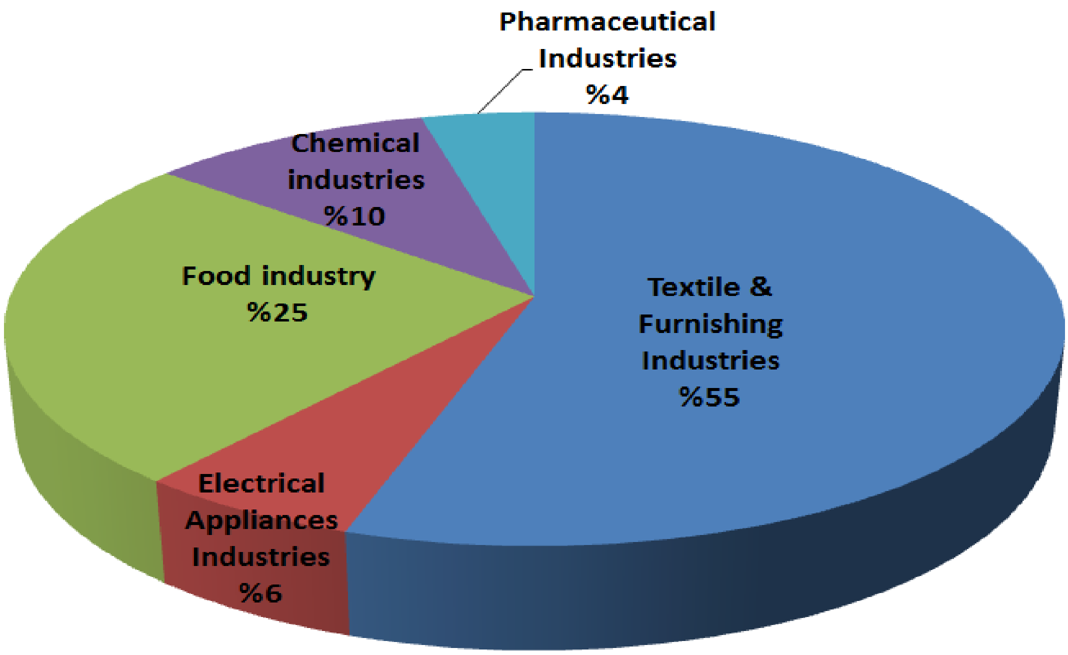


**Figure (A.4): The water consumption of the various industries in the third industrial zone and its expansion, as well as the fourth industrial zone and its extension [4].**

### 3- The project of the construction of the tertiary wastewater treatment plant for human wastewater

The first stage of the new tertiary wastewater treatment plant for the new city of Burj Al-Arab is completed. The station is located west of the city in the old quarry area. The project will be executed in three stages with a total design capacity of 345,000 $m^3$/ day by about 115,000 $m^3$/ day for each stage. The proposal is to be implemented in four stages and a design card of 460,000 $m^3$/ day. It is proposed that a new western industrial wastewater treatment plant with a capacity of 65,000 $m^3$/ day be constructed at the same site. This plant treats the discharges resulting from the third and fourth industrial areas and their extension, as part of the work of separating the industrial drainage from human drainage prepared by the consulting office "EGC" [4, 6].

### 4- Sanitary drainage project for the fifth industrial zone and industrial developer area (A, B, and C)

The sewerage system is currently being implemented to serve the fifth industrial zone and industrial development areas (A, B, and C). The project consists of slop lines of pottery with a flexible compass with diameters of 450 mm, 500 mm, 600 mm and slope lines of reinforced concrete with diameters of 700 mm, 900 mm, 1000 mm, and 1200 mm. The project also includes the construction of a lift station with a 900 mm GRP line [4, 6].

### 5- Works of the housing facilities of associations in the eighth district

Implementation and delivery have been completed of drinking water and sanitation network in the area of housing societies in the eighth district. The project consists of a drinking water network with its accessories. It is made up of UPVC plastic pipes with diameters ranging from 110 mm to 500 mm. The sewage network with its accessories is made up of (UPVC) plastic pipes with diameters ranging from 160 mm to 630 mm [4, 6].

## A-4: The General Plan for Urban and Industrial Development in the Burj Al-Arab City

In this sector, the necessary data will be mentioned on all the added land areas needed for all the uses distributed in the development stages in the new Burj Al Arab city as follows**:**

**Table (A.3): The needed areas of the industrial zones are distributed in the stages of development periods [4].**

| Year | 2017 | 2022 | 2027 | 2032 |
|---|---|---|---|---|
| The first industrial zone (acres) | 205 | 205 | 205 | 205 |
| The second industrial zone (acres) | 742 | 742 | 742 | 742 |
| The third industrial zone (acres) | 504 | 504 | 504 | 504 |
| The extension of the third industrial zone (acres) | 0 | 300 | 397 | 397 |
| The fourth industrial zone (acres) | 751 | 751 | 751 | 751 |
| The extension of the fourth industrial zone (acres) | 0 | 476 | 476 | 476 |
| The fifth industrial zone (acres) | 0 | 469 | 674 | 674 |
| Textile & textile industries complex (acres) | 0 | 282 | 422 | 422 |
| The engineering and chemical industries zone (acres) | 0 | 176 | 352 | 440 |
| The small industries complex (acres) | 0 | 115 | 115 | 115 |
| The workshops and stores at the second industrial zone (acres) | 127 | 127 | 127 | 127 |
| The workshops and stores at the third industrial zone (acres) | 149 | 149 | 149 | 149 |
| The valley of technology (acres) | 0 | 582 | 873 | 1038 |
| The smart village (acres) | 0 | 125 | 250 | 378 |
| The logistics area (acres) | 0 | 315 | 496 | 496 |
| The customs department and dry port (acres) | 0 | 276 | 276 | 276 |
| The free zone (acres) | 0 | 678 | 678 | 678 |

**Table (A.4): The needed for swimming pool areas, lakes in recreation areas, and club areas are distributed in the stages of development periods [4].**

| Year | 2017 | 2022 | 2027 | 2032 |
|---|---|---|---|---|
| The sporting clubs district, Total area (acres) | 200 | 645 | 645 | 645 |
| The sporting clubs district, Water bodies (acres) | 2 | 6.5 | 6.5 | 6.5 |
| The tourist resort hotel, total area (acres) | 0 | 0 | 192 | 192 |
| The tourist resort hotel, Water bodies (acres) | 0 | 0 | 1.9 | 1.9 |
| Zoo, total area (acres) | 0 | 0 | 317 | 317 |
| Zoo, water bodies (acres) | 0 | 0 | 6.3 | 6.3 |
| Fish gardens, total area (acres) | 0 | 0 | 140 | 140 |
| Fish gardens, water bodies (acres) | 0 | 0 | 2.8 | 2.8 |
| Regional and amusement parks, total area (acres) | 0 | 409 | 409 | 409 |
| Regional and amusement parks, water bodies (acres) | 0 | 0.6 | 0.6 | 0.6 |
| The total water bodies (acres) | 2 | 7.1 | 18.1 | 18.1 |
| The total water bodies (hectare) | 0.84 | 2.98 | 7.6 | 7.6 |

**Table (A.5): The needed for the tourism sector and entertainment are distributed in the stages of development periods [4].**

| Year | 2017 | 2022 | 2027 | 2032 |
|---|---|---|---|---|
| The sporting clubs district (acres) | 454 | 654 | 654 | 654 |
| The sporting clubs district (visitor) | 13884 | 20000 | 20000 | 20000 |
| The tourist resort hotel (acres) | 0 | 0 | 192 | 192 |
| The tourist resort hotel (visitor) | 0 | 0 | 30000 | 30000 |
| The galleries (acres) | 0 | 0 | 460 | 460 |
| The conference (acres) | 0 | 0 | 0 | 109 |
| Area of constructions for galleries (20%) and conference (30%) (acres) | 0 | 0 | 92 | 125 |
| The Galleries and conference (hectare) | 0 | 0 | 38.6 | 52.5 |
| The amusement parks (acres) | 0 | 409 | 409 | 409 |
| The regional parks (acres) | 0 | 358 | 358 | 358 |
| The zoo (acres) | 0 | 0 | 317 | 317 |
| The fish garden (acres) | 0 | 0 | 0 | 140 |
| The hotels (room) | 0 | 200 | 600 | 800 |

**Table (A.6): The needed areas of construction are distributed in the stages of development periods [4].**

| Uses | Until 2017 | 2017-2022 | 2022-2027 | 2027-2032 | Total area (acres) |
|---|---|---|---|---|---|
| Residential uses | 2707 | 1651 | 2076 | 2013 | 8447 |
| Total domestic services | 274 | 305 | 179 | 367 | 1125 |
| Total services of the city center | 567 | 714 | 307 | 116 | 1805 |
| Regional services | 511 | 553 | 1196 | 216 | 2476 |
| Total industrial zones | 3376 | 1538 | 909 | 254 | 6130 |
| Total commercial areas | 99 | 98 | 0 | 76 | 273 |
| Total recreational areas | 454 | 558 | 317 | 140 | 1469 |
| Total tourist areas | 63 | 52 | 706 | 179 | 1000 |
| Total investment Services areas | 1052 | 599 | 554 | 128 | 2334 |
| Agricultural services center and dairy projects, and to feed and abattoir | 89 | 151 | 71 | 64 | 375 |
| Future uses and cemetery area | 321 | 268 | 0 | 0 | 589 |
| Treatment plants | 404 | 0 | 0 | 0 | 404 |
| The total (acres) | 9970 | 6487 | 6415 | 3553 | 26427 |
| The total (hectare) | 4188 | 2725 | 2694 | 1492 | 11099 |

**Table (A.7): The areas of universities and research centers are distributed in the stages of development periods [4].**

| Year | 2017 | 2022 | 2027 | 2032 | Capacity (visitor) | The Density (visitor/ acres) |
|---|---|---|---|---|---|---|
| Mubarak academy for scientific research | 226 | 226 | 226 | 226 | 2000 | 8.85 |
| Egyptian, Japanese university | 93 | 183 | 183 | 183 | 11000 | 60.11 |
| Private universities and Alexandria university | 192 | 384 | 618 | 668 | 130000 | 194.61 |
| Research city and technological institutes | 0 | 128 | 278 | 278 | 10200 | 36.69 |
| Alexandria library | 0 | 0 | 16 | 16 | 1000 | 62.5 |
| Training center for industrial zones | 47 | 90 | 90 | 90 | 1800 | 20 |

**Table (A.8): The number of users of the university areas and research institutes are distributed in the stages of development periods [4].**

| Year | Number of visitors (visitor) | | | |
|---|---|---|---|---|
| | 2017 | 2022 | 2027 | 2032 |
| Mubarak academy for scientific research | 2000 | 2000 | 2000 | 2000 |
| Egyptian, Japanese university | 5590 | 11000 | 11000 | 11000 |
| Private universities and Alexandria university | 37365 | 73730 | 120269 | 130000 |
| Research city and technological institutes | 0 | 4696 | 10200 | 10200 |
| Alexandria library | 0 | 0 | 1000 | 1000 |
| Training center for industrial zones | 940 | 1800 | 1800 | 1800 |
| The total number of users (user) | 45895 | 93226 | 146269 | 156000 |

**Table (A.9): The total number of beds in hospitals and medical centers are distributed in the stages of development periods [4].**

| Year | 2017 | 2022 | 2027 | 2032 |
|---|---|---|---|---|
| Number of beds (compartments, beds) | 210 | 2810 | 6110 | 6210 |

# APPENDIX B

# HEAD CALCULATION OF TRANSFER AND LIFTING PUMPS

# HEAD CALCULATION OF TRANSFER AND LIFTING PUMPS

## B-1: Head Calculation of Transfer Pumps

Transfer pumps are used to pump the clarified seawater to the pressure required by the pre-treatment stage, which its head can be calculated as follows:

Outlet pressure (H) = suction pressure HLP (2 bar) + differential pressure sand filter (1 bar) + differential pressure cartridge filter (1 bar) + differential pressure pipes (0.5 bar) = 4.5 bar (B. 1)

Outlet pressure (H) = Required pressure at the top outlet (4.5 bar).

Where the pressure and feed flow to the filtration plant are known, the transfer pumps can be chosen using a coverage chart, which makes it possible to make a preliminary selection through a group of pump sizes based on a specific impeller speed [58].

## B-2: Head Calculation of Lifting Pumps

This pump is used to lift water from the production tank to the ground tanks in the new city of Burj Al Arab. The total head of the lifting pump $(\boldsymbol{H_P})$ can be calculated as follows:

$$H_P = H_{static} + H_l = H_{static} + (H_F + H_M) \tag{B.2}$$

where, $H_P$ = Total head; $H_{static}$ = Static head; $H_l$ = Lost head; $H_F$ = Friction losses; $H_M$ = Minor losses [51].

### 1- Static Head ($\mathbf{H_{static}}$) Calculation

The length of force mainline between the RO plant and Burj Al-Arab reservoirs =16 Km. The elevation of RO plant location = 18 m; the elevation of Burj Al-Arab reservoirs = 25 m (as mentioned in **step 6** in the **sector (6.3), Chapter (3)**).

- The Static head ($H_{static}$) = 25 - 16 = 7 m.

### 2- Friction Losses ($\boldsymbol{H_F}$) Calculation

$$H_F = \frac{8 \times f \times L \times {F_d}^2}{\pi^2 \times g \times D^5} \text{ (Darcy - Weisbach Formula)} \tag{B.3}$$

where, $f$ = Coefficient of friction (Darcy coefficient); $L$ = The length of force mainline;

$F_d$ = The design flow rate; $D$ = Pipe diameter (m) [51].

❖ **The force main design:**

$F_d$ **(Maximum daily discharge + fire discharge)** = 254000 $m^3$/ day = 2.94 $m^3/s$.

Assume using concrete pipe 1500 mm, Taken between V = (1 - 2) m/ s.

$2.94 = \frac{\pi D^2}{4} * V$, ⇨ V = 1.66 m/s. This is value between V = (1 - 2) m/s) ⇨ (OK)

*(f)* For concrete (0.012 - 0 .020) ⇨ take *f* = (0 .013)

Accordion to the Egyptian code for the foundations of the design and implementation conditions for pipelines used in drinking water and sewage networks [ 51].

- **Equation (B.3)** is applied and friction losses of lifting pump ($\boldsymbol{H_F}$) for three suggested configurations of PV-RO plant are calculated as follows:

$$H_F = \frac{8\times f\times L\times {F_d}^2}{\pi^2\times g\times D^5} = \frac{8\times 0.013\times 16000\times 2.94^2}{\pi^2\times 9.81\times 1.5^5} = 19.6 \text{ m}$$

### 3- Minor Losses ($\mathbf{H_M}$) Calculation

Minor losses($H_M$) are caused by a sudden change in water flow as a result of a pipe connected to a tank or in pipe attachments such as elbows, methods, jointers, and cocks [51].

Minor losses are calculated from the equation:

$$H_M = \frac{K_M\times V^2}{2\times g} \tag{B.4}$$

where, $K_M$ = Minor losses coefficient.

For valves (1100 - 1500) mm (maximum distance between valves 2000m)

$$\text{Butterfly valves needed} = \frac{\text{force main length}}{\text{maximum distance between valves}} = \frac{16 \text{ km}}{2 \text{ km}} = 8 \text{ valves} \tag{B.5}$$

$$\text{Washing valves needed} = \frac{\text{force main length}}{\text{maximum distance between valves}} = \frac{16 \text{ km}}{2 \text{ km}} = 8 \text{ valves} \tag{B.6}$$

- **Table (B.1)** Shows coefficient depends on water flow in elbows, valves, Etc ($K_M$).

- **(Tables (B.2 –B.5))** are used for calculation $K_M$ (minor losses).

**Table (B.1): The coefficient depends on water flow in elbows, valves, Etc ($K_M$) [51].**

| Items | $K_M$ | No. Items | Total $K_M$ |
|---|---|---|---|
| Entrance valve | 1 | 1 | 1 |
| Exit valve | 0.5 | 1 | 0.5×1= 0.5 |
| Butterfly valve | 0.4 | 8 | 0.4×8 =3.4 |
| Non-return valve | 4.0 | 1 | 4×1= 4 |
| Washing valve | 0.4 | 8 | 0.4×8 = 3.4 |
| Elbow 45° | 0.2 | 2 | 0.2×2 = 0.4 |
| $\sum(K_M)$ | 12.7 | | |

- **Equation (B.4)** is applied and minor losses ($H_M$) of the lifting pump for three suggested configurations of PV-RO plant is calculated as follows:

$$H_M = \frac{K_M\times V^2}{2\times g} = \frac{12.7\times 1.66^2}{2\times 9.81} = 1.8 \text{ m (Minor losses (H}_\text{M}\text{))}$$

## 4- Total Head $(H_P)$ Calculation

- **Equation (B.2)** is applied and the total head $(H_P)$ of the lifting pump for three suggested configurations of PV-RO plant is calculated as follows**:**

$$H_P = H_{static} + (H_F + H_M) = 7 + (19.6 + 1.8) = 28.4 \text{ m} \approx 2.84 \text{ (bar)}$$

**• Some design criteria are shown in the following table:**

**Table (B.2): Coefficient of friction values for various types of pipes [51].**

| Type of pipes | $f$ |
|---|---|
| Asbestos Cement pipes | 0.012 - 0.020 |
| UPVC pipes | 0.008 - 0.012 |
| GRP pipes | 0.008 - 0.012 |
| Concrete pipes | 0.012 - 0.020 |
| Cast Iron pipes | 0.012 - 0.020 |

**Table (B.3): Minor losses coefficient valves for various components [51].**

| Items | $K_M$ |
|---|---|
| Entrance | 1 |
| Exit | 0.5 |
| Valve | 0.4 |
| Non-return valve | 4.0 |
| Washing valve | 0.4 |
| Elbow 45° | 0.2 |

**Table (B.4): The maximum distance between wash valves [51].**

| Line diameter (mm) | Valve diameter (mm) | The maximum between valves (m) |
|---|---|---|
| Up to 600 | 150 | 1000 |
| 700 – 1000 | 200 | 1500 |
| 1100 – 1500 | 250 | 2000 |
| 1600 – 2000 | 350 | 2500 |
| More than 2000 | 400 | 3000 |

**Table (B.5): The maximum distance between the isolation valves [51].**

| Line diameter (mm) | The maximum distance between valves (m) |
|---|---|
| Up to 600 | 1000 |
| 700 - 1000 | 1500 |
| 1100 - 1500 | 2000 |
| 1600 - 2000 | 2500 |
| More than 2000 | 3000 |

# APPENDIX C

# PV SYSTEM DESIGN SOFTWARE PROGRAM

# PV SYSTEM DESIGN SOFTWARE PROGRAM

## C-1: Introduction

In the twentieth century, the computer has become part of everyday life in most engineering fields. PVsyst V6.86 is a PC software package for the study, sizing, and data analysis of complete PV systems. This software is geared to the needs of architects, engineers, researchers. It is also very helpful for educational training. In the following section, PVsyst V6.86 software program is briefly discussed which is also used during the design in **Chapter (4)** [60]**.**

PVsyst V6.86 offers two levels (**Preliminary design** - **Project design**) of PV system study, roughly corresponding to the different stages in the development of real projects **[60]**. PVsyst V6.86 is divided into four input files **(**see **Figure (C.1))**, namely**:**

1) **Preliminary design:** This is the pre-sizing step of a project**.**

2) **Project design:** It aims to perform a thorough system design using detailed hourly simulations [60]**.**

Within the framework of a "project", the user can perform different system simulation runs and compare them. He has to define the plane orientation (with the possibility of tracking planes or shed mounting) and to choose the specific system components. He is assisted in designing the PV array (number of PV modules in series and parallel), given a chosen inverter model, battery pack, or pump [60]**.**

In a second step, the user can specify more detailed parameters and analyze fine effects like thermal behavior, wiring, module quality, mismatch and incidence angle losses, horizon (far shading), or partial shadings of near objects on the array, and so on. For pumping systems, several system designs may be tested and compared to each other, with a detailed analysis of the behaviors and efficiencies [60]**.**

Results include several dozens of simulation variables, which may be displayed in monthly, daily, or hourly values, and even transferred to other software. The "Loss Diagram" is particularly useful for identifying the weaknesses of the system design. An engineer report may be printed for each simulation run, including all parameters used for the simulation, and the main results [60]**.**

A detailed economic evaluation can be performed using real component prices, any additional costs, and investment conditions [60]**.**

3) **Databases:** the database management for meteorological data and PV components**.**

Creation and management of geographical sites, generation, and visualization of hourly meteorological data, import of meteorological data from several predefined sources, or custom ASCII files. Database management of manufacturers and PV components, including PV modules, Inverters, Regulators, Generators, Pumps,…, etc [60]**.**

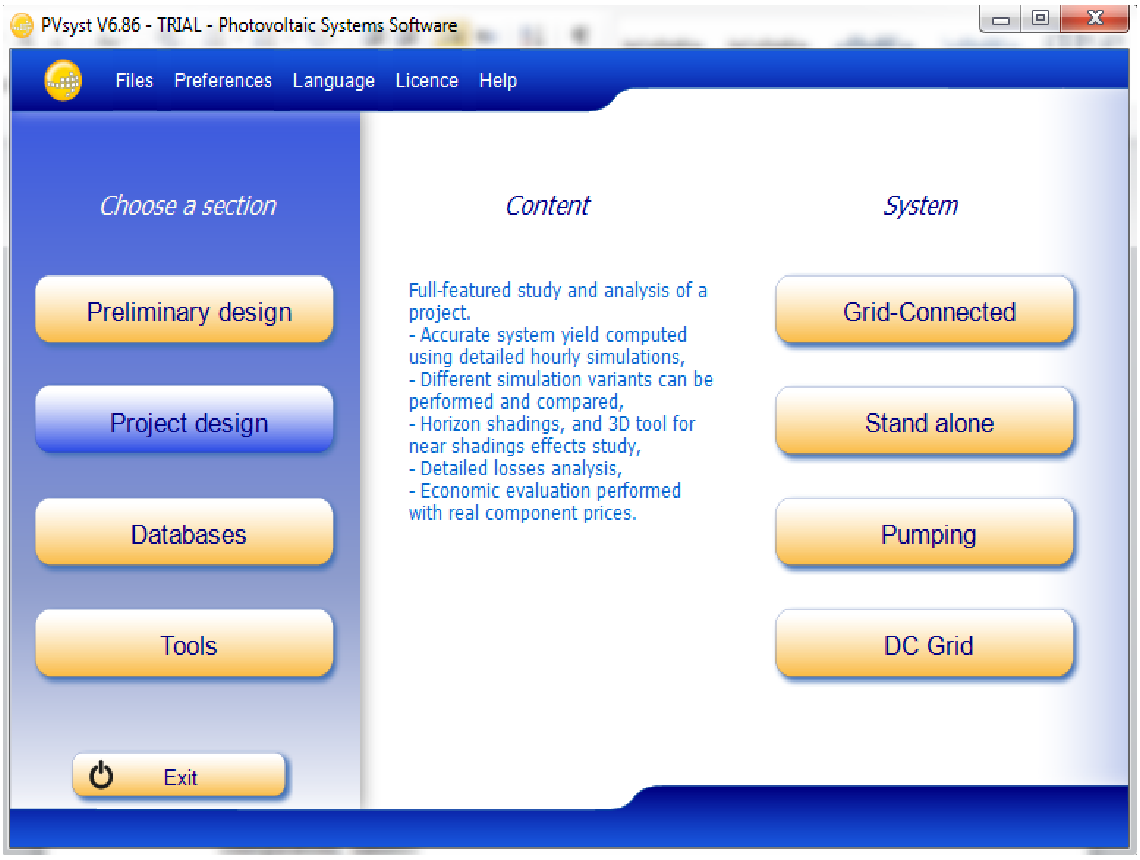


**Figure (C.1): The main window for a PVsyst V6.86 software program [60].**

**4) Tools :**

**Measured data analysis:** when a PV system is running and carefully monitored, this part (located in the "Tools" part) permits the import of measured data (in almost any ASCII format), to display tables and graphs of the actual performances, and to perform close comparisons with the simulated variables. This is gives a means of analyzing the real running parameters of the system, and identify even very small irregularities. Included are also some specific tools useful when dealing with solar energy systems: tables and graphs of meteo data or solar geometry parameters, irradiation under a clear day model, PV-array behavior under partial shadings or module mismatch, optimizing tools for orientation or voltage,…, etc [60]**.**

- PV system at PVsyst V6.86 software program **(Project design level)** is divided into four configurations **(**see **Figure (C.1))**, namely**:**

  **1) Grid-connected system;**
  **2) Stand-alone system;**
  **3) Pumping system;**
  **4) DC Grid system.**

❖ Two configurations only used for design PV systems in this search, as follows:

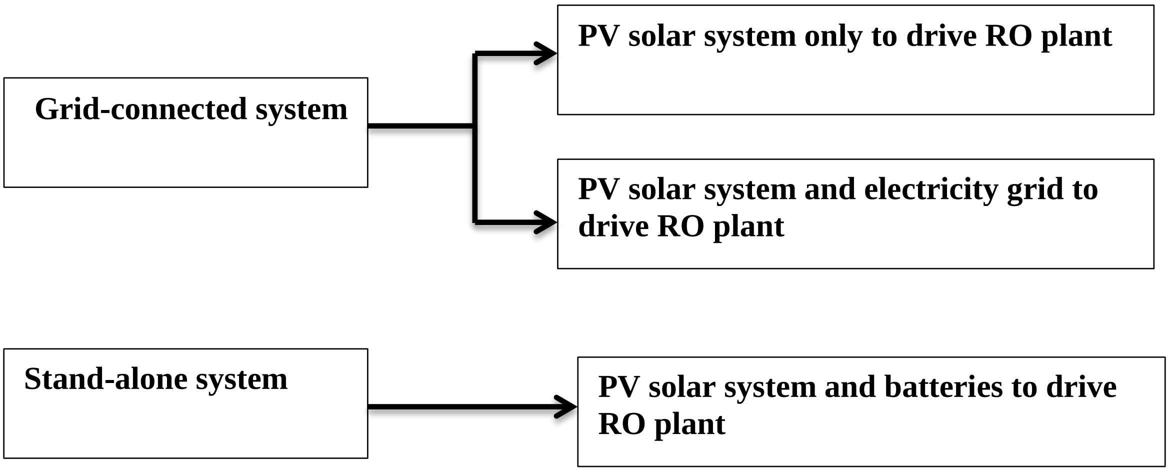


## C-2: PV System Design in PVsyst V6.86 Software Program

In this search, solar energy was considered a renewable energy source for the RO plant. SO, the feasibility study of the PV-RO plant was investigated for the three suggested configurations mentioned in **the sector (3.5)** in **Chapter (3).**

The total required electrical power capacity (30 MW → **the outcome of step (6**) in **Chapter (4)**) to operate the RO desalination plant by solar energy was divided into (30) units, each unit with a generating capacity of (1 MW). Each unit has its own electrical cable, and these units are connected to the main electrical panel and special electrical switchgear. The availability of connecting to the electricity grid or batteries is taking into consideration in PV configurations that needed it. The PV system LCOE calculations will be made on only one generating unit with a capacity of only 1 MW. This is because all units have the same conditions, components, costs, and capacities for all generating units (with a capacity of 1MW), so the economic study (LCOE) of the generated unit energy cost (USD/ KWh) from a single generation unit equals the generated unit energy cost (USD/ KWh)of combined generating units**.**

PVsyst V6.86 software program was used to design, optimize, sizing PV arrays and battery banks and analyze the performance of the designed PV system. The input data of details of the defined site was obtained from (**Table (3.7)** in **Chapter (3)**). The input data of system parameters used in designing the PV was obtained from (**Table (3.8)** in **Chapter (3)**)**.**

❖ **The process of designing a PV system in PVsyst includes the following basic steps:**

1. Project – define the location and meteorological data**;**
2. Orientation – define module azimuth and tilt**;**
3. System – choose the system modules, inverters, and electrical design**;**
4. Module Layout**;**
5. Detailed Losses – mismatch**;**
6. Simulation – view a summary of the system's energy output**.**

## Step 1: Project

Choose **(Project Design)** and then **(Grid Connected)** or **(Stand-alone)** in the main PVsyst screen (see **Figure (C.1)**) [60]**.**

Click on the **(New Project)** button and then click on the **(Choose Site)** button to select the correct project site and meteorological file (the meteorological file will often be automatically associated with the chosen site) (see **Figure (C.2)**) [60]**.**

In order to add a new site to PVsyst, click on **(Databases)** in the main PVsyst screen and then **(Geographical Sites)** [60]**.**

Choose **New** and locate your site on the **(Interactive Map)** tab, or type the geographical location in the search box. Click **(Import)** and then click on the **(Import)** button with the sun icon. Click **(OK)** and then **(Save)**. When prompted to save the hourly values, click **(Yes)** and then **(Close)** and **(Exit)** (see **Figure (C.3)**) [60]**.**

The definitions of a geographical site are in the form of a PDF file, and we can get it by press the **(print)** button. The definition of a geographical site file (PDF form) was created by PVsyst (see **Figure (C.4)**) [60]**.**

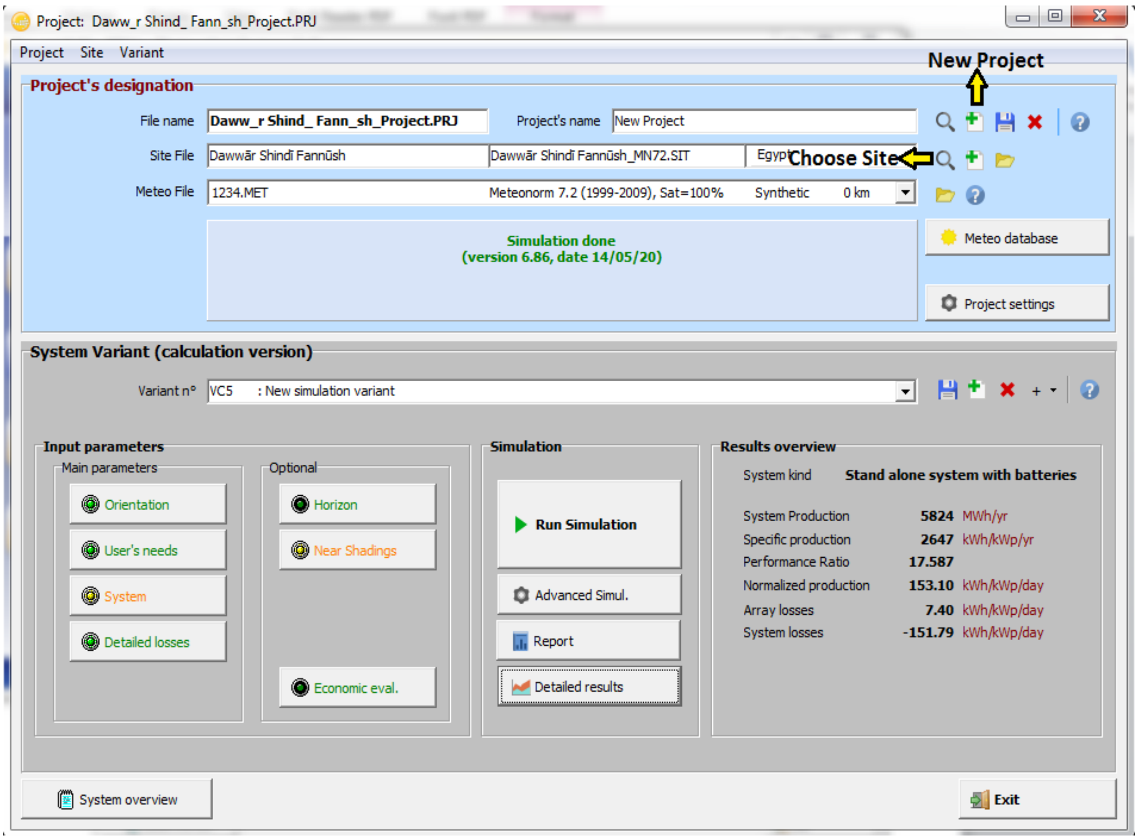


**Figure (C.2): The project window for a PVsyst V6.86 software program [60].**

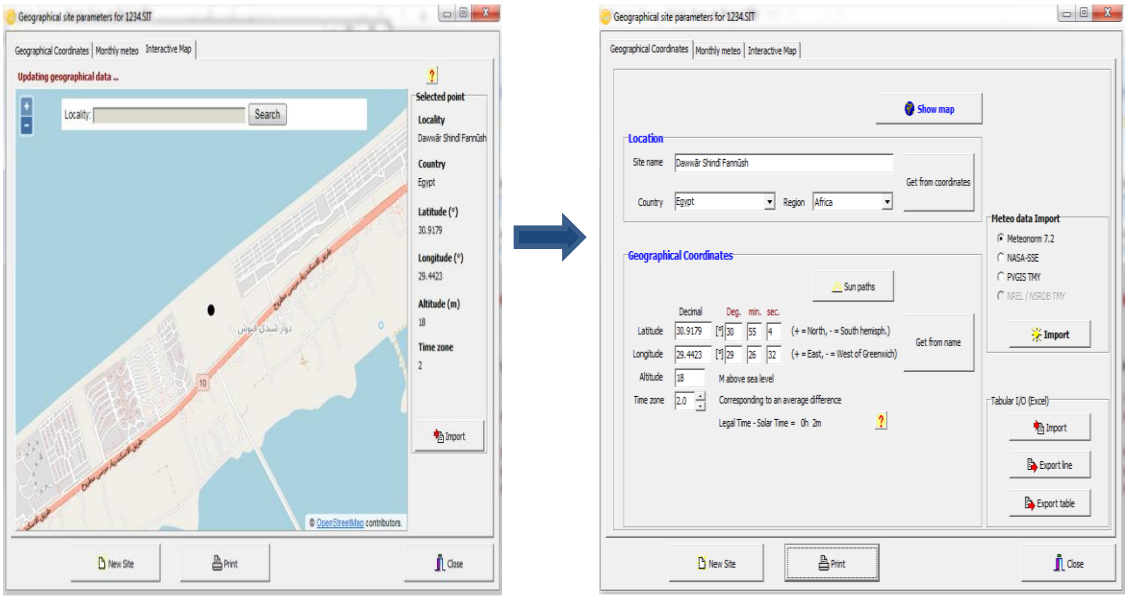


**Figure (C.3): The geographical site window for a PVsyst V6.86 software program [60].**

| PVSYST V6.86 | | 23/05/20 | Page 1/1 |
|---|---|---|---|

Definition of a geographical site

**Geographical Site** **Dawwār Shindī Fannūsh** Country **Egypt**

File 1234.SIT of 05/05/20 11h53

**Situation**
Time defined as

| | | | |
|---|---|---|---|
| Latitude | 30.92° N | Longitude | 29.44° E |
| Legal Time | Time zone UT+2 | Altitude | 18 m |

**Monthly Meteo Values** Source 1234

| | Jan. | Feb. | Mar. | Apr. | May | June | July | Aug. | Sep. | Oct. | Nov. | Dec. | Year | |
|---|---|---|---|---|---|---|---|---|---|---|---|---|---|---|
| Hor. global | 3.26 | 4.15 | 5.51 | 6.81 | 7.63 | 8.11 | 8.08 | 7.25 | 6.17 | 4.85 | 3.84 | 3.07 | 5.73 | kWh/m².day |
| Hor. diffuse | 1.15 | 1.56 | 1.94 | 2.09 | 2.11 | 1.92 | 1.70 | 1.94 | 1.79 | 1.52 | 1.11 | 1.09 | 1.66 | kWh/m².day |
| Extraterrestrial | 5.80 | 7.17 | 8.71 | 10.20 | 11.11 | 11.45 | 11.29 | 10.58 | 9.30 | 7.71 | 6.17 | 5.39 | 8.75 | kWh/m².day |
| Clearness Index | 0.562 | 0.579 | 0.633 | 0.667 | 0.686 | 0.708 | 0.716 | 0.685 | 0.663 | 0.629 | 0.622 | 0.569 | 0.656 | |
| Amb. temper. | 13.3 | 13.8 | 16.7 | 19.3 | 22.8 | 25.6 | 27.9 | 27.9 | 25.9 | 23.1 | 18.9 | 15.0 | 20.9 | °C |
| Wind velocity | 3.0 | 3.5 | 3.4 | 3.6 | 3.4 | 3.5 | 3.7 | 3.3 | 3.1 | 2.7 | 2.5 | 2.7 | 3.2 | m/s |

**Solar paths at Dawwār Shindī Fannūsh, (Lat. 30.9179° N, long. 29.4423° E, alt. 18 m) - Legal Time**

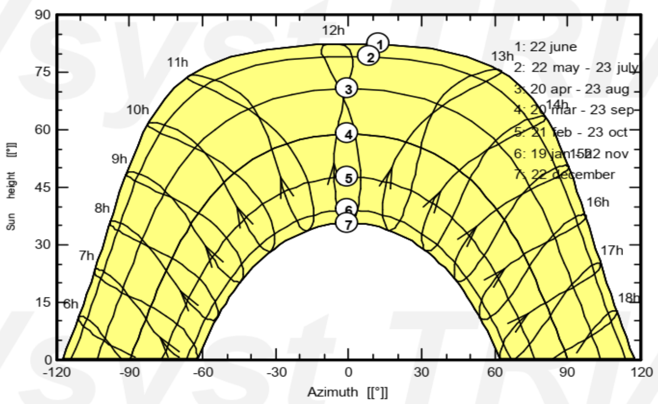


PVsyst Evaluation mode

**Figure (C.4): The definitions of a geographical site file (PDF form) created by PVsyst [60].**

## Step 2: Orientation

Once the geographical location and climate file have been chosen, the array's azimuth and tilt are defined. PVsyst offers different options to fit various types of projects, including simple fixed tilted plane, multiple orientations (up to 8 orientations), seasonal tilt adjustments, 'unlimited sheds' for large systems, sun shields (modules mounted to facades of buildings) as well as various kinds of tracking arrays, both single and double-axis. Two-axis tracking is selected in this project (see **Figure (C.5)**) [60]**.**

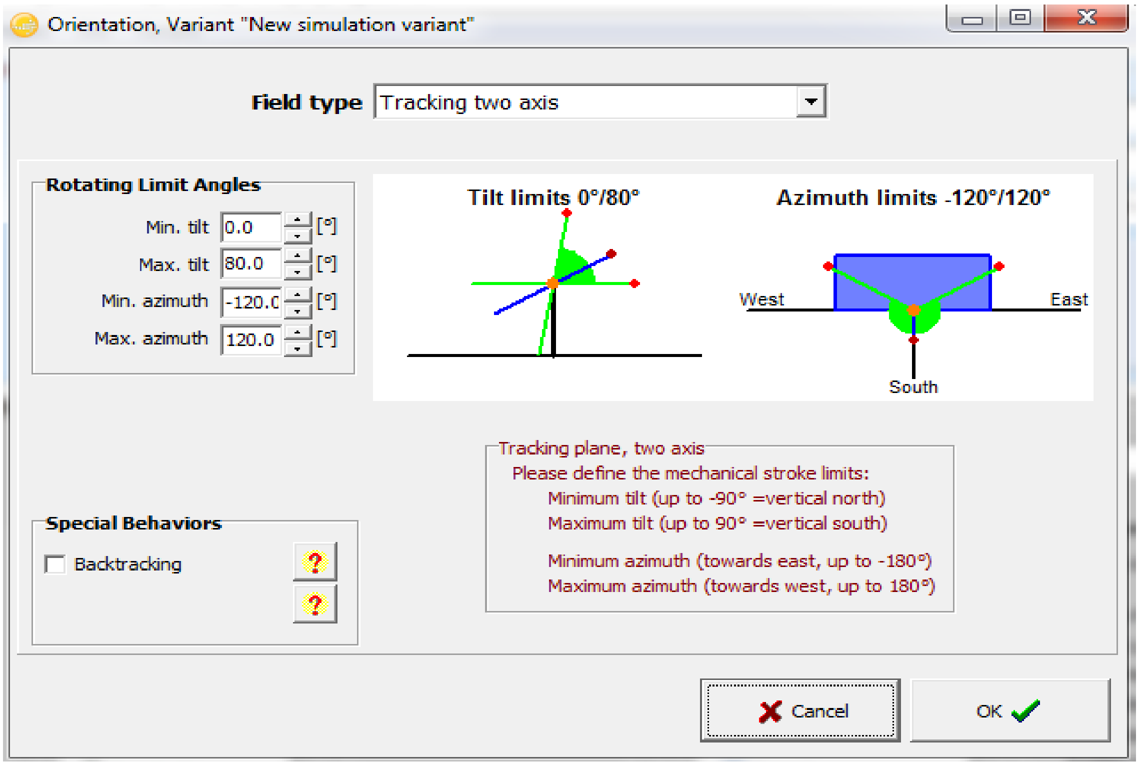


**Figure (C.5): The orientation window for a PVsyst V6.86 software program [60].**

## Step 3: System

The input data of system parameters used in designing the PV was obtained from **(Table 3.12** in **Chapter (3))**. The main system parameters, including module and inverter model, system capacity, string lengths, etc. (see **Figure (C.6)**). The Stand-alone system has additional parameters parameter that is storage (see **Figure (C.7)**). This is where PVsyst advantages become apparent [60]**.**

- Planned power (1000 KW = 1MW) is entered (see **Figure (C.6)** & **Figure (C.8)).**

The system parameters characteristics are in the form of a PDF file, and we can get it by press the **(print)** button. The system parameters characteristics file (PDF form) was created by PVsyst (see **Figures (C.9 - C.11)**) [60]**.**

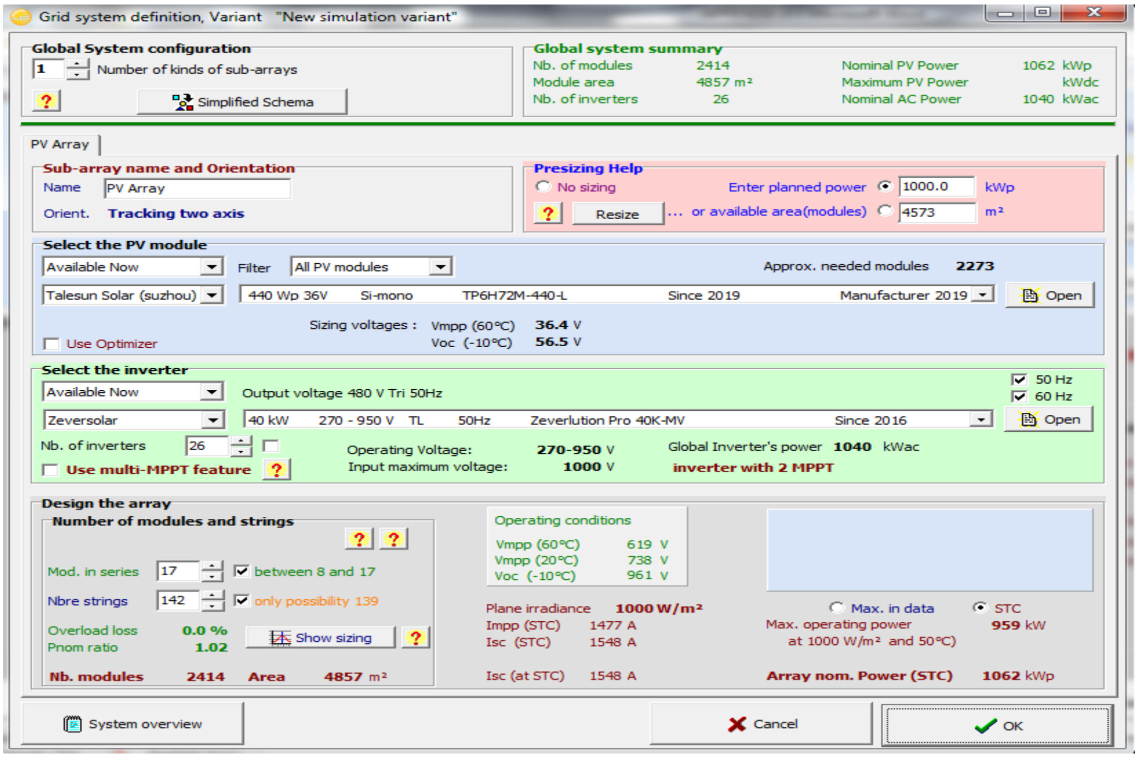

Figure (C.6): The grid system window for a PVsyst V6.86 software program [60].

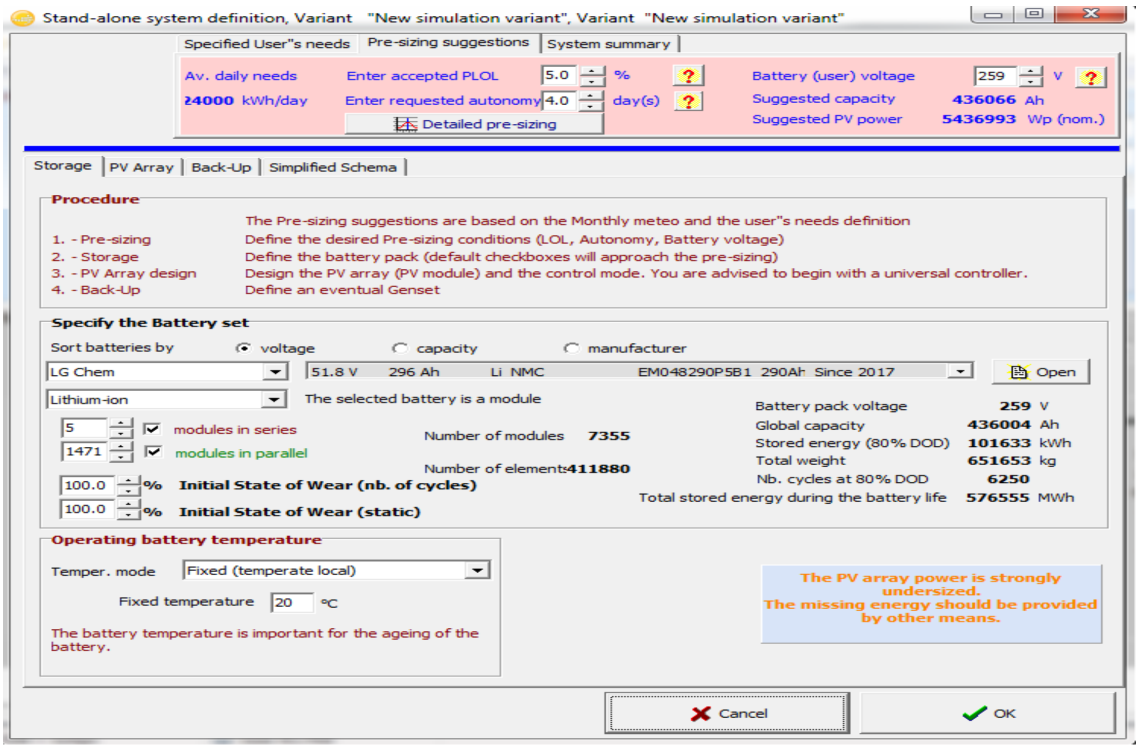

Figure (C.7): The stand-alone system window for a PVsyst V6.86 software program [60].

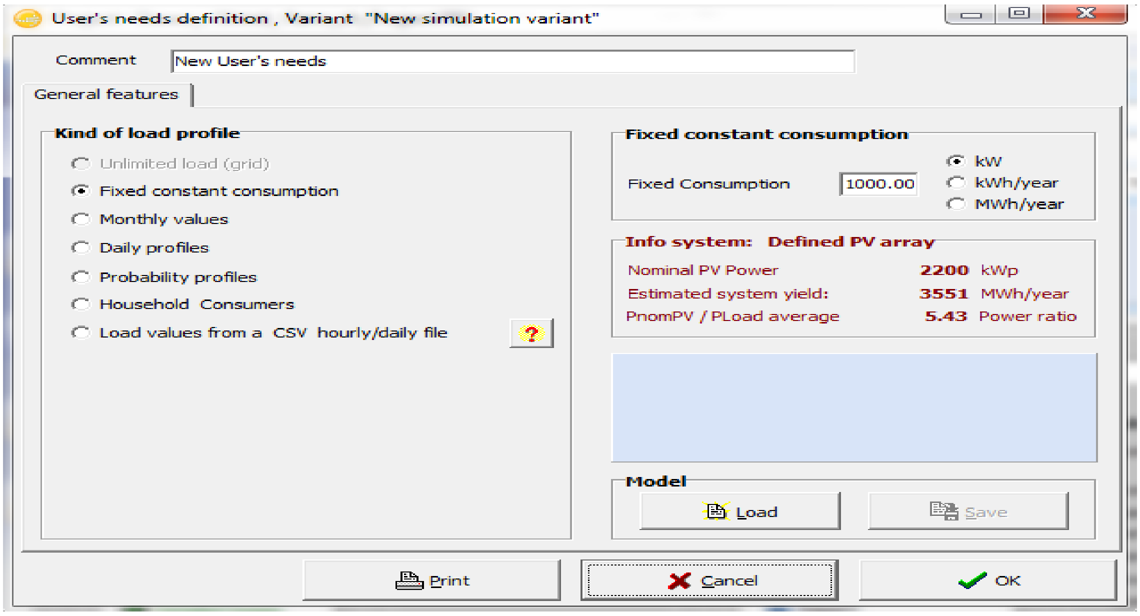


**Figure (C.8): The user's need's definition window for a PVsyst V6.86 software program [60].**

| PVSYST V6.85 | | 05/05/20 | Page 1/1 |
|---|---|---|---|

### Characteristics of an inverter

| | |
|---|---|
| Manufacturer, model : | **Zeversolar, Zeverlution Pro 40K-MV** |
| Availability : | Prod. Since 2016 |
| Data source : | Manufacturer 2017 |

**270**

| | | | | | |
|---|---|---|---|---|---|
| Operating mode | | **MPPT** | | | |
| **Minimum MPP Voltage** | **Vmin** | **N/A V** | Nominal PV Power | Pnom DC | 41 kW |
| **Maximum MPP Voltage** | **Vmax** | **950 V** | Maximum PV Power | Pmax DC | 51 kW |
| Absolute max. PV Voltage | Vmax array | 1000 V | Maximum PV Current | Imax DC | N/A A |
| Min. Voltage for PNom | Vmin PNom | 540 V | Power Threshold | Pthresh. | 25 W |
| **"String" inverter with input protections** | | | Number of string inputs | | 8 |
| **Multi MPPT capability** | | | Number of MPPT inputs | | 2 |
| Behaviour at Vmin/Vmax | | Limitation | Behaviour at Pnom | | Limitation |

**Output characteristics (AC grid side)**

| | | | | | |
|---|---|---|---|---|---|
| Grid Voltage | Unom | 480 V | **Nominal AC Power** | **Pnom AC** | **40 kWac** |
| Grid frequency | Freq | 50 Hz | Maximum AC Power | Pmax AC | 40 kWac |
| | | Triphased | Nominal AC current | Inom AC | 48 A |
| | | | Maximum AC current | Imax AC | 48 A |

| | | | |
|---|---|---|---|
| **Efficiency defined for 3 voltages** | 600 V | 720 V | 800 V |
| Maximum efficiency | 98.4 % | 98.8 % | 98.7 % |
| European average efficiency | 98.2 % | 98.6 % | 98.5 % |

**Remarks and Technical features**

Technology: TL, 16 kHz, IGBT
Protection: -25 - +60°C, IP 65: outdoor installation
Control: LCD, Graphic

| Sizes: | |
|---|---|
| Width | 510 mm |
| Height | 710 mm |
| Depth | 260 mm |
| Weight | 58.00 kg |



**Figure (C.9): The characteristics of an inverter file (PDF form) created by PVsyst [60].**

| PVSYST V6.86 | | 05/05/20 | Page 1/1 |
|---|---|---|---|

## Characteristics of a PV module

Manufacturer, model : **Talesun Solar (suzhou), TP6H72M-440-L**

Availability : Prod. Since 2019

Data source : Manufacturer 2019

| | | | | | | | |
|---|---|---|---|---|---|---|---|
| **STC power (manufacturer)** | **Pnom** | **440** | **Wp** | **Technology** | | **Si-mono** | |
| Module size (W x L) | | 1.002 x 2.008 | m² | Rough module area | Amodule | 2.01 | m² |
| Number of cells | | 2 x 72 | | Sensitive area (cells) | Acells | 1.81 | m² |

**Specifications for the model (manufacturer or measurement data)**

| | | | | | | | |
|---|---|---|---|---|---|---|---|
| Reference temperature | TRef | 25 | °C | Reference irradiance | GRef | 1000 | W/m² |
| Open circuit voltage | Voc | 50.8 | V | Short-circuit current | Isc | 10.90 | A |
| Max. power point voltage | Vmpp | 42.3 | V | Max. power point current | Impp | 10.40 | A |
| => maximum power | Pmpp | 439.9 | W | Isc temperature coefficient | muIsc | 5.5 | mA/°C |

**One-diode model parameters**

| | | | | | | | |
|---|---|---|---|---|---|---|---|
| Shunt resistance | Rshunt | 400 | ohm | Diode saturation current | IoRef | 0.018 | nA |
| Serie resistance | Rserie | 0.22 | ohm | Voc temp. coefficient | MuVoc | -170 | mV/°C |
| | | | | Diode quality factor | Gamma | 1.01 | |
| Specified Pmax temper. coeff. | muPMaxR | -0.39 | %/°C | Diode factor temper. coeff. | muGamma | -0.001 | 1/°C |

**Reverse Bias Parameters, for use in behaviour of PV arrays under partial shadings or mismatch**

| | | | | | | |
|---|---|---|---|---|---|---|
| Reverse characteristics (dark) | BRev | 3.20 | mA/V² | (quadratic factor (per cell)) | | |
| Number of by-pass diodes per module | | 3 | | Direct voltage of by-pass diodes | -0.7 | V |

**Model results for standard conditions (STC: T=25°C, G=1000 W/m², AM=1.5)**

| | | | | | | | |
|---|---|---|---|---|---|---|---|
| Max. power point voltage | Vmpp | 42.6 | V | Max. power point current | Impp | 10.33 | A |
| Maximum power | Pmpp | 440.2 | Wc | Power temper. coefficient | muPmpp | -0.38 | %/°C |
| Efficiency(/ Module area) | Eff_mod | 21.9 | % | Fill factor | FF | 0.795 | |
| Efficiency(/ Cells area) | Eff_cells | 24.3 | % | | | | |

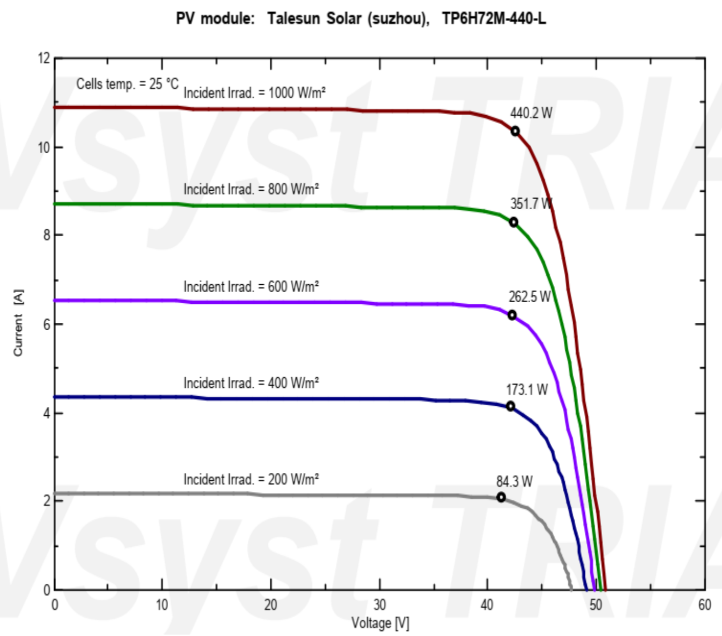


PVsyst Evaluation mode

**Figure (C.10): The characteristics of a PV module file (PDF form) created by PVsyst [60].**

| PVSYST V6.86 | | 05/05/20 | Page 1/1 |
|---|---|---|---|

**Characteristics of a battery**

| | |
|---|---|
| Manufacturer, model : | **LG Chem, EM048290P5B1 290Ah** |
| Availability : | Prod. Since 2017 |
| Data source : | Datasheet 2019 |



| | | |
|---|---|---|
| Sizes: | Width | 445 mm |
| | Height | 110 mm |
| | Depth | 1162 mm |
| | Weight | 88.60 kg |

**Basic parameters**

| Technology | **Lithium-ion, NMC** | | **Per cell** | **Whole battery** |
|---|---|---|---|---|
| Number of cells | | NCells | | 14 Cells |
| Nominal Voltage | | Vnom | 3.7 V | 51.4 V |
| Nominal Capacity (at discharge rate of 10 hours) | | Cnom | 74 Ah | 3.81 kWh |
| Internal resistance | | Int. Res. | 2.2 mOhm | 30 mOhm |
| Coulombic efficiency (without gassing) | | Eff. I | 96 % | |

**Secondary and model parameters**



| | | | |
|---|---|---|---|
| Linear part of the voltage Voc : intercept SOC=0 | Alpha Voc | 3.700 V | 51.80 V |
| Linear part of the voltage Voc : slope vs SOC | Beta Voc | 700 mV | 9.80 V |
| Voltage temp. coeff. | mu Voc | mV/°C | mV/°C |
| Reference temperature | T ref | 25 C | |
| Self-discharge current (20°C) | Iself ref. | 1.1 mA | 0.79 Ah/month |

**Physical characteristics**

| | |
|---|---|
| Sizes (W x H x D) | 0.45 x 0.11 x 1.16 m x m x m |
| Weight | 89 kg |



**Figure (C.11): The characteristics of a PV battery file (PDF form) created by PVsyst [60].**

## Step 5: Detailed Losses – Mismatch

The input data of detailed losses parameters that were used in designing the PV was obtained from **(Table 3.12** in **Chapter (3))**. The main system detailed losses, including mismatch losses and module quality loss, ohmic wiring losses, annual soil losses, light induced degradation (LID), thermal loss factor. (See **Figure (C.12)**) [60]**.**

## Step 6: Simulation

Once the system parameters have been defined, click on the **(Simulation)** button. Upon completion of the simulation, a report will be available for viewing and printing [60]**.**

The simulation report is in the form of a PDF file, and we can get it by press the (print) button [60]**.**

- The simulation results report (PDF form) was created by PVsyst for PV solar system only to drive RO plant configuration and PV solar system and electricity grid to drive RO plant configuration (See **Figures (C.13 – C.16)**) [60]**.**

- The simulation results report (PDF form) was created by PVsyst for PV solar system and batteries to drive RO plant configuration (See **Figures (C.17 – C.20)**) [60]**.**

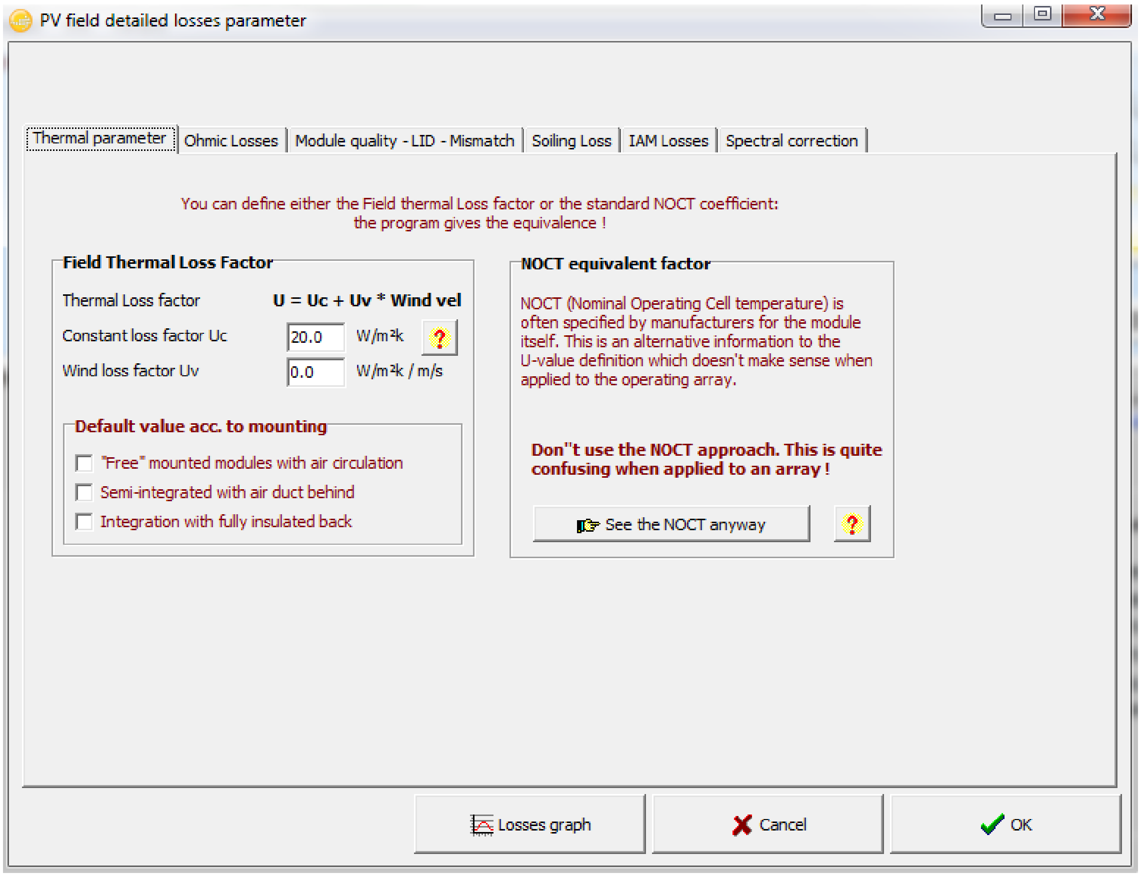


**Figure (C.12): The detailed losses parameters window for a PVsyst V6.86 software program [60].**

After the design of the PV system using the PVsyst V6.86 software program and obtaining the outputs, the financial variables and plant lifetime, capital costs values, operating costs values, grid-level system costs values, and external or social costs values mentioned in **Tables (3.10 -3.16)** in **Chapter (3)** are used as input data of **Equations (3.35)** to estimate the LCOE of PV generated power for each configuration**.**

**Table (C.1**) shows design parameters of the designed (1 MW) PV system, including the total number of PV modules, PV modules in series, PV strings, number of inverters, number of batteries, PV system energy ($E_{SYS}$), solar fraction and the unit energy cost for all PV system configurations (USD/ KWh)**.**

| PVSYST V6.86 | | 05/05/20 | Page 1/4 |
|---|---|---|---|

## Grid-Connected System: Simulation parameters

**Project :** **New Project**

| | | | | | |
|---|---|---|---|---|---|
| **Geographical Site** | **Dawwār Shindī Fannūsh** | | | Country | **Egypt** |
| **Situation** | Latitude | 30.92° N | | Longitude | 29.44° E |
| Time defined as | Legal Time | Time zone UT+2 | | Altitude | 18 m |
| | Albedo | 0.20 | | | |
| **Meteo data:** | **Dawwār Shindī Fannūsh** | Meteonorm 7.2 (1999-2009), Sat=100% - Synthetic | | | |

**Simulation variant :** **New simulation variant**

Simulation date 05/05/20 15h11

| | | | | |
|---|---|---|---|---|
| **Simulation parameters** | System type | **No 3D scene defined, no shadings** | | |
| **Tracking plane, two axis** | Minimum Tilt | 0° | Maximum Tilt | 80° |
| Rotation Limitations | Minimum Azimuth | -120° | Maximum Azimuth | 120° |
| **Models used** | Transposition | Perez | Diffuse | Perez, Meteonorm |
| **Horizon** | Free Horizon | | | |
| **Near Shadings** | No Shadings | | | |
| **User's needs :** | Unlimited load (grid) | | | |

**PV Array Characteristics**

| | | | | |
|---|---|---|---|---|
| **PV module** Si-mono | Model | **TP6H72M-440-L** | | |
| Original PVsyst database | Manufacturer | Talesun Solar (suzhou) | | |
| Number of PV modules | In series | 16 modules | In parallel | 142 strings |
| Total number of PV modules | Nb. modules | 2272 | Unit Nom. Power | 440 Wp |
| Array global power | Nominal (STC) | **1000 kWp** | At operating cond. | 902 kWp (50°C) |
| Array operating characteristics (50°C) | U mpp | 611 V | I mpp | 1477 A |
| Total area | Module area | **4571 m²** | Cell area | 4122 m² |
| **Inverter** | Model | **Zeverlution Pro 40K-MV** | | |
| Original PVsyst database | Manufacturer | Zeversolar | | |
| Characteristics | Operating Voltage | 270-950 V | Unit Nom. Power | 40.0 kWac |
| Inverter pack | Nb. of inverters | 25 units | Total Power | 1000 kWac |
| | | | Pnom ratio | 1.00 |

**PV Array loss factors**

| | | | | |
|---|---|---|---|---|
| Array Soiling Losses | | | Loss Fraction | 3.0 % |
| Thermal Loss factor | Uc (const) | 20.0 W/m²K | Uv (wind) | 0.0 W/m²K / m/s |
| Wiring Ohmic Loss | Global array res. | 7.0 mOhm | Loss Fraction | 1.5 % at STC |
| LID - Light Induced Degradation | | | Loss Fraction | 2.0 % |
| Module Quality Loss | | | Loss Fraction | -0.8 % |
| Module Mismatch Losses | | | Loss Fraction | 1.0 % at MPP |
| Strings Mismatch loss | | | Loss Fraction | 0.10 % |

Incidence effect (IAM): Fresnel AR coating, n(glass)=1.526, n(AR)=1.290

| 0° | 30° | 50° | 60° | 70° | 75° | 80° | 85° | 90° |
|---|---|---|---|---|---|---|---|---|
| 1.000 | 0.999 | 0.987 | 0.962 | 0.892 | 0.816 | 0.681 | 0.440 | 0.000 |

Spectral correction FirstSolar model. Precipitable water estimated from relative humidity

| Coefficient Set | C0 | C1 | C2 | C3 | C4 | C5 |
|---|---|---|---|---|---|---|
| Monocrystalline Si | 0.85914 | -0.02088 | -0.0058853 | 0.12029 | 0.026814 | -0.001781 |



**Figure (C.13): The simulation results report (PDF form) created by PVsyst for PV solar system only to drive RO plant configuration and PV solar system and electricity grid to drive RO plant configuration, page number (1) [60].**

| PVSYST V6.86 | | 05/05/20 | Page 2/4 |
|---|---|---|---|

## Grid-Connected System: Main results

**Project :** **New Project**

**Simulation variant :** **New simulation variant**

| | | | | |
|---|---|---|---|---|
| **Main system parameters** | System type | **No 3D scene defined, no shadings** | | |
| PV Field Orientation | Tracking two axis | | | |
| PV modules | Model | TP6H72M-440-L | Pnom | 440 Wp |
| PV Array | Nb. of modules | 2272 | Pnom total | **1000 kWp** |
| Inverter | Model | Zeverlution Pro 40K-MV | Pnom | 40.0 kW ac |
| Inverter pack | Nb. of units | 25.0 | Pnom total | **1000 kW ac** |
| User's needs | Unlimited load (grid) | | | |

| | | | | |
|---|---|---|---|---|
| **Main simulation results** | | | | |
| System Production | **Produced Energy** | **2564 MWh/year** | Specific prod. | 2565 kWh/kWp/year |
| | Performance Ratio PR | 80.71 % | | |

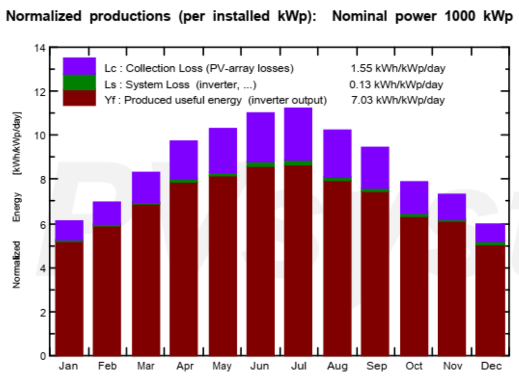


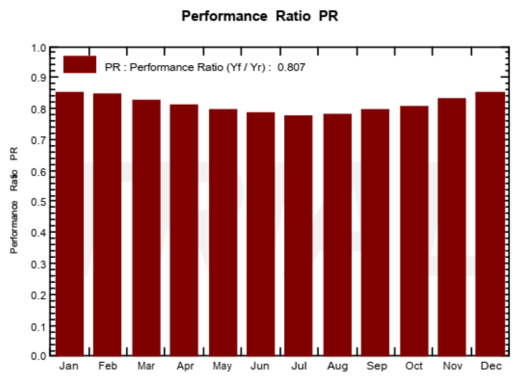


**New simulation variant**

**Balances and main results**

| | GlobHor kWh/m² | DiffHor kWh/m² | T_Amb °C | GlobInc kWh/m² | GlobEff kWh/m² | EArray MWh | E_Grid MWh | PR |
|---|---|---|---|---|---|---|---|---|
| **January** | 101.1 | 35.71 | 13.32 | 188.7 | 181.3 | 163.0 | 160.3 | 0.850 |
| **February** | 116.2 | 43.82 | 13.83 | 194.6 | 186.8 | 167.6 | 164.9 | 0.847 |
| **March** | 170.9 | 59.98 | 16.70 | 257.6 | 247.2 | 216.6 | 212.9 | 0.827 |
| **April** | 204.2 | 62.69 | 19.34 | 291.3 | 279.9 | 240.5 | 236.3 | 0.812 |
| **May** | 236.4 | 65.39 | 22.84 | 318.7 | 306.4 | 257.7 | 253.0 | 0.794 |
| **June** | 243.2 | 57.47 | 25.55 | 329.5 | 317.2 | 263.3 | 258.5 | 0.785 |
| **July** | 250.6 | 52.66 | 27.85 | 347.3 | 334.5 | 274.5 | 269.4 | 0.776 |
| **August** | 224.7 | 60.12 | 27.94 | 316.3 | 304.2 | 251.5 | 246.9 | 0.781 |
| **September** | 185.1 | 53.64 | 25.88 | 282.5 | 271.6 | 228.1 | 224.0 | 0.793 |
| **October** | 150.2 | 47.17 | 23.12 | 244.6 | 235.0 | 200.6 | 197.1 | 0.806 |
| **November** | 115.1 | 33.36 | 18.94 | 220.6 | 212.3 | 185.9 | 182.7 | 0.828 |
| **December** | 95.1 | 33.77 | 14.99 | 185.8 | 178.6 | 160.3 | 157.6 | 0.849 |
| Year | 2092.7 | 605.77 | 20.90 | 3177.4 | 3055.2 | 2609.6 | 2563.7 | 0.807 |

| Legends: | | | | |
|---|---|---|---|---|
| | GlobHor | Horizontal global irradiation | GlobEff | Effective Global, corr. for IAM and shadings |
| | DiffHor | Horizontal diffuse irradiation | EArray | Effective energy at the output of the array |
| | T_Amb | T amb. | E_Grid | Energy injected into grid |
| | GlobInc | Global incident in coll. plane | PR | Performance Ratio |



**Figure (C.14): The simulation results report (PDF form) created by PVsyst for PV solar system only to drive RO plant configuration and PV solar system and electricity grid to drive RO plant configuration, page number (2) [60].**

| PVSYST V6.86 | | 05/05/20 | Page 3/4 |
|---|---|---|---|

## Grid-Connected System: Loss diagram

**Project :** **New Project**

**Simulation variant :** **New simulation variant**

| | | | | |
|---|---|---|---|---|
| **Main system parameters** | System type | **No 3D scene defined, no shadings** | | |
| PV Field Orientation | Tracking two axis | | | |
| PV modules | Model | TP6H72M-440-L | Pnom | 440 Wp |
| PV Array | Nb. of modules | 2272 | Pnom total | **1000 kWp** |
| Inverter | Model | Zeverlution Pro 40K-MV | Pnom | 40.0 kW ac |
| Inverter pack | Nb. of units | 25.0 | Pnom total | **1000 kW ac** |
| User's needs | Unlimited load (grid) | | | |

**Loss diagram over the whole year**

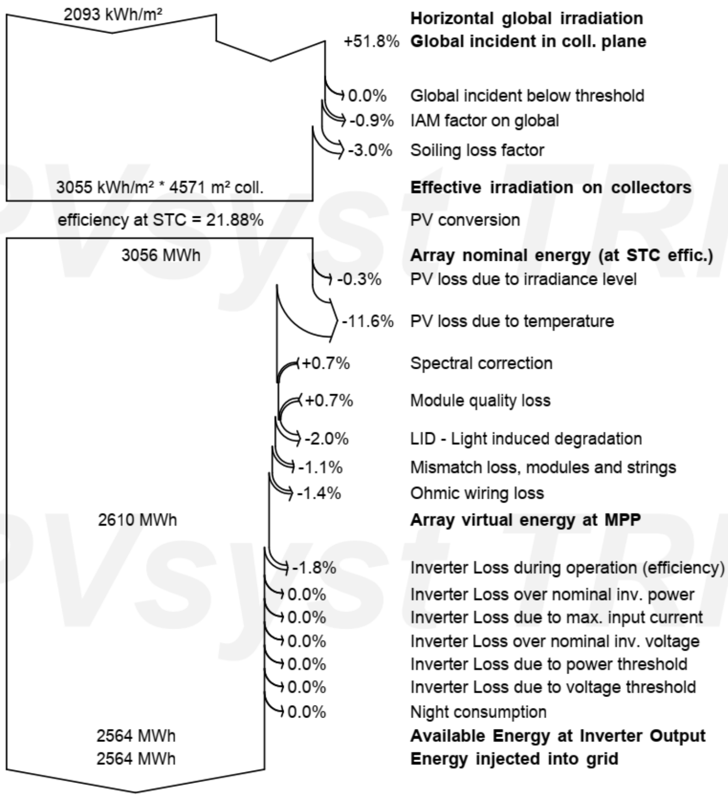






**Figure (C.15): The simulation results report (PDF form) created by PVsyst for PV solar system only to drive RO plant configuration and PV solar system and electricity grid to drive RO plant configuration, page number (3) [60].**

| PVSYST V6.86 | | 05/05/20 | Page 4/4 |
|---|---|---|---|

## Grid-Connected System: P50 - P90 evaluation

**Project :** **New Project**

**Simulation variant :** **New simulation variant**

| | | | | |
|---|---|---|---|---|
| **Main system parameters** | System type | **No 3D scene defined, no shadings** | | |
| PV Field Orientation | Tracking two axis | | | |
| PV modules | Model | TP6H72M-440-L | Pnom | 440 Wp |
| PV Array | Nb. of modules | 2272 | Pnom total | **1000 kWp** |
| Inverter | Model | Zeverlution Pro 40K-MV | Pnom | 40.0 kW ac |
| Inverter pack | Nb. of units | 25.0 | Pnom total | **1000 kW ac** |
| User's needs | Unlimited load (grid) | | | |



**Evaluation of the Production probability forecast**

The probability distribution of the system production forecast for different years is mainly dependent on the meteo data used for the simulation, and depends on the following choices:

| | | | | |
|---|---|---|---|---|
| Meteo data source | | Meteonorm 7.2 (1999-2009), Sat=100% | | |
| Meteo data | Kind | Not defined | Year | 1995 |
| Specified Deviation | Year deviation from aver. | 3 % | | |
| Year-to-year variability | Variance | 0.5 % | | |

The probability distribution variance is also depending on some system parameters uncertainties

| | | | |
|---|---|---|---|
| Specified Deviation | PV module modelling/parameters | 1.0 % | |
| | Inverter efficiency uncertainty | 0.5 % | |
| | Soiling and mismatch uncertainties | 1.0 % | |
| | Degradation uncertainty | 1.0 % | |
| Global variability (meteo + system) | Variance | 1.9 % | (quadratic sum) |

| | | |
|---|---|---|
| Annual production probability | **Variability** | **48 MWh** |
| | **P50** | **2564 MWh** |
| | **P90** | **2502 MWh** |
| | **P95** | **2485 MWh** |

**Probability distribution**

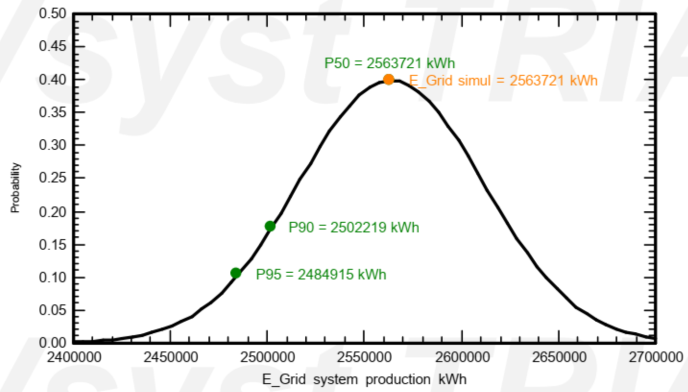






**Figure (C.16): The simulation results report (PDF form) created by PVsyst for PV solar system only to drive RO plant configuration and PV solar system and electricity grid to drive RO plant configuration, page number (4) [60].**

| PVSYST V6.86 | | 05/05/20 | Page 1/4 |
|---|---|---|---|

## Stand alone system: Simulation parameters

| | | | | |
|---|---|---|---|---|
| **Project :** | **New Project** | | | |
| **Geographical Site** | **Dawwār Shindī Fannūsh** | | Country | **Egypt** |
| **Situation** | Latitude | 30.92° N | Longitude | 29.44° E |
| Time defined as | Legal Time | Time zone UT+2 | Altitude | 18 m |
| | Albedo | 0.20 | | |
| **Meteo data:** | **Dawwār Shindī Fannūsh** | Meteonorm 7.2 (1999-2009), Sat=100% - Synthetic | | |

| | | | | |
|---|---|---|---|---|
| **Simulation variant :** | **New simulation variant** | | | |
| | Simulation date | 05/05/20 13h11 | | |

| | | | | |
|---|---|---|---|---|
| **Simulation parameters** | System type | **Stand alone system with batteries** | | |
| **Tracking plane, two axis** | Minimum Tilt | 0° | Maximum Tilt | 80° |
| Rotation Limitations | Minimum Azimuth | -120° | Maximum Azimuth | 120° |
| **Models used** | Transposition | Perez | Diffuse | Perez, Meteonorm |
| **User's needs :** | Fixed constant load | 1000 kW | Global | 8760 MWh/Year |

**PV Array Characteristics**

| | | | | |
|---|---|---|---|---|
| **PV module** Si-mono | Model | **TP6H72M-440-L** | | |
| Original PVsyst database | Manufacturer | Talesun Solar (suzhou) | | |
| Number of PV modules | In series | 1 modules | In parallel | 5000 strings |
| Total number of PV modules | Nb. modules | 5000 | Unit Nom. Power | 440 Wp |
| Array global power | Nominal (STC) | **2200 kWp** | At operating cond. | 1985 kWp (50°C) |
| Array operating characteristics (50°C) | U mpp | 38 V | I mpp | 51997 A |
| Total area | Module area | **10060 m²** | Cell area | 9072 m² |

| | | | | |
|---|---|---|---|---|
| **System Parameter** | System type | **Stand alone system** | | |
| **Battery** | Model | **EM048290P5B1 290Ah** | | |
| | Manufacturer | LG Chem | | |
| Battery Pack Characteristics | Nb. of units | 5 in series x 1488 in parallel | | |
| | Voltage | 257 V | Nominal Capacity | 441043 Ah |
| | Discharging min. SOC | 10.0 % | Stored energy | 102763.0 kWh |
| | Temperature | Fixed (20°C) | | |
| **Controller** | Model | Universal controller with MPPT converter | | |
| | Technology | MPPT converter | Temp coeff. | -5.0 mV/°C/elem. |
| Converter | Maxi and EURO efficiencies | 97.0 / 95.0 % | | |
| Battery Management control | Threshold commands as | SOC calculation | | |
| | Charging | SOC = 0.96 / 0.80 | | |
| | Discharging | SOC = 0.10 / 0.35 | | |

**PV Array loss factors**

| | | | | |
|---|---|---|---|---|
| Array Soiling Losses | | | Loss Fraction | 3.0 % |
| Thermal Loss factor | Uc (const) | 29.0 W/m²K | Uv (wind) | 0.0 W/m²K / m/s |
| Wiring Ohmic Loss | Global array res. | 0.012 mOhm | Loss Fraction | 1.5 % at STC |
| Serie Diode Loss | Voltage Drop | 0.7 V | Loss Fraction | 1.6 % at STC |
| LID - Light Induced Degradation | | | Loss Fraction | 2.0 % |
| Module Quality Loss | | | Loss Fraction | -0.8 % |
| Module Mismatch Losses | | | Loss Fraction | 1.0 % at MPP |
| Strings Mismatch loss | | | Loss Fraction | 0.10 % |





**Figure (C.17): The simulation results report (PDF form) created by PVsyst for PV solar system and batteries to drive RO plant configuration, page number (1) [60].**

| PVSYST V6.86 | | 05/05/20 | Page 2/4 |
|---|---|---|---|

## Stand alone system: Simulation parameters

Incidence effect (IAM): Fresnel AR coating, n(glass)=1.526, n(AR)=1.290

| 0° | 30° | 50° | 60° | 70° | 75° | 80° | 85° | 90° |
|---|---|---|---|---|---|---|---|---|
| 1.000 | 0.999 | 0.987 | 0.962 | 0.892 | 0.816 | 0.681 | 0.440 | 0.000 |





**Figure (C.18): The simulation results report (PDF form) created by PVsyst for PV solar system and batteries to drive RO plant configuration, page number (2) [60].**

| PVSYST V6.86 | | 05/05/20 | Page 3/4 |
|---|---|---|---|

## Stand alone system: Main results

**Project :** **New Project**

**Simulation variant :** **New simulation variant**

| | | | | |
|---|---|---|---|---|
| **Main system parameters** | System type | **Stand alone system with batteries** | | |
| PV Field Orientation | Tracking two axis | | | |
| PV modules | Model | TP6H72M-440-L | Pnom | 440 Wp |
| PV Array | Nb. of modules | 5000 | Pnom total | **2200 kWp** |
| Battery | Model | EM048290P5B1 290Ah | | Lithium-ion, NMC |
| Battery Pack | Nb. of units | 7440 | Voltage / Capacity | **257 V / 441043 Ah** |
| User's needs | Fixed constant load | 1000 kW | Global | 8760 MWh/year |

| | | | | |
|---|---|---|---|---|
| **Main simulation results** | | | | |
| System Production | **Available Energy** | **5491 MWh/year** | Specific prod. | 2496 kWh/kWp/year |
| | Used Energy | 5380 MWh/year | Excess (unused) | 0 MWh/year |
| | Performance Ratio PR | 76.96 % | Solar Fraction SF | 61.41 % |
| Loss of Load | Time Fraction | 38.2 % | Missing Energy | 3380 MWh/year |
| Battery ageing (State of Wear) | Cycles SOW | 99.5% | Static SOW | 80.0% |
| | Battery lifetime | 5.0 years | | |

Normalized productions (per installed kWp): Nominal power 2200 kWp

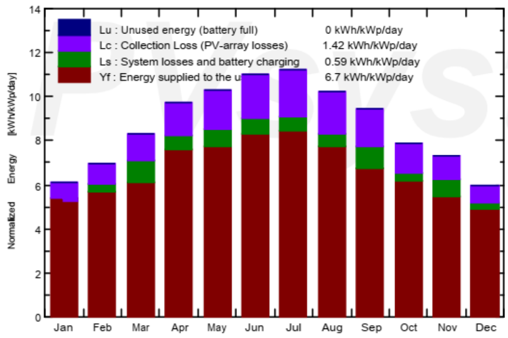


Performance Ratio PR and Solar Fraction SF

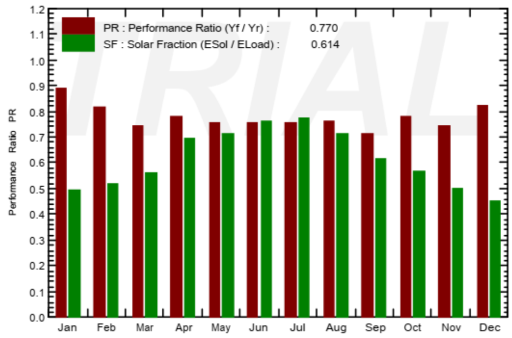


**New simulation variant**

**Balances and main results**

| | GlobHor kWh/m² | GlobEff kWh/m² | E_Avail MWh | EUnused MWh | E_Miss MWh | E_User MWh | E_Load MWh | SolFrac |
|---|---|---|---|---|---|---|---|---|
| **January** | 101.1 | 181.3 | 338.8 | 0.009 | 375.8 | 368.2 | 744.0 | 0.495 |
| **February** | 116.2 | 186.8 | 350.3 | 0.000 | 321.9 | 350.1 | 672.0 | 0.521 |
| **March** | 170.9 | 247.2 | 455.7 | 0.009 | 324.7 | 419.3 | 744.0 | 0.564 |
| **April** | 204.2 | 279.9 | 508.3 | 0.000 | 220.6 | 499.4 | 720.0 | 0.694 |
| **May** | 236.4 | 306.4 | 546.5 | 0.008 | 214.5 | 529.5 | 744.0 | 0.712 |
| **June** | 243.2 | 317.2 | 558.3 | 0.000 | 170.8 | 549.2 | 720.0 | 0.763 |
| **July** | 250.6 | 334.5 | 582.1 | 0.017 | 167.1 | 576.9 | 744.0 | 0.775 |
| **August** | 224.7 | 304.2 | 531.8 | 0.008 | 216.2 | 527.8 | 744.0 | 0.709 |
| **September** | 185.1 | 271.6 | 479.9 | 0.000 | 276.3 | 443.7 | 720.0 | 0.616 |
| **October** | 150.2 | 235.0 | 420.4 | 0.009 | 324.3 | 419.7 | 744.0 | 0.564 |
| **November** | 115.1 | 212.3 | 387.1 | 0.009 | 360.3 | 359.7 | 720.0 | 0.500 |
| **December** | 95.1 | 178.6 | 332.2 | 0.017 | 407.5 | 336.5 | 744.0 | 0.452 |
| Year | 2092.7 | 3055.2 | 5491.4 | 0.086 | 3380.1 | 5379.9 | 8760.0 | 0.614 |

Legends:

| | | | |
|---|---|---|---|
| GlobHor | Horizontal global irradiation | E_Miss | Missing energy |
| GlobEff | Effective Global, corr. for IAM and shadings | E_User | Energy supplied to the user |
| E_Avail | Available Solar Energy | E_Load | Energy need of the user (Load) |
| EUnused | Unused energy (battery full) | SolFrac | Solar fraction (EUsed / ELoad) |



**Figure (C.19): The simulation results report (PDF form) created by PVsyst for PV solar system and batteries to drive RO plant configuration, page number (3) [60].**

| PVSYST V6.86 | | 05/05/20 | Page 4/4 |
|---|---|---|---|

## Stand alone system: Loss diagram

**Project :** **New Project**

**Simulation variant :** **New simulation variant**

| | | | | |
|---|---|---|---|---|
| **Main system parameters** | System type | **Stand alone system with batteries** | | |
| PV Field Orientation | Tracking two axis | | | |
| PV modules | Model | TP6H72M-440-L | Pnom | 440 Wp |
| PV Array | Nb. of modules | 5000 | Pnom total | **2200 kWp** |
| Battery | Model | EM048290P5B1 290Ah | | Lithium-ion, NMC |
| Battery Pack | Nb. of units | 7440 | Voltage / Capacity | **257 V / 441043 Ah** |
| User's needs | Fixed constant load | 1000 kW | Global | 8760 MWh/year |

**Loss diagram over the whole year**

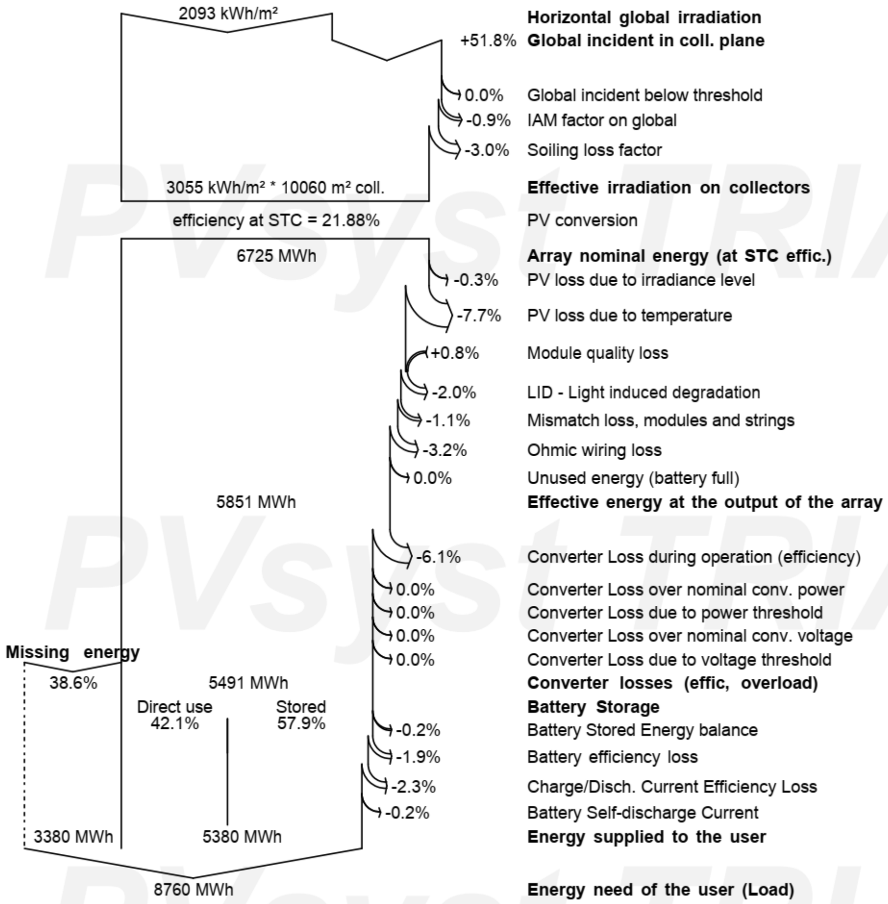






**Figure (C.20): The simulation results report (PDF form) created by PVsyst for PV solar system and batteries to drive RO plant configuration, page number (4) [60].**

**Table (C.1): The design parameters of the designed (1 MW) PV system with economic study (LCOE) for the three PV configurations; assumptions electricity cost from the grid: the base year 2020.**

| Identifier | Units | PV solar only | PV solar and batteries | PV solar and electricity grid | |
|---|---|---|---|---|---|
| | | | | PV | Grid |
| Reference output power, (Load) | KW | 1000 | 1000 | 1000 | 1000 |
| Output (STC), (Load+ storage) | KW | 1000 | 2200 | 1000 | 1000 |
| Vmpp (STC) for module | V | 42.6 | 42.6 | 42.6 | |
| Pmpp (STC) for module | W | 440.2 | 440.2 | 440.2 | |
| Total number of PV modules | Number | 2272 | 5000 | 2272 | |
| PV modules in series | Number | 16 | 1 | 16 | |
| PV strings | Number | 142 | 5000 | 142 | |
| Number of inverters | Number | 25×(40KW) | 25×(40KW) | 25×(40KW) | |
| Battery pack | Number | 0 | 7440 | 0 | |
| Performance Ratio PR | (%) | 80.71 | 76.96 | 80.71 | |
| Module efficiency (STC) | (%) | 21.9 | 21.9 | 21.9 | |
| PV System Efficiency | (%) | 17.68 | 16.85 | 17.68 | |
| PV system energy ( $E_{PV}$) | KWh/ yr | 2563700 | 5379900 | 2563700 | |
| Grid energy ($E_{el}$) | KWh/ yr | 0 | 0 | | 6196300 |
| Integrated energy ($E = E_{PV} + E_{el}$ ) | KWh/ yr | 2563700 | 5379900 | 8760000 | |
| Energy need of the user ($E_{TOTAL}$ ) | KWh/ yr | 8760000 | 8760000 | 8760000 | |
| Solar fraction ( $E / E_{TOTAL}$ ) | (%) | 29.27 | 61.41 | 100 | |
| Capital Expense | | | | | |
| PV module capital costs | USD/ kW | 600 | 600 | 600 | |
| Inverter or converter costs | USD/ kW | 266.6 | 266.6 | 266.6 | |
| Mounting structure costs | USD/ kW | 300 | 300 | 300 | |
| Balance of system (BOS) costs | USD/ kW | 540 | 540 | 540 | |
| Battery costs | USD/ kW | 0 | 3750 | 0 | |
| Capital costs ($I_{((PV)0}$ )) | USD | 1706600 | 7504520 | 1706600 | |
| Operating Expense | | | | | |
| Operating costs (Ct) | USD/ yr | 25599 | 112567.8 | 25599 | |
| Discount rate | (%) | 5 | 5 | 5 | |
| PV system lifetime (n(pv)) | Year | 25 | 25 | 25 | |
| $P_{((PV)t)} = LCOE_{(PV)}$ The unit energy cost generated from the PV system. | USD/ KWh | 0.1 | 0.21 | 0.1 | |
| The electricity energy cost from the grid | USD/ KWh | | | | 0.079 |
| Levelized transmission cost and distribution grid infrastructure | USD/ KWh | | | | $3.3 \times 10^{-3}$ |
| Emission factor for Electricity and Carbon Tax | USD/ KWh | | | | $9.7 \times 10^{-3}$ |
| $P_{((el)t)}$= The unit energy cost of conventional electricity energy | USD/ KWh | | | | 0.08 |
| $P_{((integration)t)}$ =The unit energy cost for the integration of electricity of the grid and the PV system | USD/ KWh | | | 0.086 | |
| Total System | | | | | |
| The unit energy cost for all PV system configurations | USD/ KWh | 0.1 | 0.21 | 0.086 | |

# APPENDIX D

# RO DESIGN SOFTWARE PROGRAM

# RO DESIGN SOFTWARE PROGRAM

## D-1: Introduction

In the twentieth century, the computer has become part of everyday life in most engineering fields. Major suppliers of reverse osmosis systems have developed design software programs that can simulate and optimize complex RO designs. A few of these programs can also conduct economic calculations. In the following section, IMSDesign software program is briefly discussed which is also used during the design in **Chapter (4)** [53]**.**

Hydranautics is one of the global leaders in membrane technology. Hydranautics entered the Reverse Osmosis (RO) membrane field in 1970 and is now one of the most respected and experienced companies in the industry. IMSDesign software program was developed by Hydranautics to ease the design of a membrane is driven desalination plant [53]**.**

The IMSDesign design program is divided into four input files, namely**:**

- Analysis**;**
- Design**;**
- Calculation**;**
- Post Treatment**.**

## D-2: RO Plant Design in IMSDesign Software Program

❖ For the first input **(Analysis)** window (see **Figure (D.1)**), the seawater analysis values for the Sidi Kerir region (That mention in **Table 3.3** in **Chapter 3**) are entered**.**

❖ Then you will go to the **(Design)** window **(see Figure (D.2))** and enter some data as follows**:**

a. RO plant capacity (254,000 $m^3$/ day) is inserted and divided into ten trains each train capacity of 25,400 $m^3$/ day**.**

b. The button of energy recovery devices (ERD) + (Turbo system) is selected for activation [53]**.**

c. The maximum water recovery possible during desalination is taken at 40%**.**

d. The membrane that will be selected for the designed plant is SWC6. Each train contains 318 pressure vessels. Each pressure vessel contains six spirals wound RO membranes [53]**.**

❖ To get the results, press the **(run)** button. The results are in the form of a PDF file, and we can get it by press the **(print)** button**.** The results file (PDF form) was created by IMSDesign **(**see **Figures (D.3 – D.6))** [53]**.**

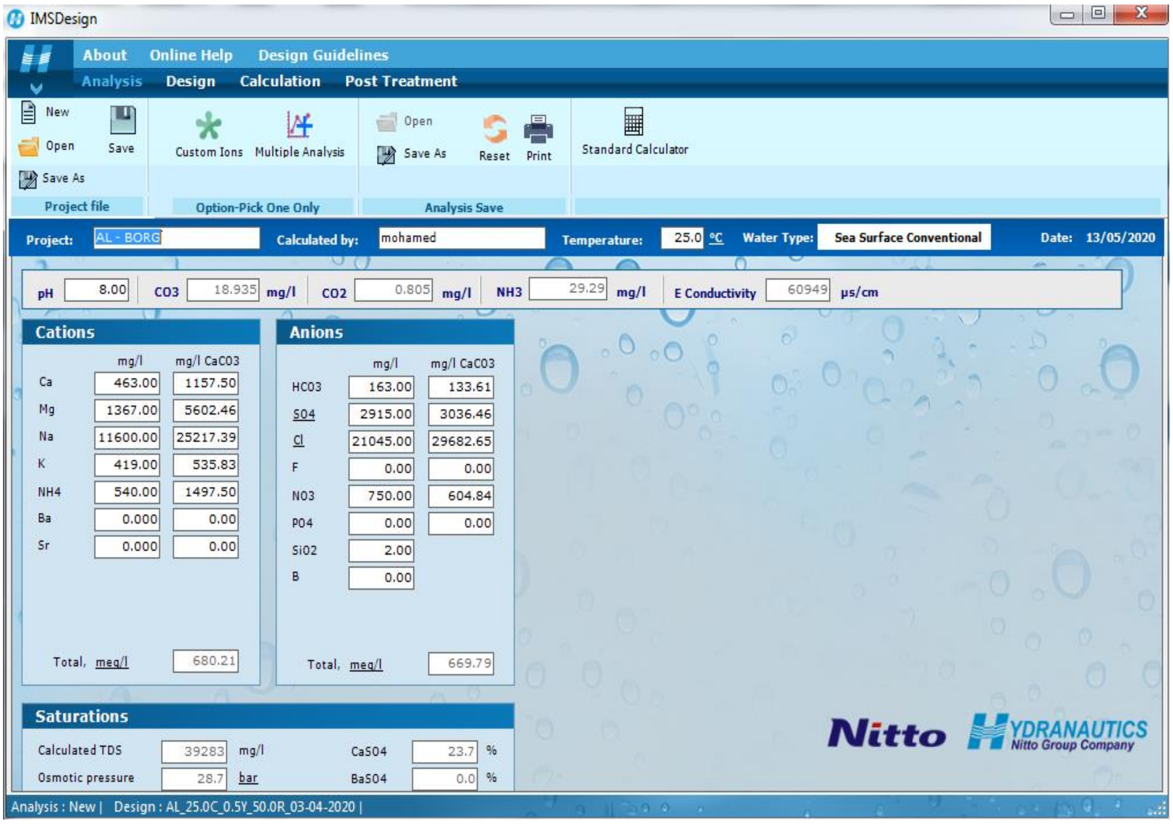

**Figure (D.1): Input and analysis window for a Reverse Osmosis element in IMSDesign [53].**

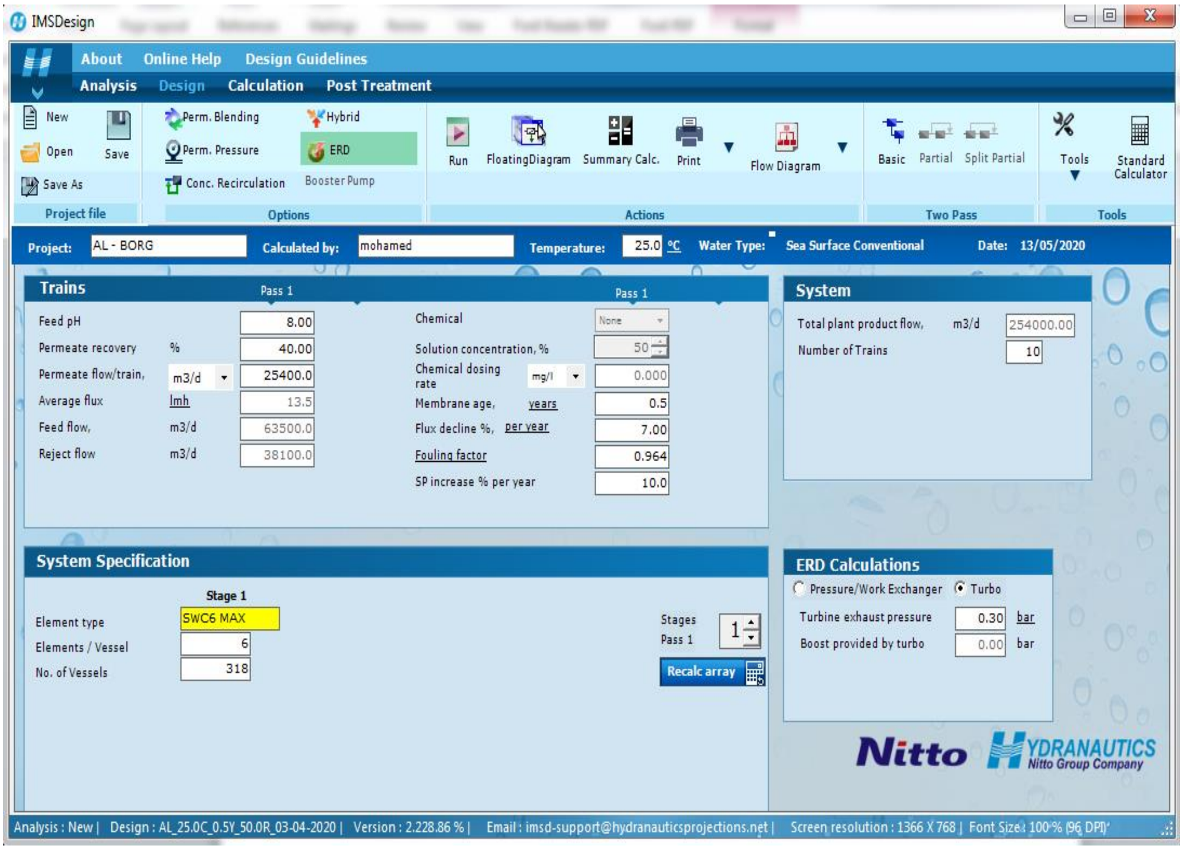

**Figure (D.2): Design window for a Reverse Osmosis element in IMSDesign [53].**

Integrated Membranes Solutions Design Software, 2018

Created on : 13/05/2020 01:53:35

Nitto HYDRANAUTICS Nitto Group Company

## Water Analysis

| | |
|---|---|
| Project name | AL - BORG |
| Water source | Sea Surface Conventional |

| | |
|---|---|
| pH | 8.00 |
| E.cond | 60948.5 µs/cm |
| CO2 | 0.805 mg/l |
| NH3 | 29.289 mg/l |
| Temperature | 25.0 °C |
| TDS | 39283 mg/l |

| Ion | mg/l | mg/l CaCO3 |
|---|---|---|
| Ca | 463.00 | 1157.50 |
| Mg | 1367.00 | 5602.46 |
| Na | 11600.00 | 25217.39 |
| K | 419.00 | 535.83 |
| NH4 | 540.00 | 1497.50 |
| Ba | 0.000 | 0.00 |
| Sr | 0.000 | 0.00 |
| | Total, meq/l | 680.21 |

| Ion | mg/l | mg/l CaCO3 |
|---|---|---|
| CO3 | 18.935 | 31.56 |
| HCO3 | 163.00 | 133.61 |
| SO4 | 2915.00 | 3036.46 |
| Cl | 21045.00 | 29682.65 |
| F | 0.00 | 0.00 |
| NO3 | 750.00 | 604.84 |
| PO4 | 0.00 | 0.00 |
| SiO2 | 2.00 | 0.00 |
| B | 0.00 | 0.00 |
| | Total, meq/l | 669.79 |

**Saturations Information**

| | |
|---|---|
| CaSO4 / KSP * 100 | 24 % |
| BaSO4 / KSP * 100 | 0 % |
| SrSO4 / KSP * 100 | 0 % |
| CaF2 / KSP * 100 | 0 % |
| SiO2 saturation | 1 % |
| Ca3(PO4)2 saturation index | 0 |
| CCPP, mg/l | 43.33 |
| Ionic strength | 0.773 |
| Osmotic pressure | 28.74 bar |



Email : imsd-support@hydranauticsprojections.net www.membranes.com +1 760 901 2500

**Figure (D.3): The results file (PDF form) created by IMSDesign software program, page number (1) [53].**

Integrated Membranes Solutions Design Software, 2018

Created on: 13/05/2020 01:46:00

Nitto HYDRANAUTICS Nitto Group Company

**Turbo( 81.5 % )**

Page : 1/4

| | | | |
|---|---|---|---|
| Project name | AL - BORG | | |
| Calculated by | mohamed | Permeate flow/train | 25400.0 m3/d |
| HP Pump flow | 2645.55 m3/h | Total product flow | 254000.00 m3/d |
| Feed pressure | 51.0 bar | Number of trains | 10 |
| Feed temperature | 25.0 °C(77.0°F) | Raw water flow/train | 63500.0 m3/d |
| Feed water pH | 8.00 | Permeate recovery | 40.00 % |
| Chem dose, mg/l, - | None | Element age | 0.5 years |
| Turbine exhaust pressure | 0.30 bar | Flux decline %, per year | 7.0 |
| Turbo boost pressure | 24.22 bar | Fouling factor | 0.96 |
| Specific energy | 2.31 kwh/m3 | SP increase, per year | 10.0 % |
| Pass NDP | 12.5 bar | | |
| Average flux rate | 13.5 lmh | | |
| | | Feed type | Sea Surface Conventional |

| Pass - Stage | Perm. Flow m3/h | Flow / Vessel Feed m3/h | Flow / Vessel Conc m3/h | Flux lmh | DP bar | Flux Max lmh | Beta | Stagewise Pressure Perm. bar | Stagewise Pressure Boost bar | Stagewise Pressure Conc bar | Perm. TDS mg/l | Element Type | Element Quantity | PV# x Elem # |
|---|---|---|---|---|---|---|---|---|---|---|---|---|---|---|
| 1-1 | 1058.5 | 8.3 | 5 | 13.6 | 1.1 | 31.2 | 1.06 | 0 | 24.2 | 49.9 | 433.7 | SWC6 MAX | 1908 | 318 x 6M |

| Ion (mg/l) | Raw Water | Feed Water | Permeate Water | Concentrate 1 |
|---|---|---|---|---|
| Hardness, as CaCO3 | 6759.96 | 6759.96 | 16.828 | 11257.6 |
| Ca | 463.00 | 463.00 | 1.153 | 771.0 |
| Mg | 1367.00 | 1367.00 | 3.403 | 2276.5 |
| Na | 11600.00 | 11600.00 | 138.300 | 19244.9 |
| K | 419.00 | 419.00 | 6.240 | 694.3 |
| NH4 | 540.00 | 540.00 | 9.174 | 875.8 |
| Ba | 0.000 | 0.000 | 0.000 | 0.0 |
| Sr | 0.000 | 0.000 | 0.000 | 0.0 |
| H | 0.00 | 0.00 | 0.000 | 0.0 |
| CO3 | 18.93 | 18.93 | 0.001 | 47.8 |
| HCO3 | 163.00 | 163.00 | 2.923 | 240.0 |
| SO4 | 2915.00 | 2915.00 | 7.287 | 4854.4 |
| Cl | 21045.00 | 21045.00 | 210.067 | 34941.7 |
| F | 0.00 | 0.00 | 0.000 | 0.0 |
| NO3 | 750.00 | 750.00 | 55.299 | 1213.4 |
| PO4 | 0.00 | 0.00 | 0.000 | 0.0 |
| OH | 0.11 | 0.11 | 0.001 | 0.2 |
| SiO2 | 2.00 | 2.00 | 0.016 | 3.3 |
| B | 0.00 | 0.00 | 0.000 | 0.0 |
| CO2 | 0.81 | 0.81 | 0.81 | 1.02 |
| NH3 | 29.29 | 29.29 | 29.29 | 29.29 |
| **TDS** | **39282.93** | **39282.93** | **433.86** | **65163.20** |
| **pH** | **8.00** | **8.00** | **6.73** | **8.08** |

| **Saturations** | **Raw Water** | **Feed Water** | **Concentrate** | **Limits** |
|---|---|---|---|---|
| CaSO4 / ksp * 100, % | 24 | 24 | 45 | 400 |
| SrSO4 / ksp * 100, % | 0 | 0 | 0 | 1200 |
| BaSO4 / ksp * 100, % | 0 | 0 | 0 | 10000 |
| SiO2 saturation, % | 1 | 1 | 2 | 140 |
| CaF2 / ksp * 100, % | 0 | 0 | 0 | 50000 |
| Ca3(PO4)2 saturation index | 0.0 | 0.0 | 0.0 | 2.4 |
| CCPP, mg/l | 43.33 | 43.33 | 94.97 | 850 |
| Ionic strength | 0.77 | 0.77 | 1.28 | |
| Osmotic pressure, bar | 28.7 | 28.7 | 47.7 | |



**Figure (D.4): The results file (PDF form) created by IMSDesign software program, page number (2) [53].**

Integrated Membranes Solutions Design Software, 2018

Created on: 13/05/2020 01:46:00

Nitto HYDRANAUTICS Nitto Group Company

**Turbo( 81.5 % )**

Project name AL - BORG Page : 3/4

Temperature : 25.0 °C Element age, P1 : 0.5 years

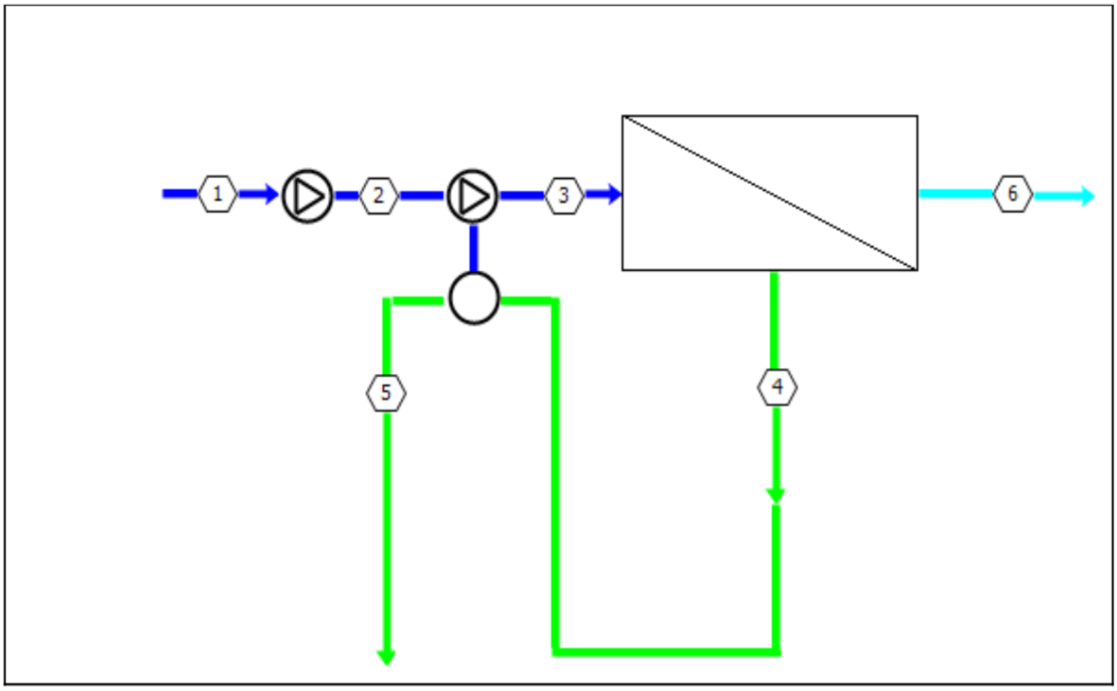


| Stream No. | Flow (m3/h) | Pressure (bar) | TDS (mg/l) | pH | Econd (µs/cm) |
|---|---|---|---|---|---|
| 1 | 2646 | 0 | 39283 | 8.00 | 60949 |
| 2 | 2646 | 26.7 | 39283 | 8.00 | 60949 |
| 3 | 2646 | 51.0 | 39283 | 8.00 | 60949 |
| 4 | 1587 | 49.9 | 65163 | 8.08 | 98375 |
| 5 | 1587 | 0.300 | 65163 | 8.08 | 98375 |
| 6 | 1058 | 0 | 434 | 6.73 | 900 |

| Pass - Stage | Element no. | Feed Pressure bar | Pressure Drop bar | Conc Osmo. bar | NDP bar | Permeate Water Flow m3/h | Permeate Water Flux lmh | Beta | Permeate (Stagewise cumulative) TDS | Ca | Mg | Na | Cl |
|---|---|---|---|---|---|---|---|---|---|---|---|---|---|
| 1-1 | 1 | 51 | 0.27 | 34.3 | 18.1 | 1.3 | 31.2 | 1.06 | 149.1 | 0.397 | 1.171 | 47.616 | 72.313 |
| 1-1 | 2 | 50.7 | 0.22 | 38.5 | 12.6 | 0.8 | 19.9 | 1.04 | 195.6 | 0.518 | 1.53 | 62.239 | 94.521 |
| 1-1 | 3 | 50.5 | 0.18 | 42 | 9 | 0.5 | 13.1 | 1.03 | 247 | 0.654 | 1.932 | 78.559 | 119.31 |
| 1-1 | 4 | 50.3 | 0.16 | 44.6 | 6.1 | 0.3 | 8.5 | 1.02 | 304.4 | 0.807 | 2.383 | 96.896 | 147.164 |
| 1-1 | 5 | 50.1 | 0.14 | 46.4 | 4.1 | 0.2 | 5.4 | 1.02 | 367 | 0.974 | 2.876 | 116.897 | 177.549 |
| 1-1 | 6 | 50 | 0.14 | 47.7 | 2.8 | 0.1 | 3.4 | 1.01 | 433.8 | 1.152 | 3.402 | 138.26 | 210.006 |



**Figure (D.5): The results file (PDF form) created by IMSDesign software program, page number (3) [53].**

Integrated Membranes Solutions Design Software, 2018

Created on: 13/05/2020 01:51:21

Nitto HYDRANAUTICS Nitto Group Company

**Turbo( 81.5 % )**

| | | | |
|---|---|---|---|
| Proiect name | AL - BORG | | |
| Calculated by | mohamed | Permeate flow/train | 25400.0 m3/d |
| HP Pump flow | 2645.55 m3/h | Total product flow | 254000.00 m3/d |
| Feed pressure | 51.0 bar | Number of trains | 10 |
| Feed temperature | 25.0 °C(77.0°F) | Raw water flow/train | 63500.0 m3/d |
| Feed water pH | 8.00 | Permeate recovery | 40.00 % |
| Chem dose, mg/l, - | None | Element age | 0.5 years |
| Turbine exhaust pressure | 0.30 bar | Flux decline %, per year | 7.0 |
| Turbo boost pressure | 24.22 bar | Fouling factor | 0.96 |
| Specific energy | 2.31 kwh/m3 | SP increase, per year | 10.0 % |
| Pass NDP | 12.5 bar | | |
| Average flux rate | 13.5 lmh | | |
| | | Feed type | Sea Surface Conventional |

| Pass - Stage | Perm. Flow m3/h | Flow / Vessel Feed m3/h | Flow / Vessel Conc m3/h | Flux lmh | DP bar | Flux Max lmh | Beta | Stagewise Pressure Perm. bar | Stagewise Pressure Boost bar | Stagewise Pressure Conc bar | Perm. TDS mg/l | Element Type | Element Quantity | PV# x Elem # |
|---|---|---|---|---|---|---|---|---|---|---|---|---|---|---|
| 1-1 | 1058.5 | 8.3 | 5 | 13.6 | 1.1 | 31.2 | 1.06 | 0 | 24.2 | 49.9 | 433.7 | SWC6 MAX | 1908 | 318 x 6M |

**CALCULATION OF POWER REQUIREMENT**

| | Pass 1 | Total system power |
|---|---|---|
| Pump/Boost pressure, bar | 26.7 | |
| Product flow, m3/d | 25400.0 | 25400 |
| Pump flow, m3/d | 63500.0 | |
| Pump efficiency, % | 87.0 | |
| Motor efficiency, % | 95.0 | |
| VFD efficiency, % | 97.0 | |
| Pumping power, BHP | 3280.6 | |
| Pumping power, kw | 2447.3 | 2447.3 |
| Pumping energy, kwh/m3 | | 2.31 |



**Figure (D.6): The results file (PDF form) created by IMSDesign software program, page number (4) [53].**

# الملخص العربى و الخلاصة و التوصيات

# الملخص العربى و الخلاصة و التوصيات

## المقدمه:

في ظل وجود الاكتظاظ السكاني في مصر في العقود الأخيرة ، كان من الضروري إنشاء وعمل توسعات فى المدن العمرانية الجديدة لاستيعاب هذا الاكتظاظ. ومن هنا، تحتاج هذه المدن الجديدة إلى مياة، و بما أن حصة مصر من مياه النيل هى ٥٥.٥ × $١٠^٩$ م$^٣$/ سنوياً، وهذه الحصة ثابتة. لذا فإن الخيار الوحيد اللازم لإدارة مواردنا المائية بكفاءة هو أما بالبحث عن موارد أخرى وتطويرها لكى تساهم مع مياه النيل فى تغطية الأحتياجات المستقبلية (مثل استخدام تحلية مياه البحر) أو بإعادة استخدام مياه الصرف الصحي المعالجة ثلاثيا فى الرى للحد من استنزاف الموارد المائية المحدودة للأجيال القادمة.

## ملخص الرسالة :

إن مدينة برج العرب الجديد هى عينة من المدن العمرانية الجديدة السكنية والصناعية الموجودة والتي تمت دراستها في هذه الرسالة، و الهدف الرئيسى من هذا الرسالة هو عمل التخطيط الأستراتيجى لمشروعات المياه الشرب و الصرف الصحى لتعزيز المرافق القائمة حاليا في مدينة برج العرب الجديدة لاستيعاب الزيادة السكانية المتوقعة حتى عام ٢٠٣٢، مع الأخذ فى الأعتبار عمل مقارنة بين التكوينات الثلاثة المقترحة للألواح الشمسية الكهروضوئية المقترنة بنظام التناضح العكسي لتحلية المياه (PV-RO) ودراسة جدوى استخدام تحلية مياه البحر عن طريق استخدام تقنية (PV-RO) كمصدر بديل ثان لمياه النيل. وذلك لتزويد المدينة بمياه الشرب لتغطية الاحتياجات المستقبلية. وهذا يتماشى مع توجيهات الحكومة في مصر.

تم تقدير مقدار الطلب على المياه وتصرفات مياه الصرف الصحي لجميع الاستخدامات. وذلك باستخدام التنبؤ بالتعداد السكاني المتوقع مع الخطة العامة للتنمية الحضرية والصناعية داخل مدينة برج العرب. ثم تطبيق القوانين ومعدلات الاستهلاك الخاصة بتقدير الطلب على المياه وتصرفات الصرف الصحي المنصوص عليها في الكود المصري لتصميم وتنفيذ مشاريع مياه الشرب والصرف الصحي. وقد تم تقييم الوضع الحالي لمرافق لمياه الشرب ومرافق الصرف الصحي في مدينة برج العرب ، وتم تحديد نقاط الضعف لوضع الحلول ضمن التخطيط الاستراتيجي المقترح في هذه الدراسة، و ايضا تم أستخدام العديد من التقنيات والبرامج المختلفة للمساعدة في اختيار الحلول المثلى.

## الاستنتاج:

بشكل عام، وفقًا للنتائج التي تم الحصول عليها من هذه الدراسة ، يمكن تمثيل الاستنتاجات الرئيسية على النحو التالي:

١- **دراسة النمو السكانى للمدينة حتى عام ٢٠٣٢:** تم عمل دراسة للتنبؤ طويل الأمد للسكان فى مدينة برج العرب الجديدة حتى سنة الهدف (٢٠٣٢) و ذلك بطريقتين هما ( الدالة الخطية – الدالة الأسية) و تم تطبيقهم بثلاث تقنيات لتشمل التقنيات التقليدية مثل استقراء منحنيات الاتجاه (Extrapolation of trend curves) ، والتقنيات الحديثة مثل الخوارزمية الجينية (GA) و أستمثال عناصر السرب (PSO). من خلال مقارنة النتائج التي تم الحصول عليها من عملية التنبؤ بعدد السكان بالطرق و تقنيات المذكورة تبين أن أفضل طرق التنبؤ طويل الأمد للسكان فى مدينة برج العرب الجديدة هى بأستخدام المعادلة الأسية مع تقنية (أستمثال عناصر السرب PSO) (٧٢٧٣٧٥ شخصًا) مقارنة بالنماذج الأخرى. ويرجع ذلك إلى أن نتائج التنبؤ السكاني باستخدام هذا النموذج هى الأقرب مع الزيادة السكان الفعلية لمدينة برج العرب الجديدة من عام ٢٠١٢ إلى عام ٢٠١٧. وايضا يتناسب معدل الزيادة المتوقع للسكان بأستخدام نموذج المعادلة الأسية مع طبيعة النمو السكاني المستقبلى في مدينة برج العرب حيث ستكون إحدى المدن الصناعية المهمة في مصر في المستقبل القريب. لذلك فإن الزيادة السكانية ستكون أسرع بسبب زيادة فرص العمل المتوقعة، وهو عامل جذب مهم للسكان. علاوة على ذلك ، يمكن تنفيذ تقنية (أستمثال عناصر السرب PSO) ببساطة، وبسرعة تقارب سريعة بدون الكثير من المعاملات، و في الوقت نفسه من السهل الوقوع في الحل الأمثل بأستخدامها.

٢- **تقديرالطلب المتوقع على المياه حتى عام ٢٠٣٢:** تم تقديرالطلب المتوقع على المياة حتى سنة ٢٠٣٢ لمدينة برج العرب الجديدة و ذلك بأستخدام معدلات أستهلاك المياة المذكور في الكود المصرى لتنفيذ مشروعات المياة الشرب و الصرف الصحى للاستخدمات المختلفة ، وكان أجمالى أقصى طلب شهرى على مياة الشرب لمدينة برج العرب الجديدة لسنة الهدف هو ٤٩٨١٨٧ متر مكعب/ يوم.

٣- **تقديرتصرفات الصرف الصحى المتوقعة حتى عام ٢٠٣٢:** تم تقدير تصرفات الصرف الصحى المتوقعة لمدينة برج العرب الجديدة حتى عام ٢٠٣٢ و كان أجمالى التصرفات الآدامية و الصناعية حوالى ٤٧٦٨٩٧ متر مكعب/ يوم.

٤- **تقييم موقف أعمال الصرف الصحي بالمدينة حتى عام ٢٠٣٢:** تم تقييم موقف أعمال الصرف الصحي و ذلك لتقدير متطلبات التخطيط الأستراتيجى لمشروعات الصرف الصحى و تمت دراسة الحلول والحصول على التوصيات بأنة لا توجد حاجة لزيادة القدرة التصميمية لمحطات رفع و معالجة مياه الصرف الصحي بمدينة برج العرب الجديدة. كونها قادرة على إستيعاب التدفقات المقدرة لمياه الصرف الصحي حتى سنة ٢٠٣٢.

٥- **تقييم موقف أعمال تغذية مياه الشرب للمدينة حتى عام ٢٠٣٢:** تم تقييم موقف أعمال تغذية مياه الشرب لتقدير متطلبات التخطيط الأستراتيجى لمشروعات التغذية و الأمداد بمياة الشرب و تمت دراسة الحلول والحصول على التوصيات بأنة هناك حاجة إلى زيادة السعة التصميمية لمرافق التغذية بمياه الشرب بمقدار ٢٥٤٠٠٠ م٣/ يوم لمدينة برج العرب الجديدة لأستيعاب الزيادة السكنية و التطور العمرانى و الصناعى فى المدينة حتى سنة ٢٠٣٢.

٦- **متطلبات التخطيط الأستراتيجى في أعمال تغذية مياه الشرب حتى عام ٢٠٣٢:** تم عمل دراسة جدوى لثلاثة تكوينات مقترحة لمحطة التناضح العكسي لتحلية المياه المقترنة بالألواح الشمسية الكهروضوئية (PV-RO)، متوفرة كبدائل لإمدادات المياه، و ذلك لاختيار أفضلهم لتزويد المدينة بالمياة حتى سنة ٢٠٣٢. هذه التكوينات هي:

- **التكوين الأول:** فى هذا التكوين يتم تشغيل محطة التناضح العكسي لتحلية المياه (RO) بالطاقة الكهربائية المنتجة من الألواح الشمسية الكهروضوئية (PV) فقط (و فى هذا التكوين تعمل المحطة فى ساعات النهار فقط لأنة لا يتم توليد كهرباء بهذه الطريقة بالليل لعدم وجود الأشعاع الشمسى اللازم لتوليد الطاقة الكهربائية).
- **التكوين الثاني:** فى هذا التكوين يتم تشغيل محطة التناضح العكسي لتحلية المياه (RO) بالطاقة الكهربائية المنتجة من الألواح الشمسية الكهروضوئية (PV) (فى ساعات النهار) و يتم الأعتماد على بطاريات تخزين كهربائية فى تخزين جزء من الطاقة المنتجة من الألواح الشمسية الكهروضوئية بالنهار للأعتماد عليها فى تشغيل المحطة (فى جزء من ساعات الليل).
- **التكوين الثالث:** فى هذا التكوين يتم تشغيل محطة التناضح العكسي لتحلية المياه (RO) بالطاقة الكهربائية المنتجة من الألواح الشمسية الكهروضوئية (PV) (فى ساعات النهار) و بالطاقة الكهربائية من الشبكة العامة للكهرباء (فى ساعات الليل).

و من نتائج مقارنة حسابات التكلفة الوحده للمتر المكعب من المياه المنتجة من للتكوينات تبين التالى:

التكوين الأول : التكلفة لكل متر مكعب من المياه المنتجة بهذا التكوين هي ٢.٢٧٨ دولار أمريكي/ متر مكعب.

التكوين الثاني : التكلفة لكل متر مكعب من المياه المنتجة بهذا التكوين هي ١.٥٨٥ دولار أمريكي/ متر مكعب.

التكوين الثالث : التكلفة لكل متر مكعب من المياه المنتجة بهذا التكوين هي ٠.٨٩٢ دولار أمريكي/ متر مكعب.

وفقا للنتائج ، فإن التكوين الثالث هو أفضل تكوين اقتصادي ، لأنه ينتج ماء بأقل تكلفة لمتر المكعب.لذا نوصى بتنفيذ مشروع نظام PV-RO يعمل بالألواح الشمسية الكهروضوئية المتكاملة مع الشبكة العامة للكهرباء (بسعة ٢٥٤٠٠٠ م٣/ يوم و بتكلفة تقديرية ٣٥٠.٥٧٣ × ١٠$^{٦}$ دولار أمريكي). وذلك للتغلب على نقاط الضعف في نظام المياه، وكذلك لمنع أي نقص في الخدمات. هناك فوائد أخرى للمشروع ، مثل تقليل الاعتماد على مياه النيل للاستفادة منه في المناطق غير الساحلية الأخرى، وكذلك تقليل الغازات الضارة الناتجة عن توليد الكهرباء بالطرق التقليدية التي تستخدم في تحلية مياه البحر.

# التوصيات:

بشكل عام، وفقًا للنتائج التي تم الحصول عليها من هذه الدراسة ، يمكن تمثيل التوصيات على النحو التالي:

١- لا حاجة لزيادة القدرة التصميمية لمحطات رفع و معالجة مياه الصرف الصحي بمدينة برج العرب الجديدة.

٢- يجب تنفيذ مشروع نظام PV-RO يعمل بالألواح الشمسية الكهروضوئية متكاملة مع الشبكة العامة للكهرباء (بسعة ٢٥٤٠٠٠ م٣/ يوم و بتكلفة تقديرية ٣٥٠.٥٧٣ × ١٠$^{٦}$ دولار أمريكي)، لتقليل الاعتماد على مياه النيل للاستفادة منه في المناطق غير الساحلية الأخرى، وكذلك تقليل الغازات الضارة الناتجة عن توليد الكهرباء بالطرق التقليدية التي تستخدم في تحلية مياه البحر.

**كلية الهندسة**
**قسم الهندسة الصحية**

# دراسة المياة والصرف الصحى بمدينة برج العرب الجديدة

رسالة مقدمة من

ضمن متطلبات درجة الماجستير
فى الهندسة الصحية

مقدمة من

محمد غريب عبدالغنى مجاهد

بكالوريوس هندسة القوى الكهربائية و الآلات - كلية الهندسة - جامعة المنوفية - ٢٠٠٧

نوفمبر ٢٠٢٠

**كلية الهندسة**
**قسم الهندسة الصحية**

## صفحة الموافقة على الرسالة

# دراسة المياة والصرف الصحى بمدينة برج العرب الجديدة

**رسالة مقدمة من**

## محمد غريب عبدالغنى مجاهد

بكالوريوس هندسة القوى الكهربائية و الآلات ـ كلية الهندسة ـ جامعة المنوفية ـ ٢٠٠٧

لجنة الحكم والمناقشة التوقيع

**الاستاذ الدكتور / فيفى محمد السيد** ..................
**أستاذ متفرغ بقسم الهندسة الصحية**
**كلية الهندسة – جامعة الإسكندرية**

**الاستاذ الدكتور / محمد طارق سرور** ..................
**أستاذ بقسم الهندسة الصحية**
**كلية الهندسة – جامعة الإسكندرية**

**الاستاذ الدكتور/ مدحت عبدالمعطى مصطفى** ..................
**أستاذ بقسم الهندسة الصحية**
**كلية الهندسة – جامعة الإسكندرية**

تاريخ مناقشة الرسالة: ١٦ / ١١ /٢٠٢٠

**كلية الهندسة**
**قسم الهندسة الصحية**

# لجنة الإشراف

إسم الطالب: محمد غريب عبدالغنى مجاهد

عنوان الرسالة: دراسة المياة والصرف الصحى بمدينة برج العرب الجديدة

إسم الدرجة: الماجستير فى الهندسة الصحية

| لجنة الإشراف | التوقيع |
| --- | --- |
| **الاستاذ الدكتوره / فيفى محمد السيد عبدالرسول**<br>أستاذ متفرغ بقسم الهندسة الصحية<br>كلية الهندسة – جامعة الإسكندرية | .................. |
| **الدكتوره / مى عبد الفتاح فايد**<br>مدرس بقسم الهندسة الصحية<br>كلية الهندسة – جامعة الإسكندرية | .................. |
| **الدكتوره / ساميه عبد الرحمن على**<br>مدرس بقسم الهندسة الصحية<br>كلية الهندسة – جامعة الإسكندرية | .................. |